

Neuromodulation of spinal networks in embryonic and larval zebrafish

Thesis submitted for the degree of
Doctor of Philosophy

Michael Jay

Department of Neuroscience, Psychology and Behaviour

University of Leicester

2015

Abstract

Neuromodulation of spinal networks in embryonic and larval zebrafish

Michael Jay

Spinal networks, once considered an inflexible ensemble of excitatory and inhibitory components organised into fixed circuits, are in fact modulated by a range of neuromodulators which impart levels of flexibility that permit adaptation to changing environments. In this thesis the roles of two known neuromodulators, nitric oxide (NO) and dopamine (DA), have been examined within the developing zebrafish nervous system.

In the first results chapter, the anatomical and functional effects of perturbing NO signalling during neuromuscular junction (NMJ) development have been investigated. This revealed that prolonged exposure to NO decreased NMJ number. Additionally, miniature end plate current (mEPC) frequency was reduced, kinetics slowed, and locomotor drive affected, suggesting NO is a potent modulator of NMJ maturation and function.

In the second and third chapters, the physiological maturation and functional roles of a population of DAergic neurons which project to spinal networks have been studied. To understand when and how cellular activity patterns develop, targeted *in vivo* electrophysiological recordings were made from dopaminergic diencephalospinal neurons (DDNs) at embryonic and larval stages, where locomotor network development and output undergo profound changes. These investigations demonstrated that DDNs functionally mature during development, engaging in low frequency tonic spiking at embryonic stages which is accompanied by high frequency bursting at larval stages. Paired recordings of DDNs with spinal neurons revealed that at free swimming (larval) stages, tonic spiking is associated with periods of locomotor inactivity, whereas bursts are associated with periods of swimming. Ablation of DDNs was sufficient to suppress locomotor output suggesting that these cells modulate spinal network excitability.

In sum, these investigations provide important insights into the roles of NO and DA during locomotor network ontogeny: NO modulates NMJ maturation while DA contributes to locomotor output.

Acknowledgements

Firstly, I would like to thank my supervisor, Joe McDermid, for his invaluable guidance throughout the course of my PhD. He has been an excellent supervisor and if it were not for his expertise and willingness to always help, I would not have achieved nearly as much as I have (and I'd probably still be wondering how to turn the rig on). I will always be indebted to Joe for giving me the opportunity to join his lab. It has been a true privilege and I cannot thank him enough.

It would also be amiss to not thank both present and past members of the lab for their help throughout my time in Leicester, both as an undergraduate and PhD student. You have all made my time in Leicester a unique experience, to say the least! I'd also like to thank all the technical staff we've had through the years that have made my life that bit easier.

Finally, I'd like to thank my parents for their support and providing me with all the opportunities which have allowed me to go to university and undertake this wonderful opportunity.

Contents

Front Matter	i
Abstract	ii
Acknowledgements	iii
Table of Contents	iv
List of Tables	x
List of Figures	xi
Abbreviations	xiv
1 Introduction	1
1.1 Central pattern generators in the spinal cord	2
1.2 Supraspinal control of locomotor networks	6
1.3 Pattern generation and neuromodulation of an invertebrate CPG network	8
1.4 Neuromodulation of vertebrate networks	10
1.4.1 Gaseous neuromodulators	11
1.4.2 Monoaminergic neuromodulators	12
1.5 Developmental roles of neuromodulators	14
1.6 Using zebrafish to study motor network development	16
1.6.1 Zebrafish exhibit a range of stereotypical behaviours during de- velopment	16
1.6.2 Development of the locomotor network	18
1.6.3 Innervation of the developing musculature	23
1.6.4 Activity patterns of the developing locomotor network	24
1.6.4.1 Coiling	24

1.6.4.2	Touch response	27
1.6.4.3	Double coiling	27
1.6.4.4	Swimming	28
1.7	Aims and objectives	31
1.8	Publications	32
2	Methods	33
2.1	Zebrafish care	34
2.2	Pharmacological reagents	34
2.2.1	Chronic drug application	35
2.2.2	Fast drug application during electrophysiological investigations	35
2.3	Electrophysiological solutions	36
2.3.1	Extracellular solutions	36
2.3.2	Intracellular solutions	37
2.4	Electrophysiology	38
2.4.1	Preparation of fish	38
2.4.2	Electrophysiological methods	38
2.4.2.1	Extracellular recording	41
2.4.2.2	Whole cell and perforated patch recording	41
2.4.2.3	Data acquisition	45
2.5	Histochemistry	46
2.6	Image acquisition	48
2.7	Laser ablation	48
2.8	Monitoring behaviour	49
2.9	Analyses	49
2.9.1	Electrophysiology	49
2.9.2	Image analysis	50

2.9.3	Behaviour	50
2.9.4	Statistics	51
3	Effects of Nitric Oxide on Neuromuscular Junction Properties	54
3.1	Introduction	55
3.1.1	Identification of nitric oxide as a signalling molecule	55
3.1.2	Isoforms of nitric oxide synthase and the production of NO	57
3.1.3	Structural and functional characteristics of NOS isoforms	59
3.1.4	NOS1 expression within the developing nervous system	60
3.1.4.1	Mammalian System	60
3.1.4.2	Xenopus	61
3.1.4.3	Zebrafish	62
3.1.5	Downstream pathways of NO within the nervous system	64
3.1.5.1	NO receptor-dependent signalling	64
3.1.5.2	NO receptor-independent signalling	69
3.1.6	Roles of NO during nervous system development	71
3.1.7	Nitric oxide as a modulator of locomotor networks	76
3.2	Aims and Objectives	78
3.3	Results	79
3.3.1	Exogenous increases in NO-dependent signalling decreases NMJ number	79
3.3.2	Inhibition of NO-dependent signalling markedly increased NMJ number	83
3.3.3	Developmental effects of NO Signalling on mEPC parameters	86
3.3.4	Developmental effects of NO signalling on the frequency of inputs	91
3.3.5	Acute perturbation of NO signalling does not affect NMJ properties	91
3.3.6	Developmental perturbation of NO signalling alters the locomotor drive for swimming	94

3.3.7	Developmental effects of NO signalling on motoneuron properties	96
3.4	Discussion	103
3.4.1	NO/cGMP-dependent regulation of NMJ formation	103
3.4.2	Use of 18- β -Glycyrrhetic acid as a gap junction blocker	106
3.4.3	NO-dependent loss of inputs modulates musculature innervation	107
3.4.4	Electrophysiological consequences of NO perturbation on NMJs	107
3.4.5	Effects of NO on locomotor drive and spinal networks	110
4	Developing Cellular Properties of Spinally Projecting DDNs	114
4.1	Introduction	115
4.1.1	Dopamine synthesis	116
4.1.2	Dopamine receptors and downstream signalling pathways	116
4.1.3	The mammalian dopaminergic system	119
4.1.3.1	Ascending DAergic pathways	119
4.1.3.2	Descending DAergic pathways	121
4.1.3.3	DA receptor expression in the mammalian nervous system	124
4.1.4	Zebrafish catecholaminergic systems	126
4.1.4.1	Catecholaminergic system ontogeny	127
4.1.4.2	Diencephalospinal DAergic inputs	129
4.1.4.3	DA receptor expression in the zebrafish larvae	131
4.1.5	Electrophysiological properties of DAergic neurons	133
4.1.5.1	Midbrain DAergic neurons have autonomous spike capability	136
4.1.5.2	Diversity amongst DAergic neuron populations	137
4.2	Aims and objectives	141
4.3	Results	142
4.3.1	Identification of DDNs	142

4.3.2	Ontogeny of synaptic inputs	146
4.3.3	Maturation of intrinsic firing properties	149
4.3.3.1	Responses to rheobase current	149
4.3.3.2	Responses to suprathreshold current	152
4.3.4	DDNs undergo depolarisation block	152
4.3.5	Ontogeny of pacemaker firing	156
4.3.6	Pacemaker firing is voltage-dependent	163
4.3.7	Ionic basis of pacemaker firing	164
4.3.8	Dopaminergic autoinhibition of autonomous DDN activity . . .	168
4.4	Discussion	174
4.4.1	DDNs innervate central and peripheral structures	174
4.4.2	Development of intrinsic spike properties	175
4.4.3	DDNs spike autonomously in an age-dependent manner	178
4.4.4	DDNs undergo depolarisation block	180
4.4.5	Developing synaptic inputs	181
4.4.6	Synaptic inputs to DDNs are suppressed by DA	183
4.4.7	DDNs undergo autoinhibition	184
5	Developing Activity Patterns and Functional Roles of DDNs	186
5.1	Introduction	187
5.1.1	Dopaminergic control of spinal networks	187
5.1.2	Mechanisms underpinning the effects of dopamine (DA) on spinal networks	192
5.2	Aims and objectives	193
5.3	Results	195
5.3.1	Ontogeny of endogenous activity patterns	195
5.3.2	Activity patterns within the dopaminergic diencephalospinal neu- ron (DDN) population	197

5.3.3	Cellular basis for observed activity patterns	199
5.3.4	Synaptic drive to DDNs	202
5.3.5	Relationship between DDN activity and motor output	203
5.3.6	Effects of DC2 DDN ablation on motor behaviour	210
5.3.7	Effects of DC2 and DC4/5 ablation on motor behaviour	216
5.4	Discussion	221
5.4.1	Ontogeny of endogenous DDN firing patterns and relationship to locomotor output	221
5.4.2	Effects of DDN ablation at beat-glide swimming stages	225
5.4.3	Contribution of synaptic inputs to activity patterns	229
5.4.4	Afferent inputs to DDNs	232
6	General Discussion	237
	References	245

List of Tables

2.1	Evan's extracellular saline	37
2.2	K-gluconate intracellular solution	40
2.3	Low Chloride intracellular solution	40
2.4	Cesium Chloride intracellular solution	40
2.5	Intra- and Extracellular solutions for experiments	42
4.1	Catecholamine groups in the larval zebrafish	128

List of Figures

1.1	Organisation of vertebrate locomotor CPG	4
1.2	Organisation of vertebrate locomotor network	7
1.3	Locomotor pattern ontogeny	19
1.4	Identified cell types within the developing zebrafish spinal cord	20
1.5	Primary motoneuron outgrowth	21
2.1	Standard preparation for electrophysiology	39
2.2	Behavioural analysis	52
3.1	Schematic of NOS expression patterns during development	63
3.2	Schematic of experimental protocol	80
3.3	Developmental increases of NO signalling decrease NMJ numbers	81
3.4	Developmental increases of cGMP signalling decrease NMJ numbers	82
3.5	Developmental inhibition of NO signalling increase NMJ numbers	84
3.6	Developmental inhibition of cGMP signalling increase NMJ numbers	85
3.7	Effects of 18- β -GA on electrical coupling between EF fibres	87
3.8	Effects of 18- β -GA on electrical coupling between ES fibres	88
3.9	Developmental perturbation of NO signalling affects EF mEPC kinetics	92
3.10	Developmental perturbation of NO signalling affects ES mEPC kinetics	93
3.11	Acute manipulation of NO levels does not affect mEPC kinetics	95
3.12	Developmental NO manipulation perturbs fictive locomotor drive to EF muscle fibres	97
3.13	Developmental NO manipulation perturbs fictive locomotor drive to ES muscle fibres	98
3.14	Developmental effects of NO on the frequency and duration on the neuromuscular drive for locomotion	99
3.15	Developmental effects of NO perturbation on intrinsic properties of motoneurons	100

3.16	Developmental effects of NO perturbation on synaptic inputs to motoneurons	101
4.1	Biosynthesis pathway for catecholamines	117
4.2	Distribution of DAergic cells in the mammalian brain	119
4.3	Distribution of DAergic receptors in the mammalian spinal cord	125
4.4	Zebrafish CAergic system ontogeny	129
4.5	Zebrafish CAergic system distribution	130
4.6	Identification of DDNs	143
4.7	DDN projection patterns within the CNS	144
4.8	DDN projection patterns within the PNS	145
4.9	Schematic overview of DDN projections	145
4.10	Ontogeny and identification of synaptic inputs	147
4.11	Glutamatergic and GABAergic mPSC kinetics at 4 dpf	148
4.12	DDN activity patterns in response to rheobase current injection	150
4.13	Phase plane plots in response to rheobase current injection	151
4.14	DDN activity patterns in response to suprathreshold current injection	153
4.15	Action potential waveforms during suprathreshold current injection	154
4.16	Phase plane plots during suprathreshold current injection	155
4.17	Depolarisation block of DDNs	157
4.18	Occurrence of action potentials during current ramps	158
4.19	Development of autonomous spike activity	159
4.20	Autonomous DDN spiking at burst swimming stages	161
4.21	Autonomous DDN spiking at beat-glide swimming stages	162
4.22	Autonomous spiking is voltage-dependent	165
4.23	Autonomous spiking is voltage-dependent	166
4.24	Ionic basis of pacemaker firing	167
4.25	DDN activity patterns are modulated by DA	170

4.26 DA hyperpolarises membrane potential following TTX application . . .	171
4.27 D ₂ receptor antagonist abolishes dopaminergic autoinhibition	172
4.28 DA modulates synaptic inputs into DDNs	173
5.1 Activity patterns of dopaminergic diencephalospinal neurons (DDNs) during development	196
5.2 Firing activity coordination between DDNs	198
5.3 Activity patterns during whole cell recordings at 1 and 2 dpf	200
5.4 Endogenous DDN activity patterns at 4 dpf	201
5.5 Synaptic drive to DDNs	204
5.6 Relationship between DDN activity and locomotor network activity at 1 and 2 dpf	205
5.7 DDN activity patterns correlate with locomotion at 2 but not 1 dpf . . .	206
5.8 Paired recordings between DDNs and MNs	208
5.9 Duration of locomotor activity is unaffected by DDN bursting	209
5.10 DDN activity patterns correlate with locomotion at 4 dpf	209
5.11 Targeted ablation at 1 days post fertilisation (dpf) causes loss of GFP positive cells	212
5.12 Selective loss of DDNs following ablation at 1 dpf	212
5.13 Identified beat-glide swim episodes in control and ablated larvae	213
5.14 Selective loss of DDNs affects locomotor output	214
5.15 Parameters of swim episodes are unaffected by DDN ablation	215
5.16 Selective loss of DC2/4/5 GFP-positive neurons following ablation . . .	217
5.17 Parameters of swim episodes are unaffected by DC2/4/5 cell ablation .	218
5.18 Swimming trajectories post DC2/4/5 cell ablation	219
5.19 Identified beat-glide swim episodes in DC2/4/5 ablated larvae	220

Abbreviations

18- β -GA	18- β -Glycyrrhetic acid
3-MT	3-methoxytyramine
6-OHDA	6-hydroxydopamine
8-CPT-cGMP	8-(4-Chlorophenylthio)-guanosine 3',5'- cyclic monophosphorothioate
AADC	aromatic L-amino acid decarboxylase
AC	adenylyl cyclase
ACh	acetylcholine
AChE	acetylcholinesterase
AChR	acetylcholine receptor
ADHD	attention deficit hyperactivity disorder
AHP	afterhyperpolarisation
AMO	antisense morpholino
AMPA	α -amino-3-hydroxy-5-methyl-4-isoxazolepropionic acid
AP	action potential
APV	(2R)-amino-5-phosphonovaleric acid
ATP	adenosine triphosphate
AVI	audio video interleave
BH ₄	tetrahydrobiopterin
BIC	bicuculline
CA	catecholamine
CaCl ₂	calcium chloride
CAergic	catecholaminergic
CaM	calmodulin
cAMP	3'-5'-cyclic adenosine monophosphate
CaP	caudal primary
CB	calbindin
cGMP	cyclic guanosine monophosphate
CiA	circumferential ascending
CiD	circumferential descending
CNG	cyclic nucleotide-gated
CNS	central nervous system
CoBL	commissural bifurcating longitudinal
CoLA	commissural longitudinal ascending
CoLo	commissural local

COMT	catechol-o-methyl transferase
CoPA	commissural primary ascending
CoSA	commissural secondary ascending
CPG	central pattern generator
CsCl	cesium chloride
CsOH	cesium hydroxide
Ctrax	California Institute of Technology Fly Tracker
D β H	dopamine- β -hydroxylase
d-tubocurarine	(+)-tubocurarine hydrochloride pentahydrate
DA	dopamine
DAergic	dopaminergic
DAh	dopamine hydrochloride
DAT	dopamine transporter
DC	diencephalic catecholaminergic cluster
DDN	dopaminergic diencephalospinal neuron
DETA/NO	diethylenetriamine/nitric oxide adduct
dlc	dorsolateral commissural interneuron
DMSO	dimethyl sulfoxide
DoLA	dorsal lateral ascending
dpf	days post fertilisation
DRG	dorsal root ganglia
dRoP	dorsal rostral primary
DSHB	Developmental Studies Hybridoma Bank, University of Iowa
EDRF	endothelial-derived relaxing factor
EF	embryonic fast
EPP	end plate potential
EPSC	excitatory post synaptic current
EPSP	excitatory post synaptic potential
ES	embryonic slow
FAD	flavin adenine dinucleotide
fEPSP	field excitatory post synaptic potential
FMN	flavin mononucleotide
GABA	γ -Aminobutyric acid
GAPDH	glyceraldehyde-3-phosphate dehydrogenase
GC	guanylyl cyclase
GIRK	G-protein-coupled inwardly rectifying potassium
GP	globus pallidus

GPCR	G-protein coupled receptor
GTP	guanosine triphosphate
GUI	graphical user interface
HCN	hyperpolarisation-activated, cyclic nucleotide-gated
HCRT	hypocretin/orexin
hpf	hours post fertilisation
I_A	transient K^+ current
I_h	hyperpolarisation-activated inward current
I_{NaP}	persistent sodium current
IC	ipsilateral caudal
IN	interneuron
IP_3	inositol 1,4,5-triphosphate
IPSC	inhibitory post synaptic current
IPSP	inhibitory post synaptic potential
ISI	interspike interval
JAABA	Janelia Automatic Animal Behavior Annotator
KA	Kolmer-Agdur
KCl	potassium chloride
KOH	potassium hydroxide
KYN	kynurenic acid
L-DOPA	L-3,4-dihydroxyphenylalanine
L-NAME	N_{ω} -Nitro-L-arginine methyl ester hydrochloride
LC	locus coeruleus
LPS	lipopolysaccharide
LTP	long-term potentiation
mAHP	medium-duration hyperpolarisation
MAO	monoamine oxidase
MCoD	multipolar commissural descending
mEPC	miniature end plate current
$MgCl_2$	magnesium chloride
MiP	middle primary
MLR	mesencephalic locomotor region
MN	motoneuron
MO	medulla oblongata
mPFC	medial prefrontal cortex
mPSC	miniature post synaptic current
MS-222	ethyl 3-aminobenzoate methanesulfonate
MSN	medium spiny neuron

NA	noradrenaline
NaCl	sodium chloride
NADPH	nicotinamide adenine dinucleotide phosphate
NAergic	noradrenergic
NaOH	sodium hydroxide
NG	nitroglycerin
NMDA	N-Methyl-D-aspartic acid
NMJ	neuromuscular junction
NO	nitric oxide
NOS	nitric oxide synthase
OB	olfactory bulb
ODQ	1H-[1,2,4]Oxadiazolo[4,3-a]quinoxalin-1-one
PBS	phosphate buffered solution
PBS-TX	phosphate buffered solution/triton-X
PD	periodic depolarisation
PDA	2,3 <i>cis</i> -Piperidine dicarboxylic acid
PDE	3'5'-cyclic nucleotide phosphodiesterases
PFA	paraformaldehyde
PIC	picrotoxin
PKA	protein kinase A
PKG	protein kinase G
pMN	primary motoneuron
PNMT	phenylethanolamine N-methyltransferase
PO	preoptic area
Pr	pretectum
PSC	post synaptic current
PT	posterior tuberculum
QX-314	N-(2,6-Dimethylphenylcarbamoylmethyl) triethylammonium bromide
RB	Rohon-Beard
Rh- α -BTX	rhodamine-conjugated α -bungarotoxin
RoP	rostral primary
SB	synaptic burst
SEM	standard error of the mean
sGC	soluble guanylyl cyclase
sMN	secondary motoneuron
SNAP	S-Nitroso-N-acetyl-DL-penicillamine
SNc	substantia nigra pars compacta
SOD	superoxide dismutase

SP	subpallium
SVZ	subventricular zone
TEA	tetraethylammonium chloride
TGF- β	transforming growth factor β
TH	tyrosine hydroxylase
TTX	tetrodotoxin
UCoD	unipolar commissural descending
ufmf	micro fly movie format
UV	ultra-violet
VaP	variable primary
VeLD	ventrolateral descending
VeMe	ventral medial
VMAT2	vesicular monoamine transporter 2
VMR	visual motor response
vRoP	ventral rostral primary
VTA	ventral tegmental area

CHAPTER

1

Introduction

The locomotor repertoire of an organism is underpinned by neuronal networks known as central pattern generators (CPGs) which in vertebrates are located in the spinal cord. These networks generate coordinated locomotor output by providing the rhythmic excitatory drive necessary for the sequential activation of muscle groups (Delcomyn, 1980; Grillner, 2003). CPGs are able to generate a basic rhythmic pattern in the absence of supraspinal input. However since locomotor output has to be flexible in order to adapt to changing environmental demands, spinal networks integrate a range of inputs which further refine their activity patterns (Le Ray et al., 2011; Sillar et al., 2014; Stein, 2014). Behaviours that require the rapid integration of information are driven primarily by classical fast synaptic transmission. However, spinal networks are also influenced by a range of molecules, known as neuromodulators, which alter the cellular and synaptic properties of constituent neurons of the CPG to offer further flexibility to motor output (Harris-Warrick, 2011; Miles and Sillar, 2011; Sillar et al., 2014; El Manira, 2014). While there has been intense interest in the modulatory actions of this diverse range of chemicals, the roles of neuromodulators, particularly within the context of control of vertebrate locomotor networks, are not fully understood. To address this gap in knowledge, I have examined the role of two neuromodulators, nitric oxide (NO) and dopamine (DA), within the development and control of spinal networks.

1.1 Central pattern generators in the spinal cord

Within the vertebrate spinal cord, the CPG which drives rhythmic locomotor output has been well characterised and appears to be conserved amongst terrestrial and aquatic

vertebrates (Grillner et al., 1995; Grillner, 2003; Kiehn and Butt, 2003; Grillner, 2006; Mueller et al., 2008; Goulding, 2009; Guertin, 2009; Stephenson-Jones et al., 2011). Some of the first clues regarding the origin of locomotor output within vertebrates were obtained from anaesthetised, spinal cord-transected cat preparations (Brown, 1911). Following transection at the lower thoracic level, the cats were found to be capable of producing “acts of progression” (i.e. rhythmic step-like movements). Importantly, since these animals were anaesthetised and thus received no proprioceptive input, Brown (1911) surmised that the spinal cord contains sufficient neuronal circuitry to generate basic locomotor patterning. It is now understood that the rhythmicity which contributes to locomotor output is underpinned by neural circuits termed CPGs (Jankowska et al. 1967a,b; see Grillner 2006 for review).

Both the *Xenopus laevis* frog embryo and adult lamprey preparation have proven to be useful models for examining the neuronal basis for locomotor rhythm generation. This is in part because both species have a relatively accessible and simple nervous system when compared to other vertebrate species. Moreover, the ability to generate fictive locomotor activity under experimental conditions facilitates electrophysiological investigation of the neuronal components which contribute to locomotor output. In both species, the CPG comprises two half-centre oscillators, with one located on either side of the spinal cord (Figure 1.1). Each half-centre oscillator can generate a rhythmic pattern, albeit at a higher frequency relative to whole spinal cord preparations (Khan and Roberts, 1982; Cohen and Harris-Warrick, 1984; Grillner and Wallén, 1980; Cangiano and Grillner, 2003). This arises because each half-centre oscillator also contains a class of inhibitory glycinergic neurons which make direct synaptic connections with neurons on the opposite side of the spinal cord (Grillner and Wallén, 1980;

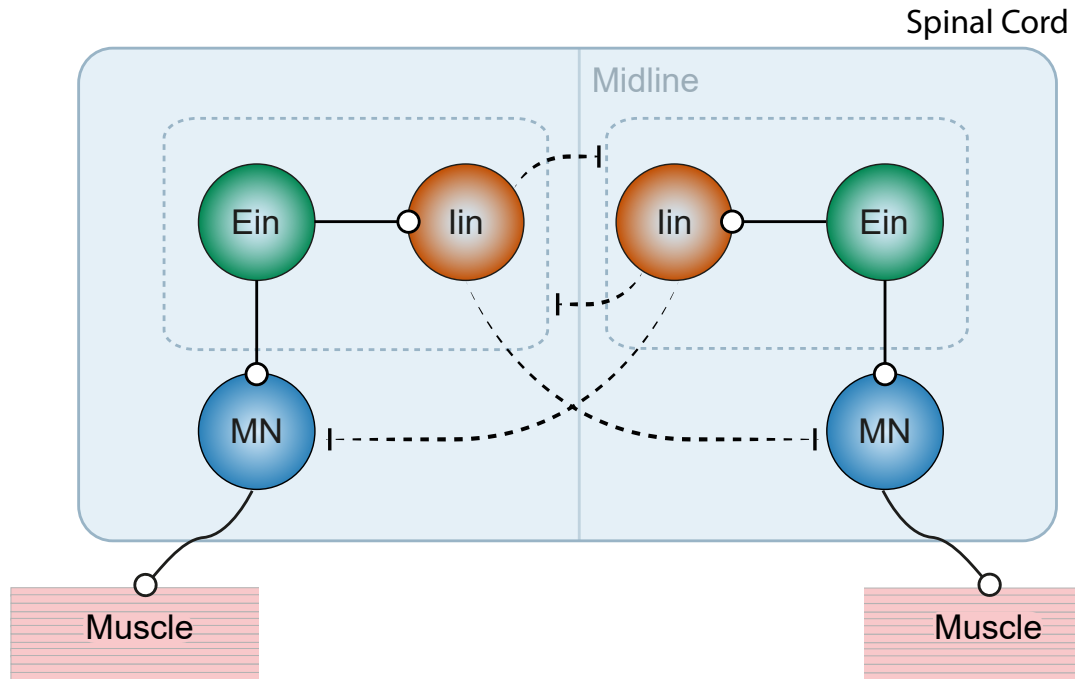


FIGURE 1.1

General organisation of the vertebrate locomotor central pattern generator. The CPG comprises excitatory glutamatergic and inhibitory glycinergic interneurons (Ein and Iin, respectively) and motoneurons (MNs). Dashed black lines represent inhibitory synaptic inputs arising from the Iins. All three components of each half-centre oscillator (dashed blue lines) receive inhibitory inputs. Eins excite (solid black lines) both MNs and Iins. MNs exit the spinal cord to innervate muscle tissue. Adapted from Grillner (2006).

Buchanan, 1982; Dale, 1985; Dale et al., 1986). Moreover, pharmacological block of glycinergic transmission perturbs alternating rhythm generation between each half-centre oscillator (Cohen and Harris-Warrick, 1984; Kato, 1990; Cowley and Schmidt, 1995; Kjaerulff and Kiehn, 1997). Thus, commissural glycinergic inhibitory interneurons are important in maintaining left-right rhythmicity and regulating the speed of the rhythm. In contrast, the ipsilateral glutamatergic interneurons within the half-centre oscillator provide sustained tonic excitation and fast, rhythmic excitation to CPG interneurons within the half-centre oscillator (Buchanan and Grillner, 1987; Soffe, 1989; Parker and Grillner, 1999, 2000; Cangiano and Grillner, 2003) (Figure 1.1).

After CPG activation, the constituent neurons of the half-centre oscillator

receive excitatory drive during a locomotor episode (Dale and Roberts, 1985; Dale and Grillner, 1986; Dale, 1986). Within both the *Xenopus* embryo and lamprey, this input arises from glutamatergic interneurons of the CPG that form monosynaptic connections with the commissurally projecting inhibitory interneurons, other excitatory ipsilateral interneurons and to the cholinergic motoneurons (Dale and Roberts, 1985; Buchanan and Grillner, 1987; Buchanan et al., 1989) (Figure 1.1). The excitatory post synaptic potentials (EPSPs) which drive CPG neurons to fire action potentials during a swim cycle can be dissected into two components (fast and slow) based on their pharmacological properties. Addition of (2R)-amino-5-phosphonovaleric acid (APV), an N-Methyl-D-aspartic acid (NMDA) receptor antagonist is sufficient to block the slow component whilst application of 2,3 *cis*-Piperidine dicarboxylic acid (PDA), an α -amino-3-hydroxy-5-methyl-4-isoxazolepropionic acid (AMPA)/NMDA receptor antagonist, is sufficient to abolish the fast component (Dale and Roberts, 1985; Dale et al., 1986; Dale, 1986). Thus, each EPSP is comprised of a slow NMDA and fast AMPA component. In *Xenopus*, the NMDA-dependent potential is sustained for \approx 200 ms and is markedly longer than that of the swim cycle (50 – 100 ms) (Dale and Roberts, 1985). This provides a tonic level of excitation for the duration of the locomotor episode which facilitates subsequent action potential generation. The fast AMPA receptor-mediated component provides further excitatory drive to initiate action potential generation within a swim episode. Spinal CPGs also receive an inhibitory post synaptic potential (IPSP) which occurs midway through the swim cycle. This is mediated by the commissurally projecting glycinergic interneurons and ensures efficient alternation between both half-centre oscillators (Buchanan and Cohen, 1982; Buchanan, 1982; Dale, 1985; Buchanan and Grillner, 1987). In addition to providing the mid-cycle inhibition, the

IPSP may also contribute to the generation of the following spikes in the swim cycle. This occurs upon termination of the IPSP when the membrane potential rebounds from its hyperpolarised state and overshoots the resting membrane potential, taking the cell toward and possibly over spike threshold (Perkel and Mulloney, 1974; Satterlie, 1985).

1.2 Supraspinal control of locomotor networks

Whilst the basic CPG circuitry is capable of producing rhythmic alternating output, it requires descending inputs in order to initiate locomotor activity (Figure 1.2). The basal ganglia, a group of evolutionarily conserved structures, are important in the execution of motor movements. The basal ganglia is composed of four nuclei: the striatum (caudate nucleus and putamen), the globus pallidus, the subthalamic nucleus and the substantia nigra (Stephenson-Jones et al., 2011; Grillner and Robertson, 2015; Nambu, 2015). Within mammals, the basal ganglia integrates afferent fibres originating in cortical and thalamic brain regions at the level of the striatum (Doig et al., 2010). The striatum is likely necessary for proper motor behaviour: in rat preparations, loss of thalamic inputs to the basal ganglia was insufficient to perturb feeding behaviour however lesions to the caudate nucleus itself abolished all feeding activity (Sorenson and Ellison, 1970). Indeed, perturbations within the basal ganglia induce a range of movement disorders (Albin et al., 1989). For example, within primates, hyperkinetic movement disorders are induced by block of activity within the substantia nigra (Crossman, 1987).

The basal ganglia project to a number of regions, including the MLR where it provides tonic inhibitory (GABAergic) input (Swanson et al., 1984; Garcia-Rill et al.,

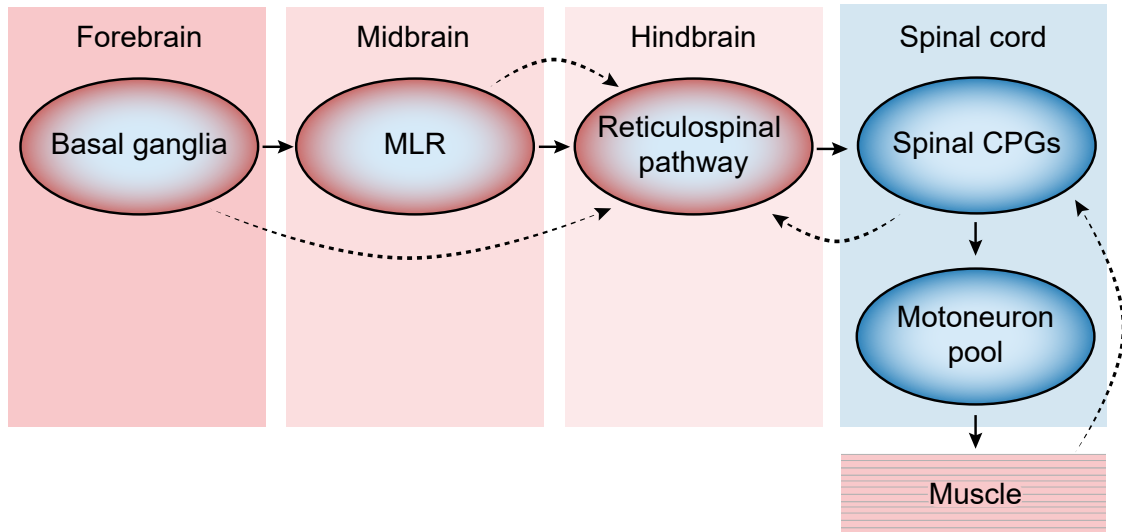


FIGURE 1.2

General organisation of the vertebrate locomotor network. All vertebrates share a similar locomotor network. Here, motoneurons (MNs) innervate the muscle and are ultimately responsible for locomotor output. Rhythmicity within locomotor episodes arises from spinal CPGs which are activated by descending reticulospinal inputs. These cells receive input from the mesencephalic locomotor region (MLR) after disinhibition from the basal ganglia. Dashed lines represent sensory feedback which converge onto the CPG and shape output. Adapted from Goulding (2009).

1985; Milner and Mogenson, 1988; Garcia-Rill et al., 1990; Alexander and Crutcher, 1990). Local infusion of bicuculline, a γ -Aminobutyric acid (GABA) receptor antagonist, within the MLR is sufficient to elicit bouts of locomotion, whereas application of excitatory neurotransmitters (glutamate, acetylcholine or norepinephrine) does not evoke locomotor activity (Garcia-Rill et al., 1985). Thus, an appropriate motor pattern is likely selected at the level of the basal ganglia and this is executed by the MLR following disinhibition. Indeed, in decerebrated lamprey preparations, electrical stimulation or local AMPA application to the MLR is sufficient to elicit bouts of locomotion (Sirota et al., 2000) in which the intensity and frequency of the stimulation correlates with behavioural output, such that stronger stimuli induce a more robust behavioural response (Sirota et al., 2000; Cabelguyen et al., 2003) and in some cases, a switch in motor pattern (Cabelguyen et al., 2003).

The MLR projects to reticulospinal neurons in the hindbrain (Garcia-Rill and Skinner, 1987; Di Prisco et al., 2000; Brocard and Dubuc, 2003; Brocard et al., 2010). These cells project caudally into the spinal cord (Metcalf et al., 1986; van Mier and ten Donkelaar, 1989; Gahtan and O'Malley, 2003) and provide excitatory drive to spinal interneurons (INs) and MNs that subsequently initiate bouts of rhythmic locomotor network activity (Buchanan and Cohen, 1982; Buchanan, 1982; Ohta and Grillner, 1989; Sirota et al., 2000; Wang and McLean, 2014).

1.3 Pattern generation and neuromodulation of an invertebrate CPG network

Owing to its accessibility, the pyloric CPG of the crustacean stomatogastric ganglion has provided a powerful opportunity to examine the effects of neuromodulators on individual neurons within an identified CPG. Here, the CPG produces rhythmic dilation and constriction of muscles within the stomach which serves to move food into the digestive tract. The neurons which constitute this CPG have been fully characterised (Maynard and Selverston, 1975) and systematic deletion of neurons within this network has elucidated their roles in generating the rhythmicity that drives this motor behaviour (Selverston and Miller, 1982; Miller and Selverston, 1982a; Eisen and Marder, 1982; Miller and Selverston, 1982b). Briefly, the pyloric network comprises 14 neurons: 8 pyloric (PY) cells, 2 pyloric dilator (PD) cells and 1 of each of the following cell types: ventricular dilator (VD), lateral pyloric (LP), inferior cardiac and anterior burster (AB). Rhythmicity within this CPG network arises from an electrically coupled network between the AB neuron, which produces rhythmic periodic depolarisations that elicit a

burst of action potentials, and two PD neurons (Maynard and Selverston, 1975; Miller and Selverston, 1982a,b). This cluster of rhythm generating cells drives the remaining ‘follower neurons’, the ventricular dilator and the constrictor motoneurons (inferior cardiac, lateral pyloric and pyloric) (Eisen and Marder, 1982).

This network receives extensive neuromodulatory inputs (see Figure 4a from Marder and Bucher, 2001) which regulate numerous aspects of the CPG and motor output (see below). Within this system neuromodulators alter the cellular and synaptic properties of constituent CPG neurons (see Harris-Warrick, 2011 for review). As a consequence, the motor output can be modified or reconfigured to produce different locomotor patterns. For example, DA, a common neuromodulator, can modify the motor pattern of the pyloric CPG by affecting the synaptic strength and cellular properties of constituent neurons (Flamm and Harris-Warrick, 1986a,b; Johnson et al., 1993b,a, 1994, 1995; Ayali and Harris-Warrick, 1999; Peck et al., 2006). Here, exogenous application of DA slows the cycle frequency of the network and changes the firing properties of individual neurons (Harris-Warrick et al., 1995). At the cellular level, DA increases firing frequency on each cycle and advances the firing phase in the LP and PY cell types. This is attributable to a decrease of the transient K^+ current (I_A) and increase of the hyperpolarisation-activated inward current (I_h) (Harris-Warrick et al., 1995; Peck et al., 2006). The I_A current is typically activated by membrane hyperpolarisation and slows the rate of membrane repolarisation proceeding an action potential. The I_h current is a hyperpolarisation activated cationic current but in contrast to I_A , depolarises the membrane following an afterhyperpolarisation (AHP).

In addition to its cellular effects, DA also modulates the synaptic connections within the pyloric network (Johnson et al., 1993a,b, 1994, 1995). The effects of DA on

synaptic connections are complex, affecting both pre- and post synaptic domains. For example, DA significantly increases the synaptic strength between the pacemaker AB cell and its chemical synaptic targets (namely the PY, LP and IC cells). By contrast, DA simultaneously decreases synaptic strength between the remaining pacemaker cells (namely the PD neurons and their targets) (Johnson et al., 1993b, 1995). DA can also affect the electrical coupling by either enhancing or weakening the connections between the pacemaker neurons (Johnson et al., 1993a). As a consequence of these cellular and synaptic effects, changes in CPG properties can arise from changing concentrations of neuromodulators which subsequently affect parameters of motor patterning (Flamm and Harris-Warrick, 1986a; Ayali and Harris-Warrick, 1999).

1.4 Neuromodulation of vertebrate networks

In comparison to invertebrate models such as the crustacean stomatogastric ganglion, the precise regulatory roles of neuromodulators upon vertebrate CPG function and locomotor patterning are less clear. This is in part due to the relative inaccessibility of spinal networks and the inability to monitor properties from identified cell populations *in vivo*. Nonetheless, some progress towards elucidating the roles of neuromodulators during locomotion has been made. Spinal networks are subject to neuromodulation by a diverse range of molecules including amino acids acting via metabotropic receptors, peptides, endocannabinoids, amines and gases such as NO. These modulators influence numerous signalling pathways which have a variety of cellular effects that afford spinal networks their flexibility.

1.4.1 Gaseous neuromodulators

Gaseous molecules were first recognised as biologically relevant modulators in the late 1980s (Ignarro et al., 1987; Palmer et al., 1987). Since then, these simple molecules have been subject to intense study and NO, perhaps the most studied, is now established as an important modulator of many processes within the nervous system. Indeed, NO can modulate ongoing locomotor activity and perturbation of NO-dependent signalling has clear behavioural consequences, affecting for example nociception and aggressive behaviour in mice (Nelson et al., 1995; Tegeder et al., 2004; Schmidtko et al., 2009) and locomotor output in lamprey (Kyriakatos et al., 2009, 2011), *Xenopus* (McLean and Sillar, 2000; McLean et al., 2001; McLean and Sillar, 2002, 2004), zebrafish (Bradley et al., 2010) and mice (Foster et al., 2014). The effects of NO on locomotor networks are varied, but tend to have primarily inhibitory roles at embryonic and larval stages, particularly in *Xenopus* (McLean and Sillar, 2000, 2002). In the *Xenopus* tadpole, NO can strongly decrease the frequency and duration of swim episodes by facilitation of glycinergic and GABAergic synapses which provide inhibitory input to spinal networks (McLean and Sillar, 2002). In postnatal mice, NO can also slow the frequency of locomotor output (Foster et al., 2014). Thus, NO appears to be a key modulator of ongoing locomotor activity in many vertebrates.

However, while the acute effects of perturbing NO-dependent signalling upon locomotor output have been examined, the contribution of NO as a modulator of locomotor network development and the consequent effects on output have not been examined in great detail. Therefore, in this thesis, I have begun to examine the modulatory actions of developmentally perturbing NO-dependent signalling in spinal networks.

1.4.2 Monoaminergic neuromodulators

Monoamines are important neurotransmitters which play key roles in numerous cognitive processes and motor functions. DA is one such monoaminergic neuromodulator. In zebrafish, the role of DA as a modulator of motor patterns has not been fully resolved nor have the effects of DA upon CPG components been examined. Nonetheless, this monoamine does appear to be an important modulator of motor output since bath application of pharmacological reagents which act as agonists or antagonists for DA receptors, can have complex effects upon locomotor activity in freely swimming larvae (Boehmler et al., 2007; Thirumalai and Cline, 2008; Irons et al., 2013; Tran et al., 2014). Chemogenetic ablation of *otpb* cells, which include descending DAergic neurons that innervate the spinal cord, can halt developmentally-associated changes in locomotor activity patterns (Lambert et al., 2012). In a similar fashion, blockade of dopamine receptors can reconfigure the output from spinal networks from mature to immature modes of locomotor output (Lambert et al., 2012). In mammals, the role of DA is similarly uncertain. In spinalised mice preparations locomotor activity can be induced by application of DA or DA receptor agonists (Lapointe et al., 2009; Sharples et al., 2015). In rat preparations locomotor-like activity can be observed following DA (Kiehn and Kjaerulff, 1996; Barrière et al., 2004) or L-3,4-dihydroxyphenylalanine (L-DOPA) (a precursor to DA) (McCrea et al., 1997) application but relative to normal locomotor output, the regularity of this activity is markedly reduced (Kiehn and Kjaerulff, 1996). In contrast, DA and DA receptor agonists fail to induce locomotor activity in spinalised cats (Barbeau and Rossignol, 1991), but do appear to modulate ongoing locomotor patterns. The role of DA in modulating ongoing output appears to

be conserved amongst other species. In both the rat and mouse for example, DA can modulate ongoing locomotor activity in isolated spinal cord preparations (Maitra et al., 1993; Seth et al., 1993; Kiehn and Kjaerulff, 1996; Barrière et al., 2004; Lapointe et al., 2009; Sharples et al., 2015). The primary source of DA arises from a population of dopaminergic (DAergic) cells located in the forebrain. Despite a clear modulatory role for DA, little is understood about the electrophysiological and functional properties of this class of DAergic cells. In this thesis, I have attempted to address this issue by examining the functional properties of these DAergic cells within an *in vivo* zebrafish preparation.

Reminiscent of the descending dopaminergic pathway, serotonergic neurons within the zebrafish emerge between 1 – 2 days post fertilisation (dpf) (McLean and Fetcho, 2004a) and by 4 dpf, a stage characterised by robust swimming (see subsection 1.6.4), serotonergic axons project down the entire rostrocaudal extent of the spinal cord (McLean and Fetcho, 2004b) suggesting a causal role for these cells in locomotor network maturation. However, in contrast to DA, perturbing serotonergic signalling at this age in zebrafish does not revert locomotor networks to immature modes of swimming. Rather, disruption of serotonin levels at 4 dpf (Brustein et al., 2003; Brustein and Drapeau, 2005) or adult stages (Gabriel et al., 2009) alters output in both fictive locomotor episodes and freely behaving zebrafish. At larval stages, exogenous increases in serotonin levels increase the incidence of fictive swim episodes (Brustein et al., 2003) whilst at adult stages, serotonin has the opposite effect, reducing the frequency of fictive episodes (Gabriel et al., 2009). In adults, these effects may arise because the mid-cycle inhibitory post synaptic current (IPSC) frequency and amplitude increase (Gabriel et al., 2009). Thus, in zebrafish, serotonin has less marked

effects on the structure of swim episodes but rather, acts to modulate levels of output in an age dependent manner. In *Xenopus*, the serotonergic inputs to the spinal cord appear to contribute to both the maturation and output of spinal networks. Here, both the anatomical and functional characteristics of the serotonergic system have been well characterised (Sillar et al., 1995; McDearmid et al., 1997; Rauscent et al., 2009). Serotonergic cells begin to project toward spinal networks by stage 28 (\approx 1 dpf), a time coincident with changes in motor pattern from immature to more mature modes of swimming (van Mier et al., 1986). Neurotoxic ablation of the serotonergic cells before they extend into the spinal cord can prevent maturation from embryonic to post-embryonic modes of locomotor output (Sillar et al., 1995). Additionally, in contrast to adult stage zebrafish where serotonin increases mid-cycle IPSP amplitude, in the embryonic and larval stage *Xenopus*, serotonin acts to reduce mid-cycle IPSP amplitude (McDearmid et al., 1997).

1.5 Developmental roles of neuromodulators

Neuromodulatory molecules can also regulate maturation and configuration of the developing nervous system. In addition to its neuromodulatory roles during locomotor activity, the NO-dependent pathway has also been implicated in many neurodevelopmental processes. One of the earliest steps during development of the nervous system is the formation of heterogeneous classes of neurons from populations of progenitor cells located throughout the developing CNS (Satou et al., 2012; März et al., 2010). Nitric oxide synthase (NOS), the enzyme which catalyses the production of NO, is distributed throughout the nervous system (Holmqvist et al., 2004; Romero-Grimaldi et al., 2008;

Cheng et al., 2003; Matarredona et al., 2004). Perturbation of NO signalling during periods of NOS expression can have significant effects upon proliferation and differentiation of progenitor cells (Luskin, 1993; Matarredona et al., 2004; Ciani, 2004, 2006). Following differentiation, neurons extend dendritic and axonal projections to target sites and NO may influence this process. For example, dendritic growth of developing chick motoneurons (Xiong et al., 2007) and cultured rat hippocampal interneurons (Shelly et al., 2010) is retarded by exogenous NOS inhibition, while axonal outgrowth is promoted (Zhao et al., 2009; Shelly et al., 2010). In contrast, in the developing zebrafish, NO tends to have inhibitory effects upon axonal outgrowth of developing motoneurons (Bradley et al., 2010). Whilst disruption of NO signalling has clear anatomical consequences to zebrafish motoneuron axon outgrowth, the physiological and functional effects of development perturbation of NO-dependent signalling has not been examined. Within this thesis, I have addressed this issue by examining the effects of perturbing NO signalling at the level of the neuromuscular junction (NMJ), the specialised connection between motoneurons and muscle fibres.

In the larval zebrafish, dopaminergic inputs extend into the spinal cord coincident with marked changes in locomotor output. Recent investigations have demonstrated that DA may promote the generation of motoneurons at the expense of interneurons (Reimer et al., 2013). In this context, the effects of DA appear to be mediated by inhibition of 3'-5'-cyclic adenosine monophosphate (cAMP) production, a suppressor of the hedgehog pathway, which in turn is known to regulate motoneuron development (Hammerschmidt et al., 1996; Reimer et al., 2013). Thus, one of the principal aims of this thesis was to characterise the electrophysiological properties during development and examine when they become integrated into spinal networks.

1.6 Using zebrafish to study motor network development

The early stage zebrafish (*Danio rerio*) has several characteristics which makes them an attractive model for studying nervous system development and function. The zebrafish is a genetically tractable organism with a sequenced genome in which approximately 70% of genes have at least one human orthologue (Howe et al., 2013). Additionally, their small size ($\approx 1 - 2$ mm), external development and transparent tissue makes their nervous system uniquely accessible to imaging and *in vivo* electrophysiological approaches (Drapeau et al., 1999). Moreover, the spinal cord of the zebrafish is simpler than that of mammals (Goulding, 2009) which permits the study of electrophysiological properties from identifiable neuron classes. Finally, since the circuitry which drives basic locomotor patterning is likely conserved amongst vertebrates (Figure 1.1), understanding the mechanisms which modulate zebrafish locomotor networks may be of relevance to all vertebrates.

1.6.1 Zebrafish exhibit a range of stereotypical behaviours during development

As development proceeds from embryonic to larval stages, zebrafish transition between several stereotypical locomotor behaviours (Figure 1.3A). The earliest motor pattern, known as coiling, is characterised by spontaneous side-to-side contractions of the trunk. This is a transient behaviour which begins at 17 hours post fertilisation (hpf), reaches a peak frequency of ≈ 1 Hz by 19 hpf and subsequently declines in frequency to ≈ 0.1 Hz by 26 hpf (Saint-Amant and Drapeau, 1998). Concurrently, embryos develop a glutamate-mediated touch response at around 20 to 21 hpf (Downes and Granato,

2006) whereby persistent tactile stimuli cause a marked increase in the frequency of coiling (Saint-Amant and Drapeau, 1998). An intermediate behaviour known as double coiling emerges at 24 hpf, which is characterised by rapid contralateral contraction of the tail proceeding a single coil (Knogler et al., 2014). By 27 hpf, embryos are largely inactive. However at this time a tactile stimulus is sufficient to elicit swim-like behaviour which is characterised by slow (≈ 10 Hz) contractions of the tail and limited forward motion (Saint-Amant and Drapeau, 1998).

At approximately 2 dpf, when zebrafish begin to hatch from their chorion (a protective membrane which envelops the embryo), swimming becomes more robust and fish are able to generate sustained bouts ($\approx 3-60$ s) of high frequency ($\approx 60-100$ Hz) locomotion known as 'burst swimming' (Figure 1.3B) (Buss and Drapeau, 2001). At this age zebrafish tend to remain stationary. However, changes in illumination or application of mechanosensory stimuli are sufficient to elicit bouts of burst swimming. These swim episodes are erratic, incorporating numerous turns which lack obvious directionality (Buss and Drapeau, 2001). Additionally at this stage the mouth has yet to open and the yolk sac provides the sole source of nourishment. Thus this mode of swimming is thought to serve only as an escape behaviour.

By 4 dpf, shortly before larvae enter free feeding stages, swim episodes become more refined and larvae engage in spontaneous episodes of 'beat-glide' swimming (Figure 1.3C). This is characterised by short (≈ 200 ms) bouts of low frequency ($\approx 25-60$ Hz) tail-beats ('beat' periods) punctuated with bouts of inactivity ('glide' periods) (Buss and Drapeau, 2001) and the incorporation of 'routine' turns which are characterised by their low angular velocity (Budick and O'Malley, 2000). In addition to beat-glide swimming, larval zebrafish also begin to incorporate other behavioural

manoeuvres in response to a range of stimuli (see Fero et al. 2011; Kalueff et al. 2013 for review) such as a struggle behaviour characterised by rostrocaudal propagation of body bends (Liao and Fetcho, 2008), C-bends where the trunk contracts on one side, forming a 'C' shape, followed by forward propulsion, J-bends which reorient the larvae and are characterised by small amplitude contractions of the tail (Budick and O'Malley, 2000; Kalueff et al., 2013) or the visual motor response (VMR), where activity levels are transiently increased following a change in illumination (Emran et al., 2010; Fernandes et al., 2012).

1.6.2 Development of the locomotor network

Lateral to the medially located notochord and spinal cord, repeated chevron-shaped units extend along the anteroposterior extent of the trunk. These repeated units, known as somites, ultimately develop into muscle tissue and become innervated by motoneurons extending from the spinal cord. Within each hemisomite there are a set of motor and interneurons which can be distinguished by differences in axonal projection patterns (Bernhardt et al., 1990; Kuwada et al., 1990a,b; Hale et al., 2001; Higashijima et al., 2004a,b; Kimura et al., 2006; Satou et al., 2012). In the developing spinal cord, neurogenesis occurs in two temporally discrete waves. The first wave of development begins at 10 hpf which generates a small number of neuronal cell types (Figure 1.4A). At approximately 16 hpf a second wave of neurogenesis begins which produces several additional neuronal classes (Figure 1.4B).

At the onset of coiling, the spinal cord comprises a relatively small number of cell types which includes three (Myers et al., 1986) to five (Eisen et al., 1990; Menelaou

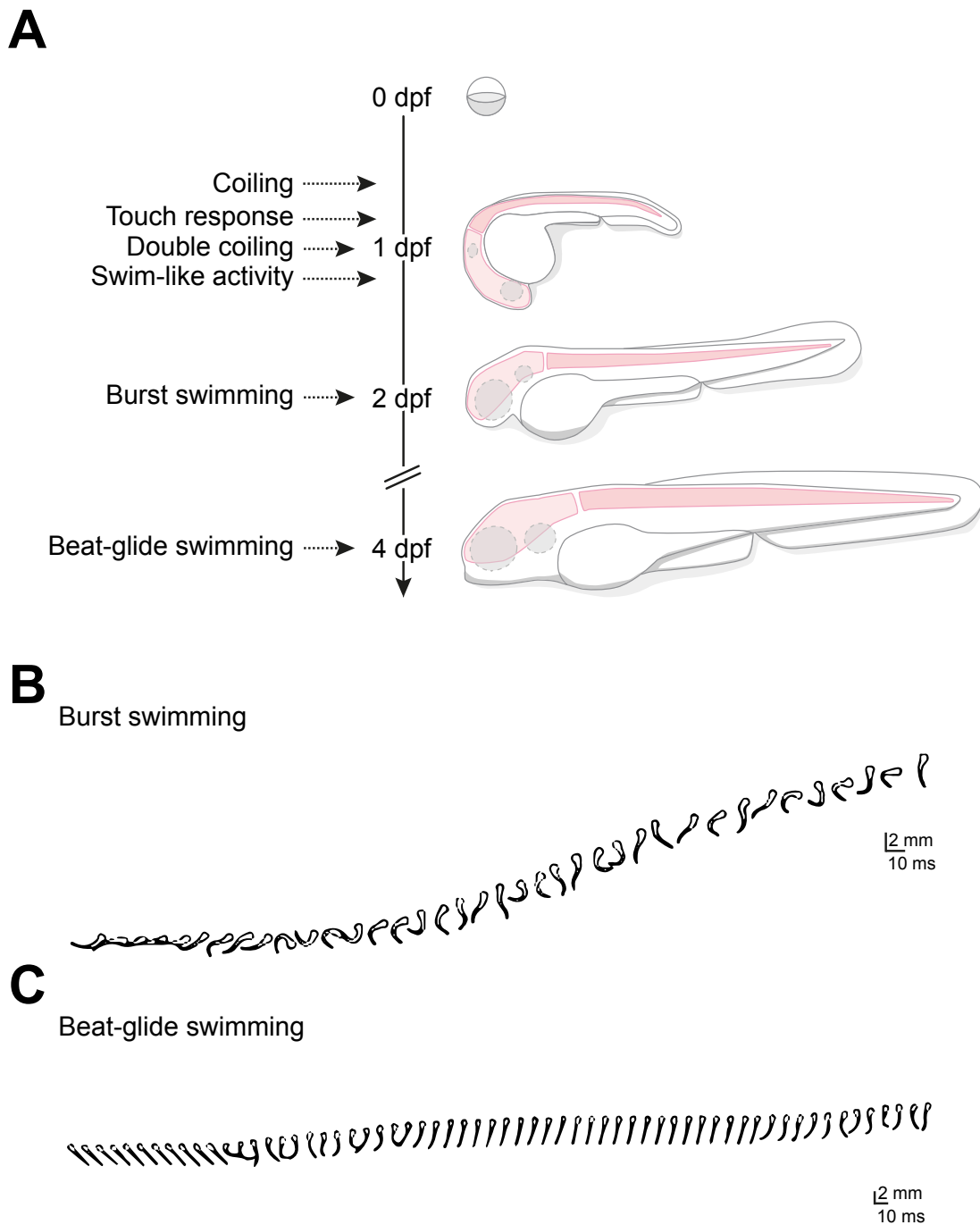


FIGURE 1.3

Stereotypical ontogeny of locomotor patterns during early zebrafish development. (A) During development, zebrafish exhibit a stereotyped sequence of behaviours. The first behaviour, coiling, appears at ≈ 17 hpf. As development proceeds, double coiling arises, followed by robust burst (2 dpf) and beat-glide (4 dpf) swimming at larval stages. During the first day of development, embryos also develop a touch response. Here, mechanosensory stimulation increases coiling frequency or at later stages elicits swim-like activity patterns. (B – C) Burst (B) and beat-glide swimming (C) episodes captured using a high speed camera. Redrawn from (Buss and Drapeau, 2001).

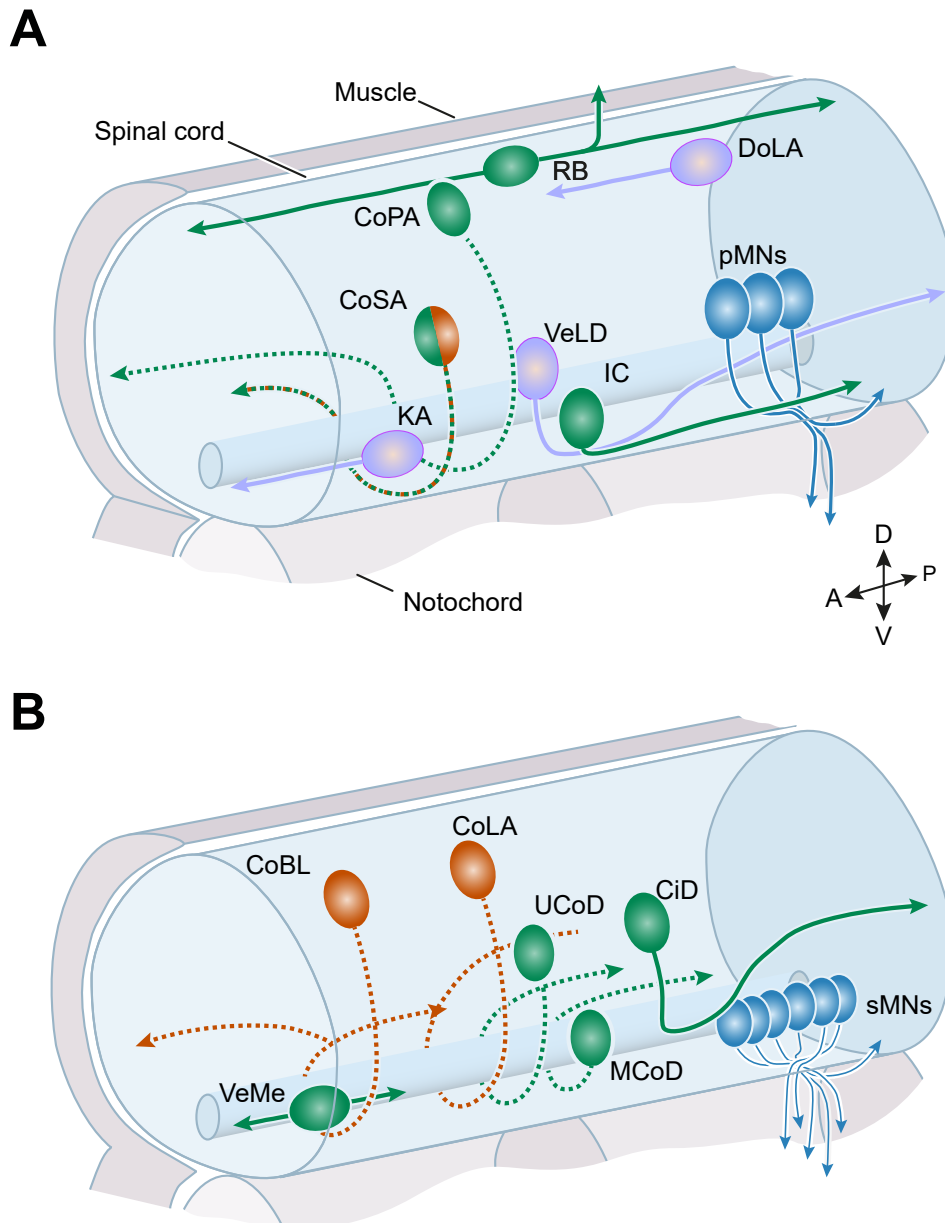


FIGURE 1.4

Schematic representation of identified cell types during development. (A – B) Cell populations identified during the first (A) and second (B) wave of neurogenesis. Solid and dashed lines represent ipsilateral and contralateral projections arising from the cell body, respectively. Colours represent the neurotransmitter phenotype: orange (glycinergic), light purple (GABAergic), green (glutamatergic), blue (cholinergic). CoSAs are a mixed population of glutamatergic and glycinergic cells (Higashijima et al., 2004a). Abbreviations: Commissural bifurcating longitudinal (CoBL), Commissural longitudinal ascending (CoLA), Commissural primary ascending (CoPA), Commissural secondary ascending (CoSA), Circumferential descending (CiD), Dorsal lateral ascending (DoLA), Ipsilateral caudal (IC), Kolmer-Agdur (KA), Multipolar commissural descending (MCoD), Rohon-Beard (RB), Primary motoneuron (pMN), Secondary motoneuron (sMN), Unipolar commissural descending (UCoD), Ventrolateral descending (VeLD), Ventral medial (VeMe).

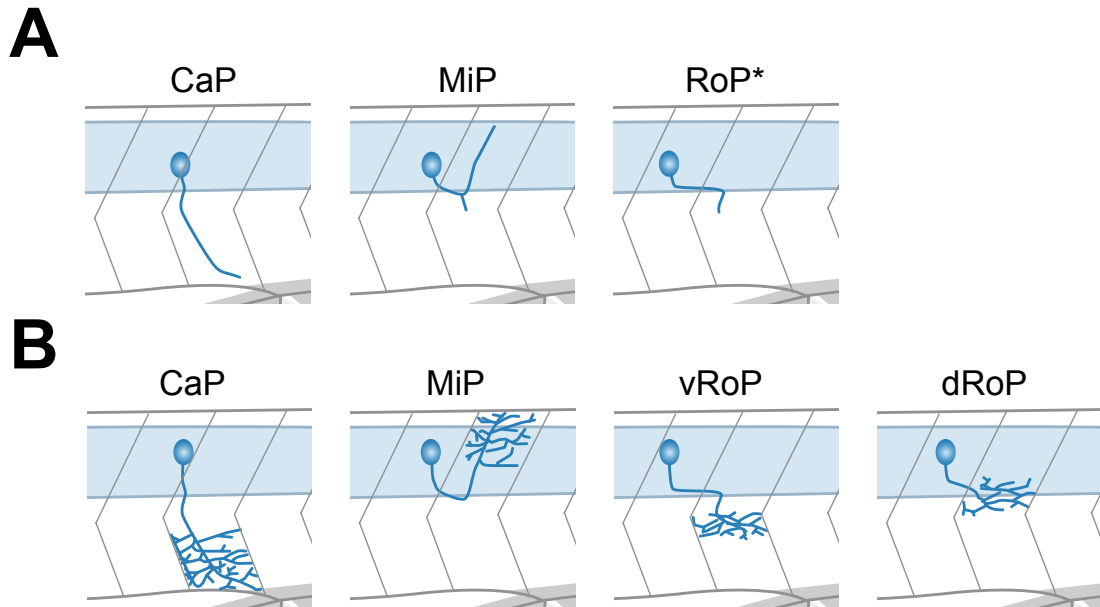


FIGURE 1.5

Schematic representation of primary motoneuron innervation patterns. (A – B) Primary motoneurons extend from the spinal cord to innervate surrounding muscle tissue. **(A)** By 1 dpf three classes of primary motoneuron have begun to extend axons toward ventral (CaP), medial (RoP) and dorsal (MiP) tissue. **(B)** By 4 dpf the primary motoneurons have innervated their stereotypical and mutually exclusive fields within the musculature. * Note that the early development of the dRoP and vRoP is currently unknown. However, the development of RoPs in general has been examined (Myers et al., 1986). Abbreviations: Caudal primary (CaP), Middle primary (MiP), Rostral primary (RoP), Dorsal rostral primary (dRoP), Ventral rostral primary (vRoP).

and McLean, 2012) classes of primary motoneurons (pMNs) and a further seven classes of INs (Bernhardt et al., 1990; Kuwada et al., 1990b; Saint-Amant and Drapeau, 2001; Park et al., 2004) (Figure 1.4A). As development progresses spinal networks begin to incorporate additional cell populations (Figure 1.4B) which presumably serve as a basis for more complex and refined motor behaviours.

The ontogeny and anatomy of these early developing cell types has been well characterised. The pMNs are amongst the earliest developing and first appear at \approx 10 hpf. They begin to exit the spinal cord shortly before the onset of coiling (Myers et al., 1986; Plazas et al., 2013) and by approximately 19 hpf, each pMN has extended axons into the somitic tissue in a stereotypical manner (Figure 1.5A) (Raamsdonk

et al., 1982; Westerfield et al., 1986; Myers et al., 1986; Plazas et al., 2013). The caudal primary (CaP) motoneuron exits the spinal cord first at ≈ 17 hpf and descends ventrally along the medial surface of the muscle tissue. The middle primary (MiP) and rostral primaries (RoPs) exit approximately an hour later but innervate the dorsal and medial tissue, respectively. A further class of motoneuron, known as the variable primary (VaP), extends an axon in approximately 50 % of somites but is subsequently eliminated by ≈ 36 hpf (Eisen et al., 1990). Thus, whilst the VaPs may contribute to coiling, they are not necessary for later modes of locomotor activity. As development progresses, the remaining four classes of pMN (CaP, MiP, vRoP, dRoP) extend axonal collaterals to innervate stereotypical domains of muscle tissue (Figure 1.5B).

At embryonic stages the INs comprise the glutamatergic Rohon-Beard (RB), GABAergic Kolmer-Agdur (KA), glutamatergic commissural primary ascending (CoPA), glutamatergic/glycinergic commissural secondary ascending (CoSA), GABAergic dorsal lateral ascending (DoLA), GABAergic ventrolateral descending (VeLD) and ipsilateral caudal (IC) cell populations (Bernhardt et al., 1990; Kuwada et al., 1990b; Saint-Amant and Drapeau, 2001). RBs, a class of mechanosensory neuron with extensive peripheral axonal projections (Metcalf et al., 1990; Reyes et al., 2004), emerge at approximately the same time as the pMNs, and by 15 hpf begin extending axons along the anteroposterior axis (Kuwada et al., 1990a). By 18–20 hpf, the DoLA, VeLD and IC cells have extended descending ipsilateral axons (Bernhardt et al., 1990; Kuwada et al., 1990b) whilst the CoPAs and CoSAs project ascending axons to the contralateral aspect of the spinal cord. The ventrally located KA cells project ascending ipsilateral axons and central canal-contacting cilia (Martin et al., 1998; Wyart et al., 2009).

As development proceeds, progressively more cell types, including motoneu-

rons and interneurons, are added to the spinal network. At ≈ 27 hpf, once the primary motoneurons have been established, approximately two dozen secondary motoneurons (sMNs) (per somite) extend from the spinal cord (Myers, 1985; Pike et al., 1992) and innervate both embryonic fast (EF) and embryonic slow (ES) muscle fibres (West-erfield et al., 1986; Pike et al., 1992; Devoto et al., 1996). Several additional interneuron classes also emerge during this second wave of neurogenesis (Bernhardt et al., 1990; Hale et al., 2001; Higashijima et al., 2004a,b; Satou et al., 2009) including: glutamatergic circumferential descending (CiD), glycinergic circumferential ascending (CiA), glycinergic commissural bifurcating longitudinal (CoBL), glutamatergic unipolar commissural descending (UCoD), glutamatergic multipolar commissural descending (MCoD), glutamatergic ventral medial (VeMe), glycinergic commissural longitudinal ascending (CoLA) and glycinergic commissural local (CoLo) cell types. CiDs, CiAs and CoBLs emerge by 22 hpf. CoBLs project commissural axons that bifurcate to project both anteriorly and posteriorly while the ipsilateral CiAs project anteriorly. CiDs project either exclusively posteriorly or bifurcate to extend axons anteriorly and posteriorly (Menelaou et al., 2014). The UCoD, MCoD and VeMe are located ventrally within the spinal cord and have contralateral descending axons. The CoLo develop by ≈ 40 hpf and project a descending commissural axon which extends $\approx 1-2$ somites (Liao and Fetcho, 2008).

1.6.3 Innervation of the developing musculature

During embryonic and larval stages there are only two types of muscle tissue, ES and EF (Raamsdonk et al., 1982). These two muscle populations are distinguishable based on their orientation and relative position within the somitic tissue; ES fibres are

superficial and run in parallel to the body axis while EF fibres are located medially and run obliquely to the anteroposterior axis (Raamsdonk et al., 1978, 1982; Buss and Drapeau, 2000). In addition to morphological differences, these muscle populations differ with respect to their functional and electrophysiological properties (Buss and Drapeau, 2000; Luna and Brehm, 2006): ES fibres are extensively electrically coupled to multiple neighbouring ES fibres and generate synaptic currents with relatively slow rise and decay kinetics. In contrast, the EF fibres exhibit less extensive electrical coupling and generate synaptic currents with relatively fast kinetics (Buss and Drapeau, 2000; Luna and Brehm, 2006).

Before the cholinergic motoneurons begin to extend into the developing muscle tissue, prepatterned acetylcholine (ACh) receptor clusters begin to form throughout the medially located EF muscle fibres (Panzer et al., 2005, 2006). As the motoneurons extend they form *en passant* synapses with the AChRs along the medial surface. Each synapse, known as a NMJ comprises a presynaptic terminal, synaptic cleft and a motor end plate. When taken to spike threshold, motoneurons release a bolus of ACh into the synaptic cleft which binds to AChRs on the muscle fibre and consequently elicits an end plate potential (EPP). These EPPs ultimately lead to muscle contraction.

1.6.4 Activity patterns of the developing locomotor network

1.6.4.1 Coiling

Coiling which is the earliest observed locomotor activity, does not require supraspinal input (Saint-Amant and Drapeau, 1998; Downes and Granato, 2006). Efforts to understand how this behaviour arises have therefore focused upon the activity patterns

of the small number of interneurons present in the embryonic spinal cord (see subsection 1.6.2). Whole-cell *in vivo* patch clamp recordings from identified spinal neurons between 20–24 hpf (Saint-Amant and Drapeau, 2001; Tong and McDearmid, 2012; Knogler and Drapeau, 2014) revealed that a small subset of cell types, namely the ICs, VeLDs, CoSAs (originally misidentified as CoPAs; see below) and pMNs are active at the onset of coiling. The electrical activity underpinning coiling persists in the presence of common ligand gated ion channel blockers (for glutamate, glycine and GABA) and botulinum neurotoxin (which inhibits neurotransmitter release) but not in the presence of heptanol, a gap junction uncoupler or following ammonia-rebound block of gap junctions (Saint-Amant and Drapeau, 2000, 2001). Thus, early stage coiling is likely to be mediated by an electrically coupled network of as few as four cell types which become rhythmically entrained.

Recently, the IC cells have emerged as likely candidates for the generation of coiling (Tong and McDearmid, 2012). These cells are restricted to the rostral region of the spinal cord, which has been identified as a region necessary for initiation of coiling (Saint-Amant and Drapeau, 1998). Moreover, unlike the VeLDs or pMNs, IC cells have pacemaker properties. These cells produce an activity pattern known as periodic depolarisations (PDs) (≈ 500 ms in duration) that propagate to muscle tissue via gap-junctions and cause ipsilateral muscle contraction (Saint-Amant and Drapeau, 2000, 2001; Tong and McDearmid, 2012). This intrinsic activity pattern is dependent upon a persistent sodium current (I_{NaP}) which slowly takes the IC cell toward spike threshold (Tong and McDearmid, 2012). Shortly after the emergence of coiling, synaptic bursts (SBs) are observed within spinal networks. In contrast to PDs which are propagated by gap junctions, SBs arise from developing contralateral synaptic inputs (Saint-Amant

and Drapeau, 2000). SBs are driven by chloride-mediated glycinergic inputs and as development continues, these synapses are thought to contribute to midcycle inhibition of the contralateral side during locomotion (Grillner and Matsushima, 1991; Saint-Amant and Drapeau, 2000).

The precise role of VeLDs during the period when coiling is observed has yet to be fully resolved. Despite being integrated into the early spinal network (Saint-Amant and Drapeau, 2001), how they contribute to coiling is unclear. However, selective inhibition of VeLDs and MNs between 18 and 19 hpf is sufficient to delay or inhibit the normal levels of correlated activity between active cell types at this age (Warp et al., 2012). Thus, VeLDs may be necessary for the transition from unpatterned network activity to rhythmic coiling-like activity. However the mechanisms underpinning this transition require further investigation.

It was originally thought that CoPAs were glycinergic and gave rise to SBs (Saint-Amant and Drapeau, 2001). However, as this cell population was later identified as glutamatergic (Higashijima et al., 2004b), this is unlikely to be the case. More recent work from the Drapeau group suggests that CoPAs were simply misidentified as CoSAs in their earlier work since both cell types have similar morphological characteristics before 24 hpf (Knogler and Drapeau, 2014). Nonetheless, by 21 hpf, effective contralateral alternation in activity patterns is seen within the spinal cord (Warp et al., 2012), which presumably arises from reciprocal inhibition by a class of commissural inhibitory interneurons. In addition to the CoPAs, CoSAs are amongst the earliest developing ($\approx 19-22$ hpf) commissurally projecting neurons in the spinal cord, and at least a proportion of these cells are glycinergic (Higashijima et al., 2004a). Thus, if functionally mature, CoSAs may contribute to the reciprocal inhibition of the contralat-

eral spinal networks. Indeed, by 5 dpf, CoSAs show robust activity patterns during a range of locomotor patterns suggesting they play an integral role in shaping locomotor output (Liao and Fetcho, 2008).

1.6.4.2 Touch response

Whilst CoPAs may not be necessary for coiling, they have been implicated in mediating the touch response which develops at ≈ 21 hpf. In *Xenopus* the excitatory dorsolateral commissural interneurons (dlcs), which are homologous to CoPAs (Higashijima et al., 2004b; Goulding, 2009), are necessary for excitation of contralateral spinal circuits in response to mechanosensory inputs (Roberts and Sillar, 1990). CoPAs appear to play a similar role within zebrafish by ≈ 24 hpf whereby sensory input from RBs is transmitted to CoPAs which subsequently initiate contralateral spinal network activity (Saint-Amant, 2006; Pietri et al., 2009; Easley-Neal et al., 2013; Knogler and Drapeau, 2014).

1.6.4.3 Double coiling

Double coiling is dependent on existing gap-junction mediated circuits and the introduction of new glutamatergic inputs (Knogler et al., 2014). First seen at 23–24 hpf, double coiling, characterised by two rapid contralateral contractions of the trunk, progressively increases in frequency such that by 28 hpf double coils are observed in more than 60 % of all motor episodes. Despite arising at approximately the same time as the touch response, mechanosensation is not necessary for double coiling as this behaviour is unaffected in a mutant line with defective sensory pathways (Knogler et al., 2014). Instead, such activity patterns arise from the integration of further cell types into the

spinal network and contemporaneous supraspinal innervation. Indeed by 24 hpf the spinal cord has the necessary circuitry to produce double coils (as seen in spinalised preparations exposed to high K^+ extracellular saline) but requires supraspinal glutamatergic inputs to initiate this behaviour (Knogler et al., 2014).

Double coiling has been linked to the functional maturation of a population of glutamatergic interneurons known as the CiDs. The CiDs have ipsilateral axons which project caudally at 1 dpf (Bernhardt et al., 1990; Knogler et al., 2014). Between 24 and 27 hpf, CiDs have extended axons caudally and the intrinsic properties of these cells have matured, such that they begin to fire multiple action potentials in response to current injection. By 27 hpf, these cells form monosynaptic connections with caudal CiDs and pMNs. Interestingly, at this age, pharmacological block of glutamatergic and glycinergic inputs has unique effects on locomotor output. Loss of glutamatergic signalling significantly reduces double coiling while block of glycinergic transmission causes a transformation from double to triple or quadruple coils (Knogler et al., 2014). Thus, CiDs may be necessary for the generation of glutamatergic-dependent ipsilateral contractions and entrainment of more caudal spinal regions during double coiling, while early developing commissural glycinergic inputs contribute to limiting contralateral activation of CPG networks.

1.6.4.4 Swimming

From 28 hpf onward, zebrafish begin to produce more swim-like behaviours and by 2 dpf can maintain sustained bouts of burst swimming (see subsection 1.6.1 and Figure 1.3B). As larvae enter their free feeding stage, swim episodes become more refined (Figure 1.3C) and begin to incorporate a range of manoeuvres in response to a variety

of stimuli (Fero et al., 2011). These include behaviours such as capture swims, which are characterised by a stereotypical series of contractions of the tail in order to reorientate toward prey followed by an increase in velocity close to the prey item (Borla et al., 2002).

By 2 dpf, glutamatergic and glycinergic synapses have formed between neurons in the spinal cord. In contrast to coiling stages where synaptic blockers do not impinge on the basic electrical activity underpinning coiling, the chemical synapses formed by 2 dpf are necessary for proper locomotor output. At this age, block of glutamatergic receptors is sufficient to abolish swimming, and inhibition of glycinergic inputs disrupts alternation between both halves of the spinal cord (Buss and Drapeau, 2001). As is the case in other vertebrates, commissural glycinergic inputs are likely necessary for left-right alternation of swimming. Indeed, impaired glycinergic signalling causes changes in spinal network activity resulting in simultaneous innervation of contralateral muscle fibres (Buss and Drapeau, 2001; Hirata et al., 2005; McDearmid et al., 2006). In freely behaving larvae, disrupted glycinergic signalling causes a shortening of body length, which may arise due to simultaneous contraction of contralateral muscle groups (Granato et al., 1996). Specific classes of commissural inhibitory interneurons (CoSA, CoBL, CoLo) have also been implicated in the control of different behaviours by 3 dpf. During examination of fictive locomotor output Liao and Fetcho (2008) observed three fictive behaviours: escape, swimming and struggling which could be characterised by their unique motor patterns. Escape responses were characterised by a single, brief short latency burst of motor activity in response to an electrical stimulus. Swimming was characterised by rhythmic bursts of motor output which progressed from head to tail. Struggling responses travelled in the opposite

direction, progressing from the tail to the head. Paired recordings between the ventral roots and the commissural inhibitory interneurons revealed CoSAs and CoBLs were active during all three behaviours, while CoLAs and CoLoS were only recruited during struggles and escape responses, respectively. Thus, commissural glycinergic inputs play an integral role in proper locomotor patterning.

By 5 dpf, CiDs have extensive ipsilateral axonal projections in both the rostral and caudal direction (Kimura et al., 2006; Menelaou et al., 2014). In other vertebrate systems, ipsilateral excitatory interneurons provide the excitatory on-cycle drive during swimming. In the zebrafish, CiDs appear to fulfil a similar role. Paired recordings of CiDs and MNs or ventral roots revealed that all cells show rhythmic membrane oscillations, and the majority fire action potentials during fictive locomotor activity (Kimura et al., 2006). Moreover, these cells form electrical and glutamatergic monosynaptic connections with MNs (Kimura et al., 2006; Bhatt et al., 2007). More detailed *in vivo* electrophysiological investigations revealed a nuanced role for different interneuron and motoneuron populations during swimming (McLean et al., 2007, 2008). During initial investigations McLean et al. (2007) noticed dorsal MNs do not fire at slow swim frequencies. Further investigation revealed a linear relationship between the position of MNs along the dorsoventral axis and the swim frequency at which the MNs were recruited. Specifically, at low swim frequencies, ventral MNs are active, and the dorsal MNs inactive. As swim frequency increases, the more dorsal MNs get recruited while the ventral MNs are inactive. Similar patterns of recruitment also extend to the ipsilateral excitatory CiDs and the commissural excitatory MCoDs. The dorsally located CiDs are preferentially recruited during swim episodes where frequencies are above approximately 30 Hz while ventrally located MCoDs are active at frequencies below

30 Hz. The opposite pattern of recruitment occurs within two classes of inhibitory interneurons. At low frequencies (below 30 Hz) the dorsal CoBLs are active while at higher frequencies the ventral CiAs are recruited (McLean et al., 2007).

1.7 Aims and objectives

The overarching aim of this thesis was to delineate the roles of two neuromodulators, NO and DA, during development and locomotor activity. The effects of NO upon the development of NMJs have been examined in the larval zebrafish. Furthermore, the first steps toward identifying the consequences of chronic NO-perturbation to developing spinal networks has been examined (Chapter 3).

Additionally, since little is known about the functional roles of DAergic inputs to spinal networks, the firing characteristics and functional properties of a population of cells which provide DAergic inputs to spinal networks within an *in vivo* zebrafish preparation have been characterised during development (Chapter 4) and their modulatory roles during locomotor output delineated (Chapter 5).

1.8 Publications

Parts of this thesis have formed the basis of the following publications. Findings that have contributed to each paper are listed underneath the respective publication and novel unpublished findings are highlighted at the bottom of this section.

- Jay, M., Bradley, S., and McDermid, J.R. (2014). Effects of nitric oxide on neuromuscular properties of developing zebrafish embryos. *PloS one*, 9(1):e86930:
 - Figure 3.3, Figure 3.4, Figure 3.5, Figure 3.6, Figure 3.7, Figure 3.8, Figure 3.9, Figure 3.10, Figure 3.11, Figure 3.12, Figure 3.13, Figure 3.14.
- Jay, M., De Faveri, F., and McDermid, J.R. (2015). Firing Dynamics and Modulatory Actions of Supraspinal Dopaminergic Neurons during Zebrafish Locomotor Behavior. *Current Biology*, 25(4):435–444:
 - Figure 4.7, Figure 4.8, Figure 4.9, Figure 4.10, Figure 4.11, Figure 4.19, Figure 4.21, Figure 4.22, Figure 4.23, Figure 5.4, Figure 5.5, Figure 5.8, Figure 5.9, Figure 5.10, Figure 5.11, Figure 5.12, Figure 5.13, Figure 5.14, Figure 5.15, Figure 5.16, Figure 5.17, Figure 5.18, Figure 5.19.
- The following data represent novel findings which may contribute to future publications:
 - Figure 3.15, Figure 3.16, Figure 4.6, Figure 4.10, Figure 4.12, Figure 4.13, Figure 4.14, Figure 4.15, Figure 4.16, Figure 4.17, Figure 4.18, Figure 4.19, Figure 4.20, Figure 4.24, Figure 4.25, Figure 4.26, Figure 4.27, Figure 4.28, Figure 5.1, Figure 5.3, Figure 5.6, Figure 5.7.

Methods

2.1 Zebrafish care

Adult zebrafish (*Danio rerio*) were maintained in accordance with established procedures (Westerfield, 2000) and in compliance with the Animals (Scientific Procedures) Act 1986. Wild-type, *ETvmat2:GFP* (Wen et al., 2008) and *HB9:GFP* (Flanagan-Steet et al., 2005) adult fish were inbred to obtain embryos as required. Upon fertilisation, eggs were harvested and incubated in embryo medium (1.5 ml of stock salts in 1 l of dH₂O) at 28.5 °C on a 14:10 hour light:dark cycle until reaching the required developmental stage. All experiments were conducted on coiling (17 – 30 hours post fertilisation (hpf)), burst (2 days post fertilisation (dpf)) or beat-glide swimming (4 dpf) stage zebrafish, which were staged in accordance with Kimmel et al. (1995).

2.2 Pharmacological reagents

The following pharmacological reagents were used during this study: 250–500 µM diethylenetriamine/nitric oxide adduct (DETA/NO) (Sigma), 0.5–1 mM N_ω-Nitro-L-arginine methyl ester hydrochloride (L-NAME) (Sigma), 500–750 µM 8-(4-Chlorophenylthio)-guanosine 3',5'-cyclic monophosphorothioate (8-CPT-cGMP) (Sigma), 500 µM 1H-[1,2,4]Oxadiazolo[4,3-a]quinoxalin-1-one (ODQ) (Ascent Scientific), 1 mM N-(2,6-Dimethylphenylcarbamoylmethyl) triethylammonium bromide (QX-314) (Tocris), 0.5–1 µM tetrodotoxin (TTX) (Abcam), 1 mM tetraethylammonium chloride (TEA) (Sigma), 100 µM 18-β-Glycyrrhetic acid (18-β-GA) (Sigma), 0.02 % ethyl 3-aminobenzoate methanesulfonate (MS-222) (Sigma), 2 M formamide (Sigma), 5 µM dopamine hydrochloride (DAh) (Sigma), 3–10 µM (+)-tubocurarine

hydrochloride pentahydrate (d-tubocurarine) (Sigma), 1–4 mM kynurenic acid (KYN) (Abcam), 25–50 μ M bicuculline (BIC) (Sigma), 1 μ M strychnine (Sigma) and 100–200 μ M picrotoxin (PIC) (Sigma).

2.2.1 Chronic drug application

In order to investigate the effects of chronic nitric oxide (NO) perturbation on neuromuscular junction (NMJ) development, 24 hpf embryos were bathed (DETA/NO and 8-CPT-cGMP) or injected (ODQ and L-NAME) with pharmacological reagents dependent on permeability of the drug. For injection, drugs were dissolved in Evan's extracellular saline containing 0.2 % fast green (Sigma) to the desired concentration. Injection needles, pulled from filamented borosilicate glass (0.78 mm inner diameter, 1 mm outer diameter, Harvard Apparatus, UK) using a P-80 micropipette puller (Sutter Instrument, USA), were backfilled with the drug solution which was pressure injected into the yolk sac. For bath application, embryos were incubated in egg water containing the drug dissolved to the desired concentration.

2.2.2 Fast drug application during electrophysiological investigations

In order to study the acute effects of pharmacological agents during electrophysiological investigations, a fast flow system (VC4³ Valve Commander, ALA Science) was used which permitted the rapid application of drugs.

2.3 Electrophysiological solutions

2.3.1 Extracellular solutions

Unless otherwise stated, preparations were continually perfused with Evan's extracellular saline (Table 2.1) during electrophysiological studies. During studies of behaviourally-relevant activity patterns 10 μM of the neuromuscular blocker d-tubocurarine was added to the Evan's extracellular saline, thereby preventing muscle contractions that would ordinarily preclude patch clamp recording. However, during examination of locomotor-related end plate potentials (EPPs) from embryonic fast (EF) or embryonic slow (ES) muscle fibres, a lower concentration (3 μM) of d-tubocurarine was used to partially block acetylcholine (ACh) receptors and reduce muscle contractions which permitted observation of synaptic drive to the muscle fibres.

For experiments in which miniature end plate currents (mEPCs) or miniature post synaptic currents (mPSCs) were examined, d-tubocurarine was substituted with 0.5 – 1 μM TTX which prohibited evoked synaptic release by block of voltage gated Na^+ channels and unmasked quantal neurotransmitter release. Additionally, when examining mPSCs, Mg^{2+} was omitted from Evan's extracellular saline in order to alleviate block of N-Methyl-D-aspartic acid (NMDA) receptors. When examining mEPC kinetics, the gap junction blocker 18- β -GA (100 μM) was included in Evan's solution to reduce currents from neighbouring muscle fibres (Luna and Brehm, 2006).

Constituent	Concentration (mM)	Supplier
NaCl	134	Fisher Scientific
KCl	2.9	Fisher Scientific
CaCl ₂	2.1	Fisher Scientific
MgCl ₂	1.2	Fisher Scientific
HEPES	10	Melford
Glucose	10	Fisher Scientific
D-tubocurarine	0.01	Fisher Scientific

TABLE 2.1
Evan's extracellular saline. pH adjusted to 7.8 with sodium hydroxide (NaOH).

2.3.2 Intracellular solutions

Various intracellular solutions (see Tables 2.2 to 2.4, page 40) were used during the course of this work (see section 2.4 for further details). Sulforhodamine B (Sigma) was routinely included in all intracellular solutions in order to facilitate visualisation of cell morphology post-recording with fluorescence microscopy. To study the projection patterns of dopaminergic diencephalospinal neurons (DDNs), neurobiotin tracer (Vector Laboratories) was instead included in the intracellular solution and preparations were subject to streptavidin histochemistry post-recording.

For perforated patch clamp recordings (see subsection 2.4.2.2), an amphotericin B stock solution was prepared on the day of recording by dissolving 1 mg of antibiotic in 1 ml of dimethyl sulfoxide (DMSO). This stock was diluted in K-gluconate intracellular solution to a final concentration of 10 $\mu\text{g ml}^{-1}$.

During investigations of synaptic drive to DDNs, interneurons (INs) or motoneurons (MNs), QX-314 and/or TEA was also included in the patch pipette solution. QX-314 blocked sodium channels and therefore prevented generation of action current.

Block of potassium channels with TEA increased the input resistance which made it easier to space clamp the cell and improved the signal to noise ratio.

2.4 Electrophysiology

2.4.1 Preparation of fish

For electrophysiological experiments, fish were removed from their chorion if required, anaesthetised in Evan's extracellular saline containing 0.02 % MS-222 and secured on their sides to a Sylgard-lined Petri dish with 25 μm diameter tungsten pins inserted through the notochord and yolk-sac (Figure 2.1A). In order to facilitate access to DDNs, one eye was removed, thereby exposing the underlying diencephalon. For recordings of spinal neurons or axial muscle fibres, the skin overlying the trunk was carefully removed with a pair of fine forceps (Dumont #5). Preparations were then transferred to the patch clamp setup and continuously perfused with Evan's extracellular saline. In order to perform whole cell recordings from EF muscle fibres or neurons within the spinal cord, further dissection of overlying tissue was necessary. Here, a broken electrode ($\approx 50\ \mu\text{m}$ diameter) was used to aspirate muscle tissue as required and expose the more medial muscle or spinal cord (Figure 2.1A).

2.4.2 Electrophysiological methods

Standard extracellular and whole cell patch clamp techniques were used to investigate the electrophysiological properties of neurons (Table 2.5, page 42; Drapeau et al. 1999; Pinault 1996; Rae et al. 1991). Electrodes (resistance = 3–10 $\text{M}\Omega$) for extracellular

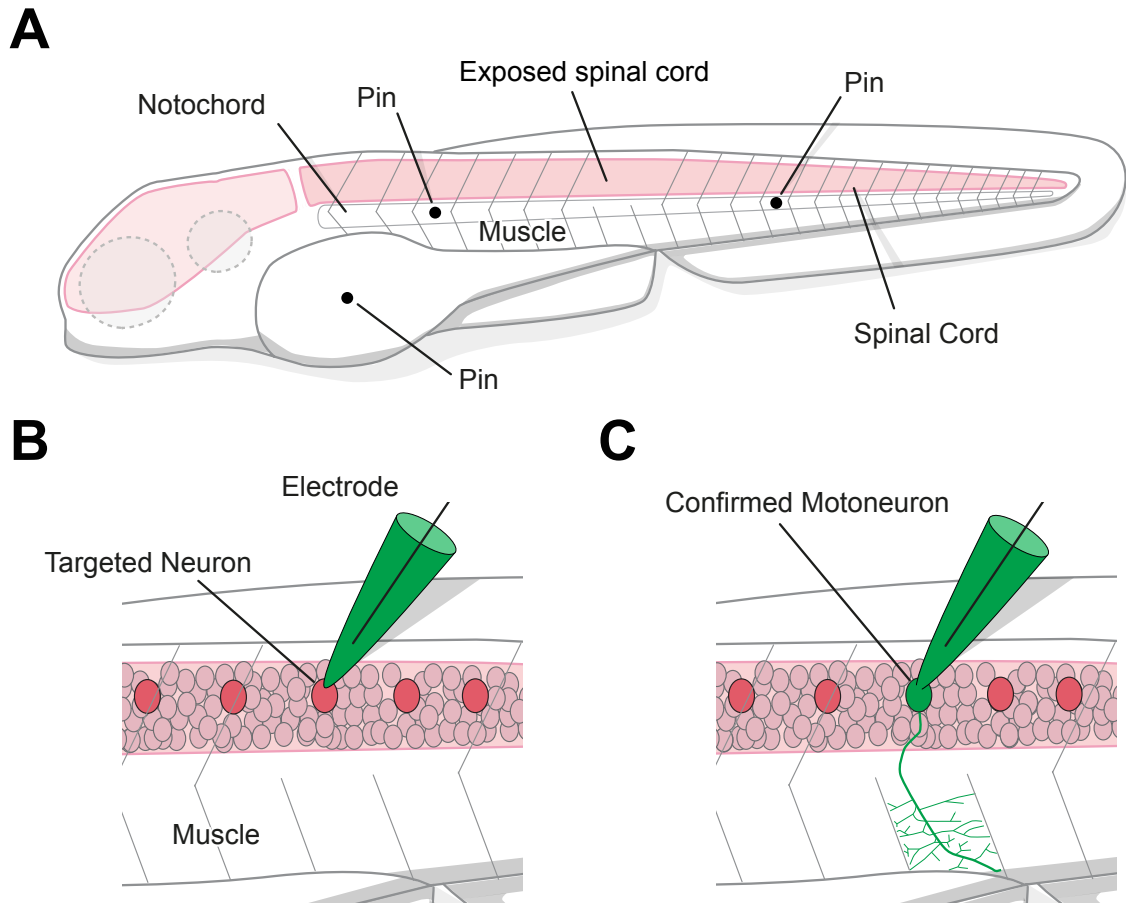


FIGURE 2.1

Standard preparation for electrophysiological investigations. (A) Larvae were secured to a Sylgard-lined dish with 25 μm tungsten pins and muscle was aspirated as necessary. (B) Specific cell types were targeted based on their stereotypical position, shape and size. (C) Dialysis with a fluorescent dye (sulforhodamine B) permitted cell morphology to be established post-recording. In this illustration, the targeted neuron was a motoneuron.

and whole cell patch clamp experiments were pulled from filamented borosilicate glass (1.5 mm outer diameter, 0.86 mm inner diameter; Harvard Apparatus, UK) using a P-80 micropipette puller (Sutter Instrument, USA). ES and EF muscle fibres could be readily distinguished from each other because ES fibres are located superficially and run in parallel along the anterior-posterior axis, while EF muscle fibres run obliquely to the anterior-posterior axis and are located medially (Raamsdonk et al., 1982). Targeted recordings from MNs and INs within the spinal cord were performed based on stereotypical dorsoventral position and soma size. Targeted recordings of DDNs in *ETv*-

Methods

Constituent	Concentration (mM)	Supplier
D-gluconic acid potassium salt	126	Sigma
NaCl	10	Fisher Scientific
MgCl ₂	2	Fisher Scientific
KCl	6	Fisher Scientific
HEPES	10	Meflord
EGTA	10	Sigma

TABLE 2.2

K-Gluconate intracellular solution. pH adjusted to 7.2 with potassium hydroxide (KOH) (Tong and McDearmid, 2012).

Constituent	Concentration (mM)	Supplier
D-gluconic acid potassium salt	125	Sigma
MgCl ₂	2.5	Fisher Scientific
HEPES	10	Melford
EGTA	10	Sigma

TABLE 2.3

Low Chloride intracellular solution. pH adjusted to 7.3 with KOH (McLean et al., 2007).

Constituent	Concentration (mM)	Supplier
CsCl	135	Fisher Scientific
MgCl ₂	2	Fisher Scientific
HEPES	10	Meflord
EGTA	10	Sigma

TABLE 2.4

Cesium Chloride intracellular solution. pH adjusted to 7.2 with cesium hydroxide (CsOH) (Tong and McDearmid, 2012).

mat2:GFP larvae were achieved by using the fluorescent features of the patch clamp microscope in order to visualise the fluorescently tagged somata.

2.4.2.1 Extracellular recording

In order to non-invasively measure the activity patterns of DDNs, loose patch methods were used. Electrodes were filled with Evan's extracellular saline, positioned over the cell of interest and small amounts of negative pressure were applied until a seal resistance of $\approx 15-50\text{ M}\Omega$ was obtained. A similar approach was taken in order to juxtacellularly label DDNs. However, electrodes were filled with Evan's extracellular saline containing 0.5% neurobiotin and repeated 0.5 Hz, 500 ms 1 nA depolarising current steps were applied for 30–45 min to facilitate transfer of neurobiotin into the targeted cell (Rae et al., 1991).

2.4.2.2 Whole cell and perforated patch recording

Once electrodes were filled with an appropriate intracellular solution (see subsection 2.3.2 and Table 2.5, page 42), they were secured to a CV-7B head stage (Axon Instruments). A small amount of positive pressure was then applied and maintained throughout the following steps in order to prevent the tip of the electrode becoming contaminated with debris in the bath. The electrode was subsequently lowered into the bath and manoeuvred into close proximity with the cell of interest using an MX7600 (Siskiyou) micromanipulator. Pipette offsets were then neutralised and a $\text{G}\Omega$ seal ('gigaseal') was established between the electrode tip and cell membrane. On occasion, cell membrane rupture would occur during gigaseal formation. In these instances, cells

Cell	Measured property	Configuration	Clamp	Intracellular Solution	Additional pharmacological agents	
					Intracellular	Extracellular
Muscle	mEPCs	Whole cell	V	K-gluconate (2.2)		TTX, 18- β -GA
Muscle	mEPPs	Whole cell	I	K-gluconate (2.2)		TTX
Muscle	Synaptic input	Whole cell	I	K-gluconate (2.2)		3 μ M d-tubocurarine
MN	Fictive swimming	Whole cell	I	K-gluconate (2.2)		
MN/IN	Recruitment	Whole cell	I	Low chloride (2.3)		
DDN	mPSCs	Whole cell	V	CsCl (2.4)		TTX, KYN*, PIC*
DDN	Activity patterns	Loose patch	I	Evan's (2.1)	Neurobiotin	KYN*, PIC*
DDN	Endogenous activity	Perforated Patch	I	K-gluconate (2.2)	Amphotericin B	KYN*, PIC*/BIC*
DDN	Synaptic input	Whole cell	I	K-gluconate (2.2)	QX-314	

TABLE 2.5

Intra- and extracellular solutions used to investigate a range of electrophysiological properties from muscle fibres (ES and EF), spinal MNs and INs, and DDNs. An asterisk denotes pharmacological reagents which were used in a subset of experiments. Voltage and current clamp experiments are denoted by a 'V' and 'I', respectively. Numbers in brackets refers to tables for the respective intracellular solution.

were excluded from analysis.

After achieving a gigaseal, a holding potential of ≈ -60 to -75 mV was applied to the tip of the electrode and pipette capacitive transients were neutralised using the electronic features of the amplifier. In order to achieve a whole cell configuration, brief bouts of negative pressure were applied. For perforated patch recordings, this step was omitted and electrical access to the intracellular environment would occur gradually over ≈ 10 – 30 min as amphotericin B diffused to the tip of the electrode. Successful access was assessed by increased cell capacitances and decreased access resistance.

On completion of whole cell recordings, cell identity was confirmed by visualising sulforhodamine B labelling under fluorescent light (Figure 2.1B,C). To confirm neuronal identity following perforated patch clamp recordings, the cell membrane was ruptured by application of negative pressure so that cells were dialysed with patch solution. Labelled cells were then visualised using fluorescence microscopy.

2.4.2.2.1 Muscle fibres

Recordings from muscle fibres were restricted to the ventral hemisomites adjacent to the yolk sac extension. For whole cell current and voltage-clamp recordings, electrodes were filled with a K-gluconate solution (Table 2.2). During current-clamp recordings of muscle fibres, cells were injected with a small amount of positive or negative current to maintain a membrane potential approximating -65 mV or -75 mV for ES or EF fibres, respectively. During voltage clamp recordings, all muscle fibres were clamped at -75 mV and series resistances compensated by $>70\%$. Fibres with access resistances $> 10\text{ M}\Omega$ were routinely excluded.

2.4.2.2.2 Spinal interneurons and motoneurons

In order to minimise any anteroposterior variation in recruitment patterns, all recordings within the spinal cord were restricted to somites 6–11 (median = 8) at 2 dpf and 8–13 (median = 10) at 4 dpf; approximately at the level of the yolk sac extension. During current-clamp recordings from spinal INs and MNs, K-gluconate based solutions were used. During paired recordings between DDNs and spinal neurons, where determining the temporal relationship between fictive swim episodes and DDN activity was of interest, a K-gluconate solution was used (Table 2.2). However, swim cycle frequency was difficult to resolve since glycinergic-mediated currents, which provide mid-cycle inhibition, are chloride-dependent (Lynch, 2004) and become depolarising from rest using this solution. Thus, in order to more easily resolve cycle frequency during fictive swim episodes, a lower chloride K-gluconate solution (Table 2.3) was instead utilised.

2.4.2.2.3 Dopaminergic diencephalospinal neurons

Loose patch methods were used to non-invasively characterise firing patterns of DDNs. Action potentials were readily observable as discrete extracellular potentials. To study synaptic input to DDNs, whole cell voltage clamp recordings were performed using electrodes filled with a CsCl based solution (Table 2.4) in the presence of Evan's extracellular saline containing 1 μ M TTX. By using this configuration, evoked spike activity was blocked and the reversal potential for Cl⁻ ions was strongly depolarised (reversal potential: \approx 0 mV). Therefore mPSCs could be resolved as large inward currents. Subsequent addition of 1 mM KYN or 100–200 μ M PIC (or 25–50 μ M BIC) allowed for the isolation of GABAergic and glutamatergic inputs, respectively.

To examine the contribution of different neurotransmitter systems to endogenous activity patterns, whole cell voltage-clamping was used to study synaptic drive. Here, electrodes were filled with K-gluconate solution containing 1 mM QX-314. Glutamatergic and GABAergic currents were isolated by voltage clamping at the reversal potential for chloride (≈ -45 mV) and cation-mediated ($\approx +5$ mV) currents, respectively.

Finally, extracellular recordings suggested DDNs have autonomous spike capability, however this was rarely observed using whole cell methods. Therefore, to examine the cellular basis of endogenous DDN activity patterns and obviate suspected washout, perforated patch clamp methods (Rae et al., 1991) were used to maintain cytoplasmic integrity.

2.4.2.3 Data acquisition

Recordings were amplified using a Multiclamp 700B (Molecular Devices, Sunnyvale, CA, USA) or an RK-400 (Biologic) amplifier. Data were digitised with an Axon Digidata 1440A (Molecular Devices, Sunnyvale, CA, USA) A-D converter connected to a PC running pClamp 10 (Molecular Devices) or a National Instruments A-D converter connected to a PC running WinEDR 3.2.7 and WinWCP 4.5.4. Raw signals were acquired at 10–30 kHz. During whole cell recordings, signals were low-pass filtered at 10 kHz and during extracellular loose patch recordings signals were band pass filtered between 1 and 4 kHz.

2.5 Histochemistry

Fish were anaesthetised in 0.02 % MS-222 and fixed in 4 % paraformaldehyde (PFA) (Fisher Scientific) dissolved in phosphate buffered solution (PBS) for 60 (1 dpf) - 90 (2 - 4 dpf) min at room temperature or overnight at 4 °C. Following fixation, preparations were extensively rinsed in PBS containing 0.1 % Triton-X 100 (herein referred to as phosphate buffered solution/triton-X (PBS-TX)). Next, larvae were transferred to blocking solution (composition: 3 % milk powder; 1 % DMSO; 0.1 % Triton-X 100 in PBS) containing primary antibody for 4 h or overnight at 4 °C before subsequent PBS-TX rinsing and transfer to fresh blocking solution containing secondary antibody. After a further 4 h (or overnight at 4 °C) of incubation, fish were rinsed and cleared in 60 % glycerol.

In fish that were used for juxtacellular neurobiotin labelling (see subsection 2.4.2.1), specimens were transferred to PBS-TX containing Cy3-conjugated streptavidin (1:100; Sigma) for 12–15 h after fixation and extensive rinsing with PBS. Following this incubation period, the fish were again rinsed in PBS-TX and transferred to fresh blocking solution containing anti-tyrosine hydroxylase (TH) antibody (1:100; Molecular Probes). Fish were incubated for 4 h at room temperature or overnight at 4 °C prior to wash and transfer to fresh blocking solution containing Cy5-labelled secondary antibodies (1:200, Invitrogen). After incubation for 4 h or overnight at 4 °C, fish were then rinsed with PBS-TX and cleared in glycerol.

For studies investigating NMJ distribution, after fixation and rinse with PBS, fish were incubated in PBS containing 1 mg ml⁻¹ collagenase (Sigma) for 16 min

before extensive rinsing in PBS-TX. Fish were subsequently transferred to blocking solution containing $10 \mu\text{g ml}^{-1}$ rhodamine-conjugated α -bungarotoxin (Rh- α -BTX). After 30 min, the fish were rinsed with PBS and placed in blocking solution containing anti-SV2 antibody (1:200, Developmental Studies Hybridoma Bank, University of Iowa (DSHB)). Fish were incubated for 4 h at room temperature or overnight at 4°C prior to wash and transfer to fresh blocking solution containing AlexaFluor 488 secondary antibody (1:500; Invitrogen). After incubation for 4 h or overnight at 4°C , fish were then rinsed with PBS-TX and cleared in glycerol.

In order to examine the spatial relationship between DDN axonal projections and MN cell bodies within the spinal cord, anti-TH primary antibodies were used in *HB9:GFP* larvae, where MNs express GFP (Flanagan-Steet et al., 2005). When examining the effects of DDN ablation on neuronal composition within the spinal cord, anti-HB9 primary antibodies were used with AlexaFluor 568 secondary antibodies.

Once cleared in glycerol, preparations were typically mounted laterally on microscope slides in order to effectively visualise DDN projection patterns throughout the central nervous system (CNS) or NMJs in the lateroventral musculature. However, to visualise GFP positive cells in the diencephalon of *ETvmat2:GFP* larvae, the brain was often removed post-clearing and mounted ventrally. In order to visualise projection patterns of TH-positive fibres in the mediolateral aspect of the spinal cord, surrounding muscle tissue and the notochord were carefully dissected from the spinal cord and the preparation mounted ventrally.

2.6 Image acquisition

During electrophysiological investigations, targeted neurons were routinely dialysed with the fluorescent dye sulforhodamine B (0.1 %). Using the fluorescence features of the patch clamp microscope and a Sunkwang SK-B140P/SO camera, a series of pictures were taken to characterise cell position and morphology.

For preparations subject to histochemistry, images were captured in 1 - 3 μm z-stack increments on an Olympus FluoView FV1000 confocal laser scanning microscope using the accompanying FluoView FV1000 software suite. During examination of NMJ distribution, image capture was restricted to the ventral musculature at the level of the yolk-sac extension. During investigations into the effects of DDN ablation on the composition of cells within the spinal cord, images of the spinal cord were restricted to somites \approx 12 – 15 (approximately the level of the yolk-sac extension).

2.7 Laser ablation

For laser ablation studies, 1 dpf (20 – 24 hpf for DC2 ablations; 30 - 32 hpf for DC2/4/5 ablations) *ETvmat2:GFP* embryos were embedded in 1.5 % low melting point agarose dissolved in egg water containing 0.02 % MS-222. GFP positive neurons were targeted for ablation by defining a region of interest within the FluoView FV1000 software. Cells were irradiated for 20 – 30 s with a UV (405 nm, 50 mW) or Argon (488 nm, 40 mW) laser set to 90 – 99 % power. Successful ablation was confirmed by examining GFP fluorescence \approx 2 h post-ablation and using GFP fluorescence/anti-TH immunohistochemistry in fixed fish at 4 dpf, once behavioural recordings had been completed.

2.8 Monitoring behaviour

Individual 4 dpf larvae were transferred to a darkened recording chamber that contained an overhead camera (Point Grey DragonFly 2) and an infrared light source for illumination (Figure 2.2A). Fish were allowed to acclimatise for 15 min before behaviour was recorded for a period of 10 min. Digital video (audio video interleave (AVI) format) recordings were acquired at 15 frames per second using Flycap2 software (Point Grey).

2.9 Analyses

2.9.1 Electrophysiology

All electrophysiological analyses were conducted offline using Clampfit (Molecular Devices). For analysis of mPSCs, mEPCs and EPPs, template matching functions were used to isolate populations of events. Captured events were manually examined and erroneous events (such as baseline noise) were excluded from further analysis. mEPC frequencies were determined by counting the number of events over 200 s. For analysis of locomotor EPPs, 30 EPPs from each swim episode were averaged and the mean rise time (10–90%), decay time (10–90%) and amplitude determined.

For analysis of DDN activity patterns during extra- and intracellular recordings, events were identified using threshold detection methods. DDN bursts were defined as periods of spiking lasting > 150 ms, comprised of ≥ 3 spikes that reached instantaneous frequencies > 20 Hz. During examination of spike rebound of autonomous

activity, the frequency was averaged over the 415 – 450 ms immediately after termination of current steps. In all whole cell recordings, a liquid junction potential of -10 mV (K-Gluconate or CsCl solution) or -16 mV (low chloride intracellular solution) was corrected for during analysis.

2.9.2 Image analysis

For analysis of NMJ distribution, all analysis was restricted to fish ranging between the ages of 48 and 52 hpf in order to minimise age-related variation in NMJ development. Furthermore, fish within each experimental replicate were age-matched to further reduce age-dependent variability. Images were obtained from the ventral somitic musculature adjacent to the yolk sac extension; approximately the same area from which mEPC recordings were conducted. Acquired images were de-convoluted using Huygens Essential software and then analysed using the ImageJ plugin SynaptcountJ.

2.9.3 Behaviour

Digital AVI format files were initially uncompressed and video colour depth changed to ‘Luminance only (Y8)’ as detailed in the Ctrax instructions (<http://ctrax.sourceforge.net/install.html#input-video-formats>). The videos were further processed in VirtualDub to maximise contrast between the larvae and arena (Figure 2.2B). The processed AVI files were subsequently converted to micro fly movie format (ufmf) video files using any2ufmf (<http://ctrax.sourceforge.net/any2ufmf.html>) and imported into California Institute of Technology Fly Tracker (Ctrax) (Branson et al., 2009) and subsequently

Janelia Automatic Animal Behavior Annotator (JAABA) (Kabra et al., 2013) for further analysis. Ctrax was initially used to obtain the coordinates and orientation of individual larvae over the 10 min recording (Figure 2.2B). After optimisation of settings, larvae were reliably tracked with nominal error rates (≈ 0.23 per fish per min of video). Any errors were corrected using the accompanying FixErrors Matlab graphical user interface (GUI).

Using JAABA, the Ctrax-derived data were classified into behavioural categories (Figure 2.2C). In order to identify episodes of a given behaviour, JAABA required an initial training period where example(s) of a behaviour and non-behaviour were manually labelled *e.g.* beat-glide swimming (behaviour) and not beat-glide swimming (non-behaviour). Once a behaviour was defined for a portion of the video, the machine learning algorithm was executed to classify the remainder of the video. The accuracy of the behavioural categorisation (behaviour or non-behaviour) was manually examined upon completion of the algorithm and retrained if necessary.

2.9.4 Statistics

All statistical analyses were performed in Graphpad Prism 6 or R v3.1.1. Normality and heteroscedasticity were first examined to determine appropriate statistical approaches. In order to examine statistical significance, the two tailed Student's t-test or the Mann Whitney U test was typically used for normal or non-normal data, respectively. However, for analysis of mEPC kinetics, in which datasets were unequal in size, non-normal and violated assumptions of equal variances between conditions, a modified Dunnett's test was used for pairwise comparisons, as described by Herberich et al. (2010).

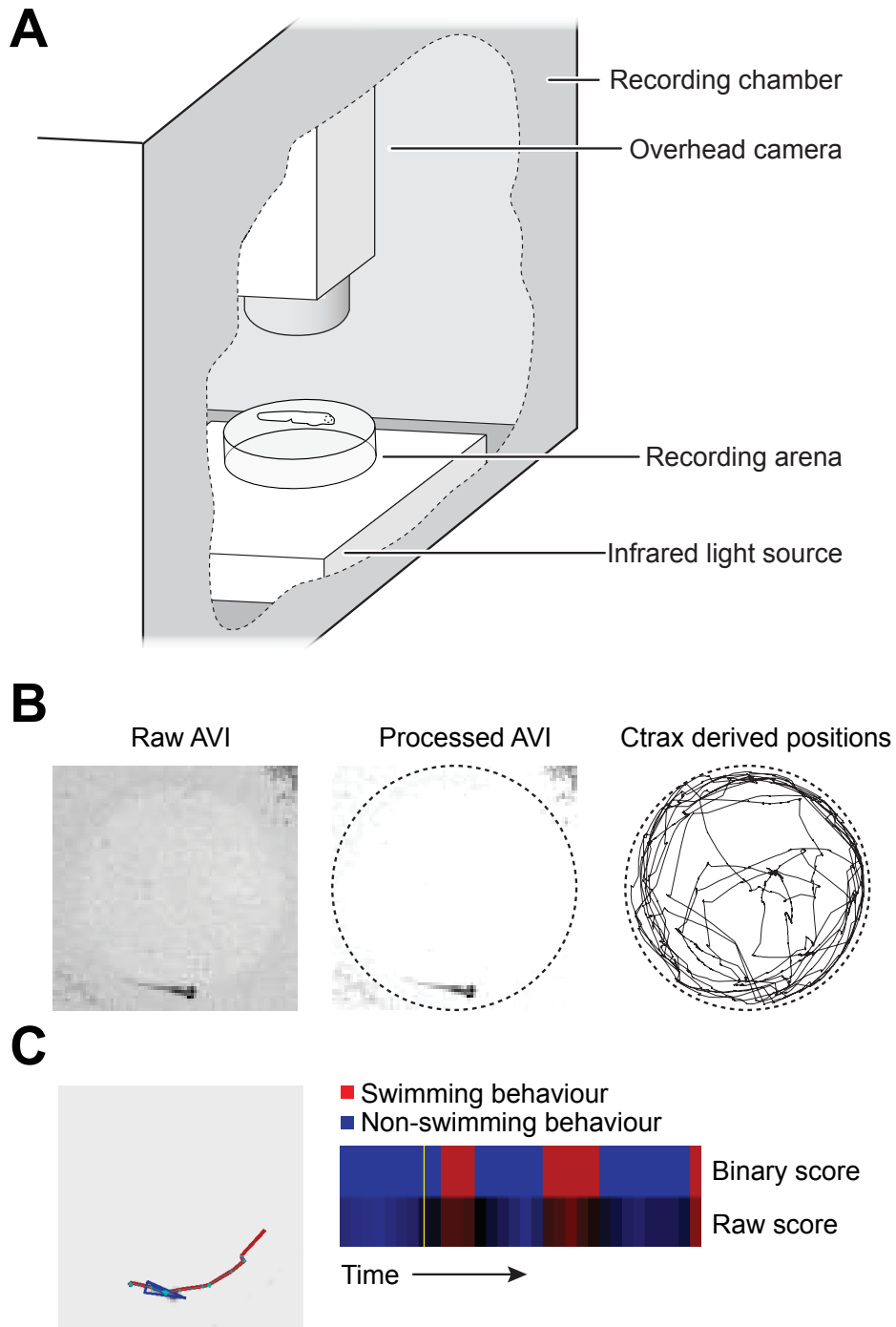


FIGURE 2.2

Equipment and analysis used to monitor behaviour. (A) Larvae were placed in a darkened recording arena on top of an infrared light source and filmed with an overhead camera. (B) Captured AVI files (left) were processed in VirtualDub (centre) (see subsection 2.9.3 for details) and opened in Ctrax to capture positional information of the larvae over time (right). (C) The Ctrax derived data was used by JAABA to categorise the videos into swimming (red) and not-swimming (blue). JAABA produced a binary and raw score. Colour saturation of the raw score indicates the confidence of the behavioural classifier.

Methods

Results within the text are presented as mean \pm standard error of the mean (SEM). Statistical significance is reported as follows: * $p < 0.05$; ** $p < 0.01$; *** $p < 0.001$. For bar charts, bars represent the mean and error bars represent the SEM. For box and whisker plots, filled circles depict raw data points, unless stated otherwise. Upper and lower hinges of the box correspond to the first and third quartiles and the whiskers extend to 1.5 x the interquartile range while the line within boxes represent median.

**Effects of Nitric Oxide on
Neuromuscular Properties of
Developing Zebrafish Embryos**

3.1 Introduction

Nitric oxide (NO) is a highly reactive free radical gas which was not considered biologically relevant until recently. Since its discovery, this simple diatomic molecule has emerged as an important modulator of a diverse range of biological processes including maintenance of vascular tone, proper immune response, locomotor network output and motor network development (Contestabile and Ciani, 2004; Bicker, 2005; Moncada and Higgs, 2006; Garthwaite, 2008; Sillar et al., 2008; Miles and Sillar, 2011; Tricoire and Vitalis, 2012; Hardingham et al., 2013). This gaseous signalling molecule has also recently emerged as a modulator of motoneuron axonal outgrowth *in vivo* (Bradley et al., 2010). While such changes are likely to have significant consequences for innervation of the surrounding musculature, these effects are not well understood. By using immunohistochemical and electrophysiological approaches, the effects of perturbing NO signalling on neuromuscular junction (NMJ) maturation have been examined within this chapter.

3.1.1 Identification of nitric oxide as a signalling molecule

Up until the late 20th century, NO was identified only as a pollutant and toxic gas. However, during the late 1970s and 1980s, three groups working independently from one another identified this molecule as an important modulator (Arnold et al., 1977; Furchgott and Zawadzki, 1980; Ignarro et al., 1987). These early investigations were originally interested in understanding the mechanisms which underpinned the effects of nitroglycerin (NG) and other nitrate-containing compounds on vasodilation of en-

endothelial tissue. NG was first described by Ascanio Sobrero in 1847 who, in addition to noting its explosive properties, also observed that small amounts of this compound was sufficient to induce a 'violent headache' (see Marsh and Marsh (2000) and Fye (1986) for reviews). By the mid 19th century, another nitrite-containing compound, amyl nitrite, was noted to induce dilation of capillaries within the frog's foot (Richardson, 1864). In 1867, small doses of amyl nitrite were prescribed to a patient suffering from angina in efforts to reduce "arterial tension" symptomatic of this condition (Brunston, 1867). This treatment quickly alleviated the patient's chest pain and soon became the *de facto* treatment for angina.

While nitrite-containing compounds had been established as vasodilators, little progress in understanding the molecular mechanisms underpinning this physiological response had been made. However several key observations during the 1970s began to address this issue. In 1977, several vasodilators were found to increase guanylyl cyclase (GC) activity (Katsuki and Murad, 1977; Katsuki et al., 1977). Based on these observations, Katsuki et al. (1977) suggested this may be caused by NO since this molecule is also known to increase GC activity (Arnold et al., 1977; Katsuki et al., 1977). Concurrent with these investigations, another group was beginning to identify the pathways which drove vasodilation in endothelial tissue (Furchgott and Zawadzki, 1980). Acetylcholine (ACh) was a known vasodilator under *in vivo* conditions, however when *in vitro* tissue preparations were exposed to ACh, vasodilation did not occur. After further investigation, Furchgott and Zawadzki (1980) discovered that vascular relaxation was dependent on endothelial cells remaining intact during tissue preparation and therefore surmised that endothelial cells released an unidentified substance, termed endothelial-derived relaxing factor (EDRF), that induced vasodilation.

The identity of EDRF remained unknown until a series of experiments conducted by Ignarro et al. (1987) and Palmer et al. (1987). First, ACh and NO induced vascular relaxation with near-identical properties; the half-life, which was inferred by the duration of vasodilation, was almost identical between ACh or NO application. Secondly, the effects of EDRF and NO upon vasodilation were inhibited by haemoglobin, a substance known to inhibit NO (Gruetter et al., 1979; Ohlstein et al., 1979). Finally, both EDRF and NO activated GC and increased cyclic guanosine monophosphate (cGMP) levels. These observations led Ignarro et al. (1987) to tentatively conclude that EDRF and NO were the same substances. At the same time, similar experiments independently confirmed EDRF and NO as the same molecule (Palmer et al., 1987).

3.1.2 Isoforms of nitric oxide synthase and the production of NO

Soon after the identity of EDRF had been established, attention turned to the substrates and enzymatic machinery which produced this gaseous molecule. By 1988, L-arginine had been identified as a putative substrate since endothelial cell tissue preparations, when bathed in this common amino acid, liberated high concentrations of NO (Palmer et al., 1988a,b; Sakuma et al., 1988). Concurrently, other researchers demonstrated that NO plays L-arginine dependent processes in both immune (Hibbs et al., 1987; Ding et al., 1988; Marletta et al., 1988) and nervous system (Garthwaite et al., 1989) functions.

It is now understood that NO is synthesised from L-arginine by nitric oxide synthase (NOS) (Bredt and Snyder, 1990). Within vertebrates there are three known isoforms: NOS1, NOS2 and NOS3. NOS1, originally referred to as neuronal NOS or

“brain NOS”, was the first to be cloned and expression patterns examined (Bredt et al., 1991a,b). This isoform, as the name suggests, is predominately found throughout the central and peripheral nervous system (Bredt et al., 1991a; Dawson et al., 1991; Snyder, 1992; Ceccatelli et al., 1994; Holmqvist et al., 2004; Rao et al., 2008; Bradley et al., 2010). However, in mammals, NOS1 is also found within skeletal muscle tissue (Marletta, 1993; Kobzik et al., 1994; Chao et al., 1996; Kapur et al., 1997; Grozdanovic and Gossrau, 1998; Ribera et al., 1998; Grozdanovic, 1999; Stamler and Meissner, 2001).

NOS2 expression is upregulated by immune system stimulation (Marletta, 1993). While some tissues, such as the uterus of rabbits (Sladek et al., 1993) and airways of humans (Nathan and Xie, 1994) have been reported to express NOS2 under physiological conditions, NOS2 is typically not constitutively expressed. Rather it is upregulated in response to a diverse range of physiological stressors which include microbial lipopolysaccharides (LPSs) (Nathan, 1992), cytokines (Schwentker et al., 2002), UV light (Warren, 1994), ozone (Pendino et al., 1993) and physical trauma (Hansson et al., 1994). In contrast to NOS1 and NOS3, NOS2 activity is not dependent on an influx of extracellular Ca^{2+} , but instead is activated by basal levels of intracellular calcium. As a consequence, when NOS2 is present, it will continuously produce NO. Nonetheless, NOS2 activity may be modulated by other mechanisms. For example, NOS2 mRNA and protein levels can be increased by several cytokines (Kinugawa et al., 1997; Pautz et al., 2010; Schmidt and Rathjen, 2010). Once produced, NOS2 protein can be degraded by other cytokines such as transforming growth factor β (TGF- β) in order to modulate NOS2 activity and reduce NO production (Vodovotz et al., 1993).

NOS3 expression appears to be restricted primarily to endothelial cells (Giaid

and Saleh, 1995; Xue et al., 1996; Wu, 2002). There have been claims that this isoform is also present within neuronal populations (Dinerman et al., 1994; O'Dell et al., 1994; Doyle and Slater, 1997) however later studies failed to detect NOS3 within neurons but rather found this isoform localised to blood vessels within the brain (Töpel et al., 1998; Blackshaw et al., 2003). Despite this, NOS3 may still serve neuromodulatory roles given the widespread vascularisation of the brain. Indeed, NO produced from NOS3 has been shown to depolarise axons of the optic nerve (Garthwaite et al., 2006), and NOS3-knockout mice suffer from disrupted synaptic plasticity in the hippocampus, cerebral cortex and striatum (Son et al., 1996; Wilson et al., 1999; Haul et al., 1999; Doreulee et al., 2003). Furthermore, knockout of NOS1 is insufficient to disrupt long-term potentiation (LTP) in hippocampal slices but double knockout of NOS1 and NOS3 can significantly impair LTP (Son et al., 1996).

3.1.3 Structural and functional characteristics of NOS isoforms

All three isoforms of NOS have common structural features. Each isoform exists as an homodimer where each monomer is comprised of an N-terminal oxygenase domain containing binding sites for haem, tetrahydrobiopterin (BH₄) and L-arginine. This is linked to a C-terminal reductase domain that contains binding sites for flavin adenine dinucleotide (FAD), flavin mononucleotide (FMN) and nicotinamide adenine dinucleotide phosphate (NADPH) (Alderton et al., 2001). Additionally, a calmodulin (CaM)-recognition site is located between the two terminals (Alderton et al., 2001).

In order for NOS to catalyse the reaction of L-arginine to NO, CaM must first bind to NOS (Spratt et al., 2006). Binding of CaM is dependent on intracellular Ca²⁺

which exposes hydrophobic sites on CaM that accommodates subsequent binding of CaM to NOS. In tissues where NOS1 and NOS3 are constitutively expressed, relatively high levels of Ca^{2+} (200 – 300 nM) are necessary to induce the conformational changes which permit the production of NO. Functionally, this is important since calcium entry into the intracellular environment as a consequence of presynaptic activity will increase levels of NO (Garthwaite, 1991, 2008). In contrast, NOS2 is active at basal levels of intracellular Ca^{2+} (< 100 nM) and therefore activity of this isoform is generally considered to be a ‘calcium-independent’ process (Balligand et al., 1994; Piazza et al., 2015). This difference in Ca^{2+} sensitivity arises because of the presence (NOS1 and NOS3) or absence (NOS2) of an auto-inhibitory loop insert in the FMN domain (Salerno et al., 1997). This insert acts to destabilise binding of CaM at low Ca^{2+} concentrations.

Finally, production of NO by all three isoforms of NOS is also dependent upon the presence of several other cofactors: BH_4 , FAD, FMN and NADPH. These either promote or stabilise the dimerisation of NOS which permits subsequent catalysis of L-arginine to NO (Ghosh, 2003; Stuehr, 2004).

3.1.4 NOS1 expression within the developing nervous system

3.1.4.1 Mammalian System

There have been several detailed studies which provide insight into the general expression patterns of NOS1 throughout the developing mammalian nervous system. During early embryonic stages (E15 – E20), NOS1-positive cells have been identified in a diverse range of brain regions including the hypothalamus (Terada et al., 1996, 2001), striatum (Samama et al., 1995), inferior colliculus (Iwase et al., 1998) and sub-

pallium (Guirado et al., 2003). During postnatal stages, NOS1 expression is observed throughout the cortex and becomes more widespread within the striatum (Giuli et al., 1994; Iwase et al., 1998; Samama et al., 1995). By postnatal day 14 (P14), most nitrergic cell populations within the brain have been established and expression of NOS1 continues through to adult stages (Dun et al., 1992; Giuli et al., 1994; Terada et al., 2001; Sardella et al., 2011).

Within the spinal cord, nitrergic cells are distributed throughout the ventral horn (Huber et al., 1995; Wetts et al., 1995; Brüning and Mayer, 1996). A further population of cells transiently express NOS1 from E15 onward until after birth (Wetts et al., 1995). By P1, nitrergic cells are distributed throughout lamina VII – VIII (with sparse labelling within laminae IX) of the lumbar spinal cord (Foster et al., 2014). At this age, nitrergic cells are non-uniformly expressed down the rostrocaudal extent of the spinal cord such that more nitrergic cells are concentrated toward the rostral segments (Foster et al., 2014). Shortly thereafter, nitrergic cells are found in the dorsal horn (laminae III – VII) (Takemura et al., 1996; Wetts et al., 1995; Foster et al., 2014) and the number of cells increases as development proceeds. This distribution persists through into adult stages with additional expression in laminae X, bordering the central canal (Spike et al., 1993; Saito et al., 1994).

3.1.4.2 *Xenopus*

In the *Xenopus* embryo nitrergic cells develop prior to hatching (stage 29 – 30) with the first observed population restricted to the caudal hindbrain (McLean and Sillar, 2001). The number of nitrergic cells in this region continues to increase and by stage 33 – 34 three discrete clusters are present, which persist through to adulthood (McLean

and Sillar, 2000, 2001). By free swimming stages (stage 43), the three nitrenergic clusters proliferate in number and extend along the anterioposterior axis. By stage 44–46, nitrenergic cells are found within the developing telencephalon, midbrain and several sensory systems (McLean and Sillar, 2001; López and González, 2002). By stage 47, a small number of labelled cells are observable in the rostral spinal cord. As larvae enter metamorphosis, NOS expression transiently increases in the spinal cord as the forelimbs begin to emerge but decreases shortly thereafter (Ramanathan et al., 2006).

3.1.4.3 Zebrafish

Several studies have elucidated the ontogeny of the nitrenergic system in the developing zebrafish (Poon, 2003; Holmqvist et al., 2004; Bradley et al., 2010). NOS1 is first observed in the developing forebrain at \approx 16 hours post fertilisation (hpf) (Figure 3.1A) (Poon, 2003; Holmqvist et al., 2004). As the nervous system matures, nitrenergic cell clusters are found distributed throughout the forebrain (Poon, 2003; Holmqvist et al., 2004) and by 35 hpf, are accompanied by a further nitrenergic cluster within the midbrain and hindbrain (Holmqvist et al., 2004). As development continues, progressively more nitrenergic cell populations emerge such that NOS is expressed within fore-, mid- and hindbrain regions (Poon, 2003; Holmqvist et al., 2004; Bradley et al., 2010). At adult stages, NOS positive cells are expressed within the hypothalamus and telencephalon (Holmqvist et al., 2000, 2007).

NOS1 expression is also observed within the spinal cord as early as 30 hpf (Figure 3.1A) (Bradley et al., 2010). At this age, 1–3 NOS1-positive cells are restricted to dorsolateral regions of the spinal cord. These cells appear to transiently express NOS1 since nitrenergic cell populations are no longer observed in the dorsal aspect from

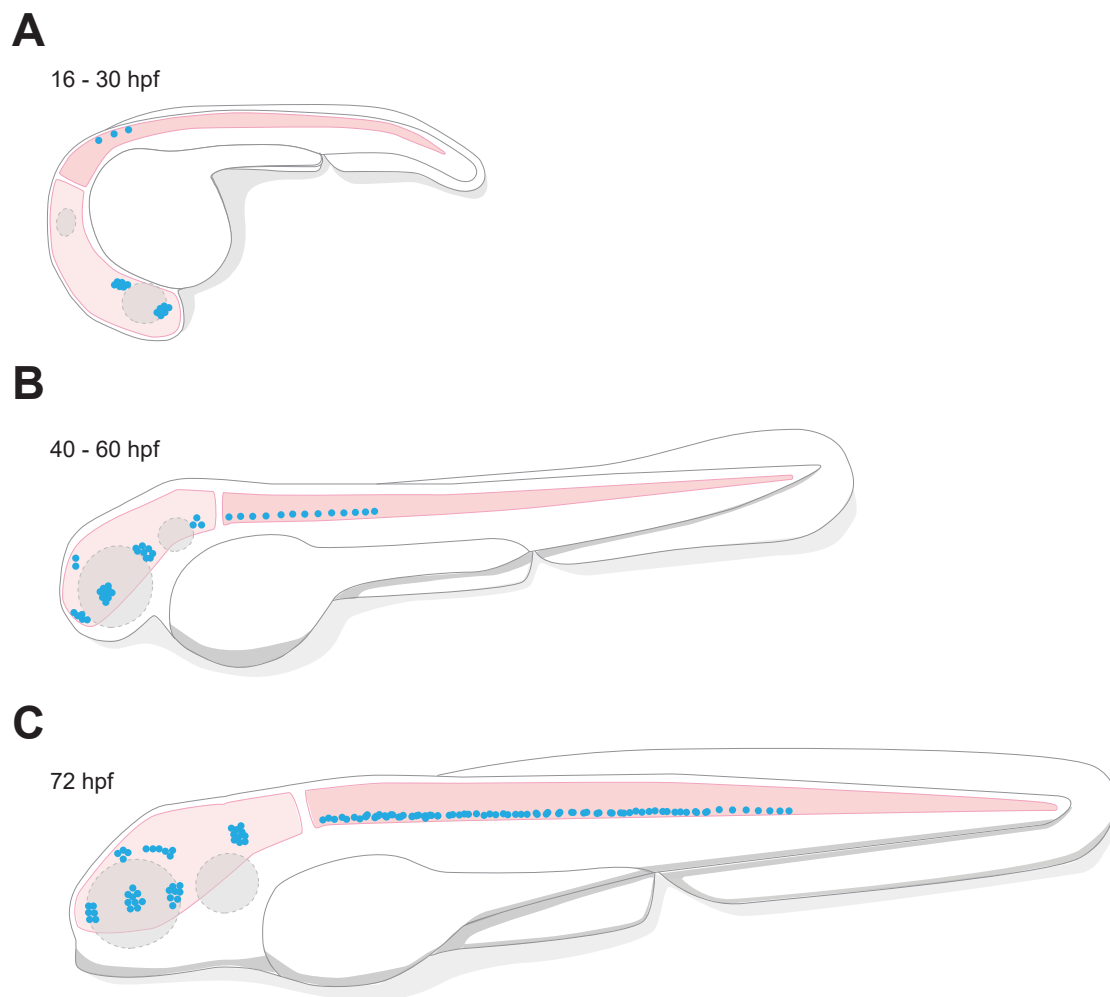


FIGURE 3.1
Schematic of NOS expression patterns during development. Nitregic cell populations increase across the first three days of development. **(A)** At 1 days post fertilisation (dpf), nitregic cells are restricted to the fore and midbrain with sparse labelling in the dorsal spinal cord. **(B)** At 2 dpf, nitregic cells populations increase throughout the forebrain. Additionally, within the spinal cord, nitregic cells are distributed along the ventral border in rostral segments. **(C)** By 3 dpf, nitregic cells are distributed down the entire extent of the spinal cord and are accompanied by nitregic cells within the fore, mid and hindbrain. Data derived from (Poon, 2003; Holmqvist et al., 2004; Bradley et al., 2010).

40–72 hpf. However, from 35 hpf onward, NOS1 is expressed in a population of ventral cells. These nitrergic cells occur in greater number and extend down somites 1–7 (Bradley et al., 2010) (Figure 3.1B). By 72 hpf, the number of nitrergic cells markedly increase and are now observed within the majority of somites (Figure 3.1C) (Holmqvist et al., 2004; Bradley et al., 2010).

3.1.5 Downstream pathways of NO within the nervous system

NO freely diffuses across cell membranes and exerts its effects by direct binding to intracellular components. Thus, unlike classical chemical transmitters, the actions of NO are not restricted to synaptic domains but are instead limited principally by its short 4–15 s half-life which permits diffusion up to 200–300 μm from the point of production (Lancaster, 1994, 1997). Thus, it is perhaps unsurprising that NO influences numerous physiological processes. The effects of NO are achieved in NO receptor-dependent and receptor-independent processes, which are briefly summarised below.

3.1.5.1 NO receptor-dependent signalling

The first, and to date, only known downstream receptor for NO is soluble guanylyl cyclase (sGC) (Gerzer et al., 1981; Förstermann et al., 1986; Garthwaite, 2008). Catalytic activity of this enzyme is substantially increased by binding of NO. sGC is a heterodimeric protein composed of two subunits, α and β (Gerzer et al., 1981; Kamisaki et al., 1986). There are two isoforms of each sGC subunit (α_1 , α_2 , β_1 , β_2) which can generate several protein products, however only the $\alpha_1\beta_1$ and $\alpha_2\beta_1$ heterodimers are thought to be functionally active (Russwurm and Koesling, 2002; Koesling et al.,

2004). The $\alpha_1\beta_1$ heterodimer is expressed throughout most tissues while $\alpha_2\beta_1$ expression is more restricted and is the predominant isoform within the brain (Mergia et al., 2003). Each heterodimer comprises a haem-binding region, a dimerisation domain and a catalytic domain. The haem-binding region acts as a NO receptor (Bellamy and Garthwaite, 2002). Binding of NO induces a conformational change in the protein and enzyme activation. Upon activation, catalysis of guanosine triphosphate (GTP) to cGMP increases several hundred-fold (Hardman and Sutherland, 1969; Chrisman et al., 1975). cGMP is an ubiquitous second messenger molecule which can act upon numerous targets (see Francis et al. (2010) for review). However, the primary target of this cyclic nucleotide is protein kinase G (PKG), which phosphorylates target proteins to regulate their activity levels (Schlossmann and Hofmann, 2005; Francis et al., 2010).

3.1.5.1.1 PKG-dependent mechanisms

Mammalian systems contain two PKG genes: *prkg1* and *prkg2*. The former encodes two isoforms, PKGI α and PKGI β , which differ in their N-terminus. This variation results in differential sensitivity to cGMP whereby the PKGI α isoform is approximately 10-fold more sensitive than PKGI β (Ruth et al., 1991). While both isoforms are present within the nervous system, their expression levels and spatial distribution are discrete. PKGI β is the predominant form expressed throughout many brain regions including the cerebellum, hippocampus, hypothalamus, amygdala, olfactory bulb, retina and cerebral cortex (Feil et al., 2005). In contrast, PKGI α is restricted to cerebellar Purkinje cells and nociceptive neurons of the dorsal root ganglia (Feil et al., 2005).

PKG is a major downstream effector that can phosphorylate a vast array of

target proteins, discussion of which is beyond the scope of this text, however extensive reviews can be found elsewhere (Wang and Robinson, 1997; Francis et al., 2010). However, a common function of PKG-mediated activity is to modulate intracellular calcium levels, which can have important functional consequences for action potential generation and signal transduction. For example, L-type Ca^{2+} channels, which permit calcium influx following membrane depolarisation, are subject to phosphorylation by PKG. Phosphorylation of these channels is sufficient to markedly slow the kinetics and inactivate this channel (Hell et al., 1993; Nishimura et al., 1992; Meriney et al., 1994). N-type Ca^{2+} channels are also phosphorylated by PKG but the functional consequences are not yet known (Hell et al., 1994). Other targets of PKG include the inositol 1,4,5-triphosphate (IP_3) receptors which mediate Ca^{2+} levels by releasing Ca^{2+} from intracellular stores. These receptors, which are ubiquitous throughout the nervous system (Sharp et al., 1993, 1999), contain a phosphorylation site for PKG at Ser-1755. When phosphorylated at this site, Ca^{2+} release is inhibited (Tertyshnikova et al., 1998; Murthy, 2001).

PKG is also known to phosphorylate and modulate the activity of other ion channels. For example, PKG-mediated phosphorylation of large-conductance calcium-activated potassium channels (BK_{Ca}) promotes channel opening and, under normal physiological conditions, the efflux of potassium ions from the intracellular environment and subsequent hyperpolarisation of the membrane (White et al., 1993; Hall and Armstrong, 2000). This is likely achieved by phosphorylation of a serine residue (Ser-1072) since a point-mutation here is sufficient to abolish the effects of NO and PKG on this channel (Fukao et al., 1999). Thus, NO can modulate excitability of neurons by inducing PKG-dependent phosphorylation of ion channels.

3.1.5.1.2 PKG-independent mechanisms

In addition to its actions mediated via PKG, cGMP can also directly modulate the activity of cyclic nucleotide-gated (CNG) channels (Kaupp and Seifert, 2002). These channels are nonselective-cation channels and under physiological conditions conduct inward Na^+ and Ca^{2+} currents (Kaupp and Seifert, 2002). The role of these channels is perhaps best understood in retinal photoreceptors, where CNG channels were first discovered (Fesenko et al., 1985). Under dark conditions, CNG channels localised to the cell membrane of rod cells are activated by the binding of cGMP and produce a steady inward current. However, when exposed to light, cGMP is hydrolysed and CNG channels close thereby limiting calcium influx. However, independent of illumination, a $\text{Na}^+/\text{Ca}^{2+}-\text{K}^+$ exchanger continuously removes Ca^{2+} from the intracellular environment. Thus, when CNG channels are closed, intracellular Ca^{2+} concentrations decrease and when sufficiently low, GC-activating proteins are activated which increases cGMP production, reopening of CNG channels and restoration of the dark state of the cell (Kaupp and Seifert, 2002).

Hyperpolarisation-activated, cyclic nucleotide-gated (HCN) channels are similar to CNG channels such that their activity is modulated by cyclic nucleotides (Biel et al., 2009; Wenker et al., 2012; Kopp-Scheinflug et al., 2015). However, these channels are strongly voltage-dependent such that they are activated during hyperpolarisation. Instead of opening or closing HCN channels, both cGMP and 3'-5'-cyclic adenosine monophosphate (cAMP), a closely related cyclic nucleotide, can shift the activation curves to more positive or negative potentials (Baruscotti et al., 2005). The currents carried by these channels have been implicated in maintaining basal levels of activity and rhythmicity in many neuronal networks (McCormick and Pape, 1990; Dossi

et al., 1992). HCN channels comprise a tetrameric complex of subunits encoded by 4 genes (HCN1 – 4). The effects of NO and cGMP upon these channels is dependent upon the composition of subunits. This is because each subunit differs in activation kinetics, voltage-dependent activation and sensitivity to cyclic nucleotides (Kopp-Scheinpflug et al., 2015).

3.1.5.1.3 Inactivation of cGMP signalling

The primary mechanism of cGMP breakdown is achieved by the 3'5'-cyclic nucleotide phosphodiesterases (PDEs) (Menniti et al., 2006). These enzymes are primarily responsible for the inactivation of cGMP and cAMP (Menniti et al., 2006). Within mammals, 11 families, comprising over 50 unique PDEs have been identified. Each PDE isozyme comprises an N-terminal, a catalytic and a C-terminal domain (Menniti et al., 2006). Additionally, each isozyme contains a well conserved glutamine switch which facilitates cyclic-nucleotide binding. The orientation of the glutamine within the catalytic domain dictates cyclic nucleotide-specificity. The N-terminal domain, which undergoes extensive splicing, contains unique sites that are involved in regulating enzyme activity. The catalytic domain, located near the C-terminal is generally well conserved within each family, but is relatively dissimilar between families (20–45 %) (Menniti et al., 2006; Francis et al., 2010).

3.1.5.2 NO receptor-independent signalling

3.1.5.2.1 Nitrosylation

Nitrosylation is the incorporation of an nitric oxide moiety into another molecule, which occurs at high concentrations of NO (Hanafy et al., 2001). High concentrations of NO are necessary for two reasons. Firstly, nitrogen dioxide (NO₂), a key component necessary for nitrosylation, is produced following bimolecular collision of two NO molecules. Secondly, a third NO molecule is then oxidised by NO₂ to form dinitrogen trioxide (N₂O₃). After formation, N₂O₃ quickly decomposes into a nitrosonium (NO⁺) and nitrite ion (NO₂⁻). NO⁺ then forms covalent bonds with secondary amines, phenolics and thiols.

This process has been implicated in several biological processes. For example, NO⁺ transfer to a critical cysteine residue (Cys 399) of an N-Methyl-D-aspartic acid (NMDA) receptor subunit significantly depresses activity levels (Lei et al., 1992; Lipton et al., 1993; Choi et al., 2000; Lipton et al., 2002). Additionally, nitrosylation has been identified as a regulator of apoptosis (Sen et al., 2008). Here, nitrosylation of glyceraldehyde-3-phosphate dehydrogenase (GAPDH) induces formation of a GAPDH-Siah1 protein complex that translocates to the cell nucleus to initiate and mediate cell death. However, the physiological relevance of nitrosylation has been questioned, particularly within the context of mediating NMDA receptor activity (Hopper et al., 2004; Garthwaite, 2008). Inhibition of NMDA receptors by NO-dependent mechanisms has previously been reported (Manzoni et al., 1992; Murphy et al., 1994; Murphy and Bliss, 1999). However, these results were reliant upon NO donors that had off-target effects (Manzoni et al., 1992), or used caged NO that was released by ultra-violet

(UV) light (Murphy et al., 1994; Murphy and Bliss, 1999). When hippocampal slices were subject to high, non-physiological concentrations of NO or UV light, there was no observable effect on field excitatory post synaptic potentials (fEPSPs) mediated by NMDA receptors (Hopper et al., 2004), but application of both conditions simultaneously was sufficient to irreversibly depress NMDA receptor-mediated currents. Thus, the previously reported effects of NO upon NMDA receptor functioning may not occur under physiological conditions (Hopper et al., 2004).

3.1.5.2.2 Nitration

Under normal physiological conditions, superoxide (O_2^-) is produced as a byproduct of oxygen metabolism and is dismutated into hydrogen peroxide (H_2O_2) by superoxide dismutase (SOD) in order to protect the intracellular environment from free radical damage (H_2O_2 is quickly broken down into H_2O and O). However in the presence of high concentrations of NO, O_2^- reacts with NO to produce peroxynitrite, which decomposes into nitrogen dioxide (NO_2^\bullet) and a highly reactive hydroxyl radical (OH^\bullet) (Francis et al., 2010). Since the hydroxyl radical can interact with most biological molecules, it's not considered a viable signalling molecule (Adams et al., 2015). While this process may not be relevant to modulating signalling pathways, both macrophages and neutrophils use peroxynitrite in order to neutralise foreign bodies. After engulfing foreign substances, such as microbes, NADPH oxidises superoxide and NOS2 generates NO. These combine to create peroxynitrite which subsequently kills the engulfed pathogen. However, dysregulation of this process and overproduction of peroxynitrite can have detrimental consequences. For example, DNA and mitochondrial damage are known to occur after increased levels of peroxynitrite. Indeed, peroxynitrite has been

implicated in a number of disease states such as amyotrophic lateral sclerosis (Zhu et al., 2006), Parkinson's disease (Ebadi et al., 2005), atherosclerosis (White et al., 1994) and heart disease (Pacher et al., 2007).

3.1.6 Roles of NO during nervous system development

The NO-dependent pathway has been implicated in many neurodevelopmental processes. One of the earliest stages during nervous system ontogeny is the formation of heterogeneous neuron classes from populations of progenitor cells located throughout the developing CNS (März et al., 2010; Satou et al., 2012). NOS1 is expressed within many of these regions (Holmqvist et al., 2004; Romero-Grimaldi et al., 2008; Cheng et al., 2003; Matarredona et al., 2004) and perturbation of NO signalling during periods of NOS1 expression can have significant effects upon proliferation and differentiation of these progenitor cells. For example, within the postnatal subventricular zone (SVZ), a source of precursor cells which differentiate into interneurons later in development (Luskin, 1993), transient increases in NOS1 expression correlate with a decrease in cell proliferation. Pharmacological inhibition of NOS at this stage can enhance cellular proliferation by up to 30 % (Moreno-López et al., 2000, 2004; Carreira et al., 2013). In contrast, the addition of NO donors has the opposite effect, slowing or inhibiting cell proliferation (Matarredona et al., 2004). This inhibitory role for NO during early development appears to be consistent with processes occurring within other areas of the nervous system and between species. For example, in the developing cerebellum, NO inhibits cell proliferation (Ciani, 2004, 2006) while in the developing *Xenopus*, endogenous NOS inhibition is sufficient to increase proliferation in the optic tectum (Peunova et al., 2001). This suppressive role for NO also persists

into adulthood (Packer et al., 2003). While the majority of neurogenesis occurs during embryonic development, several brain regions, including the SVZ continue to generate neurons at adult stages. Either NOS1 knockout or local injection of NOS inhibitors is sufficient to enhance proliferation in this region (Packer et al., 2003).

Shortly after differentiation, neurons also undergo a period of neuriteogenesis where nascent neurites acquire their dendritic or axonal properties. While there has been little focus on the role of NO in the early stages of neurite specification, recent evidence has demonstrated that cGMP and cAMP modulate this process (Shelly et al., 2010). In dissociated rodent hippocampal neurons, decreased cAMP or increased cGMP levels creates a bias toward axonal (rather than dendritic) specification (Shelly et al., 2010). Conversely pharmacological inhibition of sGC increases dendritic specification.

Proliferation and differentiation of cells is followed by migration from the proliferative zone to the final location within the CNS. NO and the cGMP-dependent pathway have also been implicated in this process. In contrast to the earlier stages of proliferation where NO has broadly inhibitory roles, NO appears to facilitate cellular migration in a number of species and experimental paradigms. Pharmacological inhibition of NOS or PKG is sufficient to significantly retard the migration of cultured human progenitors in an *in vitro* environment (Tegenge and Bicker, 2009; Tegenge et al., 2011a,b). Similarly, in embryonic (E15) mice cortical slices, the inhibition of sGC or PKG activity is sufficient to slow the rate of migration and the percentage of motile cells (Mandal et al., 2013).

Despite the paucity of literature examining the role of NO and cGMP as a modulator of neurite specification, a larger body of work has examined the role of

these molecules during neurite outgrowth. When NO-dependent signalling is inhibited, neurite extension of dissociated hippocampal neurons in mice (Ditlevsen et al., 2007) and rats (Shelly et al., 2010) is markedly reduced. In the developing chick embryo, motor neuron dendritic growth and branching is retarded following NOS, sGC or PKG inhibition (Xiong et al., 2007). NO/cGMP signalling has also been shown to facilitate neurite extension in embryonic chick dorsal root ganglia (DRG) and retinal ganglion cells (Schmidt et al., 2002; Steinbach et al., 2002), and rat cerebellar granular cells (Xiang et al., 2002). These effects are also consistent within *in vivo* locust (*Locusta migratoria*) studies. During extension and migration of enteric neurons, there are high levels of NO and cGMP expression (Haase and Bicker, 2003; Knipp and Bicker, 2009; Stern et al., 2010). However, shortly after these midgut neurons reach their target sites, NO/cGMP levels markedly decrease, which suggests a role for NO in this process. Indeed, pharmacological inhibition of NOS, sGC or PKG activity is sufficient to significantly block neuronal migration, and these effects are rescued by subsequent addition of protoporphyrin IX (which activates sGC) (Stern and Bicker, 2010) or cGMP (Haase and Bicker, 2003), thus demonstrating the NO-dependent pathway as an important facilitator of cellular migration. However, there are several contradictory studies suggesting that NO has inhibitory roles during neurite extension. In cultured dentate granule cells, exogenous increases in NO concentrations retarded neurite outgrowth in a cGMP-dependent manner (Yamada et al., 2006) and similarly, extension of chick DRG neurites is halted by NO donors (Gallo et al., 2002; He et al., 2002). Growth cones are dynamic structures at the distal tip of the neurite which detect extracellular signals and facilitate outgrowth (Lowery and Vactor, 2009). These structures can also be strongly affected by NO levels. Thus, the reported inhibitory effects of NO dur-

ing neurite outgrowth may, in part, be attributable to the effects of NO upon growth cones. Indeed, addition of NO donors can induce growth cone collapse in cultured dentate granule cells (Yamada et al., 2006), DRG neurons (Hess et al., 1993), and retinal ganglion cells (Gallo et al., 2002). Growth cones comprise of bundles of actin filaments, known as filopodia, which are fundamental for axonal growth and response to guidance cues (Lowery and Vactor, 2009). These structures are also affected by changing NO levels. For example, low concentrations ($\approx 100 \mu\text{M}$) of NO donors can cause a transient elongation and reduction in number of filopodia (Van Wagenen and Rehder, 1999; Trimm and Rehder, 2004). At high concentrations (1 mM), NO donors induce growth cone collapse and neurite retraction (Trimm and Rehder, 2004).

As axons extend they begin to form synaptic connections with their respective targets. In studies examining the nascent visual system, NO has been proposed to control the activity-dependent refinement of synaptic connections. Ganglion cells from the retina synapse with neurons in the superior colliculus. However during development, the projections of these cells form excess synaptic connections that undergo significant refinement. Perturbation of NO signalling, either by NOS inhibition or NOS (NOS1 and NOS3) knockout is sufficient to disrupt the refinement of retinotectal projections in chicks (Wu et al., 2001), mice (Wu et al., 1994, 2000) and rats (Campello-Costa et al., 2000). Nitric oxide also modulates the synaptic connections between motoneurons and muscle fibres. When motoneurons exit the spinal cord they form specialised synaptic connections, known as NMJs, with the surrounding muscle tissue. However, before this occurs, pre-patterned ACh receptor (AChR) clusters begin to form throughout the muscle tissue (Lin et al., 2001; Flanagan-Steet et al., 2005; Panzer et al., 2005, 2006). As the cholinergic motoneurons begin to project into the periphery they pref-

erentially extend toward, and form *en passant* synapses with the prepatterned ACh receptor clusters. In cultured myotubes, inhibition of NOS during this critical period of NMJ development is sufficient to significantly reduce aggregation of AChRs, while increases in NO signalling have the opposite effect (Jones and Werle, 2000; Godfrey and Schwarte, 2010). Further investigations within *Xenopus* preparations confirmed NO as a modulator of AChR aggregation and additionally identified cGMP and PKG as important downstream targets for this process (Godfrey and Schwarte, 2003; Schwarte and Godfrey, 2004; Godfrey et al., 2007).

Previous work has also shown that the NO signalling pathway regulates the axonal arborisation of zebrafish primary motoneurons (pMNs) (Bradley et al., 2010). Within zebrafish, a class of interneurons lying ventral to developing motoneurons begins to express NOS1 from ≈ 30 hpf onward, a period characterised by extensive axonal arborisation. As arborisation of motoneuron axons progresses, the levels of NOS1 mRNA expression within this class of nitrergic interneurons intensifies to the extent where NOS1 is expressed down the length of the spinal cord. This expression continues through until at least 72 hpf (Bradley et al., 2010). When NOS1 expression is perturbed with antisense morpholinos (AMOs), there is a significant increase in pMN branch number by 48 hpf (Bradley et al., 2010). Similarly, when NOS and downstream components of the NO-dependent pathway are inhibited with pharmacological agents, there are similar increases; application of N_{ω} -Nitro-L-arginine methyl ester hydrochloride (L-NAME) or ODQ, inhibitors of NOS and sGC, respectively, caused an increase in pMN branching. Moreover, when NO signalling is exogenously increased by application of NO donors (diethylenetriamine/nitric oxide adduct (DETA/NO)) or a cGMP analogue (8-(4-Chlorophenylthio)-guanosine 3',5'-cyclic monophosphoroth-

ioate (8-CPT-cGMP)), similar sized decreases can be observed.

3.1.7 Nitric oxide as a modulator of locomotor networks

Once spinal networks become functional, they are influenced by a range of neuromodulators including NO. Generally, NO has primarily suppressive effects during immature stages of locomotor output. However, as species exit embryonic and larval stages, the effects of NO upon central pattern generators (CPGs) may become facilitatory.

In the developing *Xenopus* tadpole, nitrergic cell populations develop contemporaneously with emerging locomotor output. During ongoing locomotor activity, NO acts to suppress spinal CPG activity at embryonic and larval stages via potentiation of the inhibitory synapses (McLean and Sillar, 2000, 2002). Here, bath application of an NO donor, S-Nitroso-N-acetyl-DL-penicillamine (SNAP), strongly decreased the duration (by $\approx 75\%$) and cycle frequency of swim episodes. Conversely, inhibition of endogenous NOS activity had the opposite effect, increasing both swim episode duration and cycle frequency (McLean and Sillar, 2000, 2002). These effects are attributable to selective facilitation of both glycinergic inputs, which provide midcycle inhibition during a swim episode, and GABAergic inputs that prematurely terminate swim episodes (Roberts and Blight, 1975; McLean and Sillar, 2002; Perrins et al., 2002).

As development continues and *Xenopus* tadpoles enter free feeding stages, the role of NO may switch to become facilitatory (Combes et al., unpublished observations, see Sillar et al. 2008). Although the role of NO requires further investigation in adult *Xenopus*, there is strong evidence to suggest that, in the adult lamprey, NO-

dependent endocannabinoid signalling has a net-excitatory effect upon spinal networks (Kyriakatos et al., 2009; El Manira and Kyriakatos, 2010; Song et al., 2012). In the lamprey spinal cord, NOS positive cells are distributed down the entire rostrocaudal extent of the spinal cord (Kyriakatos et al., 2009). Incubation with NOS or sGC inhibitors is sufficient to slow the frequency of pharmacologically induced swim episodes suggesting that NO acts via a cGMP-dependent mechanism to excite spinal networks. Exogenous increases in NO-dependent signalling had the opposite effect, significantly increasing swim frequency (Kyriakatos et al., 2009). Furthermore, in contrast to larval *Xenopus*, NO enhanced on-cycle glutamatergic drive and inhibited the midcycle glycinergic inputs within the adult lamprey spinal cord.

Despite extensive expression of NOS within the terrestrial spinal cord, little work has investigated whether NO has modulatory roles here. However, recent work has identified a role for NO at postnatal stages (Foster et al., 2014). Bath application of NO donors to spinal cord preparations during pharmacologically induced fictive locomotor output was sufficient to slow the frequency of output by up to $\approx 60\%$. Additionally, low doses increased, while high doses decreased, the amplitude of fictive locomotor output. These effects were modulated in a cGMP-dependent manner since application of cGMP analogues mimicked the effects of NO. Finally, by using disinhibited spinal cord preparations in which glycinergic and GABAergic inputs were blocked, Foster et al. (2014) demonstrated that NO is likely affecting the excitatory inputs to spinal CPGs.

NO also works in concert with a range of other neuromodulators to impart flexibility to locomotor networks. For example, concomitant release of endocannabinoids and NO upon lamprey spinal networks induces long term changes in locomotor

frequency, midcycle inhibition and excitatory synaptic drive (Kyriakatos and El Manira, 2007). While the precise mechanisms are unknown, NO and endocannabinoids appear to act in a synergistic manner to facilitate complementary roles. In a similar fashion, noradrenaline (NA) and NO play complementary roles within the *Xenopus* tadpole to potentiate inhibitory glycinergic and GABAergic inputs (McLean and Sillar, 2004). Here, NA acts directly upon the commissurally projecting glycinergic interneurons, while NO modulates the activity of the descending NAergic and GABAergic inputs.

3.2 Aims and Objectives

Previous work has already demonstrated that chronic perturbation of NO-signalling is sufficient to alter motoneuron axogenesis (Bradley et al., 2010). However, how the NO-dependent pathway affects the anatomical or functional properties of developing NMJs has yet to be examined. To address this issue, two approaches were taken. Firstly, immunohistochemical studies were conducted to identify anatomical changes in NMJ formation. Secondly, in order to examine physiological consequences of perturbing nitroergic signalling, a series of *in vivo* electrophysiological recordings from muscle fibres were performed.

In this chapter, it is demonstrated that disrupting the NO-dependent pathway between 1 dpf and 2 dpf is sufficient to affect NMJ formation throughout axial muscle tissue and miniature end plate current (mEPC) kinetics at nascent NMJs. Additionally, evidence is provided to suggest there are NO-dependent effects on the maturation of locomotor activity. In summary, the work described here demonstrates that NO is an important modulatory cue for proper NMJ formation and function.

3.3 Results

3.3.1 Exogenous increases in NO-dependent signalling decreases NMJ number

In order to characterise the effects of NO/cGMP signalling on neuromuscular synapse formation, 24 hpf embryos were first exposed to the NO donor DETA/NO or the cGMP analog, 8-CPT-cGMP. Embryos were incubated in these drugs or control egg solution until 48 hpf, at which point the fish were fixed (Figure 3.2A). To identify putative NMJs, embryos were subsequently exposed to rhodamine-conjugated α -bungarotoxin (Rh- α -BTX) and anti-SV2 antibodies which enabled visualisation of the postsynaptic domain upon the muscle and the presynaptic domain located on the motoneuron, respectively (Panzer et al., 2005). For the purposes of this work, analysis was performed at 2 dpf, by which stage motoneurons have extended from the spinal cord and branched to form an easily quantifiable number of synapses with muscle fibres (Figure 3.2B) (Liu and Westerfield, 1992; Panzer et al., 2005, 2006).

Since application of DETA/NO has previously been reported to perturb axonal development (Bradley et al., 2010), the effects of this NO donor upon NMJ formation were first examined. Developmental exposure to DETA/NO from 24 to 48 hpf caused a marked decrease in the total number of NMJ puncta per somite (control = 96.27 ± 5.06 , $n = 11$; DETA/NO = 53.33 ± 2.54 , $n = 24$, $p < 0.001$) (Figure 3.3A-C). Because NO/cGMP signalling affects motor axon branch formation without impairing development of the motor root (Bradley et al., 2010), NMJ puncta along the motor axon fascicle and those located upon axonal branches were examined in detail. Here, the number of NMJ puncta along the fascicle remained unchanged (control =

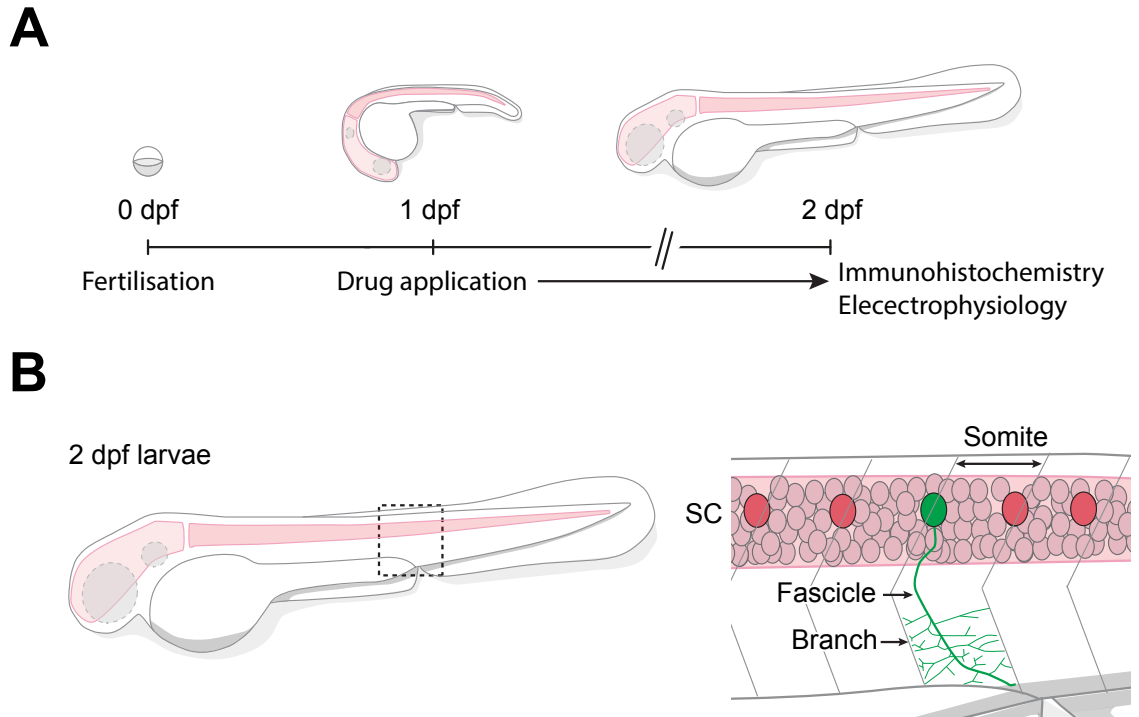


FIGURE 3.2
Schematic of experimental protocol and innervation of somitic tissue by developing motoneurons. (A) Larvae were incubated in pharmacological reagents from 1 dpf until 2 dpf, at which point fish were processed for immunohistochemical approaches or used for electrophysiological investigations. (B) Left: schematic representation of a 2 dpf zebrafish larvae. Dashed box indicates the region used for puncta analysis. Right: schematic illustration of a motoneuron extending axons along the fascicle and branching to innervate the somitic tissue.

24.82 ± 1.17 , DETA/NO = 23.17 ± 0.92 , $p > 0.05$) while a significant decrease in NMJ puncta was observed along the axonal branches (control = 71.45 ± 4.87 , DETA/NO = 30.17 ± 2.15 , $p < 0.001$) (Figure 3.3B). Since this effect could arise from changes in NMJ density along axonal branches or from changes in the absolute number of axon branches (Bradley et al., 2010), the density of branch-specific NMJ puncta was examined. Here, DETA/NO had no effect (control = 0.17 ± 0.01 puncta μm^{-1} , DETA/NO = 0.16 ± 0.02 puncta μm^{-1} , $p > 0.05$) (Figure 3.3C).

When embryos were incubated in 8-CPT-cGMP, significantly fewer NMJ puncta were observed, mirroring the effects of exogenously increased NO levels

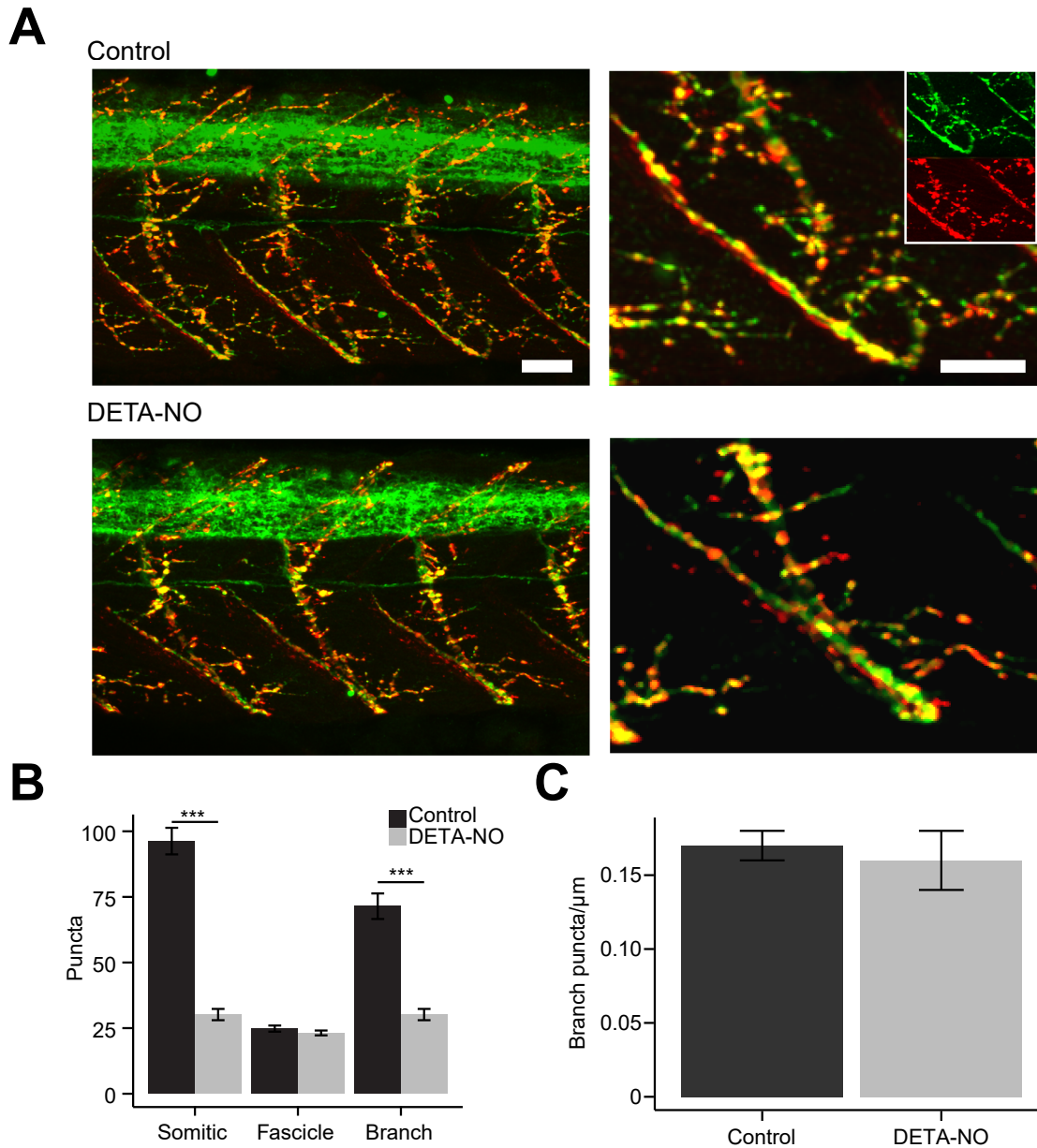


FIGURE 3.3

Developmental increases of NO signalling decreases NMJ numbers. (A) Left hand panels: lateral trunk views of anti-SV2 (green)/Rh- α -BTX (red) staining in control and DETA/NO treated zebrafish at 2 dpf. Right hand panels: expanded regions showing staining localised to a single somitic region. Insets show anti-SV2 and Rh- α -BTX images from which merged images were derived. (B) Bar chart depicting the mean (\pm standard error of the mean (SEM)) number of synapses located within each somite, along the motor fascicle and along branch-associated regions. (C) Mean density of branch-associated NMJ puncta. Scale bars in (A) = 30 μ m.

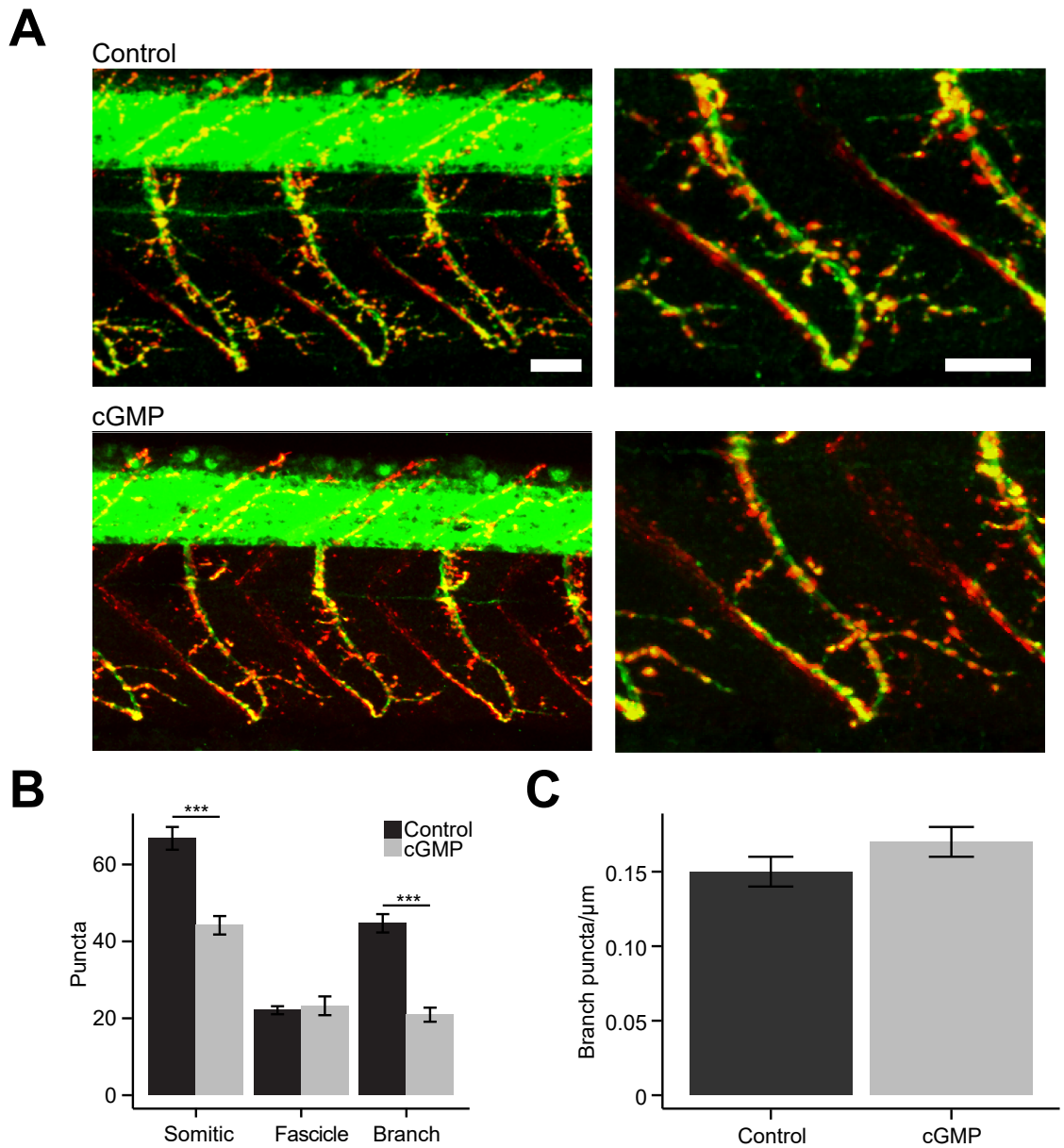


FIGURE 3.4

Developmental increases of cGMP signalling decreases NMJ numbers. (A) Left hand panels: lateral trunk views of of anti-SV2 (green)/Rh- α -BTX (red) staining in control and 8-pCPT-cGMP treated zebrafish at 2 dpf. Right hand panels: expanded regions showing staining localised to a single somitic region. (B) Bar chart depicting the mean (\pm SEM) number of synapses located within each somite, along the motor fascicle and along branch-associated regions. (C) Mean density of branch-associated NMJ puncta. Scale bars in (A) = 30 μ m.

(control = 66.80 ± 2.96 , $n = 20$; 8-CPT-cGMP = 44.19 ± 2.40 , $n = 16$, $p < 0.001$) (Figure 3.4A-C). Similarly, this effect was caused by a reduction in the number of branch-associated (control = 44.70 ± 2.39 , $n = 20$; 8-CPT-cGMP = 20.94 ± 1.83 , $n = 16$, $p < 0.001$) but not fascicular (control = 22.10 ± 1.04 , $n = 20$; 8-CPT-cGMP = 23.25 ± 2.44 , $n = 16$, $p > 0.05$) NMJ puncta (Figure 3.4B). Again, this observation could not be accounted for by a change in the density of branch-associated NMJ puncta (control = 0.15 ± 0.01 puncta μm^{-1} , 8-CPT-cGMP = 0.17 ± 0.01 puncta μm^{-1} , $p > 0.05$) (Figure 3.4C).

3.3.2 Inhibition of NO-dependent signalling markedly increased NMJ number

Next, the effects of developmental reduction of NO/cGMP levels were examined. 24 hpf embryos were exposed to L-NAME or 1H-[1,2,4]Oxadiazolo[4,3-a]quinoxalin-1-one (ODQ) in order to inhibit NOS or sGC, respectively. Both pharmacological agents had similar effects. Exposure to L-NAME (Figure 3.5A-C) (control = 80.30 ± 4.77 , $n = 20$; L-NAME = 98.56 ± 5.27 , $n = 23$; $p < 0.01$), or ODQ (Figure 3.6A-C) (control = 87.50 ± 4.10 , $n = 18$; ODQ = 116.00 ± 5.67 , $n = 12$, $p < 0.001$) significantly increased somitic puncta. Again, such effects were attributable to changes in the number of branch-associated, rather than fascicular NMJ puncta. L-NAME (control = 53.80 ± 4.24 , $n = 20$; L-NAME = 72.00 ± 4.39 ; $p < 0.001$) and ODQ (control = 58.50 ± 3.67 ; ODQ = 85.17 ± 3.67 , $p < 0.001$) markedly increased branch associated NMJ puncta. In both L-NAME (control = 0.23 ± 0.03 puncta μm^{-1} ; L-NAME = 0.19 ± 0.01 puncta μm^{-1} , $p > 0.05$) and ODQ (control = 0.19 ± 0.01 puncta μm^{-1} , ODQ = 0.21 ± 0.01 puncta μm^{-1} , $p > 0.05$) treated fish, fascicle-associated NMJ puncta remained unchanged.

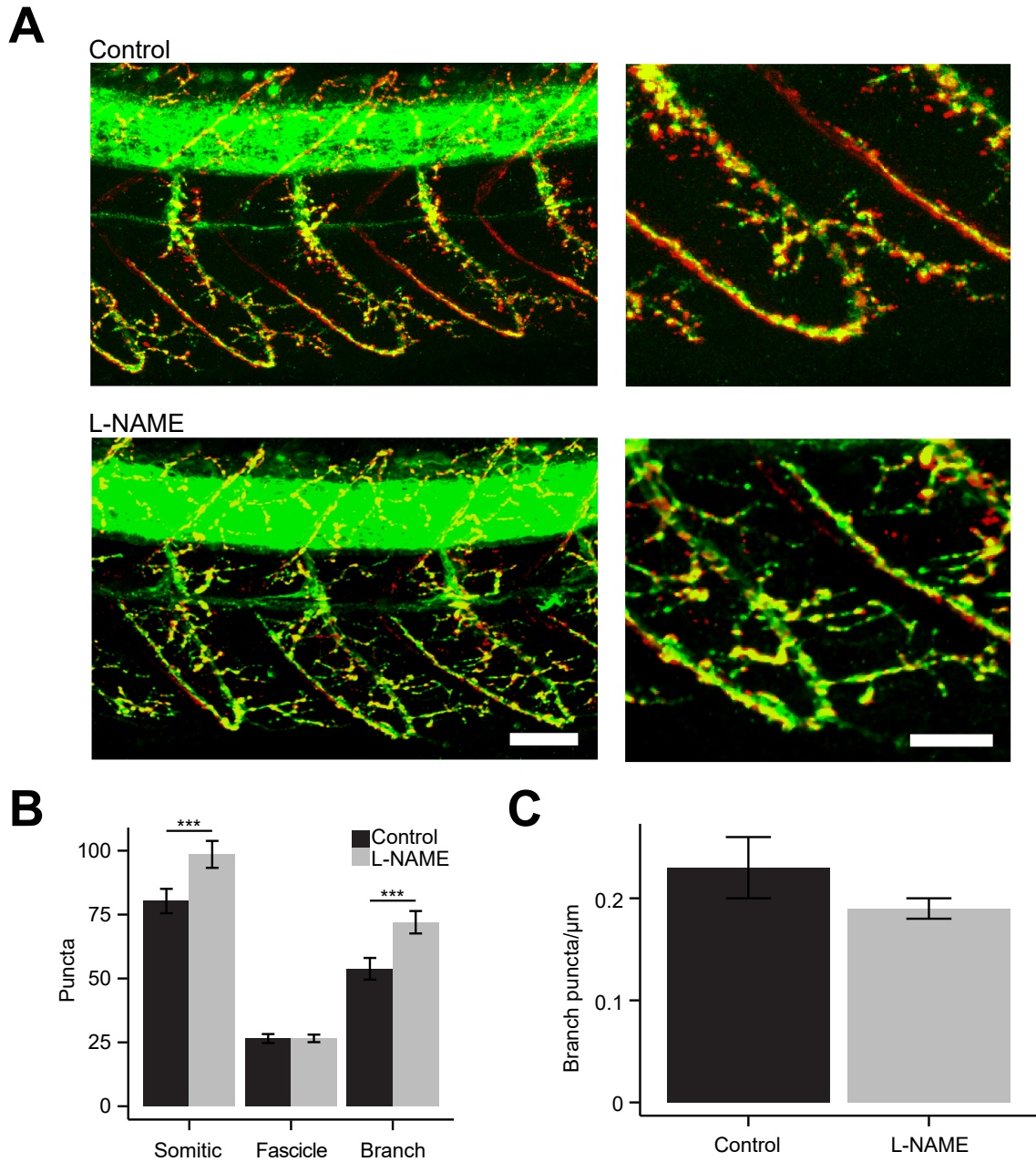


FIGURE 3.5

Developmental inhibition of NO signalling decreases NMJ numbers. (A) Left hand panels: lateral trunk views of anti-SV2 (green)/Rh- α -BTX (red) staining in control and L-NAME treated zebrafish at 2 dpf. Right hand panels: expanded regions showing staining localised to a single somitic region. (B) Bar chart depicting the mean (\pm SEM) number of synapses located within each somite, along the motor fascicle and along branch-associated regions. (C) Mean density of branch-associated puncta. Scale bars in (A) = 30 μ m.

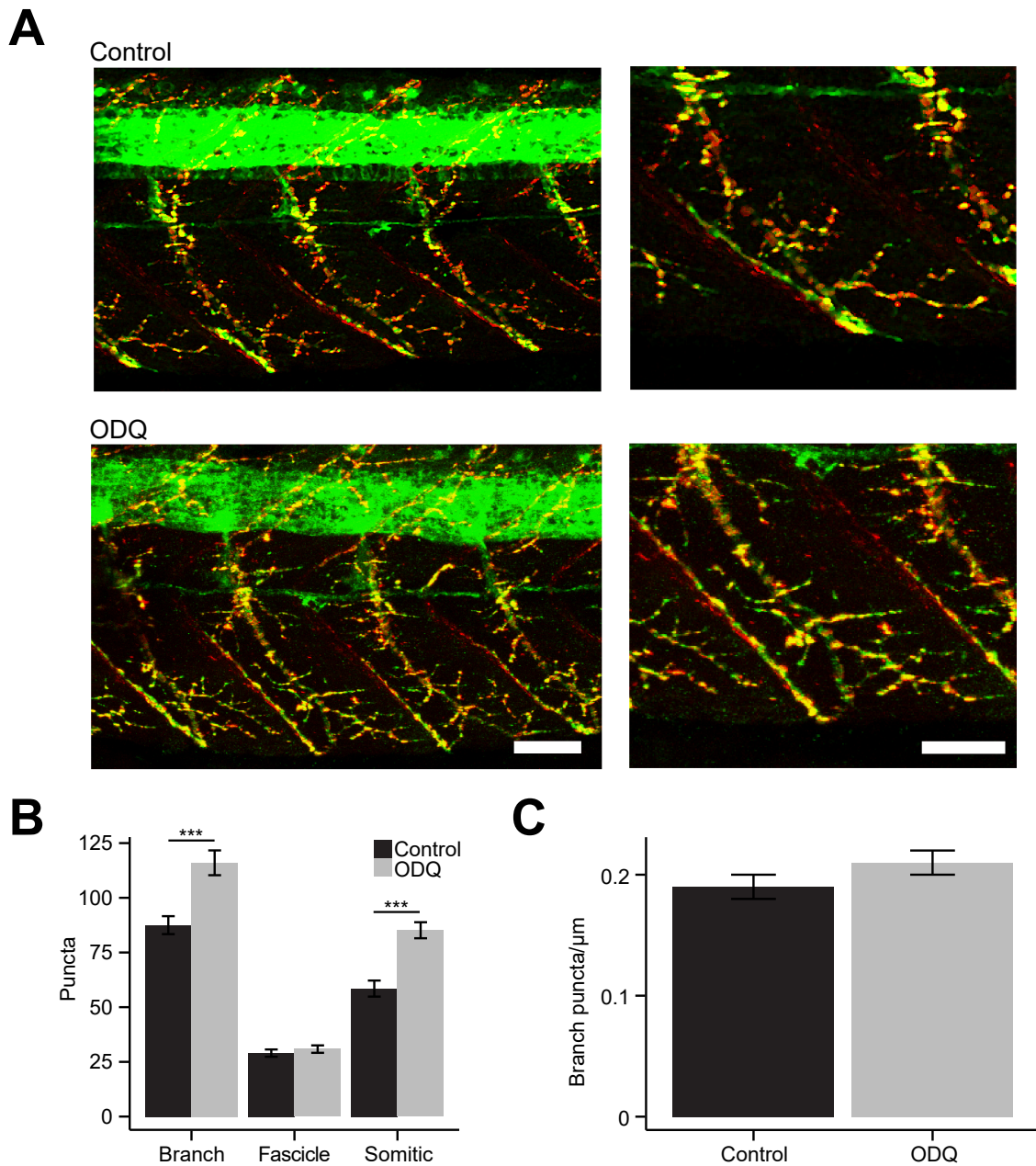


FIGURE 3.6

Developmental inhibition of cGMP signalling decreases NMJ numbers. (A) Left hand panels: lateral trunk views of anti-SV2 (green)/Rh- α -BTX (red) staining in control and ODQ treated zebrafish at 2 dpf. Right hand panels: expanded regions showing staining localised to a single somitic region. (B) Bar chart depicting the mean (\pm SEM) number of synapses located within each somite, along the motor fascicle and along branch-associated regions. (C) Mean density of branch-associated puncta. Scale bars in (A) = 30 μ m.

In sum, these results examining the anatomical consequences of NO-dependent perturbation on NMJ formation suggest that developmental increases in both NO and cGMP inhibit the formation of branch-associated NMJ puncta while decreases in NO or cGMP levels have the opposite effect. These effects arise as a consequence of inhibiting axon branch formation (Bradley et al., 2010) rather than as direct effects on the formation of branch (or fascicle) associated NMJs.

3.3.3 Developmental effects of NO Signalling on mEPC parameters

As a first step towards determining whether NO signalling affects the physiological maturation of NMJs, whole cell patch clamp recordings were made from muscle fibres in 48 hpf larvae exposed to pharmacological reagents which elevated (DETA/NO) or decreased (L-NAME) levels of NO signalling. At this age, two muscle fibre populations, termed embryonic fast (EF) and embryonic slow (ES) exist which are distinguishable based on their morphological and electrophysiological properties (see subsection 1.6.3 for details). Muscle fibres were synaptically isolated with the sodium channel blocker tetrodotoxin (TTX). Under these conditions spike-dependent neurotransmission can no longer occur but occasional synaptic events are still observed. These events, termed mEPCs, represent the stochastic release of individual quanta of ACh from the presynaptic terminal (Liley, 1956a,b; Boyd et al., 1956; Katz and Miledi, 1967). By examining the characteristics of these events, it is possible to infer the developmental state of the NMJ.

During mEPC recordings, the gap junction blocker 18- β -Glycyrrhetic acid (18- β -GA) was added to the extracellular saline in an attempt to block gap junction

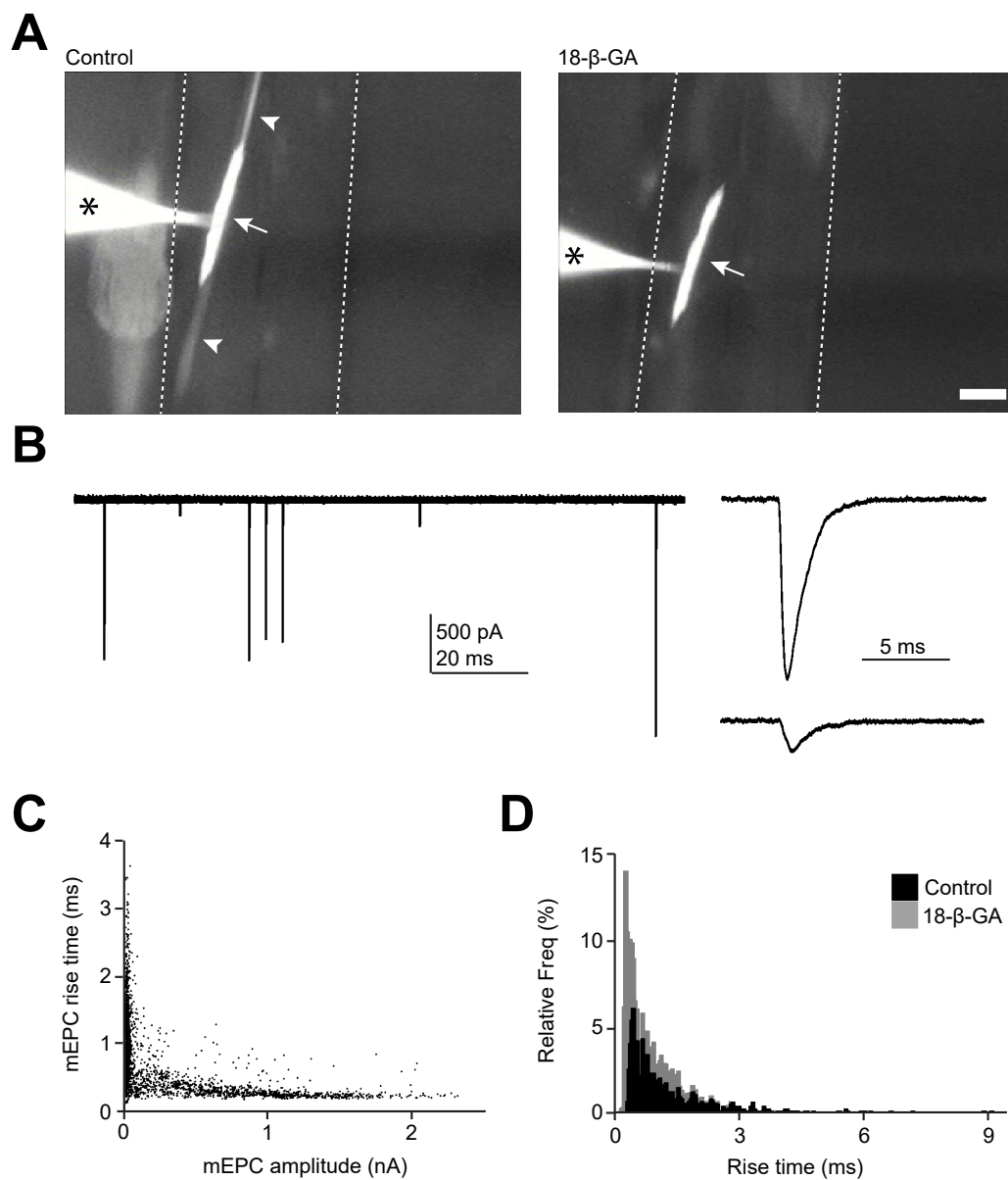


FIGURE 3.7

Effects of 18-β-GA on electrical coupling between EF fibres. (A) Images of embryonic fast (EF) muscle fibres that were dialysed with sulforhodamine B during whole cell recordings. In control saline, dye spread from the patched fibre (arrow) to neighbouring fibres (arrow heads). Preincubation with 18-β-GA abolished spread of dye. Asterisks identify the electrode. (B) Left: representative trace of mEPCs recorded from an EF fibre. Right: Example mEPCs captured on an expanded time scale. (C) mEPC amplitude versus rise time from EF fibres. (D) Histogram of mEPC rise time in control (black) and 18-β-GA treated (grey) muscle fibres. Scale bar in A = 50 μm.

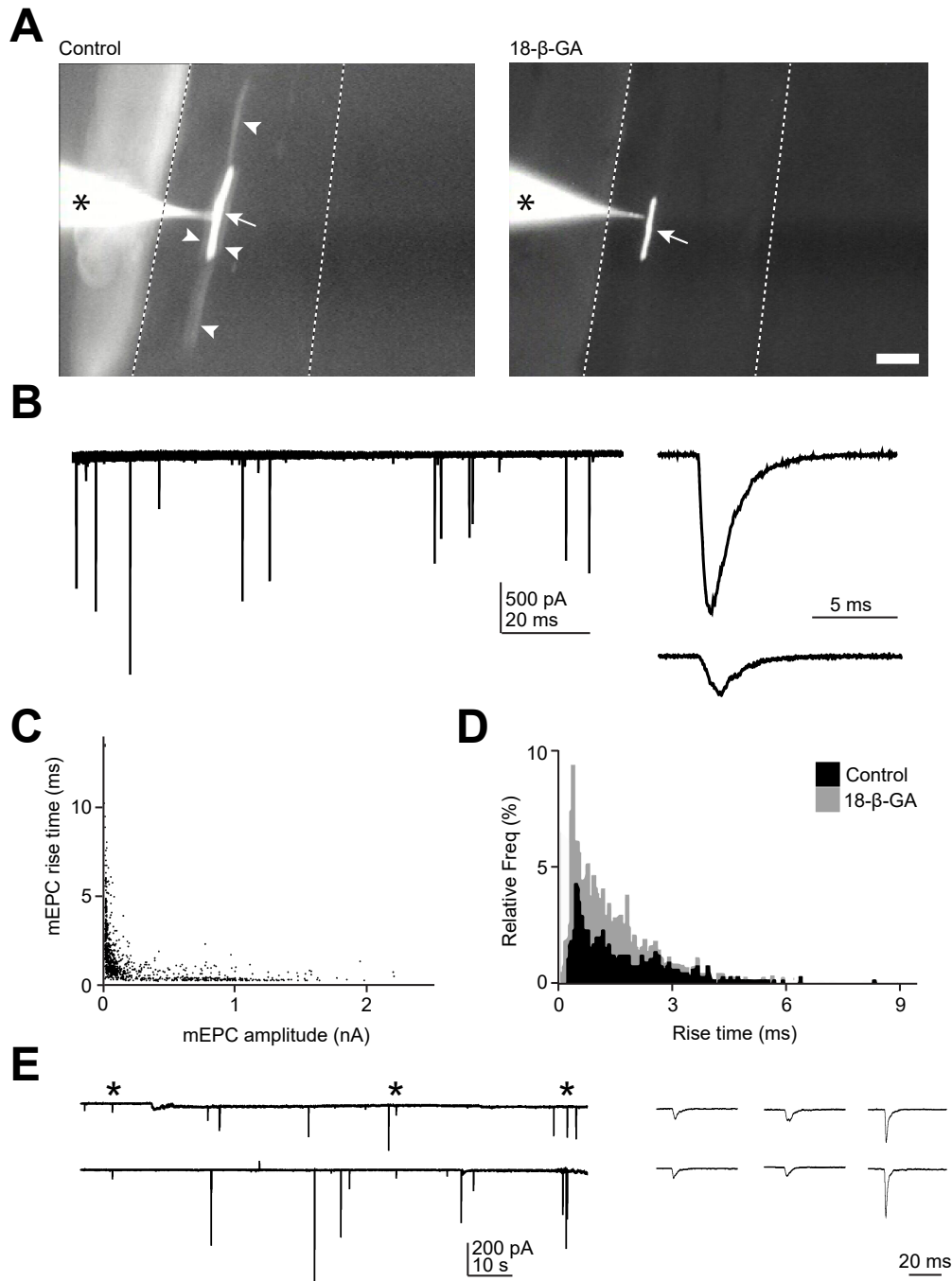


FIGURE 3.8

Effects of 18-β-GA on electrical coupling between ES fibres. (A) Images of embryonic slow (ES) muscle fibres that were dialysed with sulforhodamine B during whole cell recordings. In control saline, dye spread from the patched fibre (arrow) to neighbouring fibres (arrow heads). Preincubation with 18-β-GA abolished spread of dye. Asterisks identify the electrode. (B) Representative trace of mEPCs recorded from an ES fibre. Right: mEPCs captured on an expanded time scale. (C) mEPC amplitude versus rise time from ES fibres. (D) Histogram of mEPC rise time in control (black) and 18-β-GA treated (grey) muscle fibres. (E) Paired recording between ES fibres reveal that coincident events are occasionally observed in the presence of 18-β-GA. Asterisked events are shown with expanded time scale on the right. Scale bar in A = 50 μm.

coupling between muscle fibres (Luna and Brehm, 2006) and therefore permit examination of mEPCs arising from the isolated muscle fibre. Addition of 18- β -GA had several consequences. Firstly, it abolished spread of dye to neighbouring muscle fibres (Figure 3.7A, Figure 3.8A). Secondly, it significantly increased membrane resistance (control EF = $11.76 \pm 3.04 \text{ M}\Omega$, 18- β -GA EF = $166.30 \pm 19.23 \text{ M}\Omega$, $p < 0.001$; control ES = $19.76 \pm 4.16 \text{ M}\Omega$, 18- β -GA ES = $159.60 \pm 37.23 \text{ M}\Omega$, $p < 0.01$). Third, the mean amplitude of mEPCs was significantly altered (control EF = $73.16 \pm 2.92 \text{ pA}$, 18- β -GA EF = $783.80 \pm 14.22 \text{ pA}$, $p < 0.001$; control ES = $55.58 \pm 1.72 \text{ pA}$, 18- β -GA ES = $626.10 \pm 19.86 \text{ pA}$, $p < 0.001$).

Unexpectedly, a proportion of events with small amplitudes and slow kinetics persisted in both muscle fibre populations (Figure 3.7B-D, Figure 3.8B-D). To examine the origin of these events, a series of paired recording were conducted between neighbouring muscle fibres ($n = 1 \text{ EF pair}$, $n = 3 \text{ ES pairs}$) in order to determine whether these slow events are mediated by 18- β -GA-resistant gap junctions. Despite prolonged (20–30 min) exposure to 18- β -GA, a proportion of contemporaneous currents with small amplitudes ($< 100 \text{ pA}$) and slow rise times ($> 0.6 \text{ ms}$) were observed in both fibre populations (Figure 3.8E). Based on these observations, these small and slow currents were considered to be 18- β -GA insensitive gap junction mediated events and were therefore excluded from further analysis.

Analysis of mEPCs from EF muscle fibres of DETA/NO and L-NAME treated larvae revealed marked differences relative to control conditions (Figure 3.9A–G). The amplitude of mEPCs was significantly reduced in both condition, as revealed by cumulative probability distributions (Figure 3.9B) and analysis of mean amplitudes (Figure 3.9C; control = $783.80 \pm 14.22 \text{ pA}$, $n = 47 \text{ fibres}$; DETA/NO = $498.20 \pm 20.22 \text{ pA}$,

$n = 17$ fibres; L-NAME = 661.40 ± 13.01 pA, $n = 46$ fibres; $p < 0.001$). Moreover, increased levels of NO (DETA/NO) significantly slowed the rise time (Figure 3.9D,E; control = 0.321 ± 0.002 ms, $n = 47$ fibres; DETA/NO = 0.430 ± 0.005 ms, $n = 17$ fibres; $p < 0.001$) and half-width (control = 1.207 ± 0.019 ms, $n = 47$ fibres; DETA/NO = 1.859 ± 0.044 ms, $n = 17$ fibres; $p < 0.001$) of mEPCs. Reduced levels of NO-signalling had the opposite effect on half-width (control = 1.207 ± 0.019 ms, $n = 47$ fibres; L-NAME = 1.083 ± 0.003 ms, $n = 46$ fibres; $p < 0.001$) but did not affect rise time (Figure 3.9D,E; control = 0.321 ± 0.002 ms, $n = 47$ fibres; DETA/NO = 0.430 ± 0.005 ms, $n = 17$ fibres; $p < 0.001$).

In comparison to EF muscle fibres, perturbation of NO-signalling had similar but not identical effects on ES mEPC kinetics (Figure 3.10A—G). While the amplitude of mEPCs derived from EF fibres was significantly reduced by DETA/NO treatment, this was not the case for ES fibres. Here, DETA/NO did not alter amplitude (control = 634.70 ± 19.83 pA, $n = 24$ fibres; DETA = 661.00 ± 27.30 pA, $n = 33$ fibres; $p > 0.05$). However, L-NAME treatment did significantly reduce the amplitude of these events (control = 634.70 ± 19.83 pA, $n = 24$ fibres; L-NAME = 480.60 ± 13.38 pA, $n = 38$ fibres; $p < 0.001$). ES mEPC rise time (Figure 3.10D,E) significantly increased in DETA/NO treated fish (control = 0.293 ± 0.006 ms, $n = 24$ fibres; DETA/NO = 0.328 ± 0.007 ms, $n = 33$ fibres; $p < 0.001$) but not after L-NAME treatment (control = 0.293 ± 0.006 ms, $n = 24$ fibres; L-NAME = 0.287 ± 0.005 ms, $n = 38$ fibres; $p > 0.05$). Similarly, ES mEPC half-width (Figure 3.10F,G) increased after DETA/NO treatment (control = 1.239 ± 0.034 ms, $n = 24$ fibres; DETA/NO = 1.435 ± 0.039 ms, $n = 33$ fibres; $p < 0.001$). Additionally, the half-width of ES fibres after L-NAME treatment was marginally, but significantly, reduced (control = 1.239 ± 0.034 ms, n

= 24 fibres; L-NAME = 1.142 ± 0.026 ms, n = 38 fibres; $p < 0.05$). In sum, these results suggest that developmental manipulation of NO levels is sufficient to perturb the electrophysiological properties of both embryonic muscle populations.

3.3.4 Developmental effects of NO signalling on the frequency of inputs

Finally the frequencies of mEPCs in both EF and ES muscle fibres were examined. After 18- β -GA application, neither DETA/NO nor L-NAME significantly affected the frequency of EF mEPCs (control = 0.12 ± 0.02 Hz, n = 47; DETA/NO = 0.10 ± 0.03 Hz, n = 17; L-NAME = 0.11 ± 0.02 Hz, n = 46, $p > 0.05$, data not shown) or ES mEPCs (control = 0.08 ± 0.01 Hz, n = 24; DETA/NO = 0.06 ± 0.01 Hz, n = 33; L-NAME = 0.08 ± 0.01 Hz, n = 38; $p > 0.05$, data not shown).

However, during current clamp recordings in which 18- β -GA was excluded from the extracellular saline, DETA/NO decreased (control EF = 0.96 ± 0.07 Hz, DETA/NO treated EF = 0.49 ± 0.07 Hz; control ES = 1.26 ± 0.09 Hz, DETA/NO treated ES = 0.95 ± 0.09 Hz, $p < 0.05$, data not shown) whereas L-NAME increased (control EF = 0.96 ± 0.07 Hz, L-NAME treated EF = 1.24 ± 0.10 Hz; control ES = 1.26 ± 0.09 Hz, L-NAME treated ES = 1.71 ± 0.14 Hz, $p < 0.01$, data not shown) the number of synaptic events.

3.3.5 Acute perturbation of NO signalling does not affect NMJ properties

In order to investigate whether acute manipulation of NO signalling had an effect upon the physiological properties of larval NMJs, DETA/NO (n = 3 EF, n = 3 ES) or L-NAME (n = 4 EF, n = 3 ES) was added to the extracellular saline for 10 min after obtaining

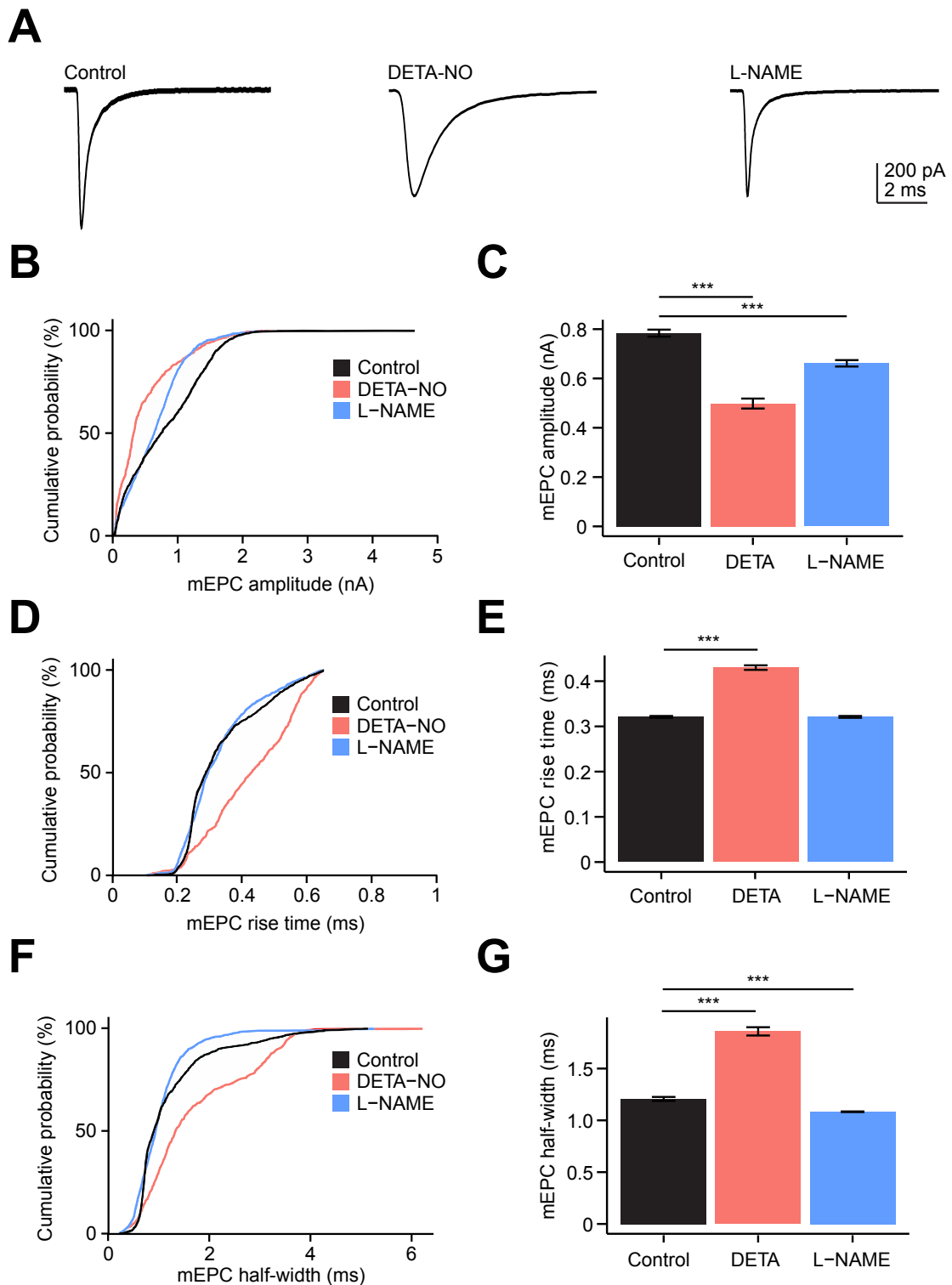


FIGURE 3.9

Developmental perturbation of NO signalling affects EF mEPC kinetics. (A) Average traces of mEPCs captured from EF fibres from control larvae (left) and after chronic DETA/NO (middle) or L-NAME (right) treatment at 2 dpf. (B – G) Cumulative percentage plots and bar charts of EF mEPC amplitude (B, C), rise time (D, E) and half-width (F, G).

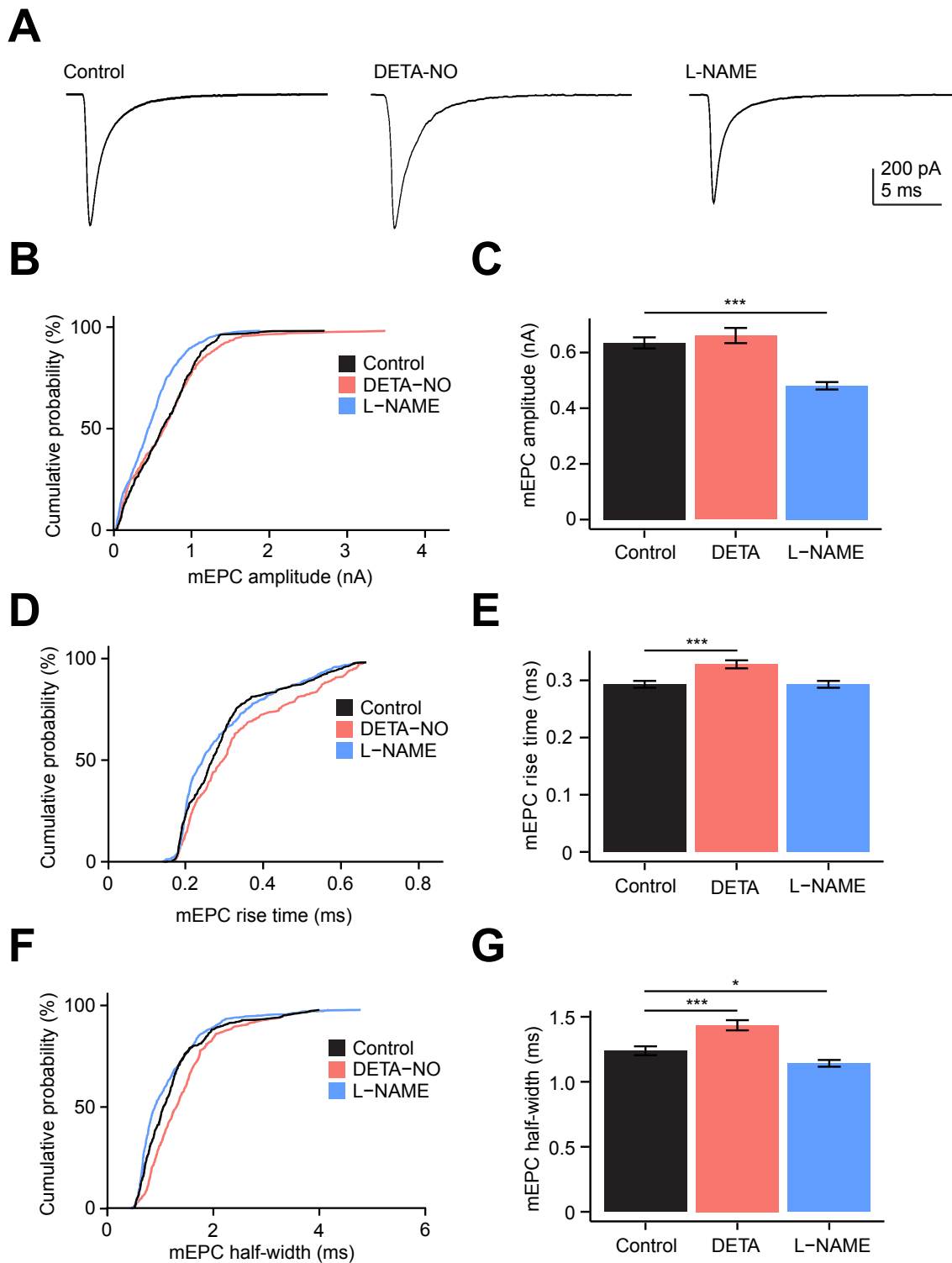


FIGURE 3.10

Developmental perturbation of NO signalling affects ES mEPC kinetics. (A) Average traces of mEPCs captured from ES fibres from control larvae (left) and after chronic DETA/NO (middle) or L-NAME (right) treatment at 2 dpf. (B – G) Cumulative percentage plots and bar charts of ES mEPC amplitude (B, C), rise time (D, E) and half-width (F, G).

whole cell configuration (Figure 3.11A — D). Exposure to either pharmacological agent failed to alter the frequency, amplitude, rise time or half-width of EF or ES mEPCs (Figure 3.11E — H). Thus, transient manipulation of NO signalling does not affect the electrophysiological properties of NMJs at this age.

3.3.6 Developmental perturbation of NO signalling alters the locomotor drive for swimming

Next, the effects of perturbing NO signalling upon locomotor drive to muscle fibres was examined in both EF (Figure 3.12) and ES (Figure 3.13) fibres. First, in order to do this, 18- β -GA was excluded from the extracellular saline and TTX was replaced with a low concentration of (+)-tubocurarine hydrochloride pentahydrate (d-tubocurarine) which permitted observation of the synaptic drive to muscle fibres under more physiological conditions.

Developmental DETA/NO exposure (Figure 3.12A,B) caused a significant decrease in locomotor end plate potential (EPP) amplitude (Figure 3.12D; control = 0.94 ± 0.03 mV; DETA/NO = 0.82 ± 0.05 mV, $p < 0.05$) and increase in rise time (Figure 3.12E; control = 3.40 ± 0.08 ms; DETA/NO = 7.07 ± 0.36 ms, $p < 0.01$) and decay time (Figure 3.12F; control = 12.21 ± 0.08 ms; DETA/NO = 22.24 ± 0.80 ms, $p < 0.001$). Developmental L-NAME exposure also significantly altered the synaptic drive to EF fibres (Figure 3.12A,C). Locomotor EPP amplitudes increased (Figure 3.12D; control = 0.94 ± 0.03 mV; L-NAME = 1.17 ± 0.04 mV, $p < 0.001$) and rise times decreased (Figure 3.12E; control = 3.40 ± 0.08 ms; L-NAME = 2.96 ± 0.08 ms, $p < 0.05$). However, decay times were not affected (Figure 3.12F).

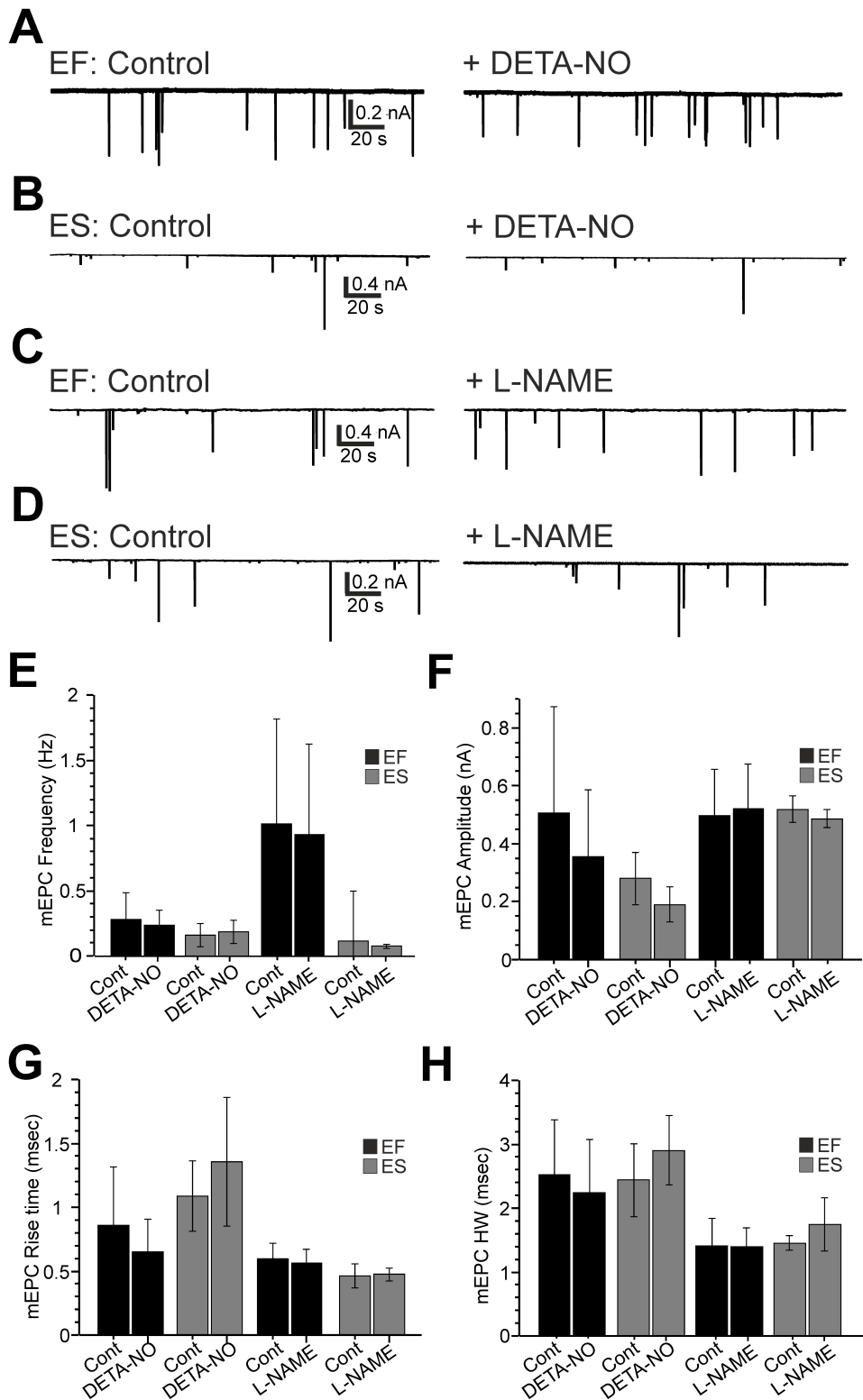


FIGURE 3.11

Acute manipulation of NO levels does not affect mEPC kinetics. (A – D) Representative traces of EF and ES mEPCs in control conditions and after a 10 minute exposure to either DETA/NO (A,B) or L-NAME (C,D). (E – H) Bar charts depicting effects of acute DETA/NO/L-NAME application on mean mEPC frequency (E), amplitude (F) rise time (G) and half-width (H).

Recordings of EPPs from ES fibres also revealed that perturbing NO signalling had marked effects. While neither DETA/NO nor L-NAME affected the amplitude of EPPs (Figure 3.13D), both treatments did significantly affect rise and decay kinetics. Here, DETA/NO dramatically increased EPP rise time (Figure 3.13E; control = 7.02 ± 0.13 ms; DETA/NO = 11.27 ± 0.32 ms, $p < 0.001$) and decay time (Figure 3.13F; control = 20.66 ± 0.29 ms; DETA/NO = 31.29 ± 5.20 ms, $p < 0.001$) durations whereas L-NAME treated fish exhibited a significant decrease in rise (Figure 3.13E; control = 7.02 ± 0.13 ms; L-NAME = 4.80 ± 0.11 ms, $p < 0.001$) and decay time (Figure 3.13F; control = 20.66 ± 0.29 ms; L-NAME = 17.30 ± 0.27 ms, $p < 0.001$).

The frequency and duration of motor episodes was also examined. In order to do this, data from both EF and ES recordings were pooled. In comparison to control fish, EPP frequency of fish raised in DETA/NO was significantly lower at the start, middle and end of the swim episode (Figure 3.14A; $p < 0.001$). Conversely, the frequency of EPPs recorded from L-NAME treated fish was significantly higher throughout the swim episode (Figure 3.14A; $p < 0.001$). Additionally, the duration of fictive swim episodes was significantly shorter in both conditions (Figure 3.14B; control = 15.60 ± 1.98 s; DETA/NO = 4.53 ± 0.60 s; L-NAME = 6.34 ± 0.90 s, $p < 0.001$).

3.3.7 Developmental effects of NO signalling on motoneuron properties

The observation that developmental perturbation of nitrgergic signalling affects parameters of locomotor drive to larval muscle fibres suggested that the electrophysiological properties of spinal networks may also be modified by NO. Therefore, the intrinsic electrophysiological properties of motoneurons were examined after chronic perturba-

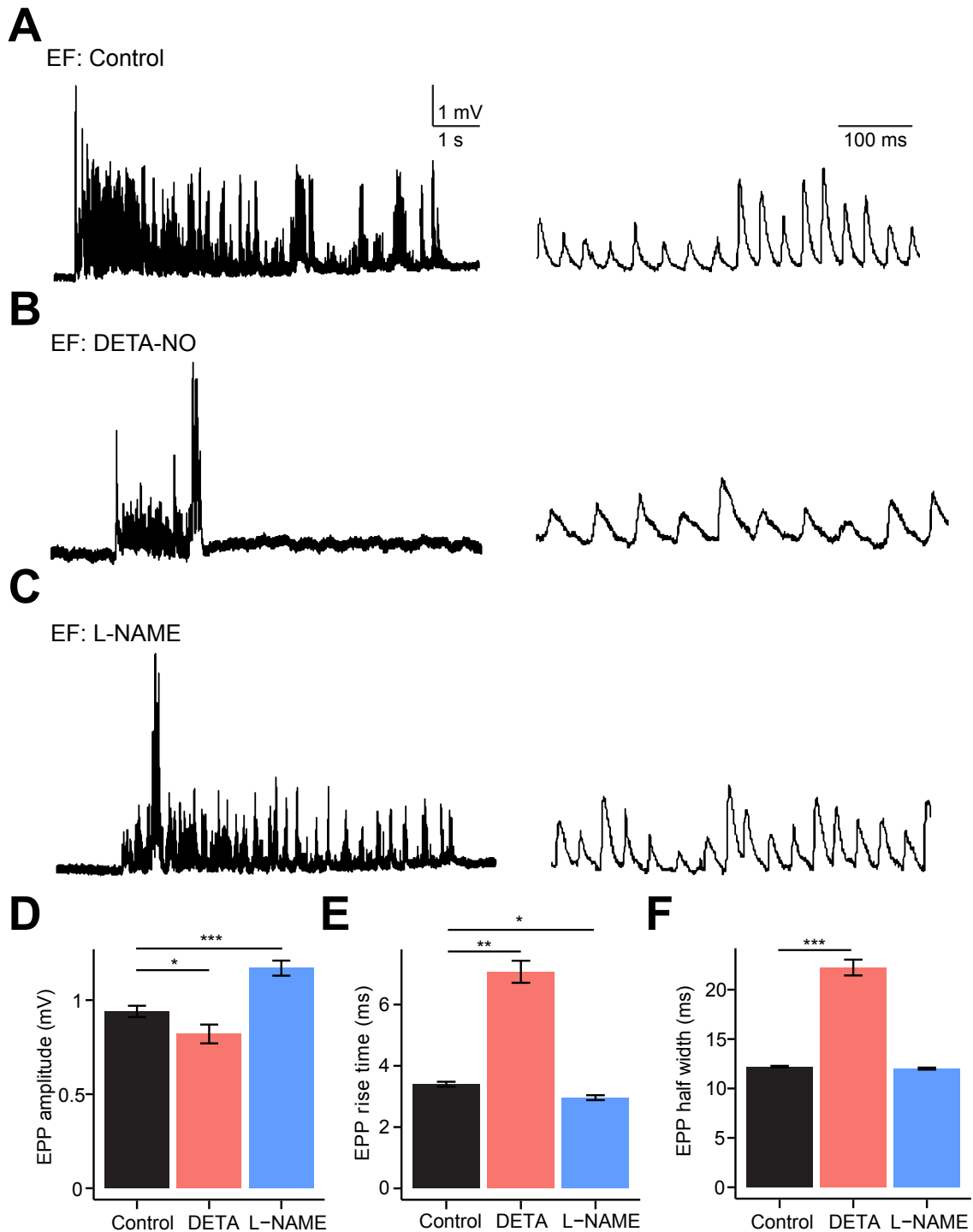


FIGURE 3.12
Developmental NO manipulation perturbs fictive locomotor drive to EF muscle fibres. (A – C) Voltage recordings of locomotor-related drive obtained from embryonic fast (EF) fibres of 2 dpf fish raised in control saline (A), DETA/NO (B) and L-NAME (C). (D – F) Mean EPP amplitude (D), rise time (E) and decay time (F) measured during episodes of fictive swimming.

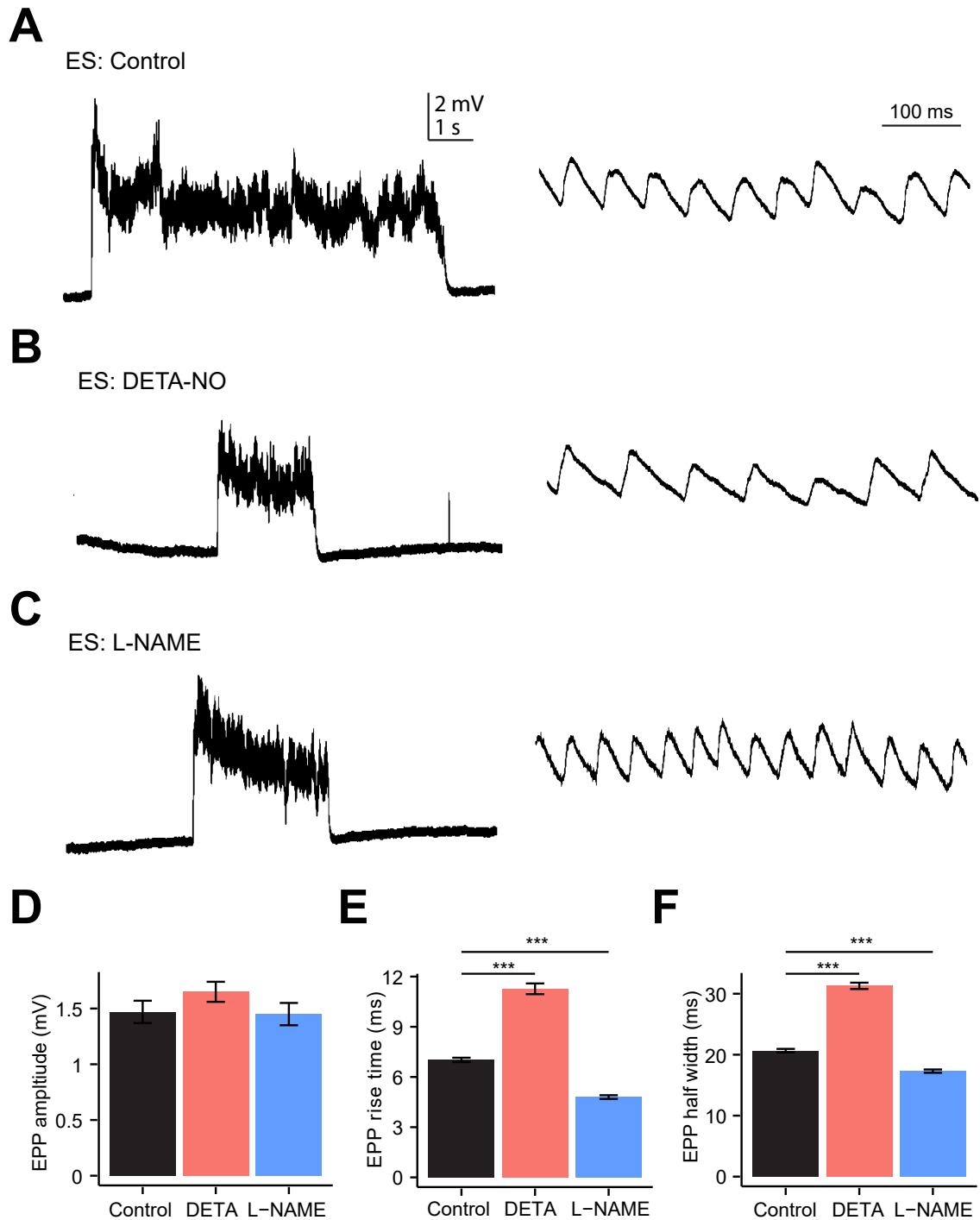


FIGURE 3.13

Developmental NO manipulation perturbs fictive locomotor drive to ES muscle fibres. (A – C) Voltage recordings of locomotor-related drive obtained from embryonic fast (ES) fibres of 2 dpf fish raised in control saline (A), DETA/NO (B) and L-NAME (C). (D – F) Mean EPP amplitude (D), rise time (E) and decay time (F) measured during episodes of fictive swimming.

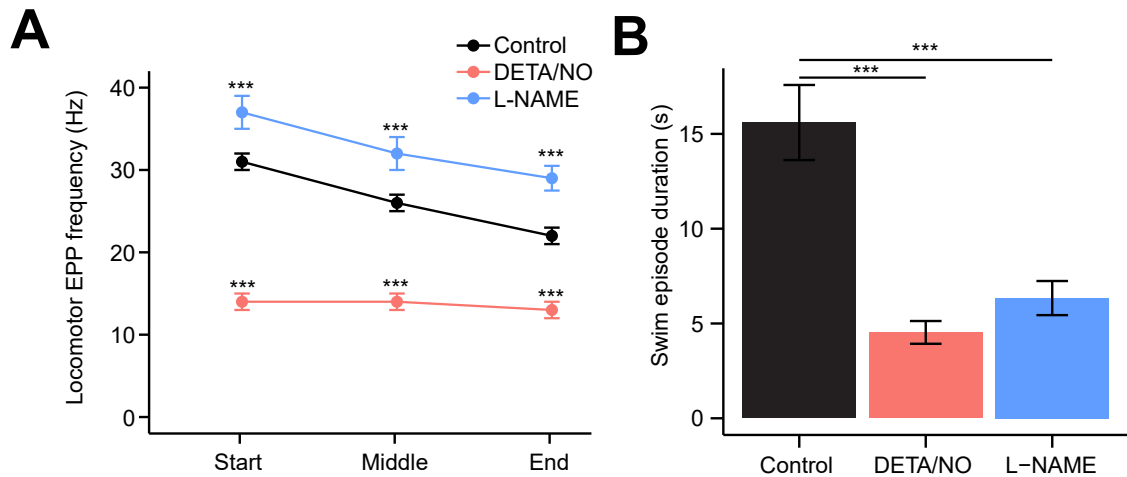


FIGURE 3.14

Developmental effects of NO on the frequency and duration on the neuromuscular drive for locomotion. (A) Line graph of mean (\pm SEM) locomotor-related EPP frequency at the beginning, middle and end of evoked fictive swim episodes in control fish and fish exposed to DETA/NO or L-NAME during development. (B) Bar chart showing mean duration of fictive motor episodes in control, DETA/NO and L-NAME treated fish.

tion of NO signalling. A series of whole cell patch clamp recordings were conducted from identified motoneurons of 2 dpf zebrafish raised in control saline, DETA/NO or L-NAME (Figure 3.15). Mean input resistance (control = 132.63 ± 8.18 M Ω , DETA/NO = 129.55 ± 9.69 M Ω ; L-NAME = 124.36 ± 13.46 M Ω ; $P > 0.05$, Figure 3.15A), rheobase (control = 100.81 ± 6.31 pA, DETA/NO = 80.00 ± 8.72 pA, L-NAME = 118.64 ± 8.74 mV; $p > 0.05$, Figure 3.15B), resting membrane potential (control = 63.46 ± 0.94 mV, DETA/NO = 62.70 ± 0.91 mV; L-NAME = 63.43 ± 0.86 mV; $p > 0.05$, Figure 3.15C), and maximum firing frequency (control = 54.79 ± 8.62 Hz, DETA/NO = 41.71 ± 11.89 Hz, L-NAME = 55.63 ± 9.75 Hz; $p > 0.05$, Figure 3.15D) were not significantly different between treatment groups.

Next, the synaptic inputs to motoneurons were examined. Here, larval zebrafish were bathed in extracellular saline containing TTX and a range of pharmacological reagents in order to isolate specific neurotransmitter systems. Glutamatergic

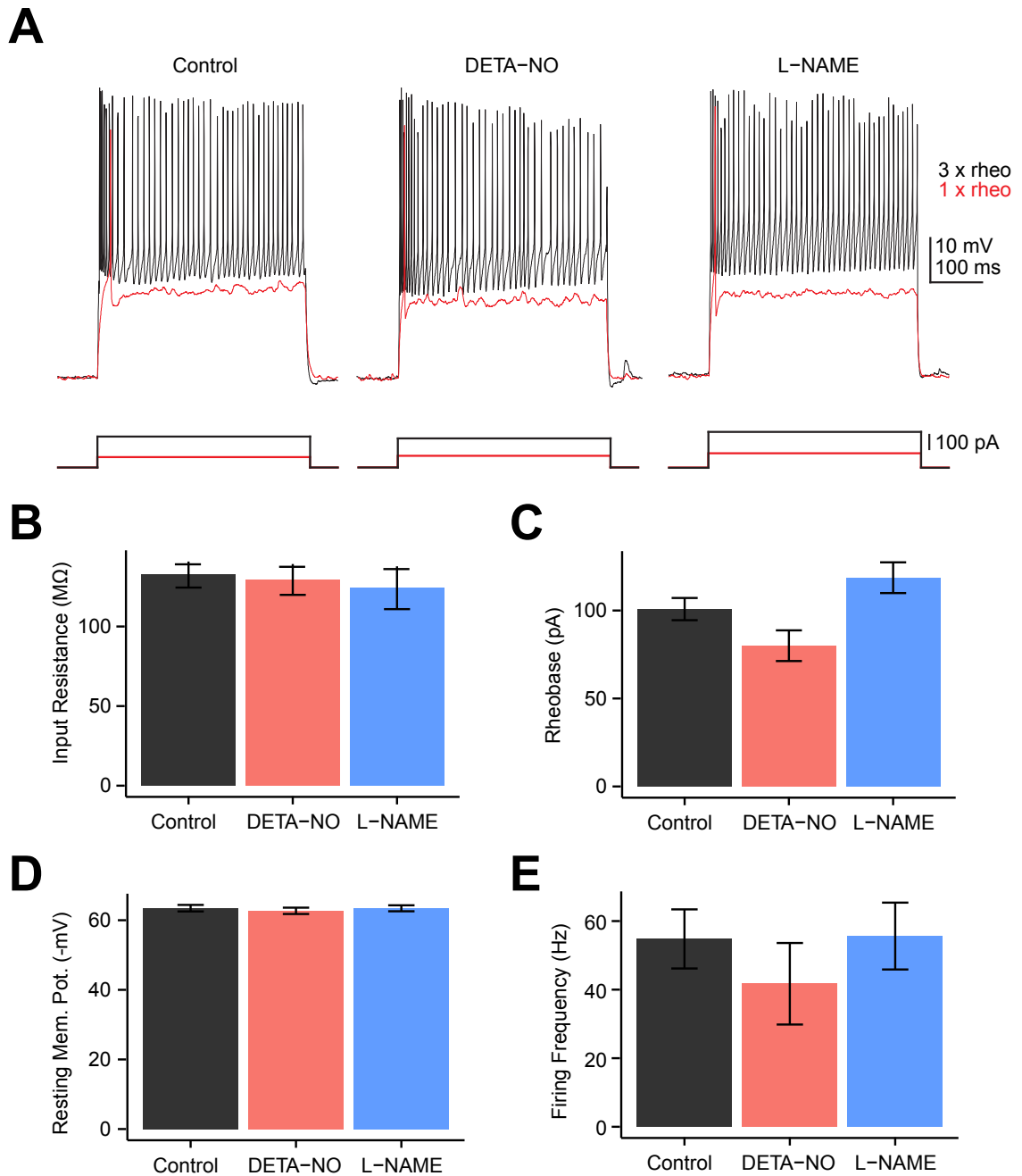


FIGURE 3.15

Developmental effects of NO perturbation on intrinsic properties of motoneurons.

(A) Rheobase current injection (red) generally evokes single action potentials. 3 x rheobase current injection (black) evokes continuous spike trains for the duration of the current step in primary motoneurons. (B – E) Bar charts depicting mean (\pm SEM) input resistance (B), rheobase (C), resting membrane potential (D) and maximum firing frequency (E) in control, DETA/NO and L-NAME conditions.

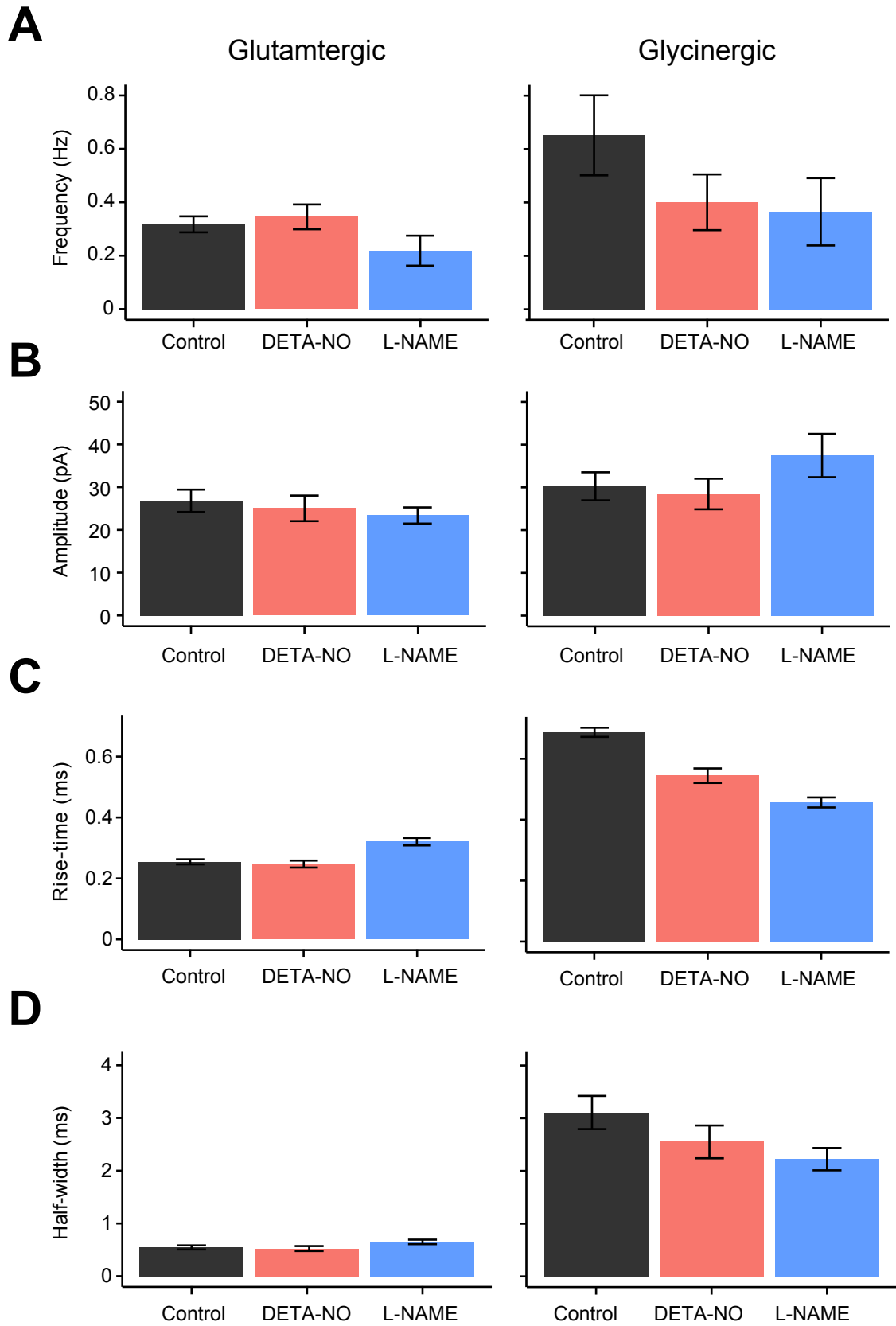


FIGURE 3.16
Developmental effects of NO perturbation on synaptic inputs to motoneurons. (A – D) Mean frequency (A), amplitude (B), rise time (C) and half-width (D) of glutamatergic (left) and glycinergic (right) miniature post synaptic currents (mPSCs).

inputs were isolated by the addition of 1 μ M strychnine and 100 μ M bicuculline in order to block glycinergic and GABAergic inputs, respectively. Analysis of presumed glutamatergic mPSCs from motoneurons revealed no significant differences between larvae raised in control saline (n = 8 fish) and DETA/NO (n = 6 fish) or L-NAME (n = 14 fish) (Figure 3.16). Specifically, the frequency (control = 0.32 ± 0.03 Hz, DETA/NO = 0.34 ± 0.04 Hz, L-NAME = 0.21 ± 0.05 Hz, $p > 0.05$, Figure 3.16A), peak amplitude (control = 26.81 ± 2.62 pA, DETA/NO = 25.05 ± 2.99 pA, L-NAME = 24.39 ± 1.89 pA, $p > 0.05$, Figure 3.16B), rise time (control = 26.81 ± 2.62 ms, DETA/NO = 25.05 ± 2.99 ms, L-NAME = 24.39 ± 1.89 ms, $p > 0.05$, Figure 3.16C) and half-width (control = 0.55 ± 0.03 ms, DETA/NO = 0.53 ± 0.04 ms, L-NAME = 0.65 ± 0.04 ms, $p > 0.05$, Figure 3.16D) of presumed glutamatergic inputs were all unchanged. Next, glycinergic inputs were examined after block of glutamatergic and GABAergic receptors with kynurenic acid (KYN) and picrotoxin, respectively. Recordings from control (n = 9 fish), DETA/NO (n = 6) and L-NAME (n = 10) raised fish revealed no significant effect of NO signalling perturbation for presumed glycinergic inputs: the frequency (control = 0.65 ± 0.14 Hz, DETA/NO = 0.40 ± 0.10 Hz, L-NAME = 0.36 ± 0.13 Hz, $p > 0.05$, Figure 3.16A), peak amplitude (control = 30.25 ± 3.28 pA, DETA/NO = 28.45 ± 3.59 pA, L-NAME = 37.45 ± 5.06 pA, $p > 0.05$, Figure 3.16B), rise time (control = 30.25 ± 3.28 ms, DETA/NO = 28.45 ± 3.59 ms, L-NAME = 37.45 ± 5.06 ms, $p > 0.05$, Figure 3.16C) and half-width (control = 3.01 ± 0.31 ms, DETA/NO = 2.55 ± 0.31 ms, L-NAME = 2.22 ± 0.21 ms, $p > 0.05$, Figure 3.16D) were all unchanged. In sum, these findings strongly suggest that developmental manipulation of NO signalling has no effect on the maturation of intrinsic motoneuron properties or the synaptic inputs to motoneurons.

3.4 Discussion

NO-dependent signalling is known to regulate axonal branching of developing motoneurons in zebrafish such that chronic inhibition of NO activity markedly increases the number of axon branches whereas exogenous increases in the levels of NO signalling has the opposite effect (Bradley et al., 2010). Whilst these observations strongly suggest that NO-dependent signalling influences zebrafish motor axon growth, the consequences for NMJ development had not been investigated in detail. The work presented in this chapter demonstrates three key findings. Firstly, disruption of NO signalling during ongoing axogenesis is sufficient to disrupt the number of NMJs within the developing musculature. Secondly, the physiological properties of these NMJs is markedly altered by NO signalling. Finally, by conducting *in vivo* recordings from unanaesthetised zebrafish larvae, it is demonstrated that developmental perturbation of NO-dependent signalling affects behaviourally relevant locomotor network output. However, these effects are unlikely to arise as a consequence of modulating the intrinsic properties of motoneurons or their synaptic inputs. In sum, these data provide *in vivo* evidence that NO signalling affects NMJ and locomotor maturation in larval zebrafish.

3.4.1 NO/cGMP-dependent regulation of NMJ formation

The findings summarised here demonstrate that exogenous elevation of NO/cGMP levels is sufficient to inhibit, whilst developmental inhibition of NO/cGMP synthesis promotes, formation of NMJs within the developing musculature. These changes likely

arise as a consequence of perturbing axonal growth, rather than a direct effect on the rate of neuromuscular junction addition: if NO was necessary for formation of NMJs along axon branches, a change in the density of axon branch-associated NMJs would be expected, yet this was not observed.

Whilst NO was observed to disrupt the absolute number of NMJs along axon branches, it did not significantly alter the number of NMJs located along the motoneuron fascicle. These results may in part be explained by the experimental protocol. Motoneurons begin to project from the spinal cord and innervate the developing muscle tissue at ≈ 17 hpf (Myers et al., 1986; Plazas et al., 2013). Within the work presented in this chapter, embryos were not exposed to pharmacological reagents until 24 hpf, by which point motoneuron fascicles have been established and they have incorporated ACh receptor clusters which form prior to neuronal innervation (Flanagan-Steet et al., 2005; Panzer et al., 2005, 2006; Jing et al., 2009, 2010). This raises the question of whether NO could modulate the development or incorporation of NMJs prior to 24 hpf. Studies examining NO-dependent regulation of NMJ formation in other vertebrate species (Jones and Werle, 2000; Godfrey and Schwarte, 2003; Schwarte and Godfrey, 2004; Godfrey et al., 2007; Godfrey and Schwarte, 2010) suggest NO/cGMP signalling can modulate the earliest stages of NMJ formation by promoting ACh receptor aggregation in muscle fibres before motoneuron innervation. However, this is unlikely to be the role of NO in zebrafish given that NOS1 expression is not observed until 30 hpf (i.e. after AChR clustering). Furthermore, expression of NOS is restricted to the spinal cord of zebrafish between 1 and 3 dpf (Poon, 2003; Holmqvist et al., 2004; Bradley et al., 2010) whilst NOS1 is expressed throughout mammalian skeletal muscle (Marletta, 1993; Kobzik et al., 1994; Chao et al., 1996; Kapur et al., 1997; Grozdanovic and

Gossrau, 1998; Ribera et al., 1998; Grozdanovic, 1999; Stamler and Meissner, 2001) which may serve as the source of NO which regulates the early stages of NMJ development. Thus the earliest stages ($\approx 17-30$ hpf) of zebrafish NMJ development are likely to be NO-independent and perturbation of NO-signalling prior to this is unlikely to have a physiological role during neuromuscular synaptogenesis along the fascicle.

In this chapter, NO appears to have primarily inhibitory effects upon axonal outgrowth, in agreement with previous reports examining the effects of NO upon motoneuron development (Bradley et al., 2010). In many other systems, NO can also modulate axonal outgrowth and synaptic inputs (Campello-Costa et al., 2000; Wu, 2002; Schmidt et al., 2002; Haase and Bicker, 2003; Tegenge et al., 2011b). In these studies, NO tends to promote axon outgrowth and refine synaptic connections. In the developing visual system for example, nascent ganglion neurons of the retina project to the superior colliculus to form a topographic representation of the visual field. These axonal projections undergo extensive refinement and reduction in number. NO has been shown to modulate this process (Campello-Costa et al., 2000; Wu et al., 2000, 2001; Schmidt et al., 2002) such that NO synthesis is necessary for the refinement of these axonal projections. Could a similar mechanism of synapse refinement account for the observed changes in the present study? In the early stages of mammalian neuromuscular synaptogenesis, muscle fibres are typically innervated by more than one motor neuron (Sanes and Lichtman, 1999). During postnatal development, excess synaptic connections are eliminated such that muscle fibres are finally innervated by one synapse (Sanes and Lichtman, 1999). However, in the developing zebrafish, motoneuron axons undergo little pruning and muscles remain polyneuronally innervated (Westerfield et al., 1986; Liu and Westerfield, 1990). Thus the role of NO at the

zebrafish NMJ is unlikely to regulate the retraction of axonal branches. Instead, NO may regulate axonal branching by modulating the rate of axonal branch outgrowth rather than pruning of excess axon branches. However, NO appears to serve inhibitory functions in zebrafish while in mammals, avian and invertebrate species, NO tends to facilitate axonal outgrowth (Schmidt et al., 2002; Steinbach et al., 2002; Xiang et al., 2002; Haase and Bicker, 2003; Xiong et al., 2007). Future investigations examining motoneuron outgrowth and branching will help elucidate the underlying function of NO.

3.4.2 Use of 18- β -Glycyrrhetic acid as a gap junction blocker

When performing experiments examining mEPC kinetics, 18- β -GA, a gap junction blocker (Davidson and Baumgarten, 1988), was included in the extracellular saline in order to reduce currents arising from electrically coupled neighbouring fibres. This drug has previously been used for the same purpose (Luna and Brehm, 2006). Addition of 18- β -GA to the extracellular saline caused several changes congruent with the premise that 18- β -GA successfully abolished currents arising from coupled fibres. In both populations of muscle fibres transcellular dye spread was successfully abolished, in agreement with Luna and Brehm (2006). Electrophysiological properties were also significantly affected: both the input resistance of the muscle fibre and amplitude of mEPCs increased. However, in contrast with other investigations (Luna and Brehm, 2006) a population of small amplitude mEPCs with slow kinetics persisted in both EF and ES muscle fibres. When conducting paired recordings between muscle fibres, these events could often be observed to occur concurrently. This observation suggests that addition of 18- β -GA is insufficient to effectively block current flow through gap junctions

and its use as a gap junction blocker should be reconsidered in future investigations.

3.4.3 NO-dependent loss of inputs modulates musculature innervation

When 18- β -GA was omitted from the extracellular saline, the frequency of mEPC events decreased after developmental increases in NO levels. The opposite was also true: decreases in endogenous NO levels significantly increased the frequency of events. These differences in frequency were not observed when 18- β -GA was included in the extracellular saline. These results, when considered in light of the effects on NMJ number and axonal branching (Bradley et al., 2010), suggest these effects arise as a consequence of alterations in innervation of the musculature.

Muscle fibres show extensive electrical coupling at embryonic stages. For example, at 1 dpf, transcellular dye spread is observed across approximately 23 ES and 8 EF muscle fibres (Buss and Drapeau, 2000). Whilst 18- β -GA fails to completely abolish electrical coupling, it does appear to significantly reduce coupling between muscle fibres as evidenced by block of transcellular dye labelling and reduced mEPC frequencies. Thus, the number of muscle fibres from which inputs could be recorded would be markedly reduced and thus may explain the observed differences here.

3.4.4 Electrophysiological consequences of NO perturbation on NMJs

To determine whether the NO-dependent modulation of NMJ number had physiological consequences, a series of *in vivo* patch clamp recordings were conducted in order to monitor mEPCs from EF and ES muscle fibres. Here, developmental manipulation of NO signalling had a marked effect in both muscle fibre populations. Previous studies

have demonstrated that the electrophysiological properties of synaptic inputs to muscle fibres change during NMJ development (Drapeau et al., 2001; Buss and Drapeau, 2000, 2002; Nguyen et al., 1999). Shortly after the developing NMJs become functional (\approx 1 dpf), synaptic inputs have small amplitudes and slow rise and decay kinetics. As development continues, mEPC amplitudes increase, while the rise and decay times shorten. In the work presented here, developmental manipulation of NO signalling had a marked effect upon mEPC kinetics in both muscle types. Exogenous elevation of NO slowed rise and decay times whilst decreased levels of NO shortened the half-width, but had no effect on rise time in both populations.

Such changes in synaptic current could arise from several contributing physiological changes. For example, ACh receptors undergo developmentally-related changes in their subunit composition which has consequential effects on their electrophysiological and functional properties (Mishina et al., 1986; Gu and Hall, 1988; Naranjo and Brehm, 1993; Missias et al., 1996; Mongeon et al., 2011; Walogorsky et al., 2012a,b; Park et al., 2014). At embryonic stages ACh receptors are composed of five subunits: $\alpha_1\beta\delta\gamma$. As the embryo develops, the γ subunit is replaced by an ϵ subunit such that by adult stages, NMJs are comprised of $\alpha_1\beta\delta\epsilon$ subunits (Mishina et al., 1986; Walogorsky et al., 2012a). Within the developing zebrafish the precise time course for the switch from γ to ϵ subunits has yet to be examined in detail. However, it would appear that ACh receptors have begun to incorporate the ϵ subunit by 48 hpf (Walogorsky et al., 2012b). This is a gradual process and appears to be complete by 8 dpf. In the *twister* mutant, the AChRs lack a functional α subunit, which renders embryonic locomotor output perturbed. Instead of engaging in stereotypical coiling behaviour, *twister* mutants exhibit co-contraction of contralateral muscle groups (Lefebvre et al.,

2004). However, as receptors begin to incorporate the ϵ subunit, AChRs functionally recover such that locomotor output is equivalent to wild-type larvae by 8 dpf (Walogorsky et al., 2012b). This process begins before 3 dpf, as evidenced by partial rescue of locomotor output in *twister* mutants by this age. Receptors which express the γ subunit generate prolonged currents whereas the ϵ subunit shortens both the rise and decay times (Naranjo and Brehm, 1993; Walogorsky et al., 2012a,b). Such changes in subunit composition may partly explain the observed changes within this study: increases in NO may have suppressed the switch from immature to mature subunits in EF fibres. However, because ES fibres do not exhibit changes in subunit composition (Mongeon et al., 2011) the slowing of rise and decay kinetics here must be attributable to other mechanisms.

Changes in the the number of ACh receptors or the concentration of acetylcholinesterase (AChE), which hydrolyses ACh and thus accelerates the decay of ACh-mediated currents, may also contribute to the observed changes (Kullberg et al., 1980; Nguyen et al., 1999). Block of AChE at embryonic stages (1 dpf) has no effect upon the kinetics of mEPCs but by larval stages (6 dpf), AChE inhibition causes a significant slowing of the mEPC decay (Nguyen et al., 1999). However, it should be noted the decay phase after AChE block is not comparable to that of embryonic mEPC kinetics suggesting several factors contribute to the observed developmentally-associated changes in mEPC kinetics. In order to elucidate the mechanisms underpinning the observed changes in physiological properties, future investigations are required. Having an understanding of the changing composition of AChR subunits, concentration of AChE and changes in ACh receptor distribution will help shed light on the potential causes of the observed changes in mEPC kinetics.

3.4.5 Effects of NO on locomotor drive and spinal networks

Previous work has identified NO as an important neuromodulator of ongoing locomotor output. The effects of acute manipulation of NO signalling have been well described in developing *Xenopus*. Here, NO tends to have suppressive effects, slowing cycle frequency and the duration of fictive swim episodes (McLean and Sillar, 2000, 2002, 2004). Similarly, within the postnatal mouse spinal cord, NO slows the frequency of fictive swim episodes (Foster et al., 2014). However, in the adult lamprey, NO plays an excitatory role, increasing swim frequency by a concomitant decrease in midcycle inhibition and increase in oncycle excitation (Kyriakatos et al., 2009).

While these investigations demonstrate that acute changes in NO levels are sufficient to modify locomotor output, the consequences of developmental perturbation of NO signalling upon locomotor network maturation have not been examined in detail. However, in freely behaving zebrafish, chronic disruption of NO signalling between 24 and 48 hpf has marked effects on locomotor output (Bradley et al., 2010) whereby developmental increases in NO significantly slows the velocity of swim episodes by $\approx 60\%$ and tail beat frequency by 20%. Conversely, inhibition of endogenous NO signalling from 24–48 hpf is sufficient to have the opposite effect whereby swim episodes are faster and tail beat frequencies increased (Bradley et al., 2010). In this chapter, the effects of perturbing NO signalling upon the neural correlate for locomotor output were examined. These results were in broad agreement with the effects of NO perturbation upon freely behaving larvae such that the frequency of drive to the muscle tissue was slower after DETA/NO (increased NO), or faster after L-NAME (decreased NO), application. The duration of fictive episodes were also significantly shortened by

both increases and decreases in NO signalling.

In addition to affecting the duration and frequency of fictive locomotor episodes, NO also affected the kinetics of locomotor-related EPPs. In EF and ES muscle fibres, DETA-NO significantly increased the rise and decay phase of EPPs. Similarly, the half-width was significantly prolonged in both muscle fibre populations. Chronic decreases in NO signalling had mostly opposite effects upon ES fibres, causing a shortening of the rise and decay kinetics. However, within EF fibres, L-NAME induced a modest decrease in rise time but failed to induce any change in half-width. Changes in the amplitude of EPPs were also observed, but these were restricted to EF fibres.

These changes may, in part, arise as a consequence of the previously discussed changes in mEPC kinetics. Specifically, DETA/NO, which slowed the rise and decay kinetics of mEPCs may also have comparable effects upon EPPs. Similarly, L-NAME decreased the kinetics of mEPCs and this would be expected to have the opposite effect. However, other factors may also contribute to this phenomenon. Interestingly, in studies examining the acute effects of NO signalling, NO tends to facilitate inhibitory synaptic input while depressing the excitatory drive to spinal networks (McLean and Sillar, 2000, 2002, 2004; Foster et al., 2014). The net effect of these short-term modifications is a significant slowing in cycle frequency, shortening of locomotor episodes and reduced synaptic drive to the periphery. In the work presented in this chapter, disruption of NO signalling over the second day of development had similar effects. Could then chronic disruption of NO levels be causing permanent changes in spinal locomotor networks? As a first step toward addressing this possibility, the electrophysiological properties of primary motoneurons in fish exposed to DETA/NO or L-NAME during development were examined. These treatments had no effect on rheobase,

firing frequency, input resistance or absolute action potential amplitude. Taken together, these findings suggest that NO does not directly modulate intrinsic excitability of primary motoneurons. Nonetheless, it remains possible that NO-dependent effects on the properties of spinal interneurons may contribute to the observed changes in locomotor patterning. Indeed, NO is known to modulate locomotor output within *Xenopus* and lamprey spinal networks by altering neurotransmitter release from premotor interneurons (McLean and Sillar, 2001, 2002, 2004; Kyriakatos and El Manira, 2007; Kyriakatos et al., 2009). However, these effects appear to be species specific. In early embryonic and larval *Xenopus* preparations (McLean and Sillar, 2001, 2002, 2004), addition of NO donors tends to have a suppressive effect on fictive swimming, shortening the duration and slowing the frequency of swim episodes. This is achieved primarily via modulation of glycinergic and GABAergic inputs to spinal motor networks and descending inputs (McLean and Sillar, 2001, 2004). In lamprey preparations, exogenous increases in NO levels have long-term consequences, inducing an increase in locomotor frequency by potentiation of excitatory inputs and inhibition of midcycle reciprocal inhibition (Kyriakatos and El Manira, 2007; Kyriakatos et al., 2009). In this chapter, developmental perturbation of NO signalling did not significantly affect the frequency or kinetics of glutamatergic and glycinergic mEPCs observed from primary motoneurons. While these data suggest that NO does not mediate the development of inputs to this neuronal population, it remains possible that NO may mediate its effects by modulating the intrinsic properties of interneurons or descending inputs. Future studies examining the effects of NO on premotor circuitry will help to resolve this issue.

Primary motoneurons, which extend from the spinal cord to innervate the musculature first, appear to exclusively innervate the EF fibres (Myers, 1985; West-

erfield et al., 1986; Liu et al., 1988). In contrast, the secondary motoneurons which have few axonal projections innervate both EF and more superficial ES fibres. Interestingly, primary motoneurons appear uniquely sensitive to NO-dependent modulation of axonal branching (Bradley et al., 2010). Thus, the observed changes in EPP amplitude may arise from a change in the innervation of EF muscle fibres.

In summary, the data presented in this chapter provide strong evidence that NO serves as a developmental regulator of NMJ maturation in zebrafish. These observations provide further support for the hypothesis that NO is a fundamentally important signalling molecule during periods of NMJ synaptogenesis and locomotor maturation.

**The Developing Cellular Properties of
Spinally Projecting Dopaminergic
Neurons**

4.1 Introduction

Dopamine (DA) is a key neurotransmitter within the central nervous system (CNS) where it plays modulatory roles in a number of behavioural processes spanning motor control, motivation, states of arousal, cognition and reward behaviour (Jackson and Westlind-Danielsson, 1994; Missale et al., 1998; Wise, 2004). Neurodegeneration or dysfunction of dopaminergic (DAergic) pathways within the nervous system can lead to an array of motor behaviour symptoms including bradykinesia, rigidity, tremors and deficits in cognitive function which are symptomatic of common neurodegenerative diseases such as Parkinson's and Huntington's disease (Mehler-Wex et al., 2006; Iversen and Iversen, 2007; Rodriguez-Oroz et al., 2009) or sensorimotor disorders such as restless leg syndrome (Ondo et al., 2000; Clemens et al., 2006; Qu et al., 2007; Earley et al., 2009).

The primary source of DA within the spinal cord arises from a population of DAergic cells located in the diencephalon (Björklund and Skagerberg, 1979; Hökfelt et al., 1979; Smeets and González, 2000; Rink and Wullimann, 2002; Qu et al., 2006; Barraud et al., 2010; Tay et al., 2011; Koblinger et al., 2014). Despite a growing body of evidence to suggest that this population of DAergic cells can influence the development and output of spinal networks, the physiological properties of these cells have yet to be described. This is in part due to the inaccessibility of this cell population in most vertebrate species, which precludes detailed *in vivo* electrophysiological analysis. In this chapter, I have begun to describe the physiological properties of the descending DAergic neurons over the first four days of zebrafish development, a period marked by profound changes in locomotor network ontogeny and output.

4.1.1 Dopamine synthesis

In vertebrates DA is synthesised from L-tyrosine in a two step process (Figure 4.1). First, L-tyrosine is converted into L-3,4-dihydroxyphenylalanine (L-DOPA) by the enzyme tyrosine hydroxylase (TH). Second, L-DOPA is converted to DA by aromatic L-amino acid decarboxylase (AADC). Production of noradrenaline (NA) or adrenaline from DA is reliant upon the presence of dopamine- β -hydroxylase (D β H) to produce NA and phenylethanolamine N-methyltransferase (PNMT) for further conversion of NA to adrenaline. Once synthesised, DA is packaged into synaptic vesicles by vesicular monoamine transporter 2 (VMAT2). Upon stimulation of the presynaptic neuron, DA is exocytosed from somatodendritic sites or into the synaptic cleft where it binds to presynaptic autoreceptors or postsynaptic receptors. The immediate effects of DA are then terminated largely by reuptake through dopamine transporter (DAT), a membrane-bound protein located near presynaptic terminals (Chen and Reith, 2000; Eriksen et al., 2010). DA can then be recycled into synaptic vesicles by VMAT2. Alternatively, DA is also subject to metabolic degradation by monoamine oxidase (MAO) or catechol-o-methyl transferase (COMT), the latter of which produces 3-methoxytyramine (3-MT), a compound largely thought to be biologically inactive but may serve some neuromodulatory roles (Sotnikova et al., 2010).

4.1.2 Dopamine receptors and downstream signalling pathways

In vertebrates the effects of DA are mediated by a family of G-protein coupled receptors (GPCRs) of which there are five types (D₁ – D₅) that can be divided into two families based on their structural, pharmacological and functional properties. The D₁-like

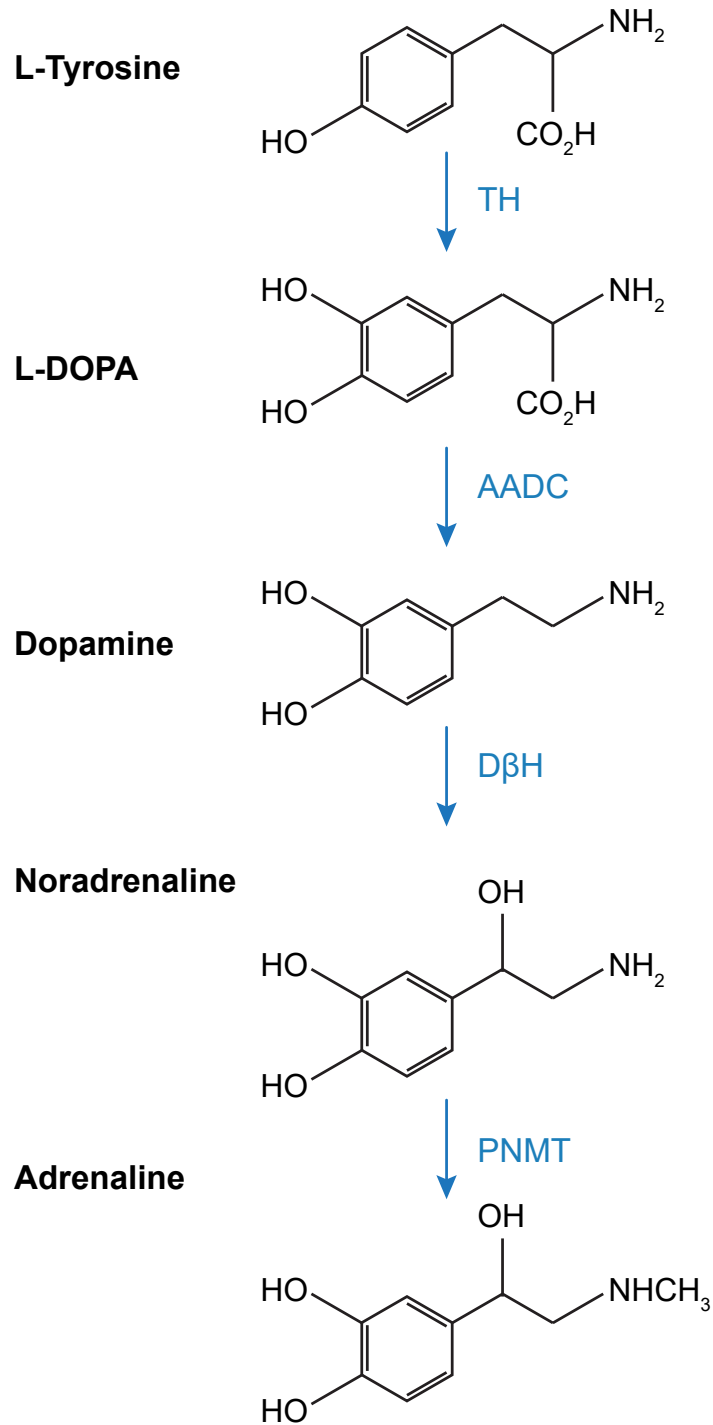


FIGURE 4.1

Biosynthesis pathway for the catecholamines. The catecholamines are derived from L-tyrosine by a number of steps. L-tyrosine is converted to L-DOPA by tyrosine hydroxylase (TH). The conversion from L-DOPA to dopamine is mediated by aromatic L-amino acid decarboxylase (AADC). If present, dopamine-β-hydroxylase (DβH) converts dopamine to noradrenaline. Finally, phenylethanolamine N-methyltransferase (PNMT) is necessary for the production of adrenaline.

family consist of the D₁ and D₅ receptors, and the D₂-like receptor family comprises the D₂, D₃ and D₄ receptors (Jaber et al., 1996; Missale et al., 1998). The distinction between both classes is based primarily on early experiments examining modulation of adenylyl cyclase (AC) activity (and subsequent 3'-5'-cyclic adenosine monophosphate (cAMP) production) by DA receptor activation (Spano et al., 1978; Keibian and Calne, 1979). The D₁-like class of dopamine receptors activate AC by coupling with the stimulatory G α_s G-protein. In contrast, the D₂-like receptors activate the inhibitory G α_i family of G-proteins which reduces levels of AC. This enzyme, AC, is responsible for the conversion of adenosine triphosphate (ATP) to cAMP, a secondary messenger implicated in many physiological processes. Thus, D₁-like and D₂-like receptors act in an antagonistic manner to modulate synthesis of cAMP. The primary target for cAMP is protein kinase A (PKA), a tetrameric enzyme consisting of two regulatory subunits bound to two catalytic subunits (Scott, 1991). Increased cellular levels of cAMP promote PKA activity by binding to the regulatory subunits which subsequently disassociate to expose the active sites of the catalytic PKA. The catalytic subunits can then phosphorylate a vast array of target proteins to modulate activity patterns (Walsh et al., 1968; Keibian and Calne, 1979; Meinkoth et al., 1993). For example, activation of PKA can increase glutamate cell surface receptor expression (Price et al., 1999; Sun et al., 2005; Gao and Wolf, 2007) or phosphorylate voltage-gated sodium channels, which reduces peak amplitude of Na⁺-mediated currents (Li et al., 1992; Murphy et al., 1993; Cantrell et al., 1997; Smith and Goldin, 1997).

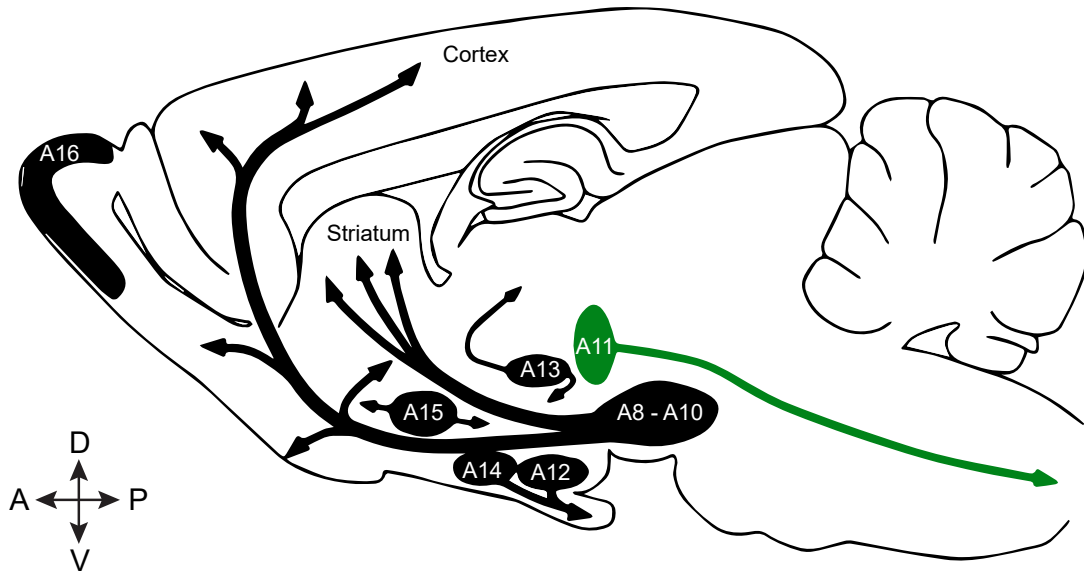


FIGURE 4.2

Distribution of DAergic cells in the adult rat brain. By adult stages, DAergic cells are distributed into nine groups, A8 – A16. The DAergic cluster which descends into the spinal cord arises from the A11 cluster (green). Redrawn from (Björklund and Dunnett, 2007).

4.1.3 The mammalian dopaminergic system

The catecholaminergic (CAergic) cell populations were first described by Dahlstroem and Fuxe (1964) whom identified twelve CAergic cell groups, designated A1 – A12. Further analysis revealed A1 – A7 as noradrenergic (NAergic) and A8 – A12 as DAergic. Subsequent studies later identified an additional five DAergic cell populations (A13 – A17) such that there are ten DAergic (Figure 4.2) and seven NAergic cell groups (see Björklund and Dunnett (2007) for review).

4.1.3.1 Ascending DAergic pathways

The majority of the DAergic cell populations contribute to four major ascending dopaminergic pathways: the mesocortical, mesolimbic, nigrostriatal and tuberoinfundibular pathways. The nigrostriatal pathway consists of DAergic neurons (A8 and

A9 cell groups) that arise in the substantia nigra and project to the striatum. This structure is involved in the generation and modulation of voluntary motor behaviour (Kravitz and Kreitzer, 2012). The DAergic projections arising from the striatum are thought to be important in this context since loss of the DAergic cells in this region is associated with Parkinson's disease in humans and perturbations of this pathway in animal models is sufficient to induce Parkinson's disease-like states (Oberlander et al., 1979; Joh and Weiser, 1993; Ichitani et al., 1994; Chang et al., 1999; Kim et al., 2003).

The mesolimbic pathway arises from the ventral tegmental area (DAergic cell group A10) and projects to subcortical limbic regions including the nucleus accumbens of the striatum, olfactory tubercle and amygdala. This pathway has been associated with numerous functions including, for example, reward behaviour. Loss of this DAergic pathway by localised injections of 6-hydroxydopamine (6-OHDA), a neurotoxic compound which preferentially destroys DAergic neurons (Kostrzewa and Jacobowitz, 1974), is sufficient to attenuate the rewarding effects of drugs (Lyness et al., 1979; Robbins and Koob, 1980; Roberts and Koob, 1982; Caine and Koob, 1994). Dysfunction of this pathway has also been implicated in other conditions including schizophrenia (Hietala and Syvälahti, 1996; Di Forti et al., 2007) and attention deficit hyperactivity disorder (ADHD) (Wu et al., 2012).

Like the mesolimbic pathway, the mesocortical pathway comprises of DAergic cells which arise from the A10 cell group. However, in contrast, these cells send projections to frontal cortex regions. This brain region has been implicated in high-level executive functions such as working memory, reasoning and problem solving (Miller et al., 2002). DAergic inputs to this region appear to be necessary for proper cognitive

activity since dysregulation of the mesocortical pathway is sufficient to perturb many of these functions (Goldman-Rakic, 1992).

The fourth ascending pathway, the tuberoinfundibular pathway, projects from the arcuate nucleus (A12) and periventricular nucleus (A14) of the hypothalamus to the pituitary gland, where it influences release of numerous hormones (Ben-Jonathan and Hnasko, 2001; Missale et al., 1998).

4.1.3.2 Descending DAergic pathways

In addition to the four major ascending pathways, a further pathway, which projects down the entire extent of the spinal cord is also present. This DAergic tract arises from the A11 population located in the hypothalamus. This small cluster of ≈ 150 – 300 neurons within the rat (Skagerberg and Lindvall, 1985) and ≈ 8000 neurons in non-human primates (Barraud et al., 2010) provides the only known source of DA to spinal networks (Björklund and Skagerberg, 1979; Hökfelt et al., 1979; Skagerberg and Lindvall, 1985; Barraud et al., 2010; Koblinger et al., 2014). Immunohistochemical approaches in a range of species have begun to characterise the composition of enzymes within the A11 population in order to elucidate their functional characteristics (Lorang et al., 1994; Ciliax et al., 1999; Qu et al., 2006; Charbit et al., 2009; Barraud et al., 2010; Koblinger et al., 2014). In adult mice, these cells contain the required enzymes for the synthesis and packaging of DA into synaptic vesicles (Charbit et al., 2009; Koblinger et al., 2014). Specifically, they are TH, AADC and VMAT2 positive. However, neither the cell bodies nor axonal projections of the A11 population contain DAT (Koblinger et al., 2014). These results are in broad agreement with human (Ciliax et al., 1999; Earley et al., 2009) and rat (Björklund and Skagerberg, 1979; Hökfelt

et al., 1979; Skagerberg and Lindvall, 1985; Lorang et al., 1994) studies which have also characterised this cell population.

In contrast to the aforementioned mice and human studies, A11 cells appear to lack AADC in non-human primates (Barraud et al., 2010). These findings have important implications for the functionality of these cells since AADC is a necessary enzyme for the conversion of L-DOPA to DA (Figure 4.1). If L-DOPA is not converted to DA by this population of cells in primates but is converted to DA in other vertebrates, what function do A11 neurons serve and are these functions species specific? Unfortunately, beyond anatomical characterisation, the physiological role of these cells has received very little attention. Nonetheless, indirect evidence suggests these cells play significant roles in locomotor network function. For example, both DA and L-DOPA are known to elicit and modulate locomotor activity whereby acute application of DA or L-DOPA can evoke air-stepping in spinalised rat and cat preparations (Jankowska et al., 1967a,b; Grillner and Zangger, 1979; Baker et al., 1984; Kiehn and Kjaerulff, 1996; McEwen et al., 1997; Barrière et al., 2004). Moreover, inhibition of DA receptors (D_1 and D_2) (McCrea et al., 1997) or AADC (Arnaiz et al., 1996) prior to L-DOPA application can prevent air-stepping. Neurons within the spinal cord are known to express AADC (Barraud et al., 2010; Wienecke et al., 2014) which suggests DA may be synthesised locally. However, methodological concerns cannot be dismissed: if levels of AADC were too low, the immunohistochemical approaches used would fail to detect AADC.

Consistent amongst all studied mammalian species, the A11 population are DAT negative (Ciliax et al., 1999; Lorang et al., 1994; Barraud et al., 2010; Koblinger et al., 2014). Whilst DAT is not a necessary component for DA release, the absence

of DAT is likely to have functional consequences since it facilitates removal of DA from the synaptic cleft. Knockout studies have shown that mice which lack DAT exhibit increased locomotor activity (Giros et al., 1996; Spielewoy et al., 2000) (although these effects may not arise as a consequence of perturbed DA signalling within the spinal network). In DAT^{-/-} mice these behavioural effects are coincident with significantly higher concentrations of DA in the striatum which clear from the extracellular space approximately 300 times slower than in wild-type mice (Jones et al., 1998). Thus, the lack of DAT is likely to have significant implications for the clearance rate of DA from the spinal cord, which may impact spinal network functionality.

There is also indirect evidence to suggest that A11 dopaminergic neurons lack D₂ autoreceptors (Pappas et al., 2008). Again, this has important functional consequences. D₂ autoreceptors regulate firing patterns, DA release and synthesis (Ford, 2014). These receptors activate G-protein-coupled inwardly rectifying potassium (GIRK) channels which strongly hyperpolarise the membrane potential to decrease firing activity (Beaulieu and Gainetdinov, 2011). This consequently decreases the probability of dopamine release (Benoit-Marand et al., 2001). To investigate the presence of D₂ autoreceptors on A11 neurons, Pappas et al. (2008) measured DA levels in the spinal cord by using implanted microdialysis probes. Block of D₂ receptors with raclopride had no significant effect on DA levels in the spinal network (but did in the striatum and nucleus accumbens). It was therefore surmised that because DA levels did not change, A11 DAergic neurons do not express D₂ receptors.

4.1.3.3 DA receptor expression in the mammalian nervous system

Both classes of DA receptor are expressed throughout the nervous system. Within the brain, D₁ receptor expression is highest in nigrostriatal, mesolimbic and mesocortical areas, including the striatum, nucleus accumbens, substantia nigra and frontal cortex. Lower D₁ receptor levels are observed toward the hippocampus, cerebellum and hypothalamic areas. Relative to the expression of D₁ receptors, D₅ receptors are expressed at low levels, primarily in cortical areas such as the prefrontal, premotor, cingulate and entorhinal cortex. Additionally, D₅ receptors are found in the substantia nigra and striatum. There is substantial overlap in expression of D₁ and D₂ receptors. Like D₁ receptors, D₂ receptors are expressed at their highest level in the striatum and nucleus accumbens. Significant levels of D₂ receptor expression is also observed in the substantia nigra, ventral tegmental area, hippocampus, olfactory tubercle and hypothalamus. D₃ and D₄ receptors are less ubiquitous, but nonetheless are expressed in many regions. D₃ receptors are found primarily within the nucleus accumbens, olfactory tubercle, striatum, substantia nigra, ventral tegmental area and hippocampus. D₄ receptors are found in the frontal cortex, amygdala, hippocampus, hypothalamus and substantia nigra.

Within the spinal cord, all five subclasses of DA receptor have been reported. However, distribution of these receptors appears to be species specific (Dubois et al., 1986; Yokoyama et al., 1994; van Dijken et al., 1996; Levant and McCarron, 2001; Zhao et al., 2007; Zhu et al., 2007, 2008; Barraud et al., 2010). Within the mouse lumbar spinal cord, all five DA receptor subtypes are found, with D₂ receptors being most prominent (Figure 4.3) (Zhao et al., 2007; Zhu et al., 2007, 2008). Across all regions, D₂ and D₅ receptors appear to be expressed by approximately 50 % of all spinal

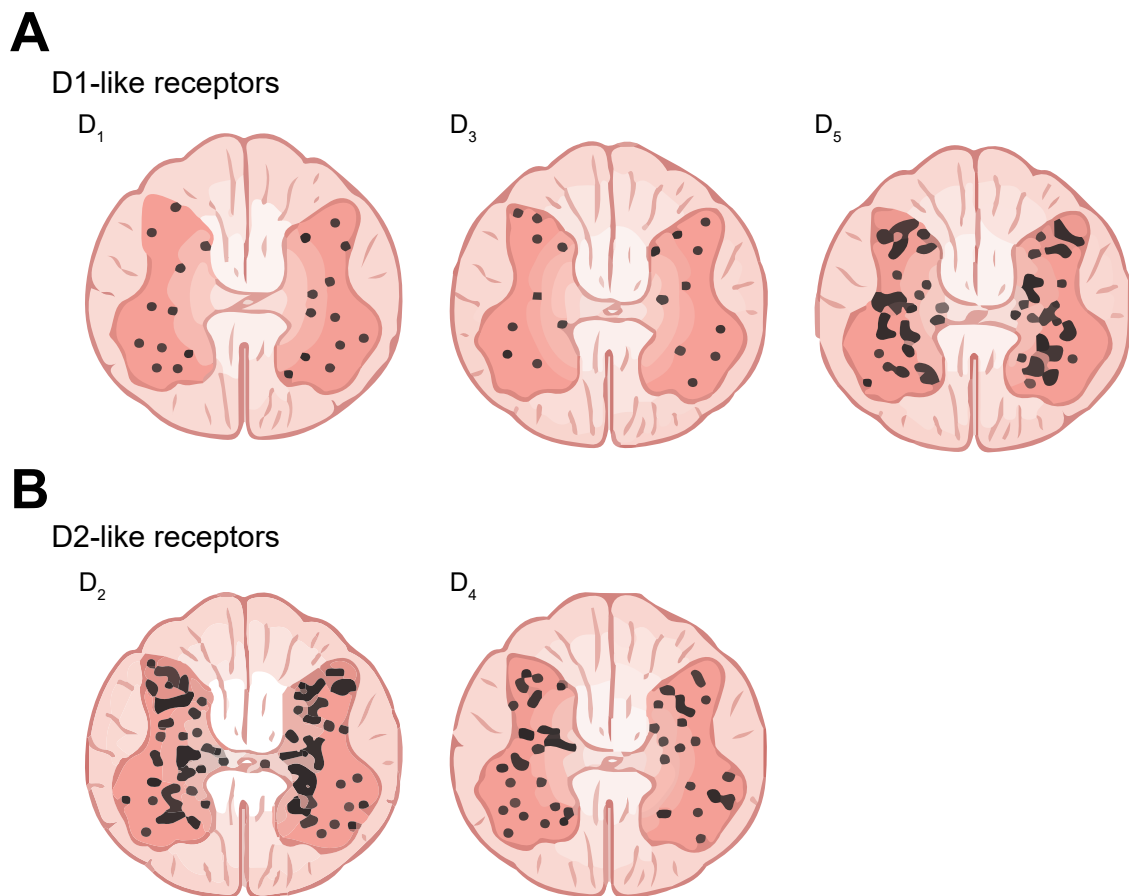


FIGURE 4.3

Distribution of DAergic receptors in the mammalian spinal cord. (A – B) Both D₁-like (A) and D₂-like (B) receptors are distributed throughout the spinal cord of mice. Adapted from Sharples et al. (2014).

neurons. A further 26 % of cells express D₄ receptors while D₁ and D₃ receptors are restricted to 17 % and 12 % of cells, respectively (Zhu et al., 2008). However, receptor labelling was found to be non-uniformly distributed throughout the major regions of the lumbar spinal cord. For all five subtypes, the highest density of receptor expression was observed in laminae IX of the ventral horn, the location of spinal motoneurons (Zhao et al., 2007; Zhu et al., 2007, 2008).

In rats, D₁ (Dubois et al., 1986), D₂ (Yokoyama et al., 1994; van Dijken et al., 1996) and D₃ (Levant and McCarson, 2001) receptor distribution has been examined in some detail within the spinal cord. D₁ receptors are concentrated toward the dorsal

horn, primarily laminae I to III (Dubois et al., 1986). D₃ receptors were distributed throughout the lumbar spinal cord with highest densities in the dorsal aspect (Levant and McCarson, 2001). As in mice, rat D₂ receptors are expressed throughout the gray matter, with higher densities toward the ventral horn, in particular laminae IX (Yokoyama et al., 1994; van Dijken et al., 1996).

While there has been little focus on other mammalian species, recent investigations of DA receptor distribution in a non-human primate have revealed that D₂, D₃ and D₅ receptor subtypes are expressed throughout the lumbar spinal cord (levels L2, L4 and L5) (Barraud et al., 2010), consistent with the aforementioned investigations in mice and rats. However, in contrast, D₁ receptor expression was not observed and the distribution of receptors was markedly different (Barraud et al., 2010). Specifically, D₂ receptors were primarily distributed in the dorsal horn (laminae I to VI), D₃ receptors were more ubiquitous, found from laminae I to X while D₅ receptor labelling was restricted to laminae I to III with sparse labelling within the ventral horn.

4.1.4 Zebrafish catecholaminergic systems

Recent investigations using immunohistochemical and genetic approaches have characterised the CAergic systems within the developing larval zebrafish (Guo et al., 1999; Holzschuh et al., 2001; Rink and Wullimann, 2002; McLean and Fetcho, 2004a; Arenzana et al., 2006; Schweitzer and Driever, 2009; Kastenhuber et al., 2010; Tay et al., 2011; Schweitzer et al., 2012) to the extent that we now have a robust understanding of DAergic and NAergic cell group ontogeny (Table 4.1) and projection patterns. By 3–4 days post fertilisation (dpf) a full complement of DAergic and NAergic tracts

have formed (McLean and Fetcho, 2004a; Arenzana et al., 2006; Sallinen et al., 2009; Kastner et al., 2010; Tay et al., 2011) which are characterised by their stereotypical positions within the brain (Table 4.1). These tracts appear to be fully developed since no additional cell groups or axonal projections are observed by adult stages (Ma, 1994b,a, 1997; Kaslin and Panula, 2001; Rink and Wullmann, 2001). NAergic cell clusters are restricted to the locus coeruleus (LC) and medulla oblongata (MO) both at larval (Ma, 1994a,b, 1997) and adult (Kaslin and Panula, 2001) stages. DAergic clusters are found throughout the telencephalon and diencephalon (Table 4.1) but notably, unlike mammals, there are no DAergic cell clusters in the mesencephalon (McLean and Fetcho, 2004a; Rink and Wullmann, 2002; Schweitzer and Driever, 2009). Thus, whether homologues for the ascending DAergic pathways exist within zebrafish is unclear.

4.1.4.1 Catecholaminergic system ontogeny

While the developmental time course of CAergic systems has not been fully resolved, several research groups have used EdU based birth-dating, *in situ* hybridisation or immunohistochemical approaches at embryonic and larval stages (Guo et al., 1999; Holzschuh et al., 2001; McLean and Fetcho, 2004a; Mahler et al., 2010) to examine CAergic system ontogeny and cell distribution. *In situ* hybridisation methods suggested the earliest developing TH positive cells were found in the diencephalon and rhombencephalon between 18 and 24 hpf (Guo et al., 1999; Holzschuh et al., 2001; Sallinen et al., 2009) whilst immunohistochemical approaches identified a population of DAergic cells in approximately the same region of the diencephalon as early as 16 hpf (McLean and Fetcho, 2004a). However, EdU-based birth-dating offers perhaps the

CA	Subdivision	Larval brain region	CA group*
DA	Telencephalon	Olfactory bulb	OB
		Subpallium	SP
	Diencephalon	Preoptic area	PO
		Prethalamus	DC1
		Posterior tuberculum	DC2
			DC3
			DC4
			DC5
			DC6
		DC7	
	Pretectum	Pr	
	Mesencephalon**	–	–
NA	Rhombencephalon	Rhombomere 1	LC
		Rhombomere 7	MO

TABLE 4.1

Catecholaminergic cell populations present within the zebrafish CNS by 4 dpf. * Catecholaminergic groups as defined by Rink and Wullimann (2002). ** No known DAergic (or NAergic) cell populations are found within the mesencephalon. Abbreviations: Catecholamine (CA), Dopamine (DA), Locus coeruleus (LC), Medulla oblongata (MO), Noradrenaline (NA), Olfactory bulb (OB), Pretectum (Pr), Preoptic area (PO), Subpallium (SP). Table adapted from Schweitzer et al. (2012).

most complete picture detailing the earliest stages of CAergic system development (Figure 4.4) (Mahler et al., 2010). Here, zebrafish embryos aged between 8 and 24 hpf were bathed in an EdU-Alexa 488 conjugate at different time points in order to determine birth date. In conjunction, standard immunohistochemical approaches against TH were used to subsequently confirm CAergic identity. This study revealed the first CAergic precursors to become postmitotic were the DAergic cells in the diencephalic catecholaminergic cluster (DC) 2 (and a proportion of DC1,3,4/5) of the diencephalon and the NAergic neurons of the LC at 8 hpf. The remaining precursors for the DAergic clusters DC1 and DC4/5 become post-mitotic between 24–30 hpf and 20–24 hpf,

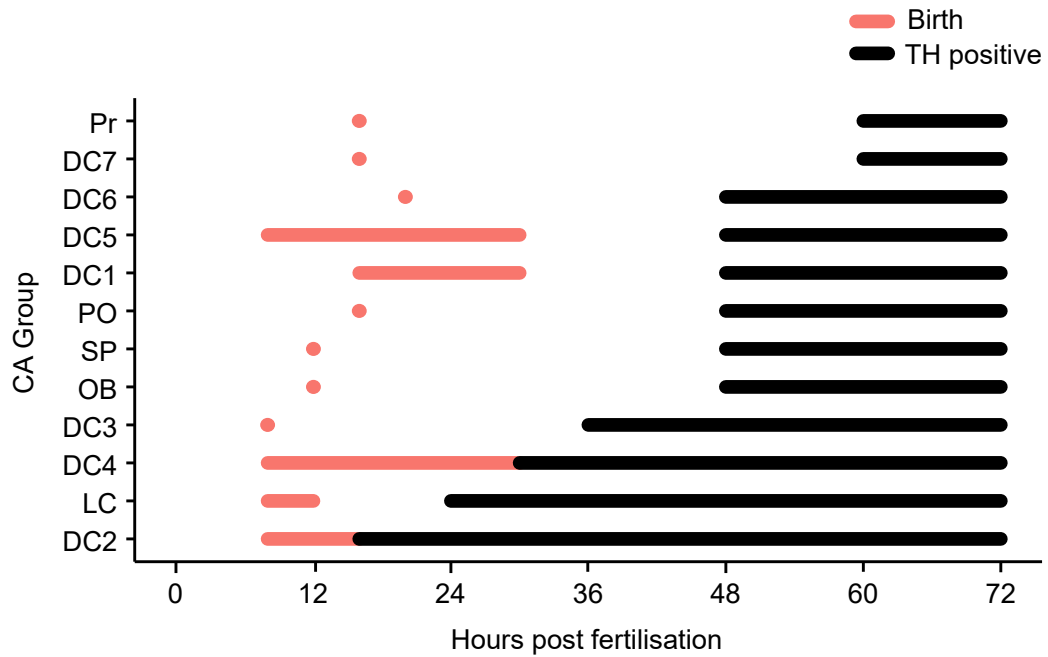


FIGURE 4.4

Development of the CAergic system during zebrafish development Ontogeny of the CAergic system as revealed by EdU-based birth dating. Red lines represent identified windows of proliferation. Red circles identify the earliest known time point of proliferation but no end point could be identified. Black lines mark the time points when each population becomes TH positive. Data derived from Mahler et al. (2010).

respectively. However, while the DC4 DAergic cells express TH from 30 hpf onward, the DC5 population are not TH positive until at least 48 hpf. For the remaining CAergic cell clusters [DC3, DC6, DC7, olfactory bulb (OB), preoptic area (PO), pretectum (Pr), subpallium (SP)] an unambiguous window of proliferation could not be determined. However, the majority of CAergic cell populations are TH-positive by 2 dpf and all CAergic cell groups are established and TH positive by 3 dpf (Figure 4.5) (Mahler et al., 2010).

4.1.4.2 Diencephalospinal DAergic inputs

Axonogenesis of the CAergic system begins early in development. The earliest developing DAergic neurons, the DC2 cluster, have extended axonal projections to the spinal

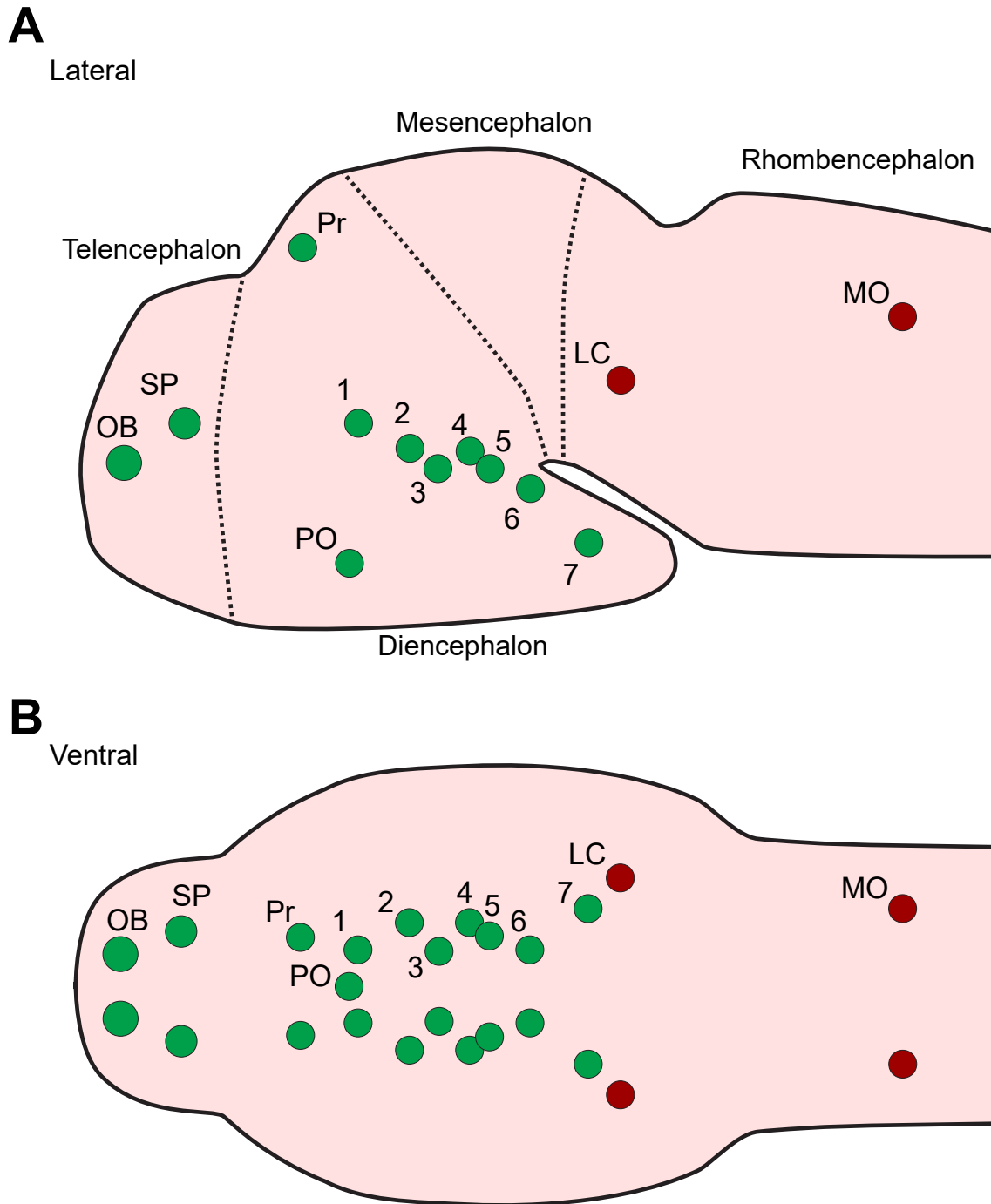


FIGURE 4.5
Distribution of the CAergic system. (A – B) Lateral (A) and ventral (B) overview of DAergic (green) and NAergic (red) cell populations. Numbered populations refer to DAergic clusters DC1 - 7. Abbreviations: Locus coeruleus (LC), Medulla oblongata (MO), Olfactory bulb (OB), Pretectum (Pr), Preoptic area (PO), Subpallium (SP). (A) and (B) are not to scale. Schematics are derived from Mahler et al. (2010).

cord by 24 hpf (McLean and Fetcho, 2004a). By 4–5 dpf, TH positive axon tracts have extended down the entire rostrocaudal extent of the spinal cord at approximately the level of the motoneuron pool (McLean and Fetcho, 2004b).

The DC2 DAergic cell cluster shares several characteristics with the supraspinal A11 DAergic cell population found within mammals which suggests they are an equivalent structure. As is the case within mammals, development of the descending DAergic pathway is dependent upon the presence of the *Orthopedia* homeobox domain protein (Wang and Lufkin, 2000; Blechman et al., 2007; Ryu et al., 2007). Moreover, the mammalian A11 population are amongst the earliest developing dopaminergic neurons (Ohyama et al., 2005; Ryu et al., 2007), have a similar anatomical location and cell morphology to the DC2 population of DAergic cells (Kaslin and Panula, 2001; Wen et al., 2008; Tay et al., 2011). However, while the mammalian A11 DAergic neurons lack DAT, at least a proportion of DC2 neurons may express it (Holzschuh et al., 2001; Xi et al., 2011).

4.1.4.3 DA receptor expression in the zebrafish larvae

While many investigations have focused on the projections of the DAergic system within the developing and adult zebrafish, relatively few studies have examined the distribution of dopamine receptors, particularly within spinal and peripheral regions. By conducting a series of whole mount *in situ* hybridisations against identified DA receptor genes, Boehmler and colleagues have taken the first steps toward examining DAergic receptor expression patterns (Boehmler et al., 2004, 2007; Li et al., 2007). In zebrafish, a gene duplication event has led to the evolution of three separate D₂ receptor genes (*drd2a*, *drd2b*, *drd2c*) and three D₄ receptor genes (*drd4a*, *drd4b*, *drd4c*)

(Boehmler et al., 2004, 2007). Interestingly, these genes may serve specific roles given their unique temporal and spatial expression patterns (see below).

D₁ (*drd1*) receptor expression is first detected at approximately 30 hours post fertilisation (hpf) in the diencephalon and lateral regions of rhombomere 4. By 36 hpf, *drd1* receptor expression is still restricted to the diencephalon and rhombomere 4 but staining is more intense (Li et al., 2007). By 5 dpf, *drd1* receptors are further found in retinal tissue, the hypothalamus and rhombomeres 3, 4, 6, and 7 (Li et al., 2007).

In comparison to D₁ receptors, *drd2a* expression is observed much earlier in development but is localised to the pineal gland between 15 – 24 hpf. By 36 hpf, *drd2a* receptors are expressed within the midbrain, rhombomere 6 and the rostral spinal cord (Boehmler et al., 2004). At 48 hpf, staining for *drd2a* receptors has spread to telencephalic regions and by 5 dpf is diffusely distributed throughout the brain. *drd2b* expression is first detected at 24 hpf and shared similar expression patterns to *drd2a*. However, staining is more prominent in the diencephalon and rhombomeres 3 – 6 with sparse labelling in the spinal cord. *drd2b* expression is restricted to these regions through to 5 dpf. *drd2c* is first observed by 24 hpf within the notochord, hindbrain (rhombomeres 1, 2, 4 and 5) and spinal cord (Boehmler et al., 2004). By 48 hpf, *drd2c* positive clusters expanded and were joined by telencephalic *drd2c* positive cells.

D₃ receptors (*drd3*) are again first observed at 15 hpf, but staining is restricted to somitic tissue (Boehmler et al., 2004). This expression is apparently transient since by 36 hpf, *drd3* expression is detected in telencephalic and hindbrain neurons but is no longer observable in the developing somites. By 48 hpf, expression is also found in the telencephalon, diencephalon and hindbrain (Boehmler et al., 2004).

Finally, all three subtypes of the D₄ receptor (*drd4a*, *drd4b*, *drd4c*) are found throughout the nervous system (Boehmler et al., 2007). The earliest to be detected is *drd4c*. By 15 hpf, *drd4c* is first expressed in the spinal cord and by 24 hpf, in the diencephalon. However, expression within these regions may be transient since at 36 hpf, 48 hpf and 5 dpf, *drd4c* is no longer found in these regions (Boehmler et al., 2004). Expression of *drd4a* is detected at 24 hpf and is restricted to the epiphysis and spinal cord. *drd4b* is also observed at this age in the telencephalon and diencephalon. By 36 hpf, *drd4a* expression has spread to the telencephalon while *drd4b* expression has become more pronounced within the telencephalon and diencephalon.

In sum, DAergic receptors are distributed throughout the zebrafish nervous system at both embryonic and larval stages, and these receptors (and their subtypes) have distinct patterns of expression. This heterogeneity in expression patterns suggest dopamine may serve distinct functional roles during development. Interestingly, DAergic receptors, or at least their mRNA products are present before DAergic neuron innervation in several regions of the nervous system. For example, *drd4c* receptors are observed down the rostral extent of the spinal by 15 hpf (Boehmler et al., 2007) but the descending DAergic inputs to this region appear between 16 and 24 hpf (McLean and Fetcho, 2004a). Thus, several cell populations may be competent to DAergic signalling as DAergic neurons reach their respective targets.

4.1.5 Electrophysiological properties of DAergic neurons

To date, most electrophysiological investigations of DA neuron firing patterns have been restricted to the midbrain. DAergic neurons in this region are of interest because, as dis-

cussed above, they contribute to three major ascending DAergic pathways (mesolimbic, mesocortical and nigrostriatal) that are associated with numerous behavioural states. Studies in the rodent substantia nigra pars compacta (SNc) (A9) and ventral tegmental area (VTA) (A10) in particular have been integral to our understanding of DAergic neuron electrophysiological properties and how they participate in behaviour.

The electrophysiological characteristics by which DAergic neurons are generally identified arise from a series of experiments by Grace, Bunney and colleagues (Bunney et al., 1973; Grace and Bunney, 1980, 1983a,c,b, 1984a; Grace and Onn, 1989; Grace, 1991). In extracellular recordings, DAergic action potentials are characterised by a relatively long half-width (2–8 ms) and an extracellular spike that consists of a positive phase with a notch soon after spike initiation and a prominent negative component (Grace and Bunney, 1983b). At rest, DAergic neurons exhibit autonomous spiking with a slow (mean = 4.5 Hz, range = 1–10 Hz) basal level of activity where each spike has long duration (Grace and Bunney, 1983b). Occasionally, DAergic cells also engage in ‘bursting’ where each burst comprises of at least two action potentials where the interspike interval (ISI) is less than 80 ms (Grace and Bunney, 1984a) with frequencies upward of 50 Hz *in vivo* (Hyland et al., 2002). Within a burst, the spikes get progressively smaller in amplitude and the ISI gets longer between each spike and terminates when the ISI increases beyond 160 ms. These bursts are generally followed by a period of inactivity (\approx 340 ms in duration) (Grace and Bunney, 1984a). Since high frequency stimulation of DAergic neurons can markedly, and in a non-linear fashion, increase DA concentrations relative to slow frequency tonic spiking (Gonon, 1988; Wightman and Zimmerman, 1990; Kawagoe et al., 1992), these two modes of firing may have important consequences for DA release at the synapse and subsequent

DA-dependent signalling.

While a proportion of the low frequency tonic spiking is maintained, bursts are abolished after disruption of afferent inputs, suggesting this activity pattern is driven by synaptic input (Overton and Clark, 1997; Khaliq and Bean, 2010). Again, since most investigations have been conducted under anaesthetic or using brain slices, how afferent inputs contribute to endogenous activity patterns has not been fully resolved (Paladini and Roeper, 2014). Nonetheless, stereological analysis of individual identified DAergic neurons within the SNc has revealed these cells have both glutamatergic and GABAergic synapses such that each DAergic neuron within the SNc has ≈ 8000 afferent synapses, 30–60% of which are glutamatergic and 40–70% are GABAergic (Henny et al., 2012). Genetic knockout or pharmacological block of N-Methyl-D-aspartic acid (NMDA) receptors in midbrain DAergic neurons is sufficient to impair bursting in both anaesthetised (Chergui et al., 1993) and free moving rats (Zweifel et al., 2009), suggesting glutamatergic inputs are necessary for this firing pattern. However, while activation of NMDA receptors using agonists depolarises the membrane and increases spike frequency of DAergic cells, it does not recapitulate the frequencies observed during *in vivo* bursting (Seutin et al., 1990). Since DAergic cells of the SNc also receive inhibitory inputs *in vivo* (Grace and Bunney, 1985) burst generation may, in part, be mediated by inhibition of GABAergic inputs (Lobb et al., 2011). Indeed, GABAergic inputs appear to be particularly relevant to burst generation since application of the GABA receptor antagonists bicuculline or picrotoxin is sufficient to significantly increase the frequency of bursts (Paladini and Tepper, 1999; Floresco et al., 2003). Dynamic clamp, a technique which introduces virtual conductances to the intracellular environment that mimic those arising from NMDA and GABA receptor

activation, has helped to address this issue (see Paladini and Roeper (2014) for review). At resting membrane potentials, Mg^{2+} blocks the pore of NMDA receptors and prohibits ion transfer. Depolarisation of the cell dislodges the Mg^{2+} ion from the pore and permits nonselective flow of cations (Blanke and VanDongen, 2009). During each action potential of a burst within a DAergic neurons, NMDA receptors undergo Mg^{2+} block which enhances the hyperpolarising phase of the action potential and alleviates depolarisation block and sodium channel inactivation. As the membrane potential then depolarises during the proceeding action potential, NMDA channels unblock and potentiate the bursting oscillation (Deister et al., 2009). Dynamic clamp methods can also be used to remove conductances. When GABA receptor conductances are removed, but NMDA-mediated conductances are left intact, DAergic neurons engage in high frequency bursting (Lobb et al., 2010). Thus, burst activity appears to arise as a balance between tonic glutamatergic inputs and GABAergic disinhibition.

4.1.5.1 Midbrain DAergic neurons have autonomous spike capability

If synaptic inputs are removed, DAergic neurons continue to produce regular spike activity which is superimposed upon slow membrane depolarisations (Grace and Bunney, 1983b, 1984b; Grace, 1991). This autonomous spiking is thought to be driven by a combination of Na^+ , K^+ and Ca^{2+} channels. However, the relative contributions of these currents varies based on the anatomical location and age of the neuron. Sodium currents were first identified as a potential mediator of pacemaker activity when tetrodotoxin (TTX) application was discovered to be sufficient to abolish action potential generation and also decreased the amplitude of the slow membrane oscillations (Grace and Onn, 1989; Nedergaard et al., 1993). However, since these slow membrane depo-

larising potentials still persist, other TTX-insensitive channels must contribute to this activity. Application of nifedipine, an L-type calcium channel blocker, after TTX application is sufficient to abolish such slow membrane oscillations, suggesting these events are calcium dependent (Nedergaard et al., 1993). Hyperpolarisation-activated, cyclic nucleotide-gated (HCN) channels also appear to contribute to pacemaker activity. When activated at hyperpolarised potentials, these channels induce a slow membrane depolarisation. This was first observed in midbrain DAergic neurons by Grace and Bunney (1983b). However, these channels appear to contribute to pacemaking in only subsets of SNc DAergic neurons (Neuhoff et al., 2002).

Interestingly, while there have been relatively few studies examining the physiological properties of DAergic neurons during development (Tepper et al., 1990, 1991; Mereu et al., 1995), recent investigations have demonstrated age- and region-dependent regulation of slow subthreshold oscillations (Chan et al., 2007). Specifically at postnatal stages (P17), SNc DA neurons rely upon Na^+ channels to produce oscillations since TTX abolished all activity. However, by adult stages, application of TTX leaves subthreshold oscillations intact within the SNc but are abolished by nifedipine. By contrast, in VTA neurons, subthreshold oscillations are driven by Na^+ at both postnatal and adult stages (Chan et al., 2007).

4.1.5.2 Diversity amongst DAergic neuron populations

In order to identify DAergic neurons *in vivo*, Bunney et al. (1973) locally applied L-DOPA to a presumed DAergic neuron while performing extracellular electrophysiological investigations. If the recorded cell contained AADC, then the L-DOPA would be converted to DA. Brain slices were processed post-recording and reacted with formalde-

hyde vapour or glyoxylic acid which permitted identification of DAergic cells because only DA reacts with these compounds to form fluorescent products. Therefore cells which had been subject to high concentrations of L-DOPA would fluoresce more strongly relative to surrounding cells. However, because electrophysiological recordings had been conducted extracellularly and L-DOPA was also applied extracellularly, it did not permit unambiguous identification of specific cells. These problems were overcome by including L-DOPA within the electrode solution and performing intracellular recordings from DA-containing neurons (Grace and Bunney, 1980) which enabled study of the electrophysiological properties of confirmed DAergic cells. These classic studies suggest midbrain DAergic neurons generate broad duration (2–8 ms) action potentials at moderate frequencies (1–30 Hz) (Grace and Bunney, 1983c,a; Grace and Onn, 1989). However, while these properties are generally applicable to DAergic neurons, a more nuanced view is beginning to emerge which suggests that DAergic cells exhibit functional diversity based on their anatomical location and projection pattern (Wolfart et al., 2001; Neuhoff et al., 2002; Margolis et al., 2006; Lammel et al., 2008, 2014).

In adult mice, two broad DAergic populations have been identified within the VTA which have unique electrophysiological properties with different axonal targets which can be further segregated into subgroups (Lammel et al., 2008). One population had stereotypical DA neuron properties. These had a low spike threshold, prominent afterhyperpolarisation (AHP), clear sag potential, broad AP (≈ 3 ms), and exhibited low frequency (≈ 2 Hz, range = 1.2–3 Hz) autonomous spiking. In contrast, the second population engaged in autonomous spiking at significantly higher frequencies (≈ 5 Hz on average, but ranging from 1–12 Hz). Unlike the first population, these cells lacked a sag potential. Additionally, this DAergic population had a prominent rebound

inhibition, whereby increasingly larger amplitude hyperpolarising steps silenced the cell for longer durations when this current injection was released. Additionally, these cells also lacked a clear AHP. Finally, the duration of these action potentials was significantly longer, attaining an average half-width of ≈ 7.5 ms. These cells also responded differently to depolarising current ramps. Both populations underwent depolarisation block, as is typical of DAergic neurons, however the DAergic cells which exhibited low frequency autonomous spiking could only attain frequencies of ≈ 10 Hz (as expected for a classical DA neuron) while the second, fast spiking population, could reach maximum frequencies upward of 20 Hz and maintain these frequencies for several seconds before there was a reduction in action potential amplitudes and eventual depolarisation block.

Mammalian DAergic neurons of the VTA and SNc express D_2 autoreceptors on the soma and dendrites (Missale et al., 1998; Beaulieu and Gainetdinov, 2011) which can regulate the activity of dopamine cells. DAergic neurons release DA from their dendrites upon depolarisation (Groves et al., 1975) and activation of the autoreceptors at somatodendritic sites hyperpolarises the membrane, inhibits autonomous spiking (Bunney et al., 1973; Lacey et al., 1987; Uchida et al., 2000) and decreases the probability of dopamine release after further synaptic input for ≈ 600 ms (Benoit-Marand et al., 2001). D_2 autoreceptors inhibit dopaminergic neurons within the VTA/SNc by activating a GIRK channel (Lacey et al., 1987; Beckstead et al., 2004). The inhibitory post synaptic currents (IPSCs) carried by these channels are relatively slow, taking ≈ 250 ms to reach peak amplitude and a further ≈ 500 ms to return to baseline (Ford et al., 2009; Courtney et al., 2012). Given the robustness of this response, D_2 autoreceptor-mediated signalling is likely an important modulator in controlling

information flow within DAergic systems (Beckstead et al., 2004; Ford et al., 2009). While all DAergic neurons are commonly thought to have autoreceptors (and this is a criterion that is commonly used to define DAergic status), Lammel et al. (2008) has recently demonstrated that subpopulations of DAergic neurons are not sensitive to extracellular DA.

Like the VTA, there is also functional heterogeneity amongst DAergic neurons in the SNc (Brown et al., 2009; Henny et al., 2012; Schieman et al., 2012). For example, within the SNc, there are populations of calbindin (CB)-positive and CB-negative DAergic cells (González-Hernández and Rodríguez, 2000; Neuhoff et al., 2002) which have markedly different electrophysiological characteristics (Neuhoff et al., 2002; Brown et al., 2009). Again, like the aforementioned VTA DAergic neurons, these subpopulations of SNc cells fired autonomously. However the CB-positive DAergic neurons fired significantly faster than the CB-negative cells. Additionally, DAergic neurons within the SNc have varied responses when presented with aversive stimuli (Henny et al., 2012). Here, the likelihood of DAergic neuron inhibition was dependent upon dendritic location and the proportion of GABAergic inputs these cells received. Therefore, in addition to varied electrophysiological properties, DAergic neurons of the SNc also have anatomical properties which dictate functional output. Thus, what was previously thought as a relatively homogeneous population of DAergic neurons with similar functional roles may in actuality have a variety of functions.

4.2 Aims and objectives

Despite a growing body of evidence to suggest dopaminergic diencephalospinal neurons (DDNs) have profound effects on the ontogeny of spinal networks (Reimer et al., 2013) and locomotor output (Thirumalai and Cline, 2008; Lambert et al., 2012; Irons et al., 2013), there is no description of their electrophysiological properties at mature stages or how these properties develop over the course of development.

Furthermore, the majority of studies which have examined the cellular basis for DAergic neuron properties have been performed within anaesthetised *in vivo* preparations or *in vitro* brain slices. This raises important questions regarding whether observed activity patterns are also seen under physiological conditions. Additionally, commonly used anaesthetics, such as chloral hydrate is metabolised to trichloroethanol. This metabolite can significantly alter firing rates in VTA DA neurons (Chen and Kandasamy, 1996; Appel et al., 2006). Indeed, when chloral hydrate is omitted and electrophysiological recordings are made from awake but paralysed animals, the frequency of bursts and tonic firing is significantly lower (Bunney et al., 1973; Steinfels et al., 1981).

In this chapter, I sought to address these issues by using targeted *in vivo* electrophysiological approaches to characterise the endogenous properties of DDNs during coiling (18 - 30 hpf), burst swimming (2 dpf) and beat-glide swimming (4 dpf) stages of development; time points in development characterised by profound changes in locomotor output (see subsection 1.6.1). The data presented in this chapter demonstrate that DDNs functionally mature across development.

4.3 Results

4.3.1 Identification of DDNs

In order to perform targeted electrophysiological investigations from DDNs, *Etvmat2:GFP* fish were used since this transgenic line expresses GFP in all DAergic cells at both embryonic and larval stages of development (Wen et al., 2008). At early embryonic stages (≈ 1 dpf) all GFP-positive cells within the posterior tuberculum (PT) are TH-positive and have extended an axon caudally toward the spinal cord (Wen et al., 2008) (Figure 4.6A). Between 1 and 4 dpf, clusters of GFP-positive, TH-negative cells begin to emerge within the PT (Wen et al., 2008). Since TH is necessary for the synthesis of DA, this suggests that these cells are not DAergic. Nonetheless, all GFP-positive cells located within the DC2 cluster of the PT are TH-positive (Wen et al., 2008) (Figure 4.6B and Figure 4.7C).

By 4 dpf, a cluster (5–7 neurons) of candidate DDNs could be observed toward the anterior border of the posterior tuberculum (Figure 4.7A,B). These cells could be readily distinguished from neighbouring GFP-positive cells as they had large diameter somata ($10.19 \pm 0.22 \mu\text{m}$), were located in a stereotypical position toward the front of the PT, and were intensely fluorescent relative to nearby GFP-positive cells. To confirm that these cells were DAergic at 4 dpf, *Etvmat2:GFP* larvae were processed for anti-TH immunohistochemistry (see section 2.5). As expected, all large, intensely fluorescent neurons in DC2 co-expressed TH (Figure 4.7C) (Wen et al., 2008). Since the only TH-positive cells in this region are DAergic (Tay et al., 2011), this suggests these cells are DAergic.

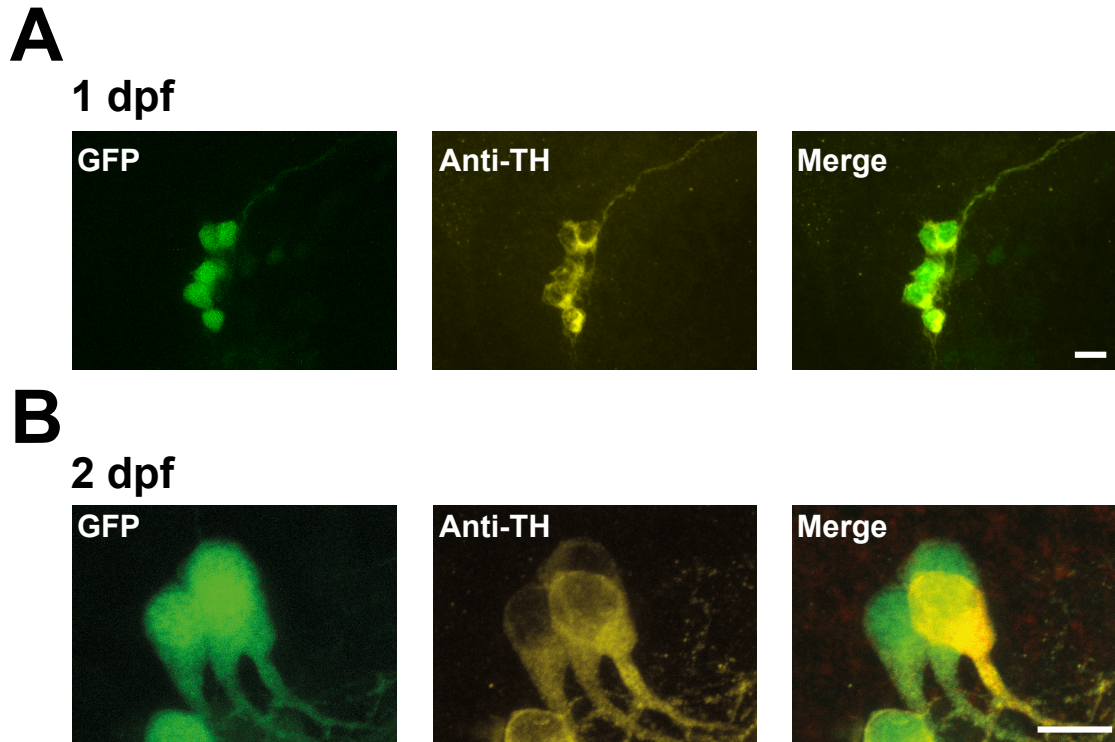


FIGURE 4.6
Identification of TH-positive cells within the posterior tuberculum of *ETV-mat2:GFP* fish at 1 and 2 dpf. (A – B) At 1 dpf (A) all GFP-positive cells within the posterior tuberculum are TH-positive. By 2 dpf (B) all cells within the DC2 cluster are TH-positive. In (A) and (B), anterior is left, dorsal is up. Scale bars = 10 μ m

In order to determine whether these DAergic cells also project to the spinal cord, individual GFP-positive cells were labelled using juxtacellular neurobiotin labelling methods. This maintained cytoplasmic integrity but allowed the axonal projection patterns of putative DDNs to be examined. As expected, all large, intensely fluorescent cells located toward the anterior of the PT that were labelled ($n = 3$) with neurobiotin branched locally but also extended a primary axon that projected caudally into the spinal cord (Figure 4.7D-F). These cells also branched at the level of the hindbrain, in agreement with previous studies (Tay et al., 2011). However, closer inspection revealed that these cells exited the CNS and branched to innervate cranial structures including the otic capsule (Figure 4.8A) and cranial neuromasts (Figure 4.8B). Additionally, peripheral processes also innervated neuromasts of the lateral

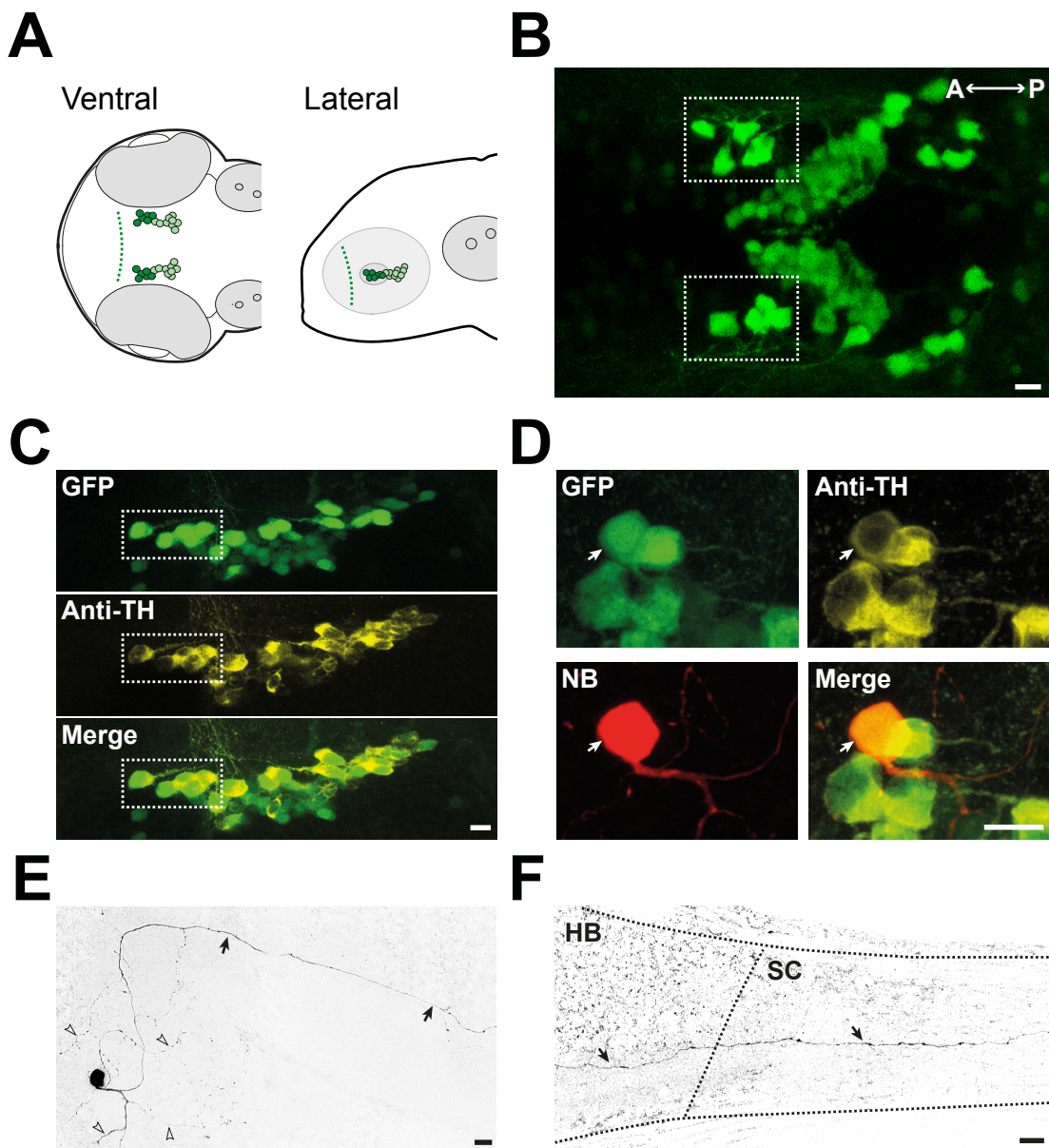


FIGURE 4.7

Identification and projection patterns of DDNs within the CNS of *ETvmat2:GFP* larvae at 4 dpf. (A) Schematic overview of *ETvmat2:GFP* positive cells in ventral (left) and lateral (right) aspects. DDNs (dark green) are located toward the anterior aspect (dashed line) of the diencephalon. (B) Ventral view of *ETvmat2:GFP* positive cells in the diencephalon. Suspected DDNs are distinguishable by intense fluorescence and large-diameter soma (dashed boxes). (C) Lateral view of GFP positive cells in the diencephalon (top). Anti-TH staining (middle) reveals anteriorly located cells are all TH positive (bottom). (D) Lateral view of a GFP-expressing neuron in the anterior diencephalon (green) labelled with neurobiotin (NB, red) and stained with Anti-TH antibodies (yellow). Merged image shows NB labelled cells are GFP and TH positive. (E – F) Lower magnification images of NB labelled cell in (D) reveals anteriorly located GFP and TH positive cells have axonal projections to the spinal cord (SC). In (C)–(H), dorsal is up and ventral is down. Scale bars in (B) — (F) = 10 μ m. (A) is not to scale.

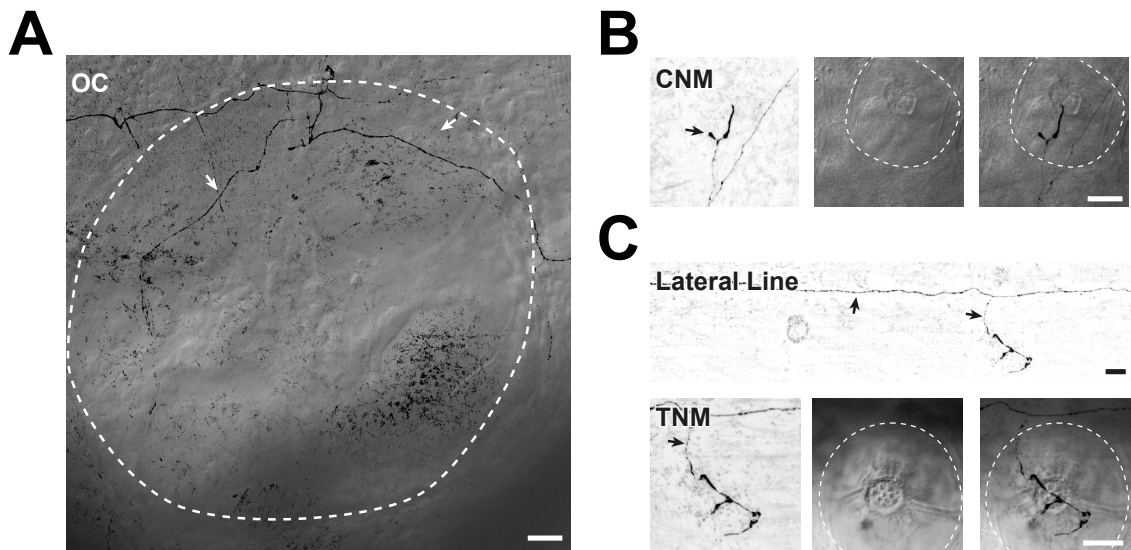


FIGURE 4.8
Projection patterns of DDNs within sensory structures of *ETvmat2:GFP* larvae at 4 dpf. (A – C) Neurobiotin labelling of DDNs reveals that at the level of the hindbrain, the primary axon branches and projects into the periphery, innervating the otic capsule (OC) (A), cranial neuromasts (CNM) (B), lateral line (top in C) and trunk neuromasts (TNM) (bottom in C). Scale bars in (A) — (C) = 10 μ m.

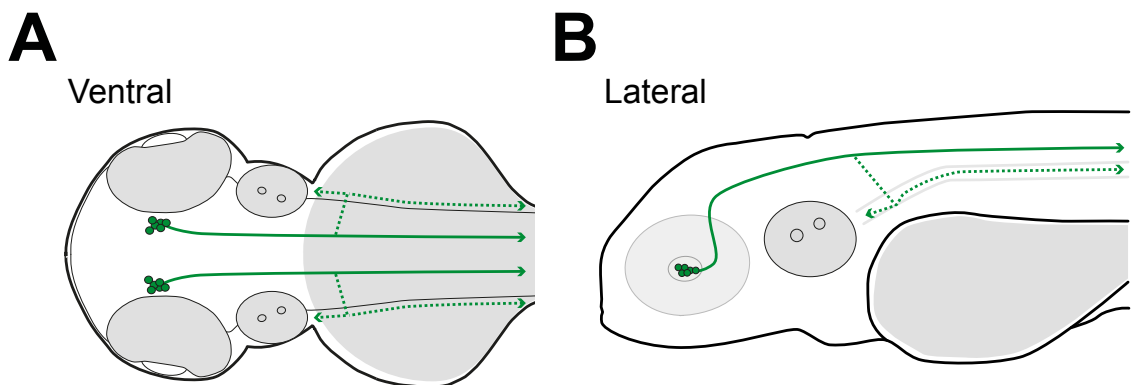


FIGURE 4.9
Schematic summary of DDN projections in *ETvmat2:GFP* larvae at 4 dpf. (A - B) Ventral (A) and lateral (B) overviews of DDN location and arborisation patterns. DDNs located in the diencephalon project caudally into the spinal cord (solid green lines) and branch at the level of the hindbrain to project into peripheral sensory systems (dashed green lines).

line (Figure 4.8C).

In sum, intensely fluorescent GFP-positive cells located toward the anterior aspect of the diencephalon belong to a class of DDNs that project to the spinal cord and peripheral sensory structures (Figure 4.9A, B). Thus, during electrophysiological investigations, recordings were restricted to the anterior diencephalon.

4.3.2 Ontogeny of synaptic inputs

To determine when synaptic inputs onto DDNs first arise during development, whole cell voltage clamp methods were used to monitor miniature post synaptic currents (mPSCs) in coiling (1 dpf), burst swimming (2 dpf) and beat-glide swimming (4 dpf) stage fish. Here, preparations were exposed to 0.5–1 μ M TTX, a voltage gated Na⁺ channel blocker. Under these conditions, spike-dependent transmission is abolished which permits observation of mPSCs that occur as a consequence of spontaneous vesicular release. In order to further characterise the nature of synaptic input, preparations were systematically exposed to channel-specific blockers.

During the early stages of coiling (20 hpf), no mPSCs were observed (n = 3 cells, data not shown). However, at later stages of coiling (22–30 hpf) synaptic inputs were apparent. Subsequent addition of picrotoxin (PIC) (50–100 μ M), a GABA_A receptor antagonist, failed to abolish this population of mPSCs (n = 3) (Figure 4.10A), suggesting these events were not mediated by GABAergic inputs. Instead, these events were presumably glutamatergic in origin because subsequent addition of kynurenic acid (KYN), a glutamate receptor antagonist, abolished all observable mPSCs (n = 3) (Figure 4.10A). Moreover, initial bath application of KYN abolished all observable activ-

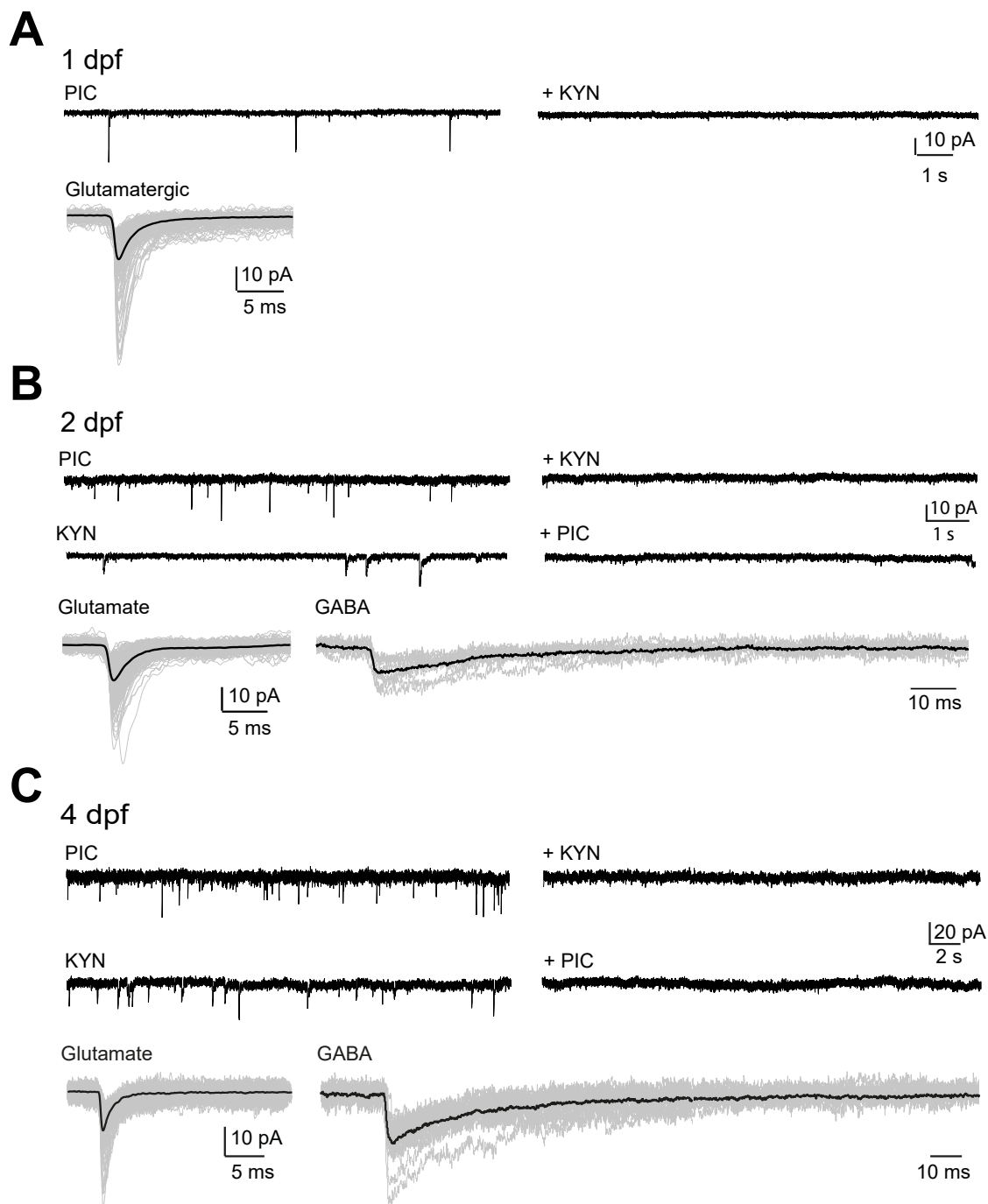


FIGURE 4.10

Ontogeny and identification of synaptic inputs during development. Identified synaptic inputs at 1 (A), 2 (B) and 4 (C) dpf at a holding potential of -75 mV. At 1, 2 and 4 dpf, addition of picrotoxin (PIC) during whole-cell DDN recordings of TTX-treated fish isolated a population of events that were abolished by application of kynurenic acid (KYN) (presumably glutamatergic). At 2 and 4 dpf, initial application of KYN isolated a second population of events that were abolished by subsequent addition of PIC (presumably GABAergic). Bottom traces in (A - C): overlays of isolated glutamatergic and GABAergic events on an expanded time scale.

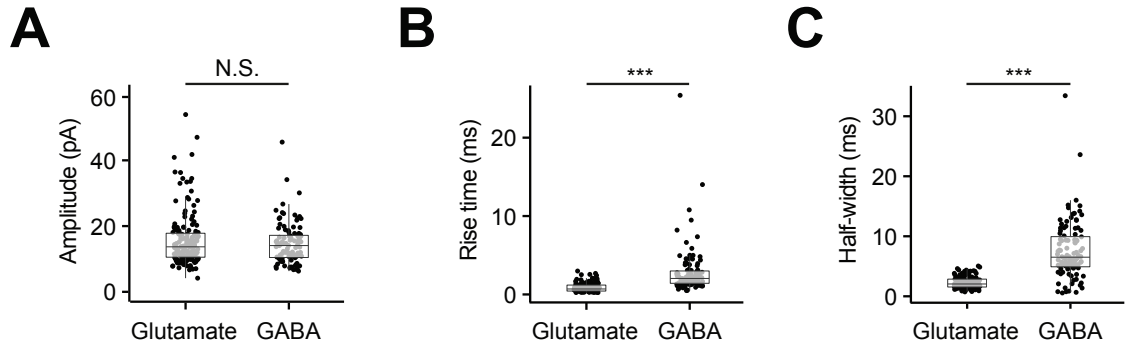


FIGURE 4.11

Glutamatergic and GABAergic mPSC kinetics at 4 dpf. (A – C) Box-and-whisker plots of glutamatergic and GABAergic 4 dpf mPSC amplitudes (A), rise times (B), and half-widths (C).

ity ($n = 3$, not shown). By burst swimming stages, picrotoxin-resistant mPSCs persisted, but a second population of events were now observable after initial bath application of KYN ($n = 3$) (Figure 4.10B). These are likely to be GABAergic as subsequent addition of picrotoxin abolished all activity. Similarly, by beat-glide swimming stages, presumed glutamatergic and GABAergic events were observable (Figure 4.10C). Further analysis of mPSC kinetics at this age revealed that glutamatergic inputs had significantly faster kinetics than GABAergic inputs (Figure 4.11). Specifically, glutamatergic mPSCs had a 10–90% rise time of 0.86 ± 0.04 ms, a half-width of 2.25 ± 0.07 ms and an amplitude of 15.68 ± 0.63 pA. GABAergic events had a similar amplitude (14.72 ± 0.63 pA, $p > 0.05$) but had a prolonged 10–90% rise time (2.86 ± 0.30 ms, $p < 0.001$) and half-width (7.63 ± 0.47 ms, $p < 0.001$). In sum, these observations strongly suggest DDNs receive glutamatergic inputs during embryonic stages and as development continues, DDNs receive both glutamatergic and GABAergic inputs.

4.3.3 Maturation of intrinsic firing properties

4.3.3.1 Responses to rheobase current

In order to examine how the firing properties of DDNs develop over the first four days of development, DDNs were synaptically isolated at 1, 2 and 4 dpf by pre-incubation with glutamatergic (2–4 mM KYN) and GABAergic (50–100 μ M PIC) receptor blockers prior to application of depolarising current steps. Since cells exhibited autonomous spiking (see subsection 4.3.5), a small amount of current was injected to maintain a potential of ≈ -75 mV. At rheobase current, neurons of 1 (n = 16), 2 (n = 24) and 4 (n = 32) dpf fish fired 1 or 2 broad-duration action potentials (Figure 4.12A). However, over the course of development, spike parameters changed significantly. Specifically, between 1 and 4 dpf, spike amplitude gradually increased (1 dpf = 23.26 ± 2.19 mV, 2 dpf = 36.57 ± 1.10 mV, 4 dpf = 42.92 ± 1.32 mV, Figure 4.12B) and spike width decreased (1 dpf = 9.63 ± 1.15 ms, 2 dpf = 4.42 ± 0.15 ms, 4 dpf = 3.25 ± 0.10 ms, Figure 4.12C). In addition, the threshold for spike activation decreased significantly across the first four days of life (1 dpf = -30.77 ± 1.73 mV, 2 dpf = -39.73 ± 0.81 mV, 4 dpf = -43.38 ± 0.72 mV, Figure 4.12D).

Phase plane plots, which display the rate of change in membrane voltage as a function of instantaneous membrane voltage, illustrated the marked developmentally-related changes in action potential dynamics, with embryonic DDNs possessing slower depolarisation and repolarisation phases when compared to post-embryonic fish (Figure 4.13). These plots also revealed the absence of a kink in the rising phase, suggestive of an action potential initiation zone close to the somatic compartment (Bean, 2007). In sum these observations suggest that the spike properties of DDNs mature over the

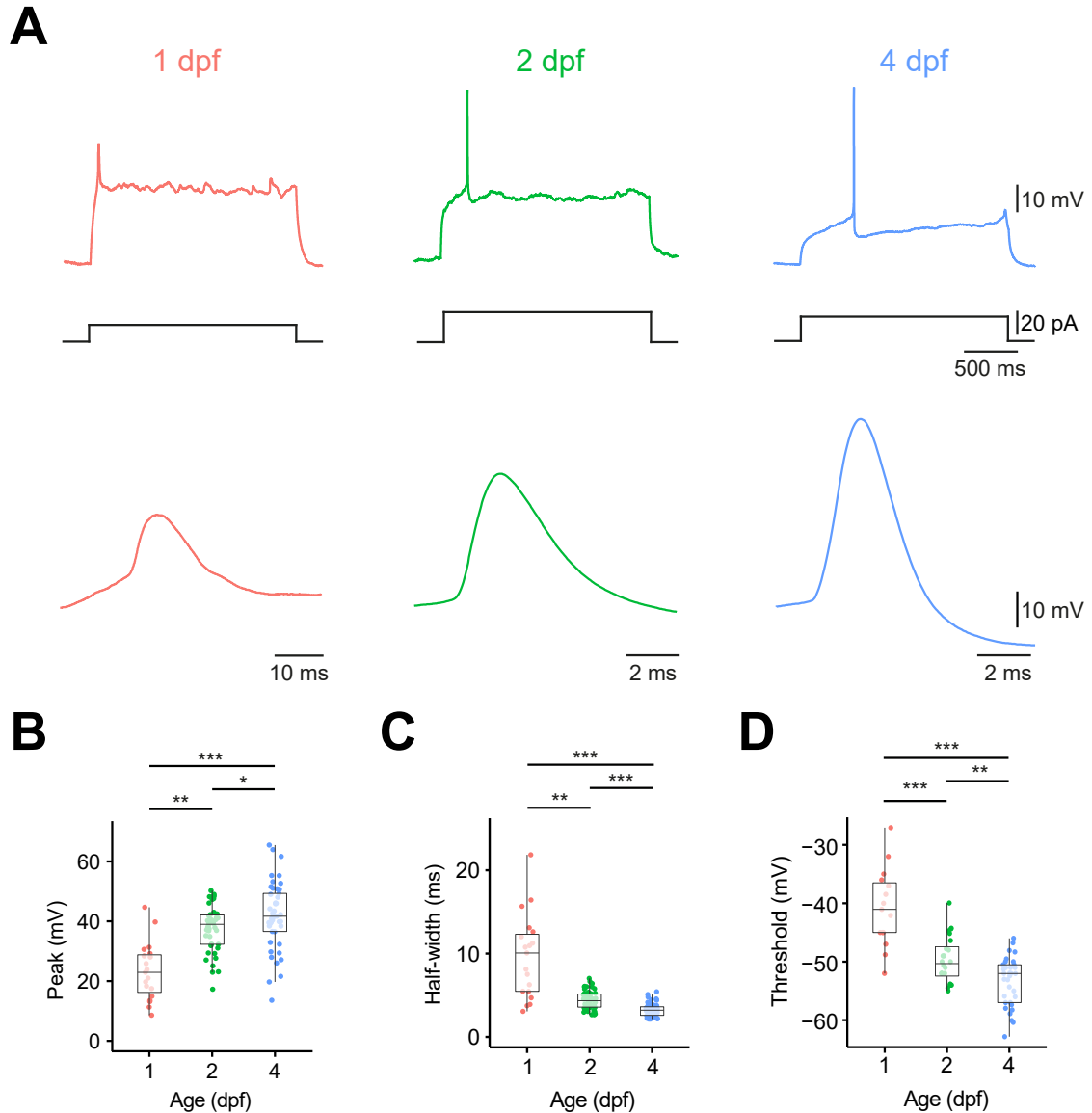


FIGURE 4.12

DDN activity patterns in response to rheobase current injection. (A) Representative whole cell patch clamp recordings in response to rheobase current from DDNs at coiling (left), burst swimming (middle) and beat-gliding (right) stages. Bottom traces represent action potentials on an expanded time scale. Note that at 1 dpf, the expanded trace is on a different time scale to 2 and 4 dpf. (B – D) Box and whisker plots of action potential peak amplitude (B), half-width (C) and spike threshold (D).

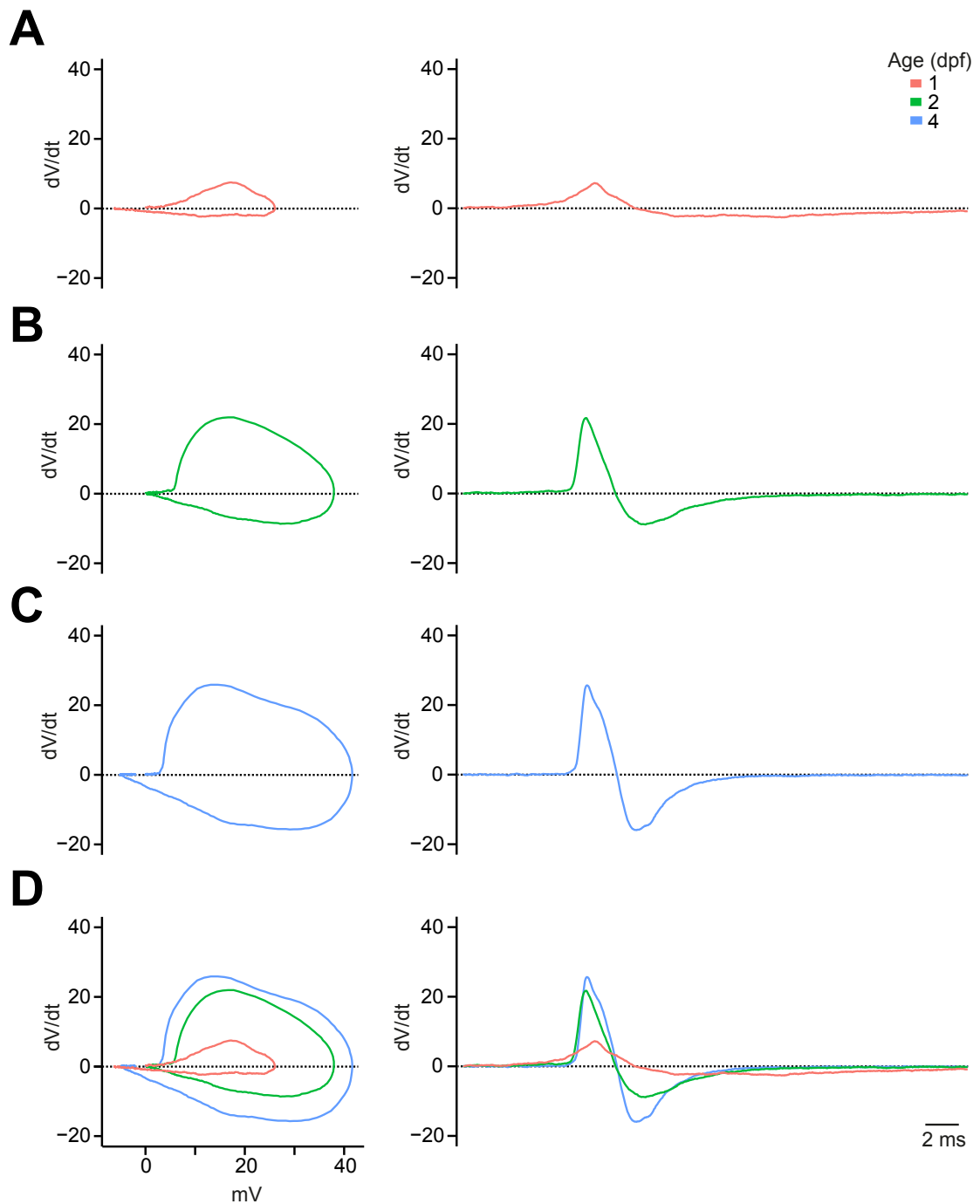


FIGURE 4.13
Phase plane plots in response to rheobase current injection. (A – C) Phase plane plots of traces from Figure 4.12A at coiling (A), burst swimming (B) and beat-gliding (C) stages. **(D)** Composite of phase plane plots in (A – C).

course of early motor development, exhibiting a gradual reduction in spike threshold, decrease in spike width and increase in spike amplitude.

4.3.3.2 Responses to suprathreshold current

Responses to suprathreshold current injection also changed across the first four days of development. At coiling stages (18–30 hpf), 1.5 and 2 x rheobase current triggered unitary ($n = 14$ of 16) or doublet ($n = 2$ of 16) action potentials (data not shown) whilst repetitive spiking responses were routinely observed at 2 dpf ($n = 24$) and 4 dpf ($n = 32$) (Figure 4.14A – B). At 2 dpf, instantaneous spike frequency decreased markedly during the duration of current steps at both 1.5 x (start of step: 13.11 ± 1.49 Hz, end of step: 4.26 ± 0.89 Hz) and 2 x (start of step: 21.40 ± 2.19 Hz, end of step: 7.56 ± 1.52 Hz) rheobase. Similarly, by 4 dpf, 1.5 x (start: 9.56 ± 1.08 Hz, end: 4.78 ± 0.72 Hz) and 2 x (start: 16.77 ± 1.49 Hz, end: 6.26 ± 0.83 Hz) rheobase current evoked a train of spikes which progressively decreased in frequency over time (Figure 4.14C,D). Additionally, consecutive spikes within each train gradually decreased in amplitude and increased in half-width (Figure 4.15). These changes were particularly apparent at 2 x rheobase, as reflected by a marked change in the rate of voltage change and peak voltage amplitude of the first five action potentials within a train (Figure 4.16A,B).

4.3.4 DDNs undergo depolarisation block

The aforementioned changes in spike parameters are indicative of depolarisation block, the process of gradual Na^+ channel inactivation leading to distortion of the action

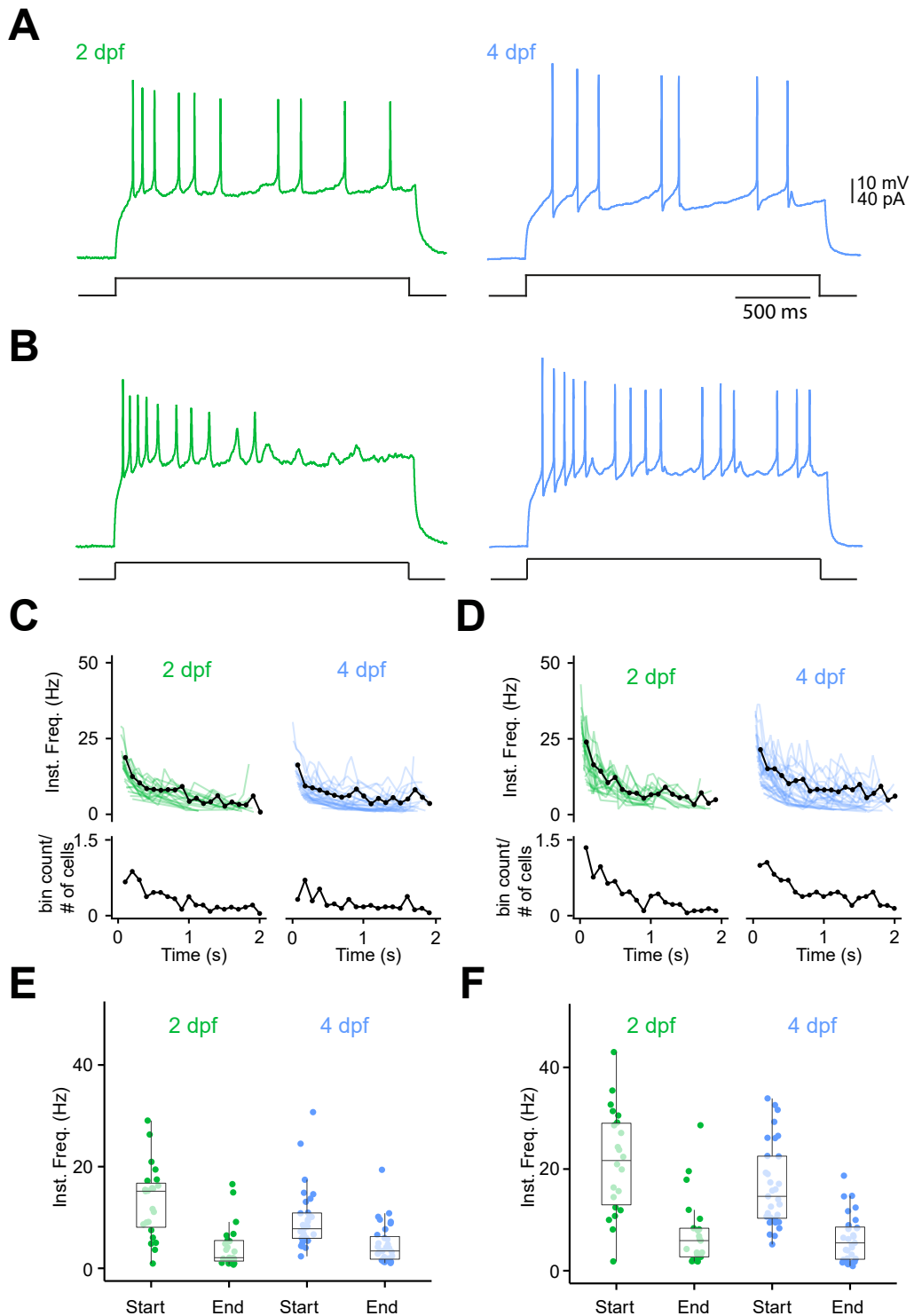


FIGURE 4.14

DDN activity patterns in response to suprathreshold current injection. (A – B) Representative whole cell patch clamp recordings in response to 1.5x (A) and 2x (B) rheobase current injection at 2 (left) and 4 (right) dpf. (C – D) Instantaneous frequency plotted as a function of time at 1.5 x (C) and 2 x (D) rheobase at 2 (left) and 4 (right) dpf. (E – F) Box plots of instantaneous frequency at the start and between the last two action potentials (end) during current steps at 1.5 x (E) and 2 x (F) rheobase.

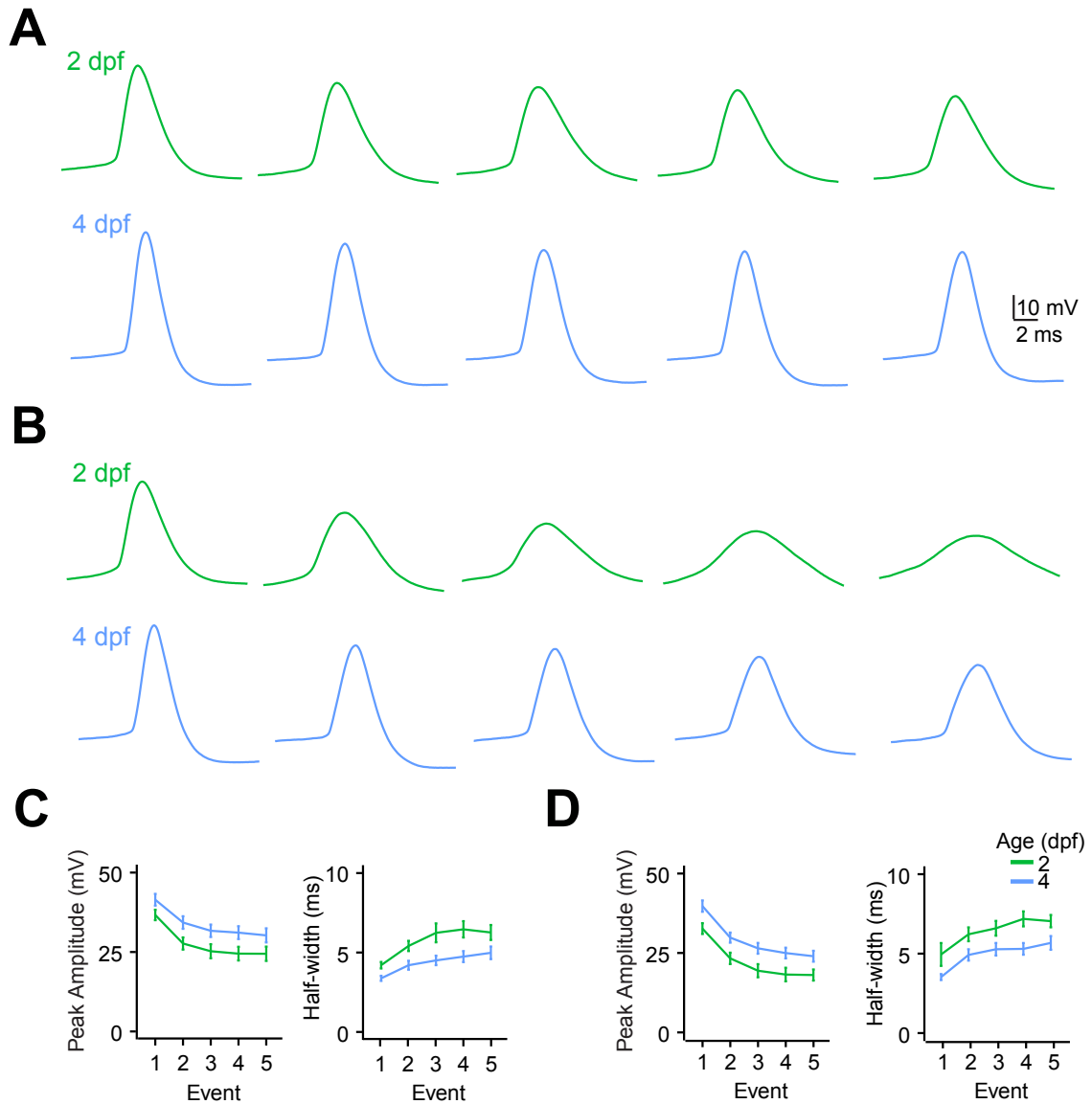


FIGURE 4.15

Action potential waveforms during suprathreshold current injection. (A) First five events from 2 and 4 dpf traces in Figure 4.14A at 1.5 x rheobase. **(B)** First five events from traces in Figure 4.14B at 2 x rheobase. **(C -- D)** Peak amplitude and half-width at 1.5 x (C) and 2 x (D) rheobase.

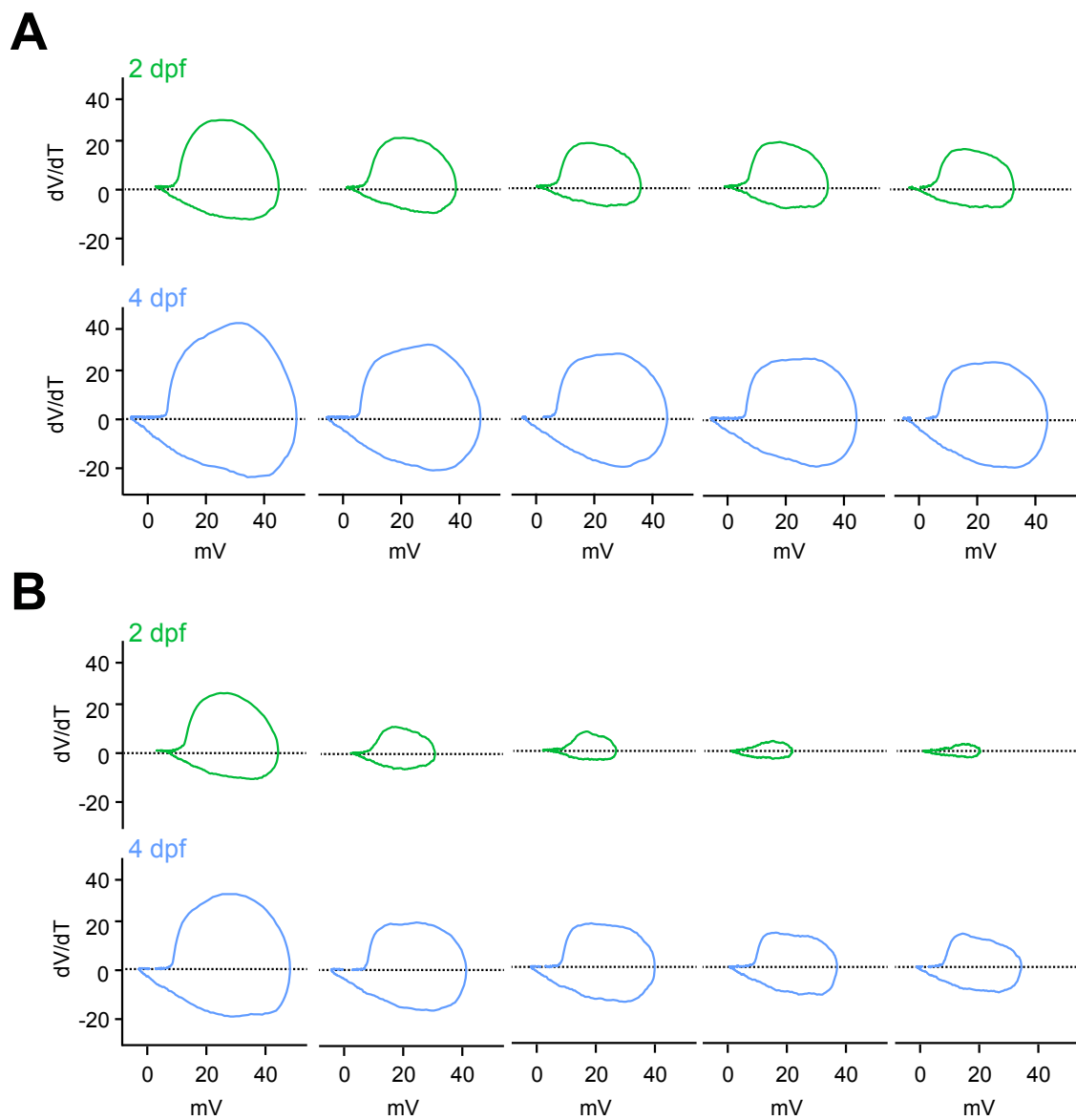


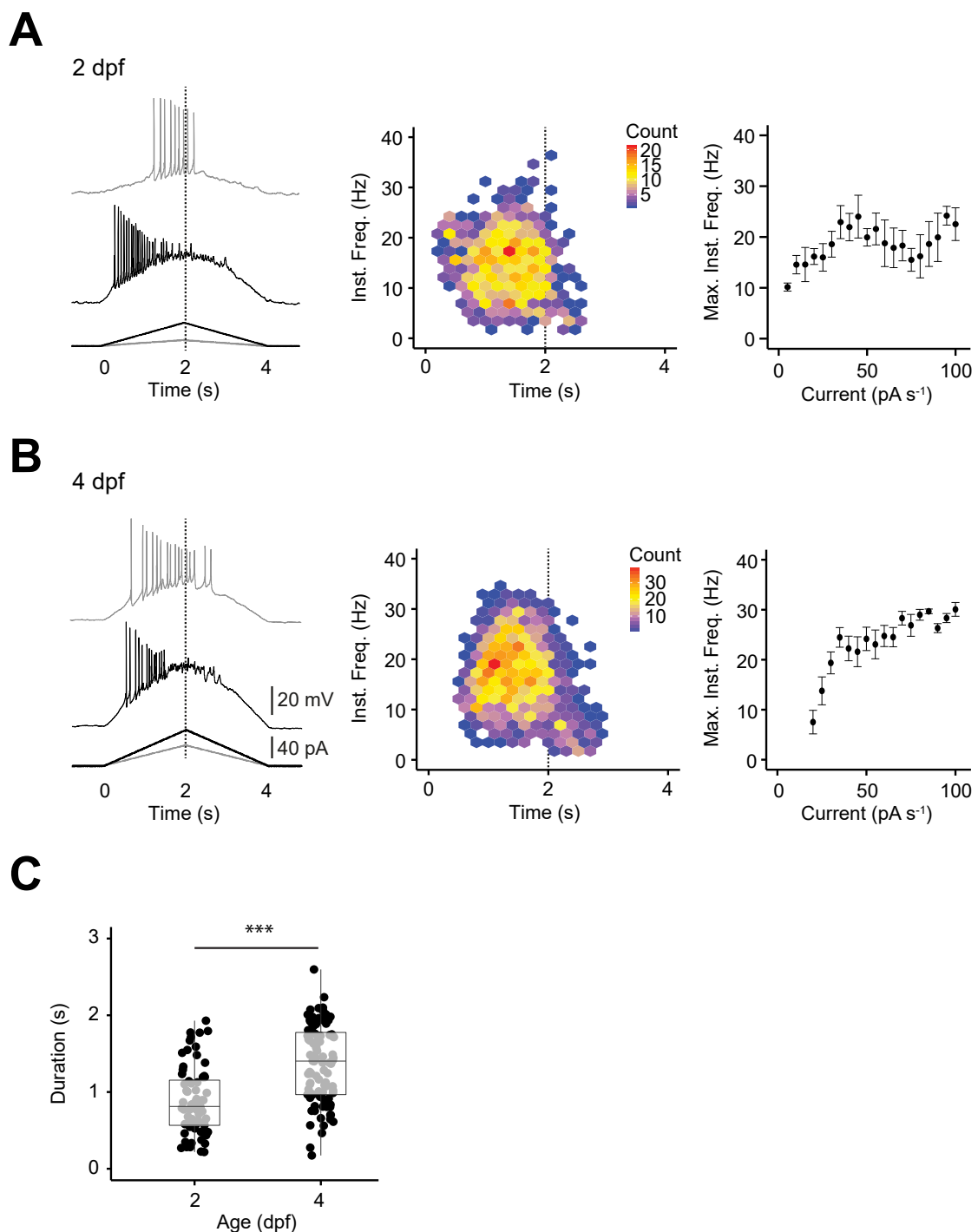
FIGURE 4.16

Phase plane plots during suprathreshold current injection. (A) Phase plane plots of first five events from 2 and 4 dpf traces in Figure 4.14A at 1.5 x rheobase. (B) Phase plane plots of first five events from traces in Figure 4.14B at 2 x rheobase.

potential waveform and ultimately spike failure (Richards et al., 1997; Lammel et al., 2008; Blythe et al., 2009). In order to investigate this process in greater detail, DDNs from 2 and 4 dpf larvae (when DDNs exhibit repetitive spiking in response to current injection), were exposed to triangular current ramps (Figure 4.17A,B). DDNs at both ages exhibited relatively mild depolarisation block when subjected to low amplitude ($20-40 \text{ pAs}^{-1}$) current ramps. However, cells underwent rapid depolarisation block when subjected to larger amplitude ($50-100 \text{ pAs}^{-1}$) current ramps, particularly at 2 dpf (Figure 4.17C, Figure 4.18B). This effect was clearly observable in hexagonal bin plots of instantaneous frequency plotted as a function of time (Figure 4.17A,B) and in plots of the spike incidence during the rising and falling phase of the current ramp (Figure 4.18A,B). These revealed a sharp decline in spike incidence and frequency near the peak of the current ramp. In sum, these results suggest that DDNs at larval stages exhibit depolarisation block when exposed to moderate levels of depolarisation.

4.3.5 Ontogeny of pacemaker firing

In order to examine whether activity patterns of DDNs were synaptically driven, kynurenic acid ($2-4 \text{ mM}$) and picrotoxin ($50-100 \text{ }\mu\text{M}$) were added to the extracellular saline in order to block glutamatergic and GABAergic inputs, respectively. During loose-patch extracellular recordings, addition of these synaptic blockers at 1 dpf ($27-35 \text{ hpf}$, $n = 8$) was sufficient to abolish all spike activity (Figure 4.19A). Surprisingly, by 2 dpf, addition of KYN and PIC failed to abolish spike activity ($n=16$, Figure 4.19B). This neurotransmitter-independent spiking occurred less frequently than under control conditions (control ISI: $1228.31 \pm 54.07 \text{ ms}$, synaptic blockers ISI: $2853.73 \pm 137.03 \text{ ms}$, $p < 0.001$, Figure 4.19C) and with a higher


FIGURE 4.17

Depolarisation block of DDNs. (A – B) Left panels: representative traces of DDN responses to low (grey) or moderate (black) amplitude depolarising triangular current ramps at burst swimming (A) and beat-glide swimming (B) stages. Middle panels: Hexagonal bin plots of instantaneous frequency over the duration of the current ramp. Dotted line represents maximum current amplitude. Right panels: Maximum observed instantaneous frequency as a function of current s^{-1} .

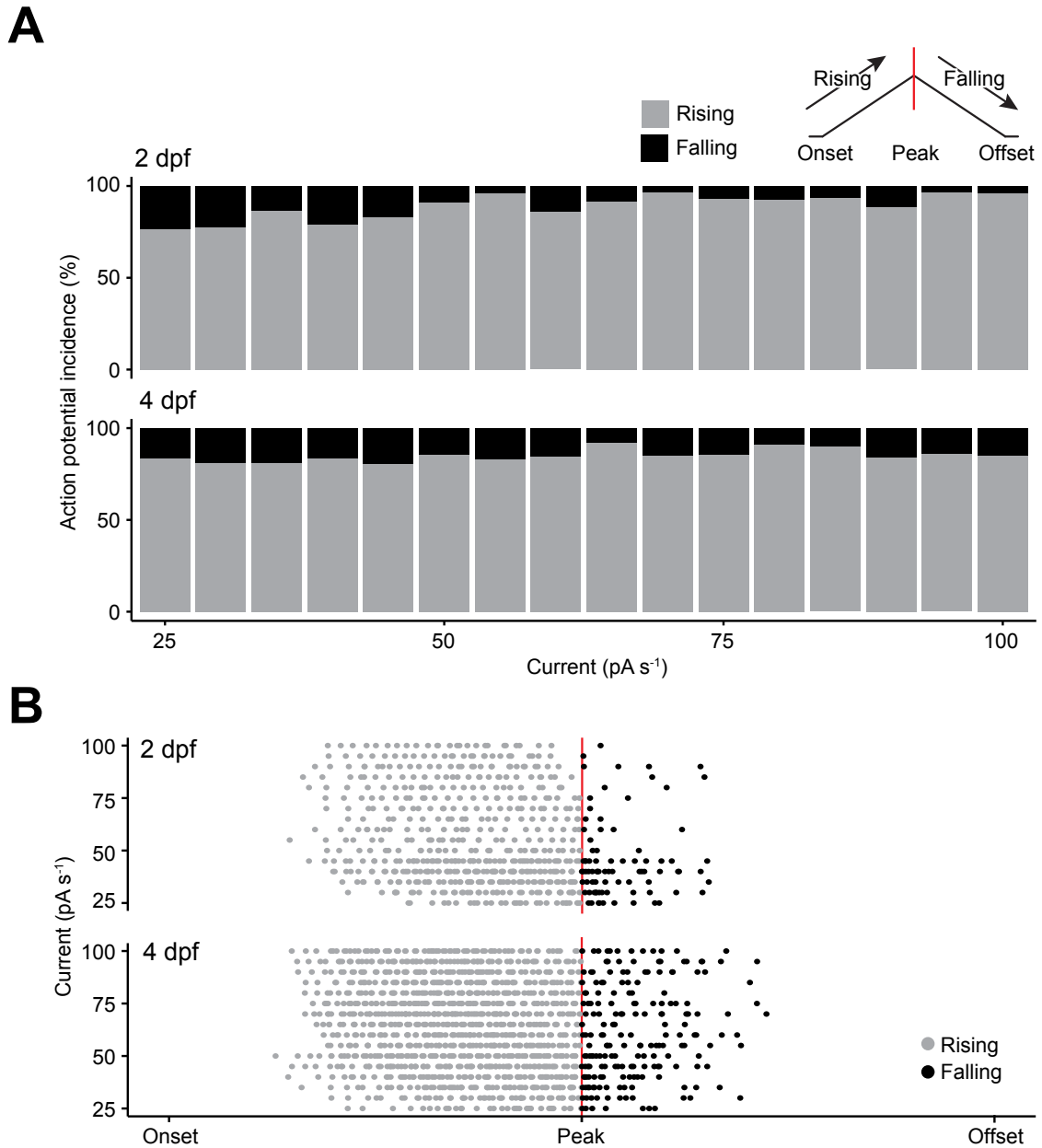


FIGURE 4.18

Occurrence of action potentials during current ramps. (A) The relative action potential occurrence during the rising phase (grey) and falling (black) phase of the current ramp at 2 (top) and 4 (bottom) dpf. (B) Action potentials during the current ramp protocol at each current ramp.

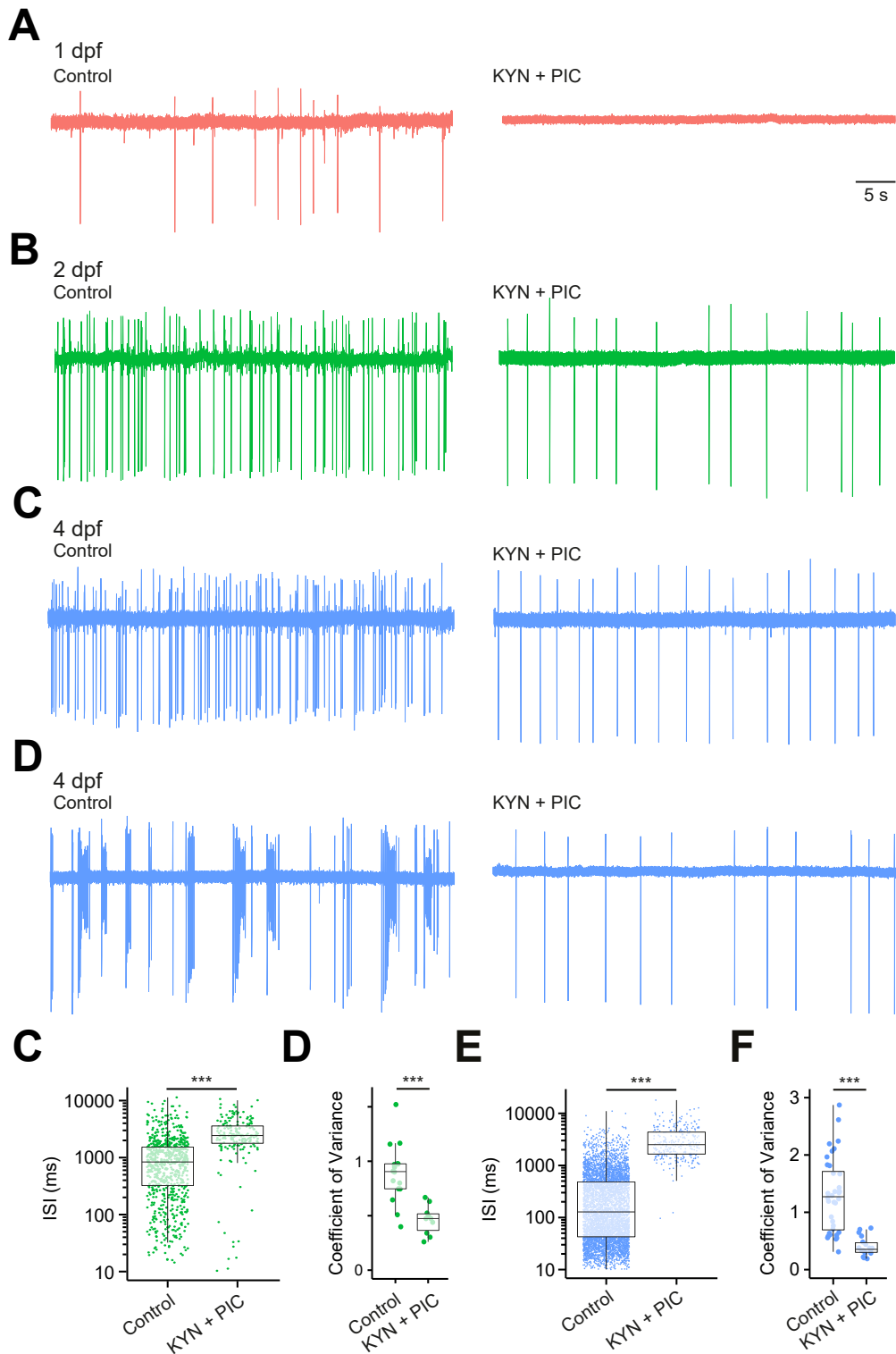


FIGURE 4.19
Development of autonomous spike activity. (A – D) Representative extracellular loose patch recordings from coiling (A), burst swimming (B) and beat-glide swimming stage (C,D) fish during control conditions (left) and after application of synaptic blockers, kynurenic acid (KYN) and picrotoxin (PIC) (right). (C – F) Box and whisker plots of interspike interval (ISI) (C,E) and the coefficient of variance (D,F) at 2 (C,D) and 4 (E,F) dpf.

regularity (control coefficient of variance: 0.88 ± 0.68 , synaptic blockers coefficient of variance: 0.46 ± 0.42 , $p < 0.001$, Figure 4.19D). These activity patterns also persisted at 4 dpf. At this age, when compared to recordings conducted in control saline, neurotransmitter-independent spiking occurred at a lower frequency, as reflected by an increase in the ISI (control ISI = 376.89 ± 8.30 ms, synaptic blockers ISI: 3285.6 ± 135.3 ms, $p < 0.001$, Figure 4.19E) and was more regular, as reflected by a marked decrease in the coefficient of variation (control coefficient of variance = 1.30 ± 0.10 , synaptic blockers coefficient of variation = 0.40 ± 0.04 , $p < 0.001$, Figure 4.19F).

In order to understand the cellular mechanisms which underpin neurotransmitter-independent spiking, perforated patch clamp recordings were obtained from DDNs at 2 and 4 dpf. At 2 dpf, maintaining electrical access via perforated patch clamp methods proved difficult. In all recordings at this age, the membrane potential drifted toward ≈ 0 mV after gaining electrical access, suggesting loss of cytoplasmic integrity and cellular degradation. In a minority of cells, this process did not occur immediately, but did occur after ≈ 30 – 60 s. Thus, while detailed analysis could not be performed at this age, activity patterns could still be characterised in this time. Irregular spike activity that appeared to be driven by a combination of synaptic input and slow membrane oscillations were observed under control conditions (Figure 4.20A). Pre-incubation with kynurenic acid (2–4 mM) and picrotoxin (50–100 μ M) revealed the presence of autonomous spiking (Figure 4.20B) that was of a non-significantly lower frequency than tonic spike activity in control saline (control frequency: 1.07 ± 0.15 Hz, synaptic blockers frequency: 0.47 ± 0.25 Hz, $P > 0.05$, $n = 3$).

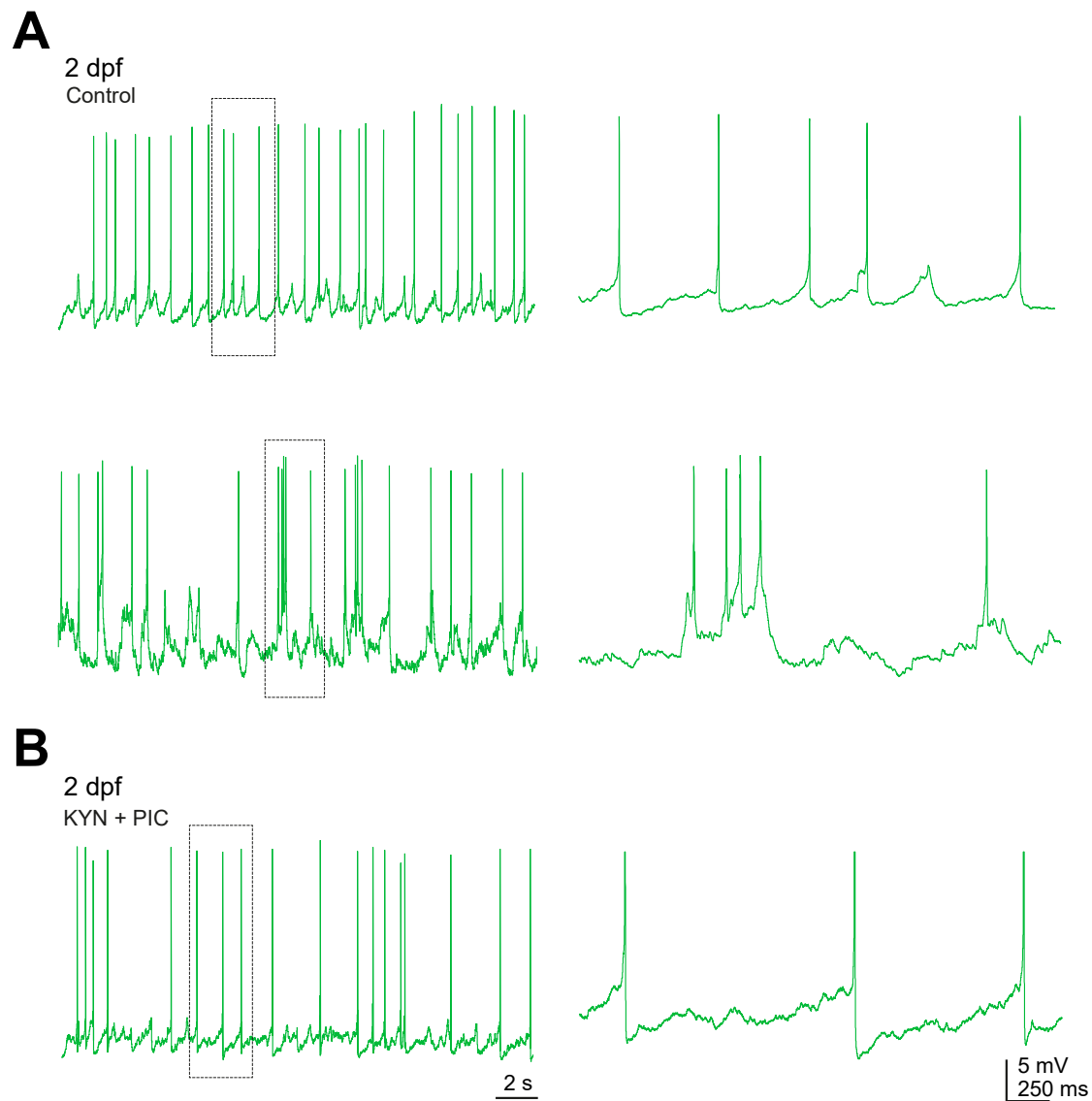


FIGURE 4.20

Autonomous DDN spiking at burst swimming stages. (A) Left hand panels: perforated patch recordings of endogenous activity at 2 dpf under control conditions in two different cells. Right hand panels: expanded regions of same traces, denoted by the dashed boxes. (B) Left hand panel: Activity patterns of a DDN after KYN and PIC application. Right hand panel: expanded region of same trace, denoted by the dashed box.

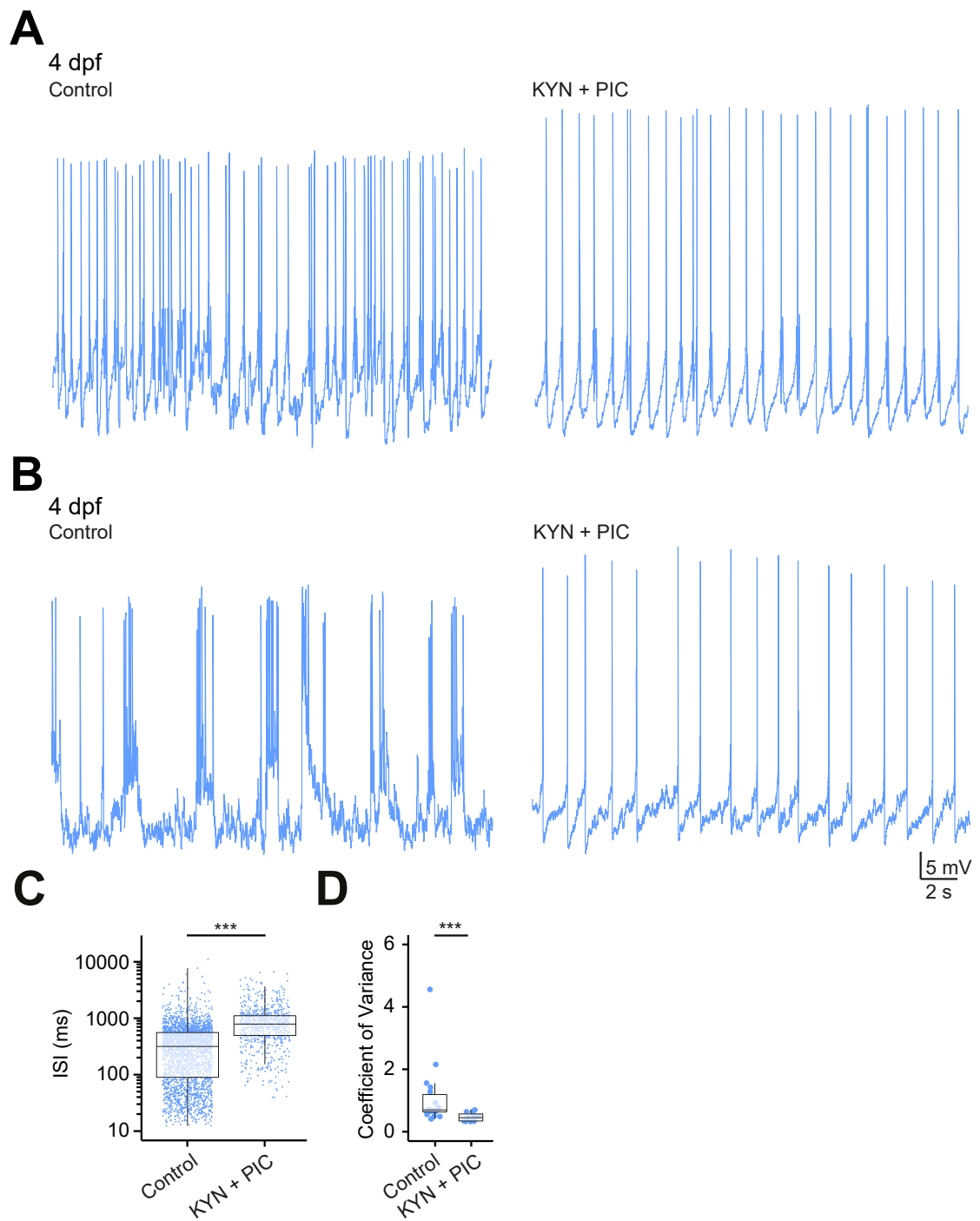


FIGURE 4.21

Autonomous DDN spiking at beat-glide swimming stages. (A – B) Activity patterns recorded from 4 dpf DDNs using perforated patch clamp methods in awake larvae before (left) and after (right) bath application of KYN and PIC. Addition of these glutamatergic and GABAergic receptor blockers unmasked autonomous spiking in cells that exhibit tonic (A) and burst (B) modes of firing. (C – D) Effects of KYN and PIC bath application on the ISI (C) and coefficient of variance (D). Scale bars of (A) and (B) are shown in (B).

By 4 dpf, perforated patch clamp recordings from DDNs could be reliably maintained for prolonged periods of time. These recordings confirmed that DDNs spike in the absence of synaptic inputs ($n = 26$). Here, incubation with kynurenic acid and picrotoxin abolished synaptic input and burst discharges without altering resting potential (control = -55.19 ± 1.28 mV, synaptic blockers = -57.83 ± 1.41 mV, $p > 0.05$). Repetitive spiking persisted in the presence of these drugs (Figure 4.21A,B). Similar to extracellular recordings, spiking was less frequent in the presence of synaptic blockers (control ISI = 401.25 ± 9.90 ms, synaptic blockers ISI = 956.18 ± 28.93 ms, $p < 0.001$, Figure 4.21C) and more regular (control coefficient of variation = 1.07 ± 0.23 , synaptic blockers coefficient of variation: 0.47 ± 0.04 , $p < 0.001$, Figure 4.21D). Thus, DDNs begin to generate autonomous spiking as zebrafish transition from embryonic forms of locomotor output to swimming stages. At 4 dpf, autonomous spikes appeared to be superimposed upon subthreshold membrane oscillations which drove the cell to spike threshold (Figure 4.22A), mirroring the membrane oscillations which underpin autonomous pacemaker activity in mammalian DAergic cell populations (Grace, 1991). For the purposes of this thesis, I will therefore refer to the slowly depolarising component as a subthreshold membrane oscillation, congruent with the mammalian literature.

4.3.6 Pacemaker firing is voltage-dependent

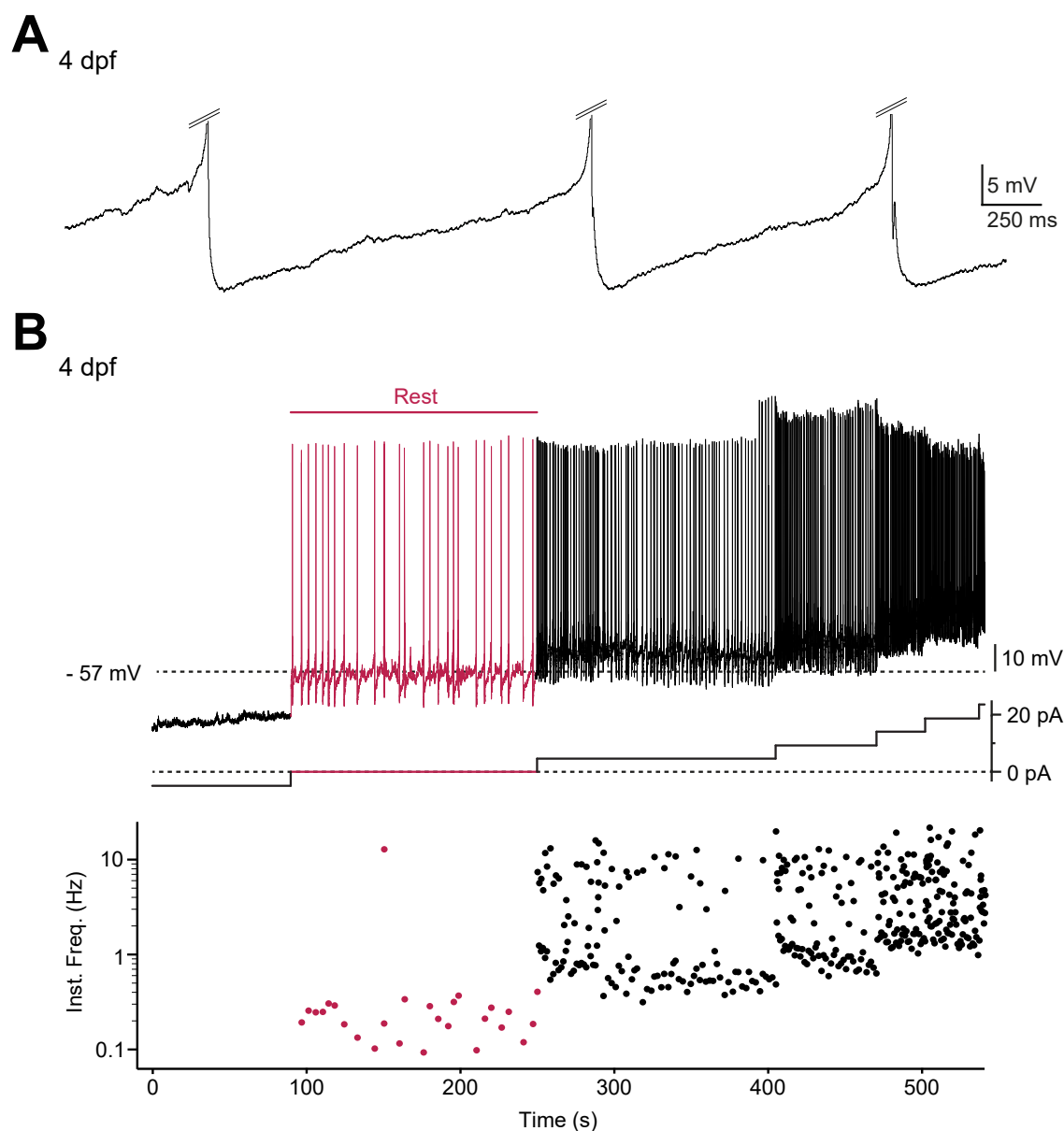
If membrane oscillations were driven by voltage-dependent conductances, their frequency should vary as a function of membrane potential. To determine whether this was the case, current was injected into DDNs of 4 dpf larvae during current clamp recordings (Figure 4.22B and Figure 4.23A-D). Injection of hyperpolarising current re-

duced the frequency of oscillations and completely silenced these events at membrane potentials negative to -64.67 ± 3.71 mV ($n = 9$). Termination of the hyperpolarising current command also caused a transient rebound in autonomous spike frequency (Figure 4.23A,D). In contrast, depolarising current increased the frequency of oscillations and action potential discharge (Figure 4.22B and Figure 4.23A-C) while release of depolarising current transiently decreased action potential frequency (Figure 4.23D). These findings suggest that autonomous spiking is driven by voltage-dependent conductances.

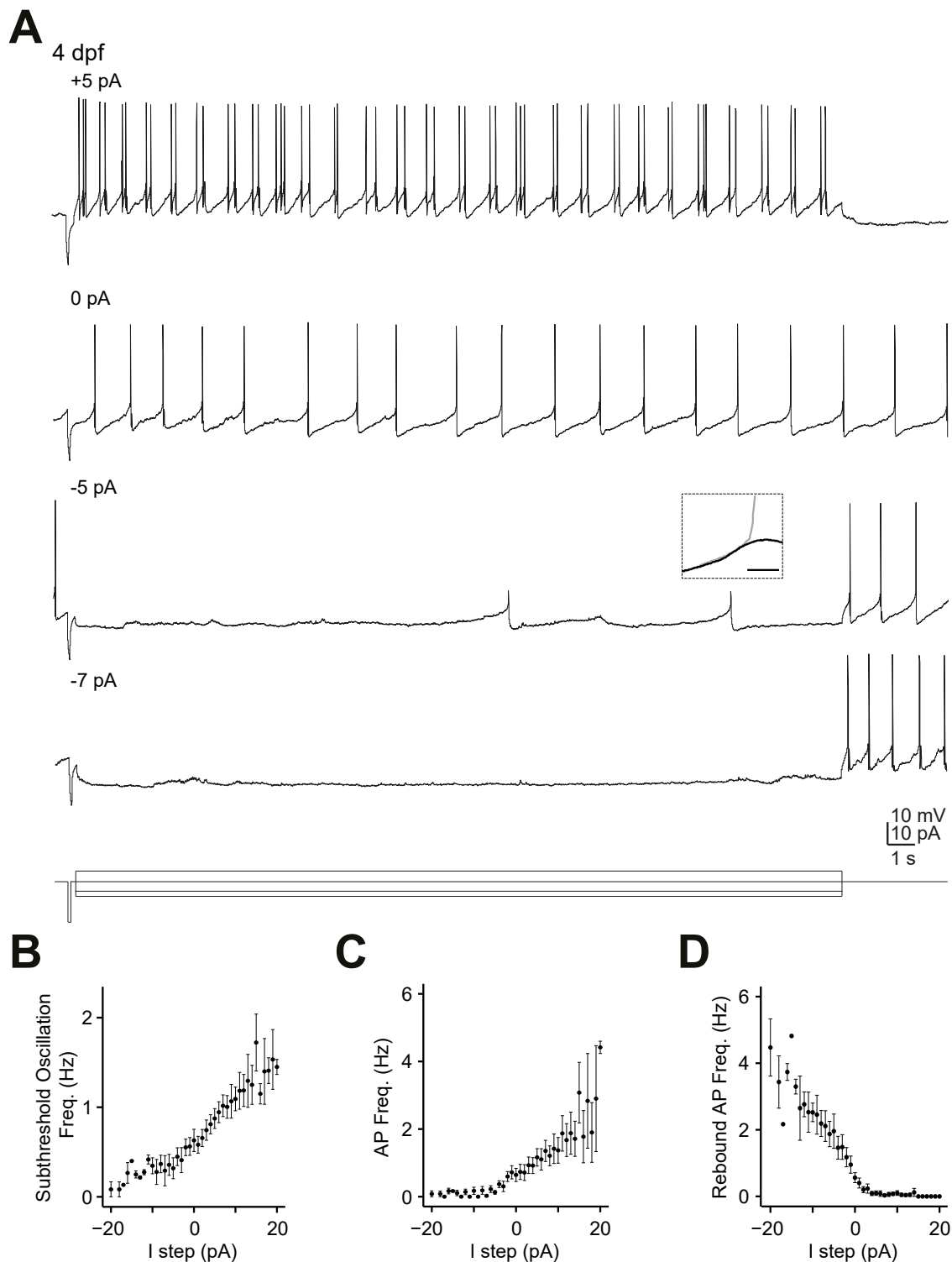
4.3.7 Ionic basis of pacemaker firing

In order to gain an initial insight into the ontogeny of intrinsic membrane oscillations, membrane responses to subthreshold current were examined during whole cell recordings. At 1 dpf, subthreshold current injection elicited steady-state membrane depolarisations (Figure 4.24A). In contrast, similar current injection at 2 and 4 dpf elicited subthreshold membrane oscillations which were characterised by a slow depolarising phase that was followed by a relatively rapid membrane hyperpolarisation (Figure 4.24A).

Studies of DAergic neurons in the mammalian midbrain suggest that autonomous spiking is underpinned by a combination of low threshold Na^+ , Ca^{2+} and hyperpolarisation-activated cation (I_h) currents (Grace and Onn, 1989; Harris, 1992; Kang and Kitai, 1993; Chan et al., 2007). To determine whether such currents contribute to the pacemaker-like activity observed in DDNs, 2 and 4 dpf larvae were first exposed to TTX ($1 \mu\text{M}$, $n = 6$). This Na^+ channel blocker abolished all action poten-


FIGURE 4.22

Autonomous spiking is voltage-dependent. (A) Expanded region showing the autonomous spike activity which facilitates pacemaker-like activity in DDNs exposed to 4 mM kynurenic acid and 100 μ M picrotoxin. Action potential discharges have been truncated (dashed lines). (B) Perforated patch clamp recording (top) showing effects of current injection (middle) on the instantaneous frequency (bottom) over a prolonged period of time. Red bar entitled 'Rest' indicates period with no current injection.


FIGURE 4.23

Autonomous spiking is voltage-dependent. (A) Depolarising steps increase, and hyperpolarising steps decrease and eventually abolish the frequency of autonomous spike activity. Inset shows the rising phase which failed to reach spike threshold (black) superimposed upon an oscillation which triggered an action potential (AP) (grey). (B – D) Subthreshold oscillation frequency (B), AP frequency (C) and rebound AP frequency (D) as a function of current injection. In (B – D) data are represented as mean \pm standard error of the mean (SEM).

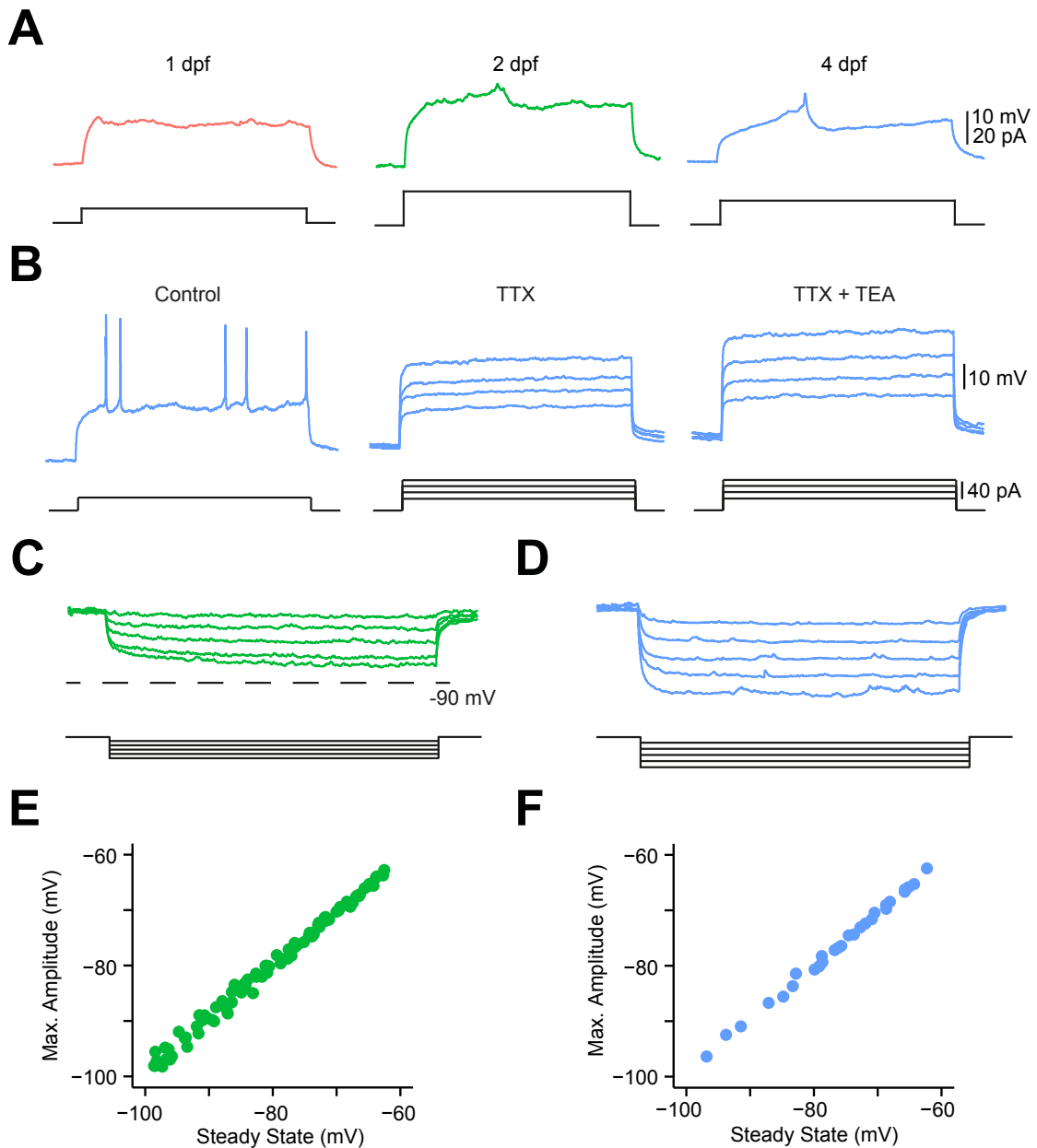


FIGURE 4.24

Ionic basis of pacemaker firing. (A) Steady state subthreshold depolarising current injection reveals a slowly developing membrane oscillation at 2 and 4 dpf, but not 1 dpf. (B) Spike activity and underlying membrane oscillations in response to suprathreshold current injection (left) were abolished by application of TTX (middle). Subsequent application of TEA (right) was insufficient to unmask underlying Ca^{2+} spikes. (C – D) Representative traces of DDN activity patterns in response to hyperpolarising current steps at 2 (C) and 4 (D) dpf. (E – F) Scatter plot of maximum observed amplitude during negative current steps vs steady state amplitude, recorded 100 ms prior to termination of current step at 2 (E) and 4 (F) dpf.

tials and subthreshold oscillations resulting in steady-state responses to membrane depolarisation (Figure 4.24B). Since subthreshold Ca^{2+} spikes may have been masked by K^+ channels (Kang and Kitai, 1993), DDNs were subsequently bathed in tetraethylammonium chloride (TEA), a K^+ channel blocker. However, steady-state membrane depolarisations were still observed in response to current injection, suggesting subthreshold Ca^{2+} conductances are not necessary for autonomous spike generation in DDNs. Finally, to test for the presence of an I_h current, DDNs were injected with hyperpolarising current steps of increasing amplitude. This should evoke a slow membrane depolarisation referred to as a sag potential if I_h currents are present. However, at both 2 (Figure 4.24C,E) and 4 (Figure 4.24D,F) dpf, these slow depolarisations were not observed, strongly suggesting that such a current does not contribute to the generation of subthreshold oscillations. In sum, these findings suggest autonomous subthreshold oscillations are mediated primarily by sodium dependent channels.

4.3.8 Dopaminergic autoinhibition of autonomous DDN activity

Midbrain DAergic neurons often exhibit sensitivity to DA release, which induces membrane hyperpolarisation, inhibits pacemaker firing, decreases DA synthesis and depresses DA release (Bunney et al., 1973; Lacey et al., 1987; Silva and Bunney, 1988; Liu et al., 1994; Kim et al., 1995; Fedele et al., 1999; Weber et al., 2001; Joseph et al., 2002). To investigate possible autoinhibitory effects of DA upon DDNs, DA was slowly perfused into the extracellular saline (Figure 4.25A). Bath application of DA (5 μM) slowed ($n = 2$ of 6) or abolished ($n = 4$ of 6) pacemaker firing in synaptically isolated cells (control = 0.65 ± 0.19 Hz, DA = 0.06 ± 0.05 Hz, wash = 0.66 ± 0.43 Hz, $p < 0.05$, Figure 4.25B). To further investigate the effects of DA, larvae were bathed in

TTX and then 5 μ M DA was added to the extracellular solution (Figure 4.26A). Here, DA had a profound effect, reversibly hyperpolarising the resting membrane potential (control = -53.9 ± 18.9 mV, DA = -63.12 ± 3.52 mV, wash = -54.68 ± 3.41 mV, $p < 0.05$, Figure 4.26A,B).

Since DAergic autoinhibition is often mediated via D₂ autoreceptors, I next asked whether preincubation with 10 μ M raclopride, a D₂-like receptor antagonist, was sufficient to reduce or abolish the inhibitory effects of DA upon intrinsic pacemaker firing. Following preincubation with raclopride, the frequency of spike discharge was 0.77 ± 0.12 Hz, which was comparable to autonomous spike frequencies in Evan's extracellular saline ($P > 0.05$). However, after preincubation with raclopride, spike discharge was not abolished following 5 μ M DA application (Figure 4.27A,B). Instead, autonomous spiking continued at a frequency of 0.77 ± 0.11 Hz ($P > 0.05$) and was of a similar frequency following washoff of DA (0.79 ± 0.14 Hz, $P > 0.05$).

Finally, the effects of DA upon synaptic inputs to DDNs were examined. Here, bath perfusion of 5 μ M DA reduced the frequency of synaptic events during whole cell voltage clamp recordings (control = 32.09 ± 3.59 Hz, DA = 8.40 ± 2.59 Hz, wash = 28.07 ± 3.39 Hz, $p < 0.01$, Figure 4.28A,B) but did not affect amplitude (control = 14.70 ± 3.45 pA, DA = 12.68 ± 3.09 pA, wash = 16.49 ± 3.90 pA, $p > 0.05$, Figure 4.28C). In sum these data suggest that both the intrinsic properties and synaptic inputs to DDNs are strongly inhibited by DA application.

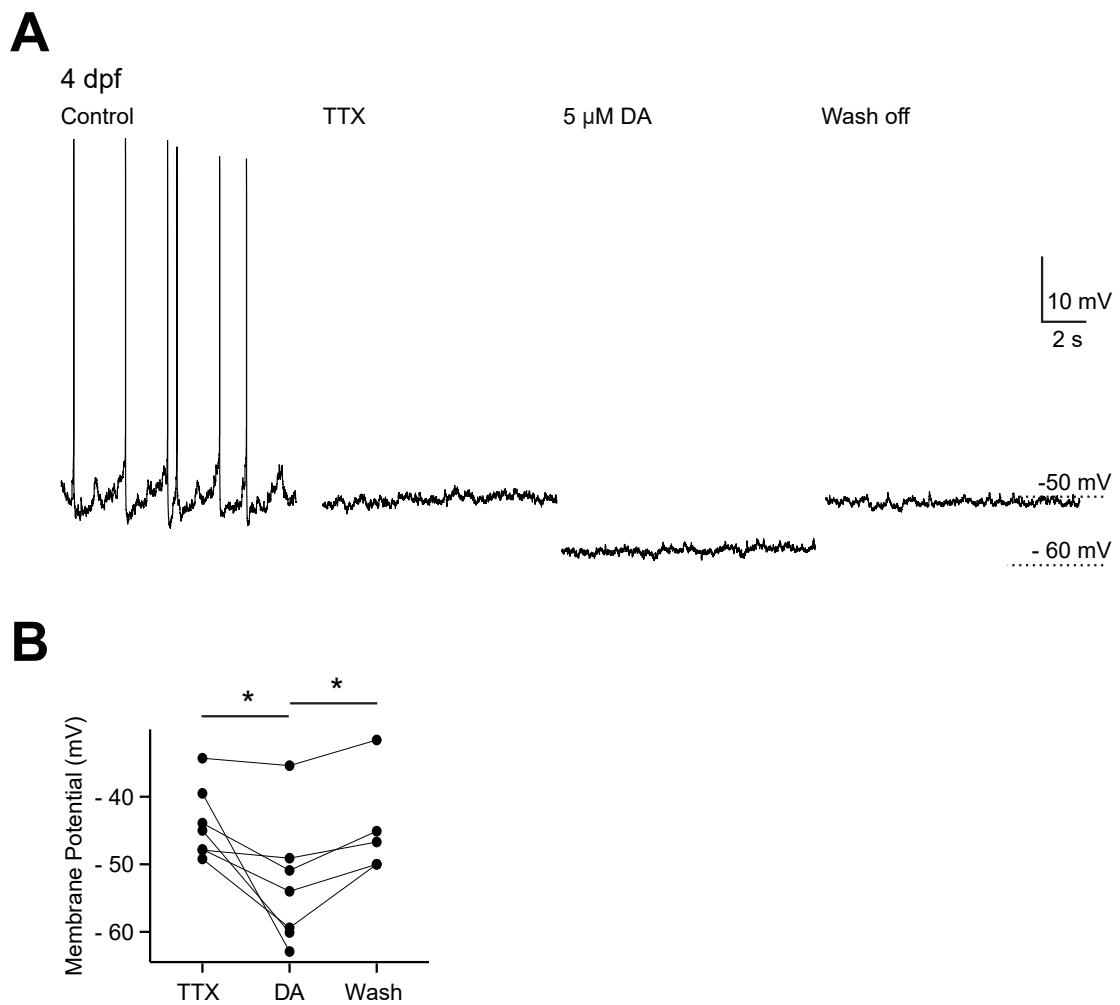


FIGURE 4.26

DA hyperpolarises membrane potential following TTX application. (A) TTX abolishes autonomous spike activity. Subsequent DA application hyperpolarising the membrane potential, which is subsequently rescued by wash off. (B) Resting membrane potential of DDNs preincubated with TTX before, during and after DA application.

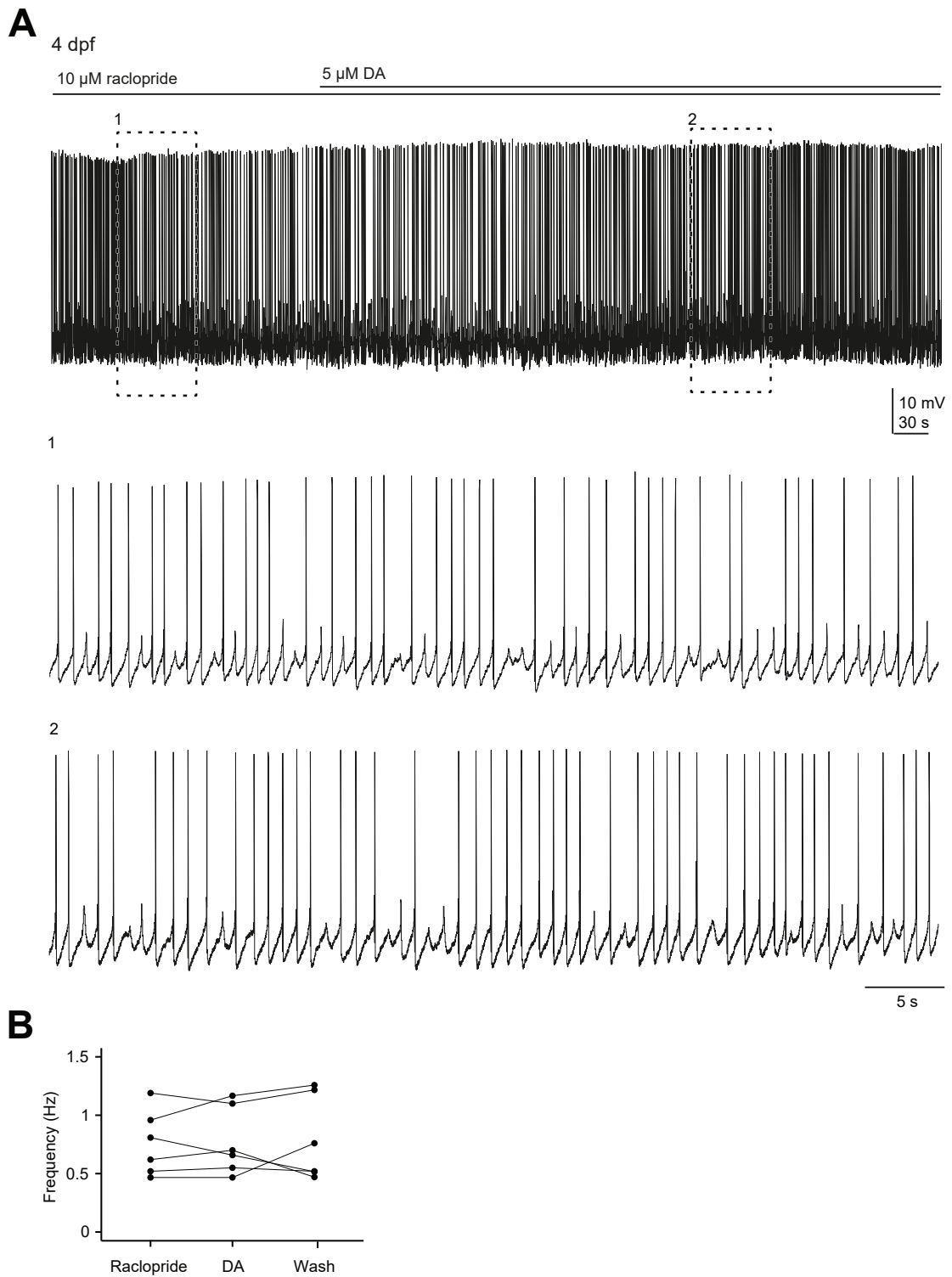


FIGURE 4.27

D₂ receptor antagonist abolishes dopaminergic autoinhibition. (A) Continuous perforated patch recording from a 4 dpf DDN preincubated with 4 mM kynurenic acid, 100 μ M picrotoxin and 10 μ M raclopride. Autonomous spiking persists following prolonged 5 μ M DA application. Bottom traces correspond to numbered dashed boxes in top trace. (B) Average autonomous action potential frequency during preincubation with raclopride, during and after DA application.

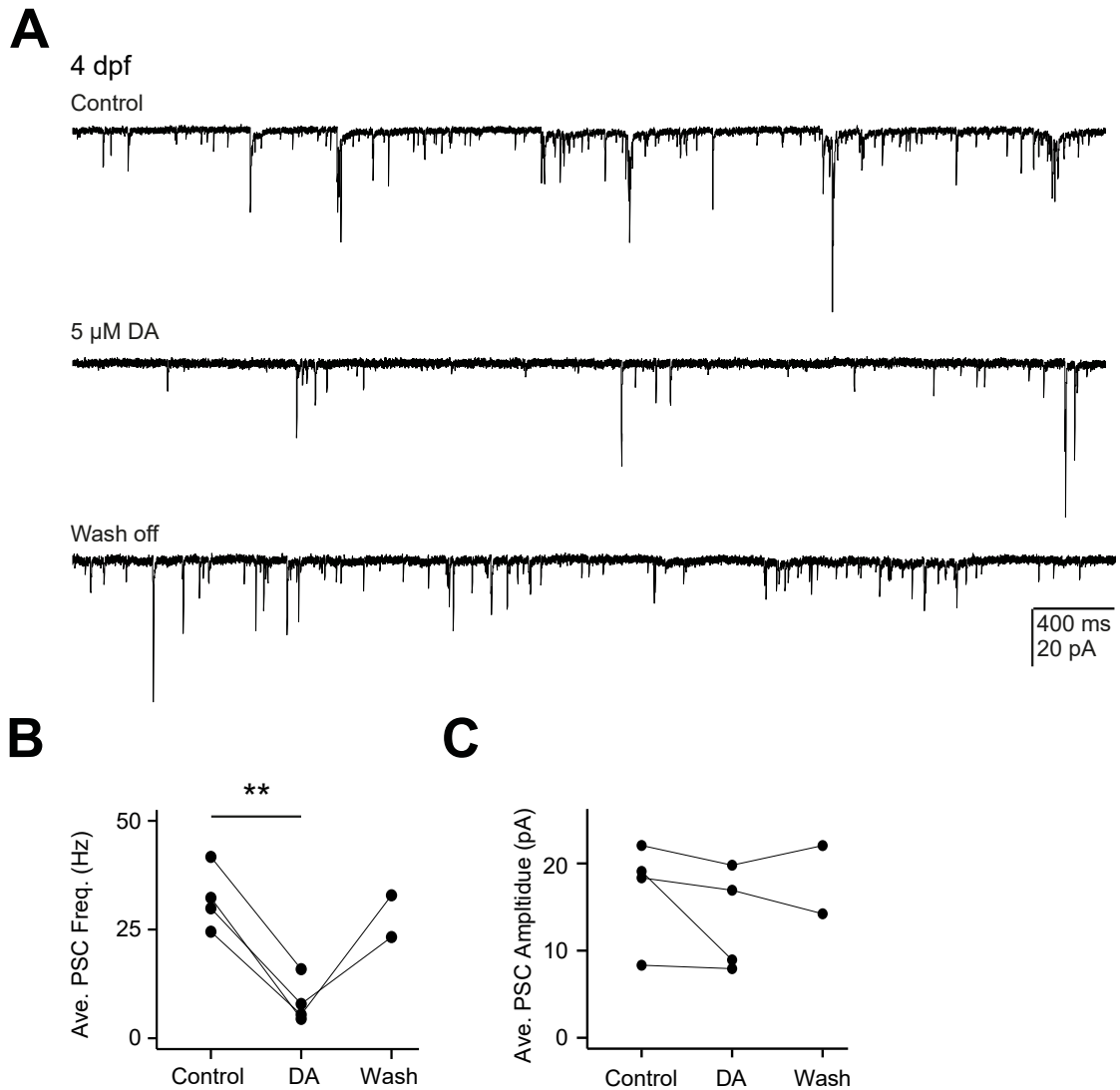


FIGURE 4.28

DA modulates synaptic inputs into DDNs. (A) Whole cell voltage clamp recordings of post synaptic currents in DDNs under control conditions (top), during (middle) DA application and after wash off (bottom). (B – C) Average frequency of synaptic input (B) and amplitude (C) before, during and after DA application.

4.4 Discussion

In this chapter, I have examined the developing electrophysiological properties of DDNs during the first four days of zebrafish development, a period marked by profound changes in locomotor output. Given that this cell population provides the only known source of DA to the spinal cord, understanding their electrical activity patterns as locomotor networks develop is necessary to fully appreciate their role in modulating locomotor network function and development. The findings presented here demonstrate that the excitable properties and endogenous activity patterns of DDNs mature progressively during early periods of motor network maturation.

4.4.1 DDNs innervate central and peripheral structures

In order to examine axonal projections, DDNs were labelled with neurobiotin. These experiments revealed that in addition to innervating the spinal cord, DDNs also innervate peripheral sensory structures including the otic capsule and neuromasts of the lateral line system. Previous work has already identified a population of diencephalic DAergic neurons which project to the periphery (Metcalf et al., 1985; Bricaud et al., 2001). However, the work presented in this chapter demonstrates that the DAergic neurons which innervate peripheral sensory structures also innervate spinal networks by 4 dpf.

The lateral line system is comprised of neuromasts distributed along the body surface of the zebrafish (Raible and Kruse, 2000; Liao, 2010). Each neuromast contains hair cells which act to detect perturbations in water flow. Self-generated movement

would activate the same sensory pathways used to detect perturbations in the environment. This reafferent input to the nervous system may therefore make it difficult to discern environmental cues from self-induced motion. One proposed mechanism to compensate for reafferent signals is that of efference copies which represent a copy of the motor pattern originating from the nervous system. These copies of the motor pattern are relayed to peripheral sensory structures in order to modulate afferent processing. Studies of *Xenopus*, dogfish and burbot have demonstrated that afferent output from the lateral line is depressed by inhibitory efferent input during swimming (Flock and Russell, 1973; Russell, 1971; Russell and Roberts, 1974; Chagnaud et al., 2015). In *Xenopus* efference copies arise from the spinal network which are subsequently transmitted to efferent neurons located in the hindbrain (Chagnaud et al., 2015). During swimming the efferent neurons, which innervate the neuromasts, are recruited to provide temporal information about the locomotor pattern and act to attenuate afferent signals (Chagnaud et al., 2015). The DAergic inputs to neuromasts reported in this chapter may also act to modulate efferent inputs to neuromasts or act post-synaptically to tune afferent inputs to the nervous system. Additionally, since DDNs spike even in the absence of synaptic input, DA may serve additional roles to modulate neuromast sensitivity during periods of locomotor inactivity.

4.4.2 Development of intrinsic spike properties

The electrophysiological responses to threshold and suprathreshold current injection were examined at embryonic coiling (1 dpf), larval burst (2 dpf) and beat-glide swimming (4 dpf) stages of development. At coiling stages, rheobase current triggered action potentials with an atypically broad half-width, small amplitude and high thresh-

old. Additionally, injection of suprathreshold current only occasionally ($\approx 10\%$ of cells) elicited multiple action potentials despite a prolonged period of current injection. By burst and beat-glide swimming stages, DDNs still fired singular action potentials at rheobase, but the half-width and activation threshold had markedly decreased. Additionally, by these ages, DDNs also fired multiple action potentials in response to suprathreshold current.

The generation and waveform of an action potential is dependent upon the composition and spatial distribution of voltage-gated ion channels (Traub and Llinás, 1977; Gao and Ziskind-Conhaim, 1998; Alessandri-Haber et al., 1999; Spitzer et al., 2000; Pineda, 2005). As neurons mature, K^+ and Na^+ currents increase which drive changes in action potential waveform (Strübing et al., 1995; Lenka et al., 2002; Benninger et al., 2003). These developmentally associated changes in waveform include increasing amplitudes and decreasing durations (Strübing et al., 1995; Gao and Ziskind-Conhaim, 1998; Lenka et al., 2002; Benninger et al., 2003). Embryonic neuron discharges are characterised by a high threshold, small amplitude action potential with a prolonged duration and slow rate of rise. In mammalian tissues, as development continues, action potentials with shorter durations and larger amplitudes are elicited at lower thresholds. Additionally, these action potentials have faster rise and repolarisation phases relative to embryonic action potentials (Strübing et al., 1995; Gao and Ziskind-Conhaim, 1998). Finally, neurons develop the capacity to spike repeatedly in response to constant depolarising current injection. At postnatal stages, K^+ channel density increases to facilitate rapid repolarisation and repetitive firing. Within the context of the work presented in this chapter, embryonic DDNs fire single, small, long duration action potentials in response to depolarising current. By 2 and 4 dpf, DDNs

develop the capacity to fire repetitively, and fire action potentials with relatively fast kinetics. These changes are similar to those previously reported in developing rat neuron populations (Strübing et al., 1995; Gao and Ziskind-Conhaim, 1998; Lenka et al., 2002; Benninger et al., 2003). Thus, these developmentally related changes in DDN action potential waveform may be dependent upon similar mechanisms.

The aforementioned effects on action potential waveform and generation are likely to have significant functional consequences. In support of this, these properties are characteristic of DAergic neurons of the SNc (Grace and Onn, 1989) and a subgroup of VTA DA neurons that, at adult stages, produce APs with atypically long (≈ 8 ms) half-widths which exhibit slow rates of depolarisation (Lammel et al., 2008) suggesting such activity patterns may be relevant to network activity. Additionally, neurons which arise from the VTA and project to the same region have unique electrophysiological characteristics. For example, half-widths have recently emerged as a reliable indicator of DAergic status, such that interneurons with relatively long half-widths are DAergic while those with short half-widths are non-DAergic, despite both populations projecting to the nucleus accumbens (Margolis et al., 2008).

As development proceeds from burst- (2 dpf) to beat-glide (4 dpf) swimming, the firing properties of DDNs mature such that action potentials are larger in amplitude with a shorter half-width and lower spike threshold. As is the case at embryonic stages, these changes may be attributable to increased expression of voltage gated Na^+ and K^+ channels (Strübing et al., 1995; Gao and Ziskind-Conhaim, 1998; Lenka et al., 2002; Benninger et al., 2003). Nonetheless, spike half-widths remained relatively broad ($\approx 3 - 4$ ms) in comparison to other neuron populations at comparable ages. For example, by 4 dpf, zebrafish excitatory interneurons and motoneurons have action potential

half-widths < 1 ms (Buss et al., 2003; Kimura et al., 2006). By larval stages, DDNs fire multiple, large amplitude action potentials in response to suprathreshold current. The instantaneous frequency of action potential discharge at 1.5 and 2x rheobase at both 2 and 4 dpf was restricted to a relatively narrow bandwidth: the highest frequencies were observed during the first 100 ms of the current step with an average peak frequency of ≈ 25 Hz (maximum observed frequency of 43 Hz). Relative to mammalian DAergic neurons, these firing frequencies are comparatively high. For example, most DAergic neurons within the SNc when challenged with depolarising current steps or ramps, can only attain frequencies up to ≈ 10 Hz, although a subpopulation can reach a maximum frequency of 20 Hz (Lammel et al., 2008). Additionally, these frequencies can only be sustained for subsecond time scales before spike-failure. Here, while frequencies declined in response to steady-state current steps, DDNs could still spike at ≈ 6 Hz at the end of a 2 s current step. Thus, in comparison to mammalian DAergic neurons, DDNs appear to exhibit robust firing patterns, yet still exhibit classical DAergic markers such as prolonged half-widths.

4.4.3 DDNs spike autonomously in an age-dependent manner

During extracellular recordings, addition of the synaptic blockers kynurenic acid and picrotoxin was sufficient to inhibit spike activity at 1 dpf but not at 2 or 4 dpf. When mammalian midbrain DAergic neurons are recorded after loss of afferent inputs, either under *in vitro* or *in vivo* anaesthetised conditions, they autonomously generate action potentials which are superimposed upon slow membrane oscillations (Grace and Bunney, 1983c, 1984a; Grace, 1991). Perforated patch clamp recordings at 4 dpf revealed the presence of autonomous spiking which persisted in the presence of these synap-

tic blockers. These findings suggest that DDNs set a basal tone of dopamine release as zebrafish enter swimming stages. As is the case in mammalian midbrain DAergic neurons (Grace, 1991; Grace and Bunney, 1983b,a; Kita et al., 1986; Grace and Onn, 1989), this autonomous DDN spiking is underpinned by voltage-dependent membrane oscillations that cyclically drive these cells to spike threshold. These oscillations are likely to be driven by Na^+ currents since addition of TTX, a voltage-gated Na^+ channel blocker, was sufficient to abolish them. In contrast, subthreshold Ca^{2+} or I_h currents are unlikely to contribute to the pacemaker activity observed here since application of TTX and TEA failed to unmask subthreshold Ca^{2+} oscillations (Kang and Kitai, 1993) and hyperpolarising current steps did not elicit sag potentials as would be expected if I_h currents contributed to the pacemaking activity (Maccaferri and McBain, 1996; Lüthi and McCormick, 1998; Biel et al., 2009). These findings stand in contrast to some studies which have reported the presence of low threshold Ca^{2+} - and I_h -dependent oscillations in mammalian DAergic neurons (Kita et al., 1986; Nakanishi et al., 1987; Grace and Onn, 1989; Nedergaard et al., 1993; Chan et al., 2007). Nonetheless, subthreshold-activating persistent Na^+ currents have been reported to drive pacemaker activity in a range of neuronal subtypes, including mammalian midbrain DAergic neurons (Uteshev et al., 1995; Taddese and Bean, 2002; Tazerart et al., 2008; Khaliq and Bean, 2010; Milescu et al., 2010; Yamada-Hanff and Bean, 2013). Interestingly there are species-specific, anatomical and age-dependent variation in the relative contributions of different ion channels to pacemaker activity (Ungless and Grace, 2012; Chan et al., 2007). For instance, at postnatal stages in mice, Na^+ channels appear to be the predominant contributor to pacemaker activity (Chan et al., 2007). As mice enter adult stages, Na^+ channels are no longer necessary to drive pacemaking, which is instead reliant upon

Ca²⁺ currents. Thus, the dependence of autonomous spiking on Na⁺ channels reported in this chapter may represent age-dependent variation. Future voltage clamp studies at larval and adult stages will help to pinpoint the subthreshold conductances required for membrane oscillations. Nonetheless, while the specific mechanisms underpinning autonomous spiking may differ from mammalian DAergic neurons, these findings lend further support to conserved physiological characteristics between vertebrate DAergic neurons.

4.4.4 DDNs undergo depolarisation block

During the course of continuous depolarising current steps, spike frequency and peak amplitude decreased while half-width increased. These changes in action potential waveform over time are indicative of depolarisation block whereby cells begin to fail to spike in response to suprathreshold current due to sodium channel inactivation (Grace and Bunney, 1986; Kuznetsova et al., 2010; Tucker et al., 2012). To investigate this possibility further here, DDNs were exposed to depolarising triangular current ramps that returned the membrane to rest preceding the peak of the ramp. During higher amplitude current ramps, DDNs robustly fired during the depolarising phase but failed to reliably spike during the declining phase of the protocol. These findings suggest DDNs undergo depolarisation block. Interestingly, mammalian midbrain DAergic neurons are thought to be particularly susceptible to depolarisation block. Indeed, one mechanism by which antipsychotic drugs are thought to act is by inducing chronic depolarisation block of hyperactive DA neurons (Chiodo and Bunney, 1983; Grace and Bunney, 1986; Grace, 1992; Valenti et al., 2011). Depolarisation block may also modulate ongoing endogenous activity patterns under physiological conditions. DAergic

neurons exhibit two primary modes of firing, low frequency tonic spiking and high frequency bursting. Computational models of midbrain DAergic neuron activity patterns suggest that the burst modes of output may terminate via depolarisation block (Oster et al., 2015). In the next chapter, I will discuss in detail the firing dynamics of DDNs but, like midbrain DA neurons, DDNs also exhibit similar modes of output: low frequency tonic spiking and high frequency bursts. Thus, the depolarisation block observed here may contribute to endogenous activity patterns and regulate DA release.

In sum, DDNs functionally mature across the first four days of development. At embryonic stages, DDNs fire small amplitude, broad action potentials at high thresholds. As development continues, spike threshold progressively decreases, action potentials become larger in amplitude and DDNs can fire multiple spikes in response to depolarising stimuli.

4.4.5 Developing synaptic inputs

In order to examine synaptic inputs, whole cell voltage clamp recordings were conducted across the first four days of development. At 1 dpf, only one population of events could be resolved, which are presumably glutamatergic since they were abolished following kynurenic acid application. By 2 and 4 dpf, two populations of events, which were distinguishable based on their kinetic and pharmacological properties were observable. Initial application of picrotoxin revealed a population of events with fast kinetics that were blocked by subsequent application of the kynurenic acid. The second population could be isolated by initial application of kynurenic acid and abolished by subsequent addition of picrotoxin. Thus, by 2 and 4 dpf, DDNs receive both gluta-

matergic and GABAergic inputs.

It is perhaps not surprising that DDNs receive glutamatergic and GABAergic inputs since these neurotransmitter systems represent the major excitatory and inhibitory inputs within the brain (Mayer and Westbrook, 1987; Meldrum, 2000; Ben-Ari et al., 2007; Li and Xu, 2008) and hypothalamic regions are known to receive glutamatergic inputs (van den Pol and Trombley, 1993). Additionally, within the zebrafish, there are extensive regions of GABAergic-positive cells distributed throughout the nervous system at embryonic and larval stages (Mueller et al., 2006; MacDonald et al., 2010; Souza et al., 2011). Interestingly, while GABAergic cells are present at 1 dpf, DDNs do not yet receive GABAergic inputs, suggesting that these synaptic connections have yet to form. Since DDNs do receive glutamatergic inputs at this age, activity patterns are presumably driven by these excitatory inputs. In support of this, block of glutamatergic inputs is sufficient to abolish all spike activity at this age (see Figure 4.19). By free swimming stages (2 and 4 dpf), DDNs receive both glutamatergic and GABAergic inputs which may contribute to activity patterns that are observed prior to synaptic blockade.

In mammalian DAergic neurons, NMDA and α -amino-3-hydroxy-5-methyl-4-isoxazolepropionic acid (AMPA) mediated currents are known to contribute to endogenous activity patterns (Chergui et al., 1994; Christoffersen and Meltzer, 1995; Tong et al., 1996; Blythe et al., 2007). In this chapter, kynurenic acid was used to confirm a population of events were mediated by glutamatergic inputs. However, this drug is a non-selective antagonist for both NMDA and AMPA receptors. Thus, the relative contribution of NMDA and AMPA to observed activity patterns could not be determined here. Further investigations using more specific pharmacological reagents will help

elucidate relative contributions.

4.4.6 Synaptic inputs to DDNs are suppressed by DA

During voltage clamp recordings of post synaptic currents (PSCs), bath application of DA significantly reduced the frequency, but not the amplitude of synaptic input to DDNs. These findings strongly suggest that afferent inputs are depressed by DA. While the afferent inputs which terminate upon DDNs have not been identified, such effects could be mediated in a D_2 -receptor dependent mechanism. For example, in the mammalian midbrain, D_2 receptors are distributed throughout the VTA and are located on non-dopaminergic neurons (Pickel et al., 2002). Additionally, glutamatergic inputs to VTA DAergic neurons are strongly depressed following DA application (Koga and Momiyama, 2000). Here, bath application of DA or the D_2 -like agonist, quinpirole, was sufficient to reduce both the amplitude and frequency of excitatory post synaptic currents (EPSCs). These effects were rescued by addition of the D_2 -like receptor antagonist sulpiride (Koga and Momiyama, 2000). Thus local DA release within the VTA could inhibit glutamatergic inputs to DAergic neurons. DAergic neurons in the VTA are also known to receive glutamatergic innervation from the medial prefrontal cortex (mPFC) (Sesack and Pickel, 1992; Carr and Sesack, 2000) which in turn project to the mPFC (Carr and Sesack, 2000) suggesting DAergic neurons in this area could indirectly inhibit their activity patterns.

4.4.7 DDNs undergo autoinhibition

During perforated patch clamp recordings of pacemaker activity in DDNs, exogenous DA application strongly inhibited autonomous spike activity in a D_2 receptor-dependent manner. These observations are consistent with findings from the mammalian midbrain. Under physiological conditions, mammalian midbrain DA neurons release DA from their dendrites and soma. In both the SNc and VTA, this locally released DA binds to autoreceptors which inhibits DA neuron activity and thus affects DA release at target sites (Bunney et al., 1973; Lacey et al., 1987; Silva and Bunney, 1988; Liu et al., 1994; Kim et al., 1995; Fedele et al., 1999; Weber et al., 2001; Joseph et al., 2002; Beaulieu and Gainetdinov, 2011). These effects are likely mediated by D_2 receptors, since inhibition of autonomous spiking can be abolished following application of D_2 receptor antagonists (Beckstead et al., 2004, 2007; Courtney et al., 2012).

The precise functional role of D_2 autoreceptors, beyond regulating DA release, is unclear. Chronic activation of D_2 -receptors can lead to a reduction in locomotor output (Missale et al., 1998). However, whether these effects are mediated via autoreceptors or postsynaptic D_2 receptors is not clear. A recent study has attempted to address this issue by selectively removing D_2 receptors from DAergic neurons in the SNc and VTA (Anzalone et al., 2012). Firstly, this study found that D_2 autoreceptors were responsible for inhibition of firing in this population of DAergic neurons. Secondly, in freely behaving mice, loss of D_2 autoreceptors had little effect on locomotor activity in mice under normal conditions. However, when presented with novel environments, these mice were hyperactive. Thus, D_2 autoreceptors may play a key role in modulating behaviour.

In mammals, D₂ autoreceptors activate GIRK channels that hyperpolarise the membrane potential (Uchida et al., 2000; Kim et al., 1995; Kuzhikandathil et al., 1998). While the mechanism underpinning the inhibitory actions of DA within zebrafish DDNs are unknown, there is extensive D₂ receptor expression localised to approximately the same region as where the DDNs are located (Boehmler et al., 2004) and relatively sparse expression of the other DA receptors (Boehmler et al., 2004, 2007; Li et al., 2007). Additionally, bath application of DA hyperpolarised the resting membrane potential after TTX treatment. Finally, preincubation with raclopride, a D₂-receptor antagonist was sufficient to abolish DA-mediated inhibition of autonomous spiking. These findings are consistent with the hypothesis of a D₂-GIRK mediated effect. If this is the case, autoreceptors may activate GIRK channels to hyperpolarise the membrane potential, decrease the frequency of the voltage-dependent subthreshold oscillations and thus decrease autonomous spiking.

In sum, the findings presented in this chapter have confirmed that a population of neurons located in DC2 are DAergic and project to the spinal cord and periphery. Additionally, the cellular basis for DAergic activity patterns at 1, 2 and 4 dpf, have been examined. This work lays the foundation for defining the functional significance of DDNs in an awake, living vertebrate.

**The Developing Activity Patterns and
Functional Roles of Spinally Projecting
Dopaminergic Neurons**

5.1 Introduction

Dopaminergic inputs to the spinal cord have been implicated as important modulators of locomotor output and, more recently, neurodevelopmental processes. However, most experiments to date examining the role of these cells have resorted to bath application of dopamine (DA) receptor agonists/antagonists or lesions of supraspinal pathways in order to elucidate the role of descending DAergic pathways. Such methods, while providing insight into the role of DAergic signalling, are often non-specific and may not fully simulate the firing properties of dopaminergic diencephalospinal neurons (DDNs) *in vivo*.

Within this chapter, I have characterised the activity patterns of a population of DDNs over the first four days of development and examined how their firing properties relate to fictive locomotor output in a paralysed, but awake, zebrafish preparation. Furthermore, by conducting specific ablation of these cells, I have begun to elucidate the modulatory actions of DDNs in free swimming larvae.

5.1.1 Dopaminergic control of spinal networks

In all vertebrates, the primary source of DAergic inputs to the spinal cord arises from a cluster of DAergic cells in the diencephalon. Despite the importance of dopamine as a modulator of spinal networks, little attention has been paid to this descending pathway. Thus, the role of DA in controlling and modulating mammalian locomotor networks is unclear. Nonetheless, several studies have examined the effects of DA on spinal network activity. When neonatal rats are suspended in the air, step-like

movements can be induced following application of L-3,4-dihydroxyphenylalanine (L-DOPA), a DA precursor, and the effects of L-DOPA are inhibited following D₁ or D₂ receptor antagonist application (Van Hartesveldt et al., 1991; McCrea et al., 1997). Similarly, using *in vitro* spinal cord preparations, locomotor-like activity can be induced by DA application (Kiehn and Kjaerulff, 1996; Barrière et al., 2004) although relative to normal locomotor output, the frequency and regularity of this activity is markedly reduced (Kiehn and Kjaerulff, 1996). In spinal cord transected adult mice preparations, locomotor activity can also be induced following application of DA or D₁/D₅ agonists (Lapointe et al., 2009). However, DA fails to induce locomotor output at neonatal stages (Sharples et al., 2015). In higher vertebrates, such as cats, DA and DA receptor agonists also fail to induce locomotor activity following spinal transection (Barbeau and Rossignol, 1991) but addition of L-DOPA, a precursor for DA and other neurotransmitters (i.e. noradrenaline and adrenaline), does (Jankowska et al., 1967a,b; Grillner and Zangger, 1979). Thus, whilst in mammals the role of DA in locomotor initiation is unclear, DA does appear to modulate ongoing parameters of ongoing motor activity in several species. These effects are mediated by D₁-like and D₂-like receptor subfamilies and, in both the rat and mouse, a growing body of evidence suggests that DA mediates excitatory effects on spinal networks via the D₁-like receptors (Seth et al., 1993; Gordon and Whelan, 2006; Han et al., 2007; Lapointe et al., 2009; Clemens et al., 2012) and inhibitory effects via activation of D₂-like receptors (Maitra et al., 1993; Clemens et al., 2012; Humphreys and Whelan, 2012).

The role of DA in modulating locomotor networks has also been examined in lower vertebrates such as the lamprey and *Xenopus*. In lamprey, there is an equivalent population to the DAergic A11 neurons which project down the spinal cord (Barreiro-

Iglesias et al., 2008), although their precise function is unknown. However, the role of a further DAergic neuron cluster which arises from the posterior tuberculum (PT) and projects to the mesencephalic locomotor region (MLR) has been elucidated (Ryczko et al., 2013). These DAergic inputs play an important role in gating locomotor activity. Electrical stimulation of the PT is sufficient to raise DA concentrations within the MLR and evoke swim episodes (Ryczko et al., 2013). Additionally, localised injection of the D₁ antagonist, SCH 23390, into the MLR reduces locomotor output, whereas injection of DA to the same region had the opposite effect. Thus, within the lamprey, DA appears to have broadly excitatory effects at the level of the MLR.

In lamprey spinal cord preparations, DA has complex effects upon rhythm generation. Harris-Warrick and Cohen (1985) found that after bath application of DA, spontaneous motor activity initially increased and then declined within 10 min. Other groups have found DA to have concentration dependent effects on ongoing locomotor output (McPherson and Kemnitz, 1994). Low concentrations (0.1 – 1 μM) of DA increased, while high concentrations (10 – 100 μM) decreased cycle frequency within swim episodes (McPherson and Kemnitz, 1994; Schotland et al., 1995). Similarly, in *Xenopus*, DA has concentration-dependent effects on fictive locomotor output. These effects appear to be mediated by differential activation of D₁ and D₂-like receptors (Clemens et al., 2012). In this preparation, low concentrations (2 μM) of DA activate D₂-like receptors while high concentrations of DA (> 50 μM) activate the low-affinity D₁-like receptors (Clemens and Hochman, 2004; Clemens et al., 2012). At low doses, DA decreased the occurrence of swim episodes over time and affected the structure of each swim episode such that the cycle frequency was significantly slower relative to control. In contrast, high doses of DA increased the occurrence of swim episodes

and accelerated the cycle frequency (Clemens et al., 2012). Thus, DA appears to alter network output by binding to DA receptors which exhibit low and high affinities for DA. Clemens et al. (2012) suggest that low levels of DA preferentially activate the high-affinity D₂-like receptor pathways which mediate inhibitory effects on spinal central pattern generator (CPG) networks whilst higher concentrations of DA would activate the lower-affinity D₁-like receptors and have excitatory effects on CPG networks which override the depressive effects of D₂ receptor activation. However, recent evidence suggests D₂ receptors can also exist in low affinity states which are not saturated under high concentrations of DA (Marcott et al., 2014). Thus the precise contributions of D₁- and D₂-receptor mediated effects may require further investigation.

In zebrafish, the precise roles of DA in modulating spinal networks are unclear. A recent investigation found that application of DA or a DA reuptake blocker can abolish spontaneous swim episodes at 3 days post fertilisation (dpf) while DA application at 5 dpf reduces motor output (Thirumalai and Cline, 2008). Yet, other investigations examining the acute effects of a range of dopaminergic agonists and antagonists found DA to have broadly excitatory roles. Both D₁-like (SKF-38393) and D₂-like (quinpirole) agonists increased locomotor activity at low concentrations while antagonists for D₁- (SCH-23390) and D₂-like (haloperidol) receptors decreased activity (Irons et al., 2013). Additionally, these drugs also reduced the stereotypical response to changes in illumination (Irons et al., 2013). Similarly, application of clozapine, a selective D₄ receptor antagonist affected locomotor activity in a dose-dependent manner (Boehmler et al., 2007): high (50 µM) concentrations abolished spontaneous swim episodes. However, larvae still swam in response to touch. At relatively low concentrations (12.5 µM), clozapine reduced output, but larvae still engaged in swimming.

Additionally, Thirumalai and Cline (2008) demonstrated that application of D₂-receptor antagonists increased the frequency of swim episodes and these effects were mediated in a 3'-5'-cyclic adenosine monophosphate (cAMP)-dependent mechanism.

In addition to modulating locomotor output, DA may also have developmental roles. Loss of early DAergic inputs to the embryonic spinal cord, or block of D₄ receptors, is sufficient to decrease the number of motoneurons and increase the number of V2 interneurons (which give rise to excitatory and inhibitory interneurons) (Reimer et al., 2013). Changes in DA levels can have profound effects on the maturation of motor network output (Lambert et al., 2012). Specifically, block of spinally projecting DAergic inputs, either by chemogenetic ablation or D₄ receptor antagonists can prevent maturation of locomotor output or revert mature modes of locomotor output (beat glide swimming) to more immature-like swimming (reminiscent of burst swimming). Interestingly, these effects can also be invoked following acute spinal cord transection. In spinalised preparations, larvae do not spontaneously engage in swimming although swim episodes can be evoked by N-Methyl-D-aspartic acid (NMDA) application (McDearmid et al., 2006). When Lambert et al. (2012) spinalised 4–7 dpf larvae and applied NMDA, swim episodes were conspicuously long, suggestive of immature modes of output. However, when DA was subsequently added to the extracellular saline, swim episodes were shortened and resembled control swim episodes. Thus, DA appears to be an important modulator for spinal network development and locomotor network output, however the precise mechanisms have yet to be elucidated.

5.1.2 Mechanisms underpinning the effects of DA on spinal networks

Since DA has been shown to effect the rhythmicity and strength of motor output, recent investigations have begun to focus on the effects of DA on CPG components (Han et al., 2007; Han and Whelan, 2009). Han et al. (2007) took advantage of a line of mice which express GFP in motoneurons and a population of interneurons in the ventral horn. The HB9 promoter is an essential homeobox gene for motoneuron differentiation but also localises to a discrete population of interneurons in lamina VIII (Hinckley et al., 2005; Wilson, 2005; Han et al., 2007). Targeted recordings from these HB9 positive motoneurons and interneurons in isolated spinal cord preparations revealed DA had a diverse range of effects on the CPG network. During ventral root recordings, bath application of DA markedly depolarised populations of motoneurons and interneurons. Whole cell methods and pharmacological investigations revealed that DA can modulate small conductance calcium-activated potassium channels (SK_{Ca}) to increase the spike frequency of motoneurons by decreasing the medium-duration hyperpolarisation (mAHP) which is driven largely by SK_{Ca} -mediated currents. Similar effects on motoneuron firing frequency have also been reported in the rat (Garraway and Hochman, 2001) and lamprey (Kemnitz, 1997). In the lamprey, DA or apomorphine (a non-selective DA receptor agonist) reduced the late AHP in motoneurons, giant interneurons and a class of mechanosensory neurons (edge cells) but did not have similar effects on other classes of interneurons (Kemnitz, 1997) suggesting DA has a selective role in modulating spinal cells. However, these effects may be species specific: in zebrafish, DA does not affect the firing frequency or other basic parameters (gain, input resistance, resting membrane potential or afterhyperpolarisation (AHP))

of identified motoneurons (Thirumalai and Cline, 2008). In mice, HB9 interneurons have an intrinsic rhythmicity and DA appears to be necessary but not sufficient to initiate these intrinsic oscillations (Han et al., 2007). Specifically, in order to evoke oscillatory activity, a combination of pharmacological reagents must be added to the extracellular solution. In the presence of tetrodotoxin (TTX), addition of NMDA and serotonin is insufficient to elicit oscillations. Similarly, application of TTX and DA fails to induce this activity (Han et al., 2007). However, inclusion of NMDA, serotonin and DA in the presence of TTX can elicit depolarising membrane oscillations. Thus, while the role of HB9 positive interneurons has not been established, DA may serve to stabilise rhythmicity in spinal networks in agreement with previous reports (see subsection 5.1.1).

Additionally, DA may serve to increase α -amino-3-hydroxy-5-methyl-4-isoxazolepropionic acid (AMPA) evoked currents within motoneurons (Han et al., 2007). These effects appear to be mediated by a D₁-like receptor mechanism, since agonism of these receptors increased the open probability and open duration of AMPA channels (Han and Whelan, 2009). However, whether this is a general principle of DAergic signalling in the spinal cord remains to be determined since DA application has generally depressive effects on evoked excitatory post synaptic potentials (EPSPs) in the rat dorsal horn (Garraway and Hochman, 2001).

5.2 Aims and objectives

Since previous reports have clearly identified descending DAergic tracts as integral to proper maturation and functioning of spinal networks, I first sought to examine the temporal emergence of DDN firing properties across embryonic (1 dpf), burst

swimming (2 dpf) and beat-glide swimming (4 dpf) stages of development. Next, the cellular bases for these activity patterns were examined. Finally, the functional roles of these cells were investigated, firstly by examining the temporal relationship between DDN activity patterns and locomotor network output and secondly by investigating the effects of DDN ablation.

5.3 Results

5.3.1 Ontogeny of endogenous activity patterns

First I sought to characterise the emergent *in vivo* activity patterns of DDNs during development. In order to understand when activity patterns emerge, non-invasive loose patch recordings were taken from DDNs across embryonic coiling (18–30 hours post fertilisation (hpf)), burst swimming (2 dpf) and beat-glide swimming (4 dpf) stages of development (Figure 5.1A-C). During early coiling periods (18–20 hpf) DDNs were completely silent ($n = 14$) (Figure 5.1A,D) which suggests that these cells are not yet functionally integrated into central networks. By 21 hpf a minority of cells ($n = 2$ of 7) began to fire sparse unitary spikes (active cells frequency = 0.17 ± 0.12 Hz, $n = 2$). As development continued, the probability of observing spike activity increased, such that between 25 and 30 hpf all recorded DDNs ($n = 27$) exhibited robust (1.28 ± 0.24 Hz) tonic spiking (Figure 5.1D).

At 2 dpf, tonic spiking was still observed in all recorded DDNs ($n = 30$, Figure 5.1B). The mean frequency of tonic spikes was comparable to that observed within the active 25–30 hpf DDNs (active 1 dpf = 1.28 ± 0.24 Hz, 2 dpf = 1.23 ± 0.15 Hz, $p > 0.05$, Figure 5.1E). In contrast to embryonic stages (18–30 hpf), in approximately 50% ($n = 14$ of 30) of 2 dpf DDNs short bursts which were characterised by discrete periods (0.39 ± 0.05 s) of high intensity spiking (21.39 ± 1.39 Hz) were observed (Figure 5.1B,F,G). By 4 dpf, both the frequency of tonic firing and incidence of high frequency bursting had increased. Relative to 1 and 2 dpf, tonic spike frequency was significantly higher by 4 dpf (4 dpf frequency = 2.23 ± 0.28 Hz, 1 dpf vs 4 dpf = $p <$

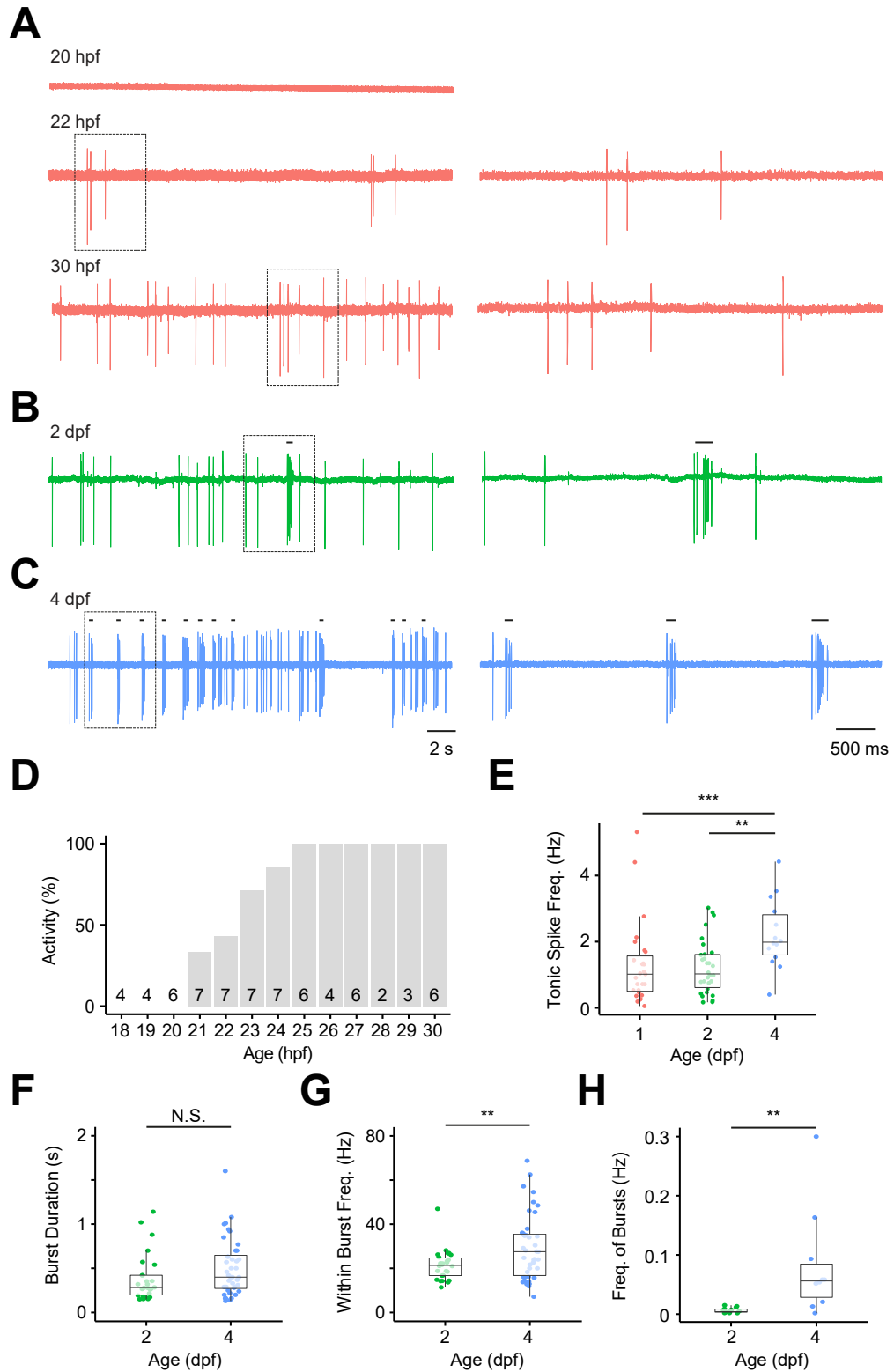


FIGURE 5.1

Activity patterns of DDNs during development. (A – C) Representative extracellular loose patch recordings from coiling (A), burst swimming (B) and beat-glide stages (C). Black bars denote bursts. (D) Onset of activity during coiling stage embryos. Number of embryos at each time point are denoted on the graph. (E) Box and whisker plot of tonic spike frequency of DDNs during development. (F – H) Box and whisker plots of burst duration (F), interburst frequency (G) and frequency of bursts (H).

0.001; 2 dpf vs 4 dpf = $p < 0.01$, Figure 5.1E) and discrete bursts of spike discharge were observed in 10 of 14 cells (71%). While bursts were of similar duration at 2 and 4 dpf (2 dpf = 0.39 ± 0.05 s, 4 dpf = 0.50 ± 0.05 s, $p > 0.05$, Figure 5.1F) the spike frequency within bursts had significantly increased (2 dpf = 21.39 ± 1.39 Hz, 4 dpf = 30.58 ± 2.29 Hz, $p < 0.01$, Figure 5.1G) and the incidence of bursts throughout the course of the recording had also significantly increased (2 dpf = 0.006 ± 0.001 Hz, 4 dpf = 0.08 ± 0.03 Hz, $p < 0.01$, Figure 5.1H).

5.3.2 Activity patterns within the DDN population

In order to examine whether DDNs were recruited in concert during tonic and burst modes of firing, a series of paired recordings were performed between both ipsilateral ($n = 8$) and contralateral ($n = 3$) pairs of DDNs. During paired recordings of ipsilaterally located cells, 98% ($n = 324$ of 332) of bursts occurred concurrently between cells with a mean delay of 11.01 ± 1.35 ms (Figure 5.2A,D,E). During contralateral paired recordings, bursts occurred contemporaneously 93% of the time, and the delay between bursts was significantly higher relative to ipsilateral pairs (mean delay = 58.18 ± 11.04 ms, $p < 0.001$, Figure 5.2B,D,E). When DDNs fired tonically, periods of coincident firing between DDN pairs (arbitrarily defined as spikes occurring in an 11 ms window, similar to the delay observed between bursts in paired DDNs) was much lower than that observed during bursting, such that only $24.9 \pm 5.4\%$ and $12.2 \pm 9.9\%$ of spikes occurred contemporaneously in ipsilateral and contralateral pairs, respectively. In sum, these findings suggest that bursts and, to some extent, tonic firing are both coordinated between DDNs on both sides of the brain.

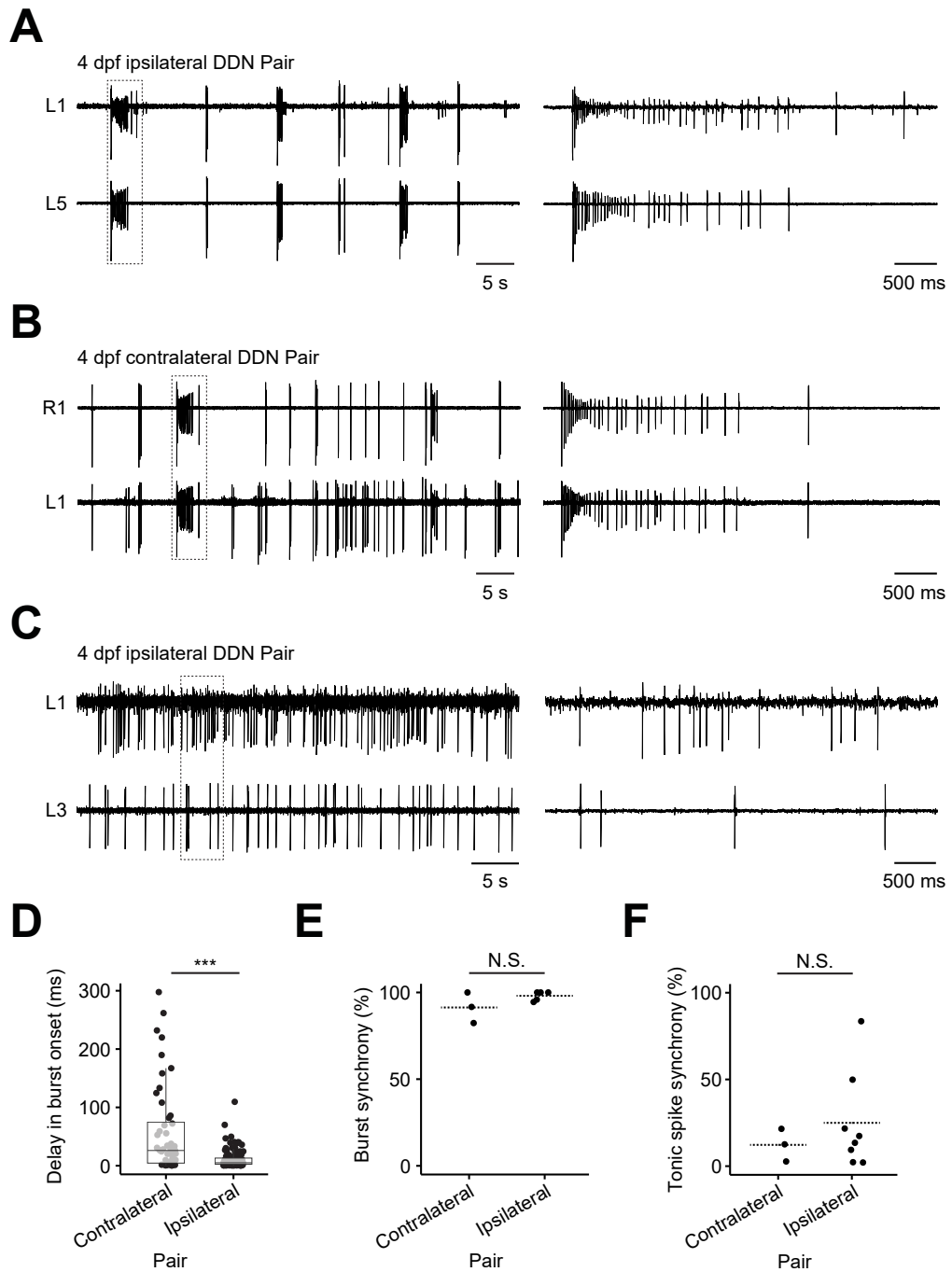


FIGURE 5.2

Firing activity coordination between DDNs. (A - C) Paired loose patch clamp recordings from ipsilateral or contralateral DDN pairs exhibiting bursting (A, B) or tonic spike (C) activity. Cells are labelled with respect to the hemisphere in which they were located ('L' = left, 'R' = right) and their relative position within the DDN cluster (1 = most anterior). (D) Box and whisker plot of delay in burst onset in ipsilateral and contralateral DDN paired recordings (E - F) Plots of spike synchrony between bursts (E) and tonic spiking during ipsilateral and contralateral DDN paired recordings.

5.3.3 Cellular basis for observed activity patterns

Whole cell and perforated patch clamp methods were used in order to monitor DDN activity and examine the cellular basis of the observed activity patterns. Since perforated patch clamp methods were difficult to perform at 2 dpf (see subsection 4.3.5), recordings at both 1 and 2 dpf were conducted in the whole cell configuration. During early coiling stages (18–20, $n = 4$), spike activity was not observed (Figure 5.3A). However, at later stages (> 20 hpf, $n = 3$), occasional spike discharges were observed (Figure 5.3A). By 2 dpf, DDNs ($n = 11$ cells) received irregular synaptic input which drove the membrane to threshold and elicited action potentials (mean frequency = 0.83 ± 0.16 Hz). Occasionally (mean frequency of occurrence = 0.03 ± 0.01 Hz), synaptic inputs elicited compound depolarisations that evoked brief (mean duration = 0.34 ± 0.05 s) high-frequency (18.78 ± 2.86 Hz) trains of action potentials (Figure 5.3B). In sum, these findings suggest embryonic DDNs are silent or fire sparse unitary action potentials whilst 2 dpf DDNs appear to generate two forms of activity: tonic spiking and burst firing.

By 4 dpf, perforated patch clamp recordings, which maintain cytoplasmic integrity, could be conducted. This permitted a thorough comparison between extracellular and intracellular conditions. Analysis of further loose patch recordings were in broad agreement with those previously reported (see above). All recorded neurons ($n = 36$) generated low frequency (1.85 ± 0.21 Hz) spiking (Figure 5.4A,G). In 78 % of DDNs ($n = 28$ of 36), this low frequency tonic spiking was interrupted by high frequency (23.03 ± 0.77 Hz) bursts that were 0.65 ± 0.05 s in duration (Figure 5.4B,C,H,I). These bursts were often observed to occur as isolated events in 28 % ($n = 8$ of 28) of those

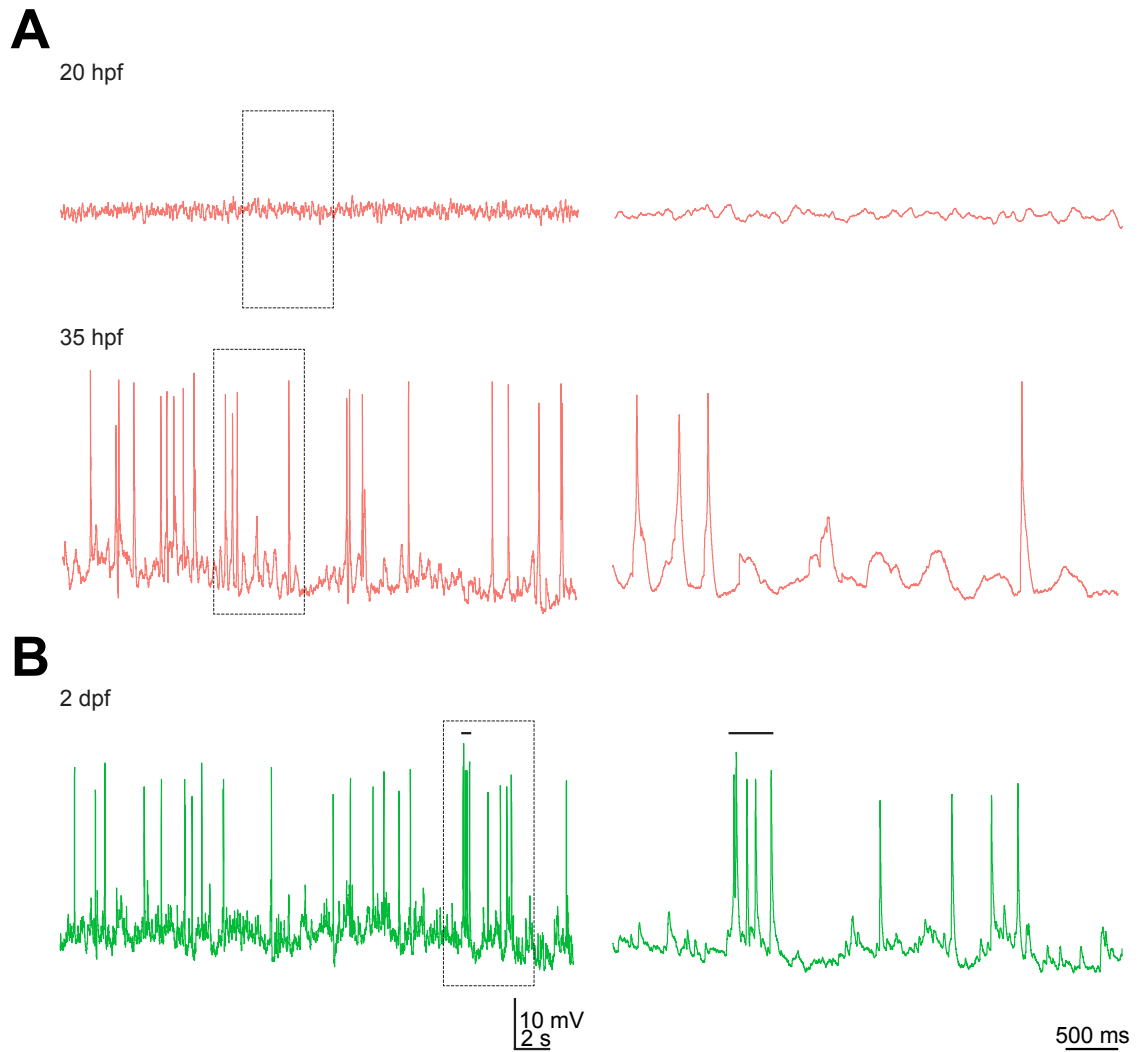
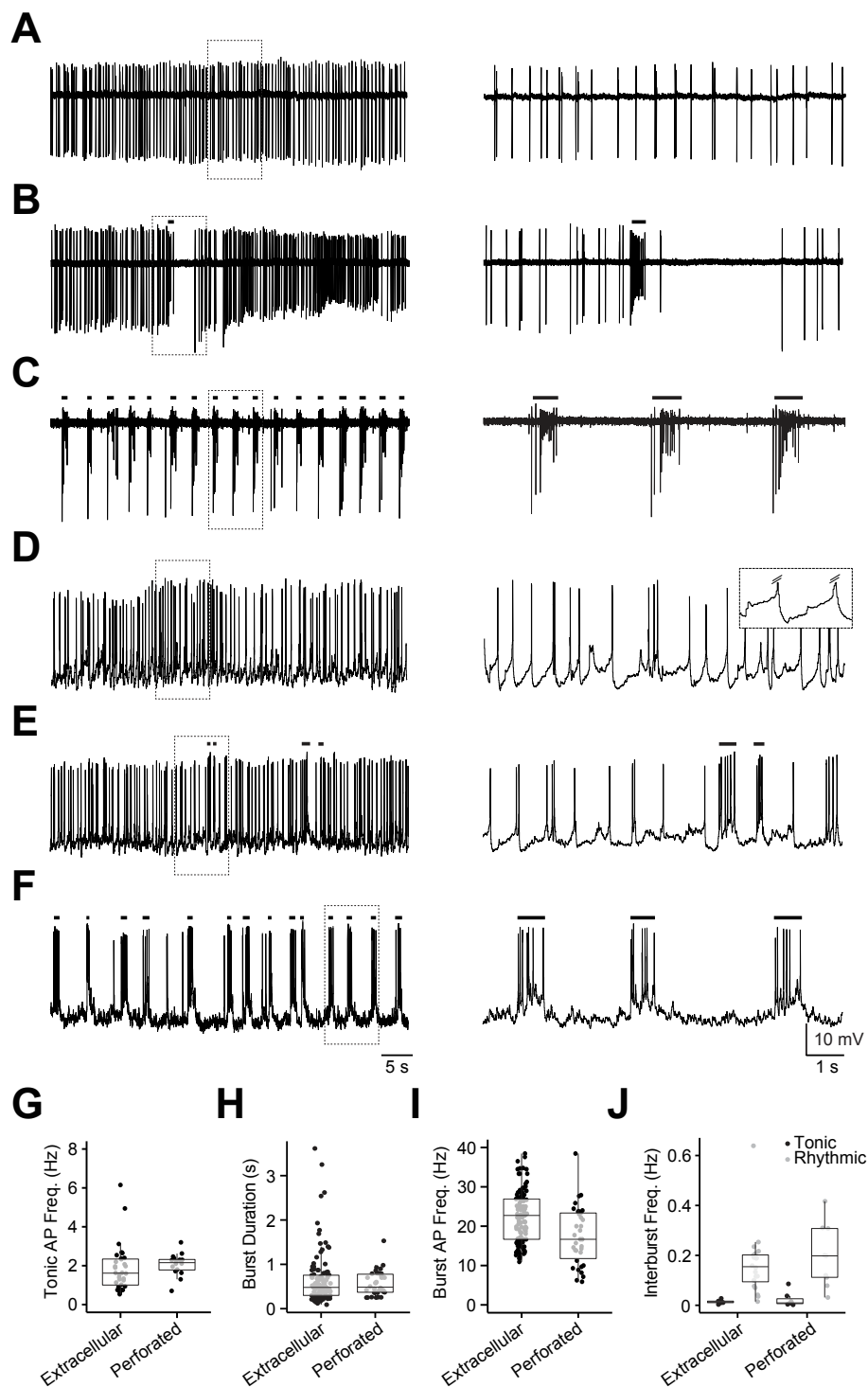


FIGURE 5.3
Activity patterns during whole cell recordings at 1 and 2 dpf. (A – B) Representative whole cell recordings from coiling (A) and burst swimming (B) stages. Black bars denote bursts.


FIGURE 5.4

Endogenous DDN activity patterns at 4 dpf. (A – F) Left: activity patterns recorded from DDNs using extracellular loose patch (A – C) and perforated patch clamp (D – F) methods at 4 dpf. Right: excerpts of activity (dashed boxes) shown on an expanded time scale. The inset in (D) shows slow membrane oscillations during periods of tonic spiking. (G – J) Box and whisker plots of tonic action potential (AP) frequency (G), burst duration (H), within burst AP frequency (I) and frequency of bursts across the duration of loose patch and perforated patch clamp recordings (J). Scale bars for time in panels (A)–(F) are illustrated in (F). Scale bars for voltage in panels (D)–(F) are illustrated in (F).

cells which exhibited bursting (Figure 5.4B). However, in 71% ($n = 20$ of 28) of cases, bursts occurred as a rhythmic train of events (Figure 5.4C). In both cases, bursts were followed by quiescent periods (mean duration = 2.63 ± 0.29 s). Perforated patch clamp recordings revealed the cellular basis of these activity patterns (Figure 5.4D-F). In current clamp mode ($n = 21$ cells), spike activity presented as irregular tonic spiking (frequency = 2.07 ± 0.14 Hz) which appeared to be driven by a combination of slowly depolarising membrane oscillations and synaptic input (Figure 5.4D). Under these conditions, bursting was also observed in the majority ($n = 17$ of 21) of neurons (Figure 5.4E,F). Again, these events either occurred in isolation ($n = 7$ of 21) or in rhythmic bouts ($n = 10$ of 21) and were typically followed by periods of quiescence (Figure 5.4E,F). In both cases, bursts were driven by depolarising inputs and were indistinguishable, lasting 0.61 ± 0.07 s containing high frequency (17.45 ± 1.27 Hz) spike discharges.

5.3.4 Synaptic drive to DDNs

In order to examine how glutamatergic and GABAergic inputs contribute to the observed activity patterns, DDNs were voltage clamped at the reversal potential for cation- (≈ 5 mV) or chloride- (≈ -45 mV) mediated currents to isolate GABAergic and glutamatergic inputs, respectively. N-(2,6-Dimethylphenylcarbamoylmethyl) triethylammonium bromide (QX-314) was also included in the intracellular solution in order to block Na^+ channels and prevent generation of action currents. Clamping at the reversal potential for cationic currents showed that presumed GABAergic currents were sparse (Figure 5.5A). However, when presumed glutamatergic inputs were isolated, irregular synaptic currents and large-amplitude compound currents were often observed (Fig-

ure 5.5B). These compound events likely underpin bursting because they occurred at a similar frequency (current clamp = 0.30 ± 0.06 Hz, voltage clamp = 0.36 ± 0.07 , $p > 0.05$) and had a similar duration (current clamp = 0.49 ± 0.02 s, voltage clamp = 0.41 ± 0.06 , $p > 0.05$) to phasic depolarisations which were observed during current clamp recordings (Figure 5.5C). These findings suggest that bursting is driven by compound glutamatergic inputs while irregular glutamatergic (and perhaps GABAergic) inputs contribute to tonic firing.

5.3.5 Relationship between DDN activity and motor output

Despite recent investigations which have implicated DAergic tracts in modulating spinal network composition (Reimer et al., 2013), maturation (Lambert et al., 2012) and ongoing locomotor output (Maitra et al., 1993; Seth et al., 1993; McPherson and Kemnitz, 1994; Schotland et al., 1995; Han et al., 2007; Clemens et al., 2012), the relationship between DDN activity patterns and motor output have not been investigated. Therefore, I sought to define the behavioural contexts associated with DDN firing patterns across embryonic (1 dpf), burst (2 dpf) and beat-glide (4 dpf) swimming stages. In order to address this issue, paired recordings were made between DDNs and spinal neurons.

Since DDNs do not spike at early embryonic stages, I focused on late stages when DDNs exhibited low frequency tonic spiking (see subsection 5.3.1). At this age, paired recordings between DDNs and spinal neurons revealed the frequency of DDN spikes did not change as a function of motor output (Figure 5.6A, Figure 5.7A). In contrast, by 2 dpf when motor output had transitioned to sustained bouts of high

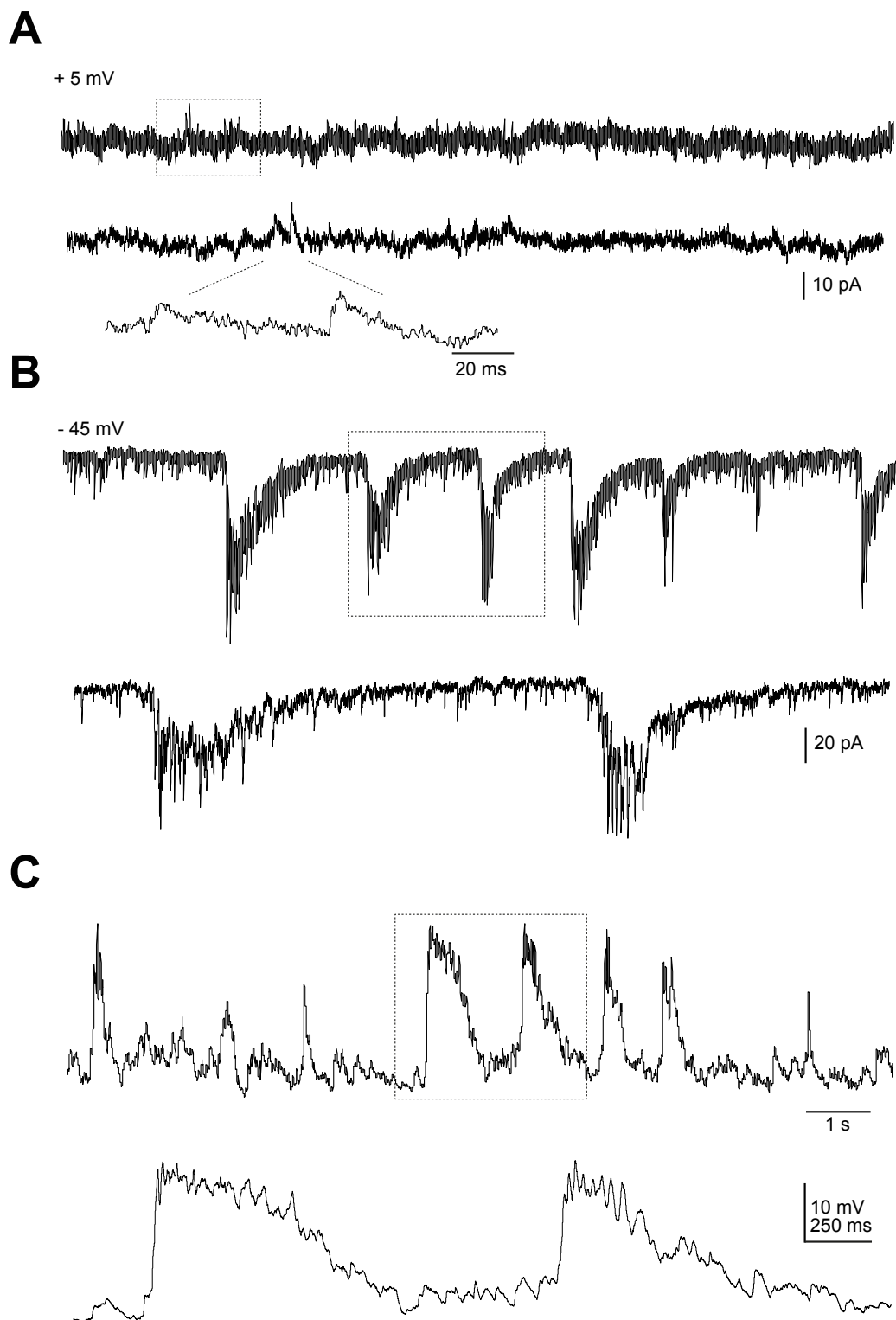


FIGURE 5.5

Synaptic drive to DDNs at 4 dpf. (A – B) Endogenous chloride (A) and cation (B) mediated currents recorded from a QX-314-dialysed DDN in a preparation bathed in Evan’s extracellular saline containing (+)-tubocurarine hydrochloride pentahydrate (d-tubocurarine). (C) Current clamp recording from the same cell as in (A) and (B). Bottom panels in (A)–(C) are excerpts (dashed boxes) of activity shown on an expanded timescale. Scale bars for time in (A)–(C) are shown in (C).

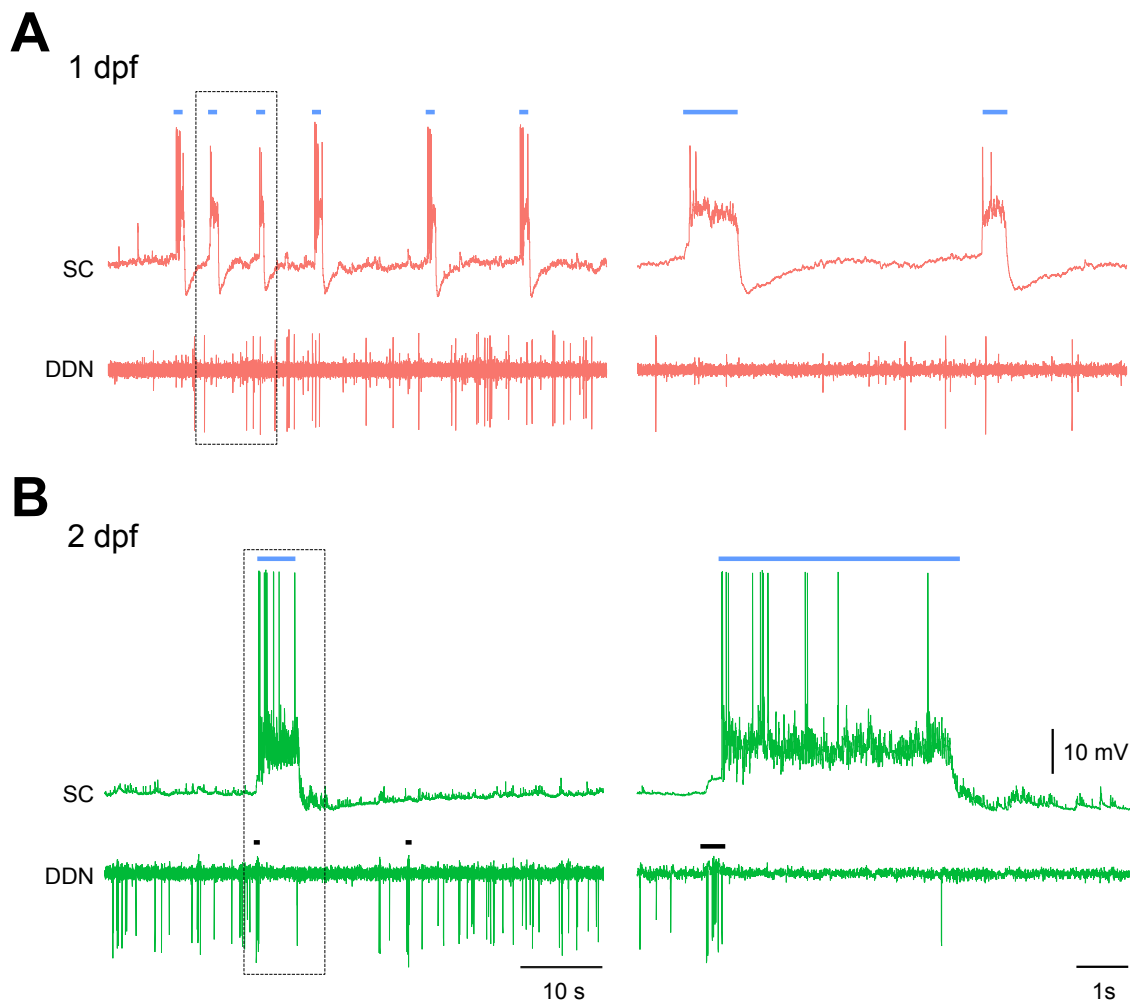


FIGURE 5.6
Relationship between DDN activity and locomotor network activity at 1 and 2 dpf.
(A – B) Paired recordings between spinal cord neurons (SC, top) and DDNs (bottom) at 1 (A) and 2 (B) dpf. Blue bars denote periods of fictive coiling (A) or burst swimming (B) and black bars denote DDN bursts.

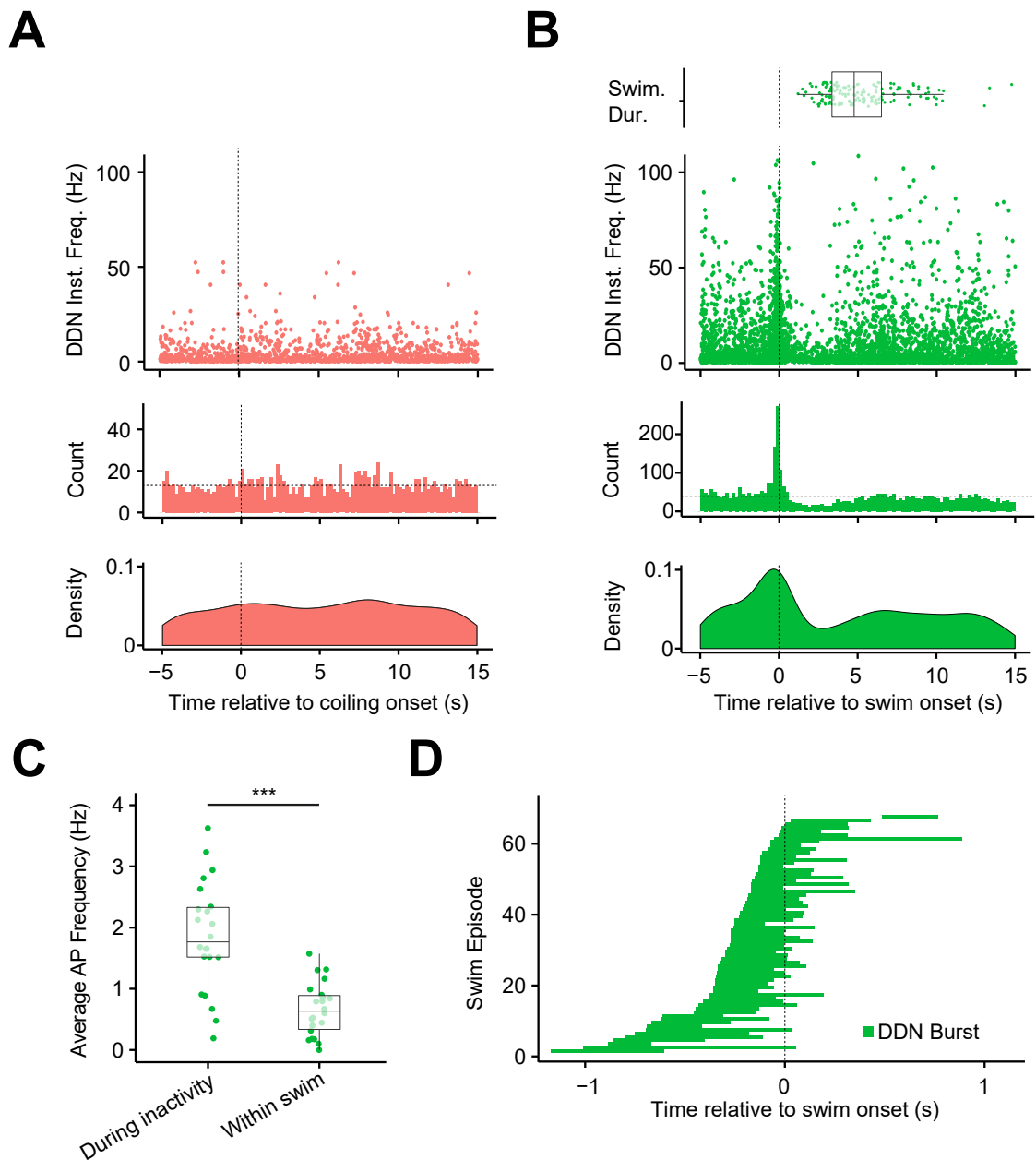


FIGURE 5.7

DDN activity patterns correlate with locomotion at 2 but not 1 dpf. (A) DDN instantaneous frequency (top), count (middle) and density (bottom) of DDN spikes relative to fictive coiling onset at 1 dpf. (B) Duration of swim episodes (top), DDN instantaneous frequency (top-middle), count (bottom-middle) and density (bottom) of DDN spikes relative to swim onset onset at 2 dpf. (C) Average DDN spike frequency during locomotor inactivity and within a swim episode. (D) DDN burst duration relative to swim onset.

frequency burst swimming, 67 of 152 (44 %) swim episodes were accompanied by a high frequency burst within the DDN (Figure 5.6B, Figure 5.7B). In 95 % of cases ($n = 64$ of 67 bursts) DDN bursts began prior to the onset of swim episodes (by 308 ± 24 ms) and on average terminated 50 ± 30 ms after the start of the swim episode (Figure 5.7D). A transient decrease in DDN spike activity was also observed during locomotor activity. During periods of swimming, the frequency of DDN spikes declined to 0.62 ± 0.07 Hz from an average spike frequency of 1.86 ± 0.19 Hz during periods when the locomotor network was not active (Figure 5.7B,C). In 40 % of swim episodes, DDNs fell completely silent.

By 4 dpf, the fictive motor pattern has again changed, and larvae now engage in beat-glide swimming. At this age, swim episodes comprise rhythmic bouts of synaptic drive separated by short silent periods when the spinal network is not recruited. Paired recordings between DDNs and motoneurons or muscle fibres at this age revealed that tonic spiking occurred when larvae were not engaged in locomotor episodes (Figure 5.8A). This is similar to the relationship between DDNs and spinal neurons at 2 dpf. However, when fish engaged in fictive swim episodes, 96 % ($n = 43$ of 45) of DDN bursts occurred contemporaneously with the beat component of swimming and had terminated prior to the onset of the glide component (Figure 5.8B).

DDN bursts did not appear to be necessary for locomotor output since a large minority (39 %, $n = 28$ of 71) of beat episodes were not accompanied by DDN bursts (Figure 5.8B,C). In support of this hypothesis, the duration of beat episodes was not significantly altered by the presence or absence of a DDN burst (mean beat duration in absence of DDN burst = 1.53 ± 0.50 s, mean beat duration in presence of DDN burst = 1.57 ± 0.44 s, Figure 5.9A). Similarly, the rest component was not affected either

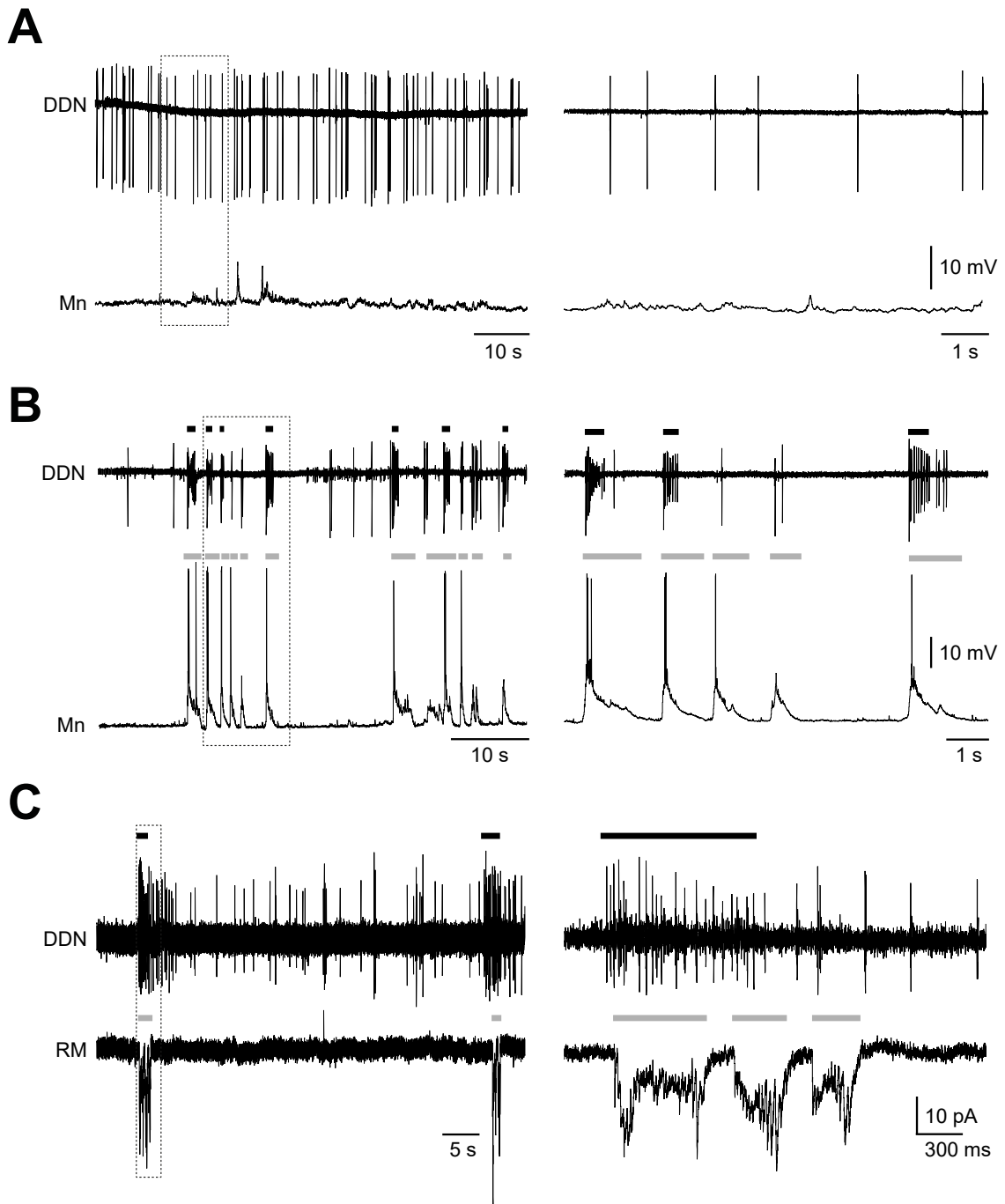


FIGURE 5.8

Paired recordings between spinal neurons and DDNs at 4 dpf. (A - B) Paired recordings between DDNs and motoneurons (MNs) reveal that DDNs spike tonically during periods of motor network inactivity (A). However, during episodes of beat-glide swimming, the MNs receive synaptic input (grey bars) and DDNs often burst (black bars) (B). **(C)** Paired recordings between DDNs and red muscle fibres (RM) reveal that DDN bursts (black bars) occur contemporaneously with synaptic drive to the muscle.

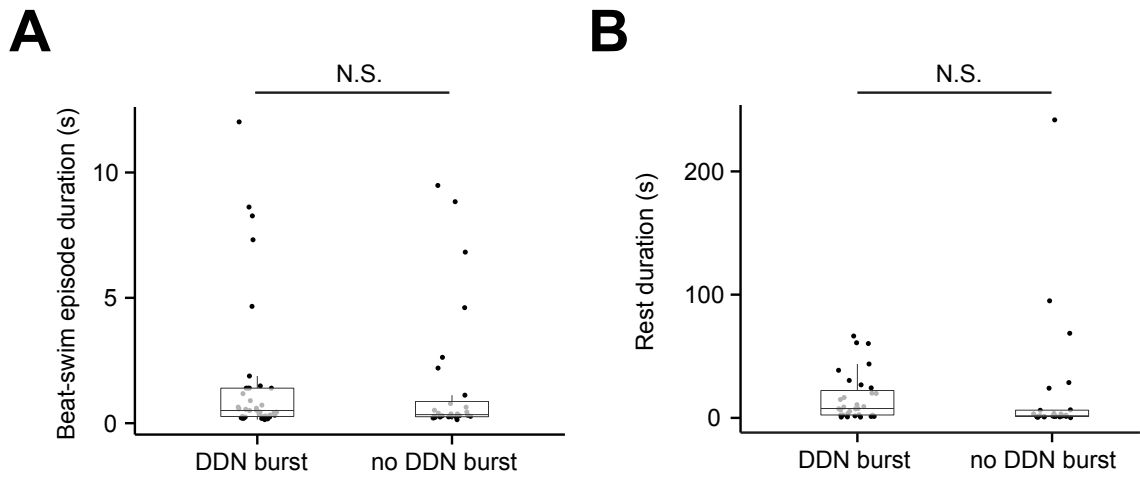


FIGURE 5.9

Duration of locomotor activity is unaffected by DDN bursting. (A - B) The duration of swim episodes (A) and the duration of rest periods between episodes of swimming (B) is unaffected by the presence or absence of DDN bursting.

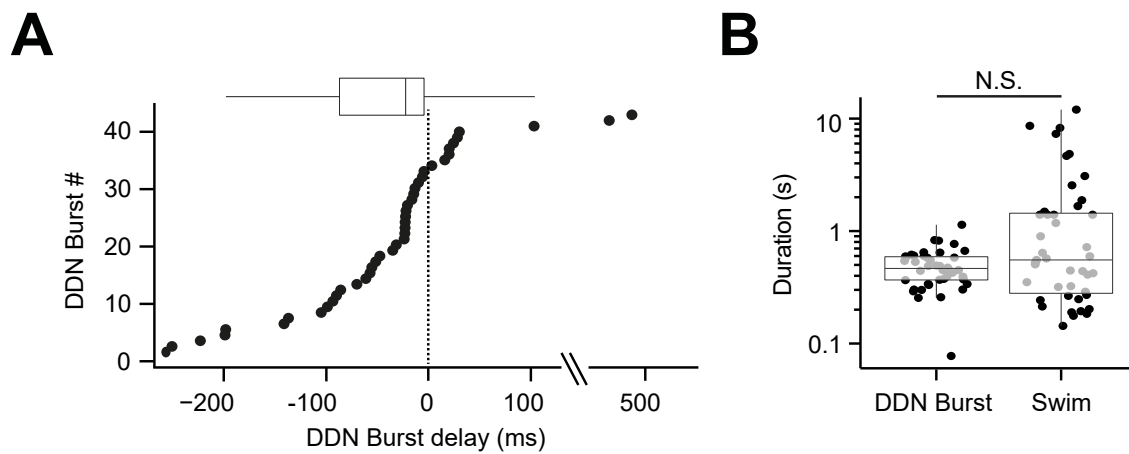


FIGURE 5.10

DDN activity patterns correlate with locomotion at 4 dpf. (A) Plot of the delay in onset of DDN burst activity relative to the onset of swim episodes (0 s, dashed line). (B) Log-scaled duration of DDN bursts and beat episodes.

(mean rest duration in absence of DDN burst = 20.3 ± 10.7 s, mean rest duration in presence of DDN burst = 16.30 ± 3.44 s, Figure 5.9B). Finally, of the 43 observed DDN bursts at 4 dpf, 77% ($n = 33$ of 43) occurred prior to the start of the beat episode (mean delay before swim onset = 74.92 ± 12.76 ms, Figure 5.10D). The remaining 33% occurred after onset of swim episodes (119.70 ± 60.01 ms) (Figure 5.10D).

In sum, these findings suggest that although burst activity is rarely observed during periods of locomotor inactivity, they are not necessary for the initiation of swim episodes. Indeed, at 2 dpf, only 44% of swim episodes occurred contemporaneously with DDN burst activity. While at 4 dpf, the incidence of coincident swimming and DDN bursting was higher (95%), a minority of swim episodes did occur in the absence of bursting. Furthermore, based on the temporal onset of DDN bursting, DDNs may serve different functions during burst swimming (2 dpf) and beat-glide swimming (4 dpf). At 2 dpf, DDN bursts typically started and terminated near the onset of swimming. However, by 4 dpf, DDN bursts occur during the beat component of the swim episode.

5.3.6 Effects of DC2 DDN ablation on motor behaviour

Thus far, electrophysiological investigations have focused upon the DDNs which arise from the DC2 cluster. In order to understand the behavioural function of this physiologically defined cell population, these cells were laser ablated and locomotor activity examined. By 4 dpf, larvae engage in beat-glide swimming, and previous reports (Lambert et al., 2012) have indicated that perturbation of descending dopaminergic inputs is sufficient to revert this refined output to more immature burst-like modes of swimming. However, the methods used to reduce DAergic signalling in spinal net-

works (chemogenetic ablation of *otpb* neurons or spinal transection) were non-specific and likely to disrupt other descending pathways that may also influence behaviour, including noradrenergic (Tay et al., 2011), hypocretin/orexin (HCRT) (Faraco et al., 2006; Prober et al., 2006; Appelbaum et al., 2009), serotonergic (McLean and Fetcho, 2004a; Lillesaar et al., 2009) and reticulospinal (Mendelson, 1986; Sato et al., 2007) pathways. Thus, for the purposes of this study, a more specific means to reduce DAergic signalling within the spinal cord was attempted.

Since DDNs are amongst the earliest developing population of DAergic neurons within the brain (see subsection 4.1.4.1), I asked whether targeted laser ablation of anteriorly located GFP positive cells within the PT at 20–24 hpf was sufficient to reduce the number of DDNs at 4 dpf. A single brief bout ($\approx 30–45$ s) of irradiation from the laser was typically sufficient to reduce GFP expression in the targeted region (Figure 5.11A,B). This appeared to be specific since neighbouring GFP positive cells outside of the targeted region (by $\approx 20–50$ μm) were unaffected by this treatment (data not shown).

In order to examine whether this method successfully ablated DDNs, 4 dpf larvae subject to ablation at 1 dpf were fixed and processed for anti-TH immunohistochemistry and compared to control fish (Figure 5.12A,B). This revealed a marked and significant decrease in the number of large, intensely fluorescent GFP positive cells located toward the anterior of the posterior tuberculum (control = 10.50 ± 0.37 cells; ablated = 1.18 ± 0.48 cells; $p < 0.001$, Figure 5.12A cf. Figure 5.12B). These findings suggest that ablation of anterior PT GFP-positive cells at 1 dpf causes selective loss of DDNs located in DC2 by 4 dpf.

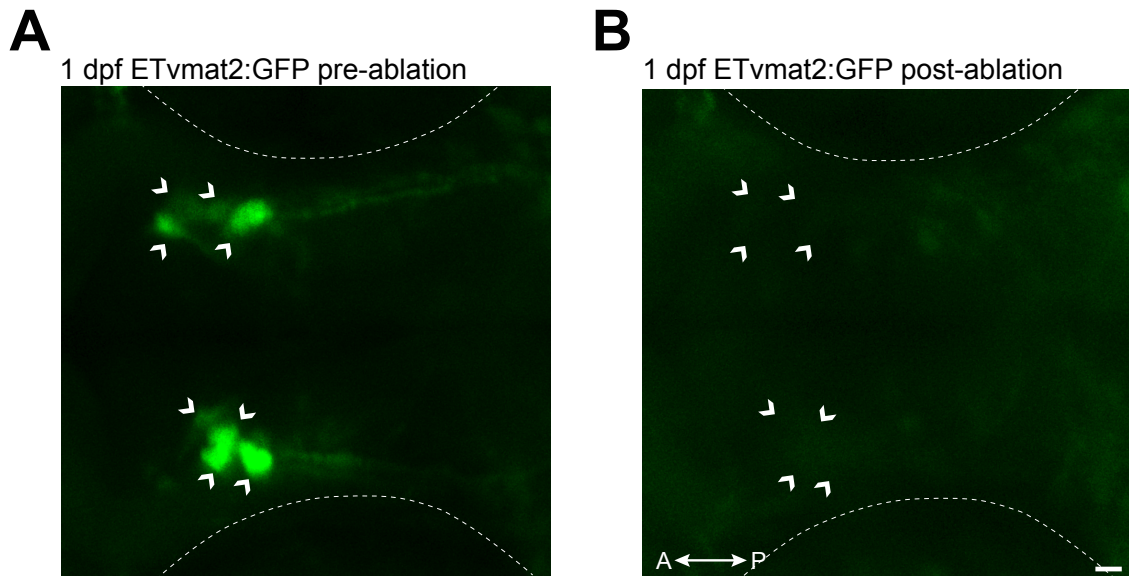


FIGURE 5.11
Targeted ablation at 1 dpf causes loss of GFP positive cells. (A) Brief bouts of irradiation with a UV or Argon laser caused the loss of *ETvmat2:GFP* positive cells (white arrow heads) in embryonic (16–24 hpf) zebrafish. Scale bar = 10 μ m.

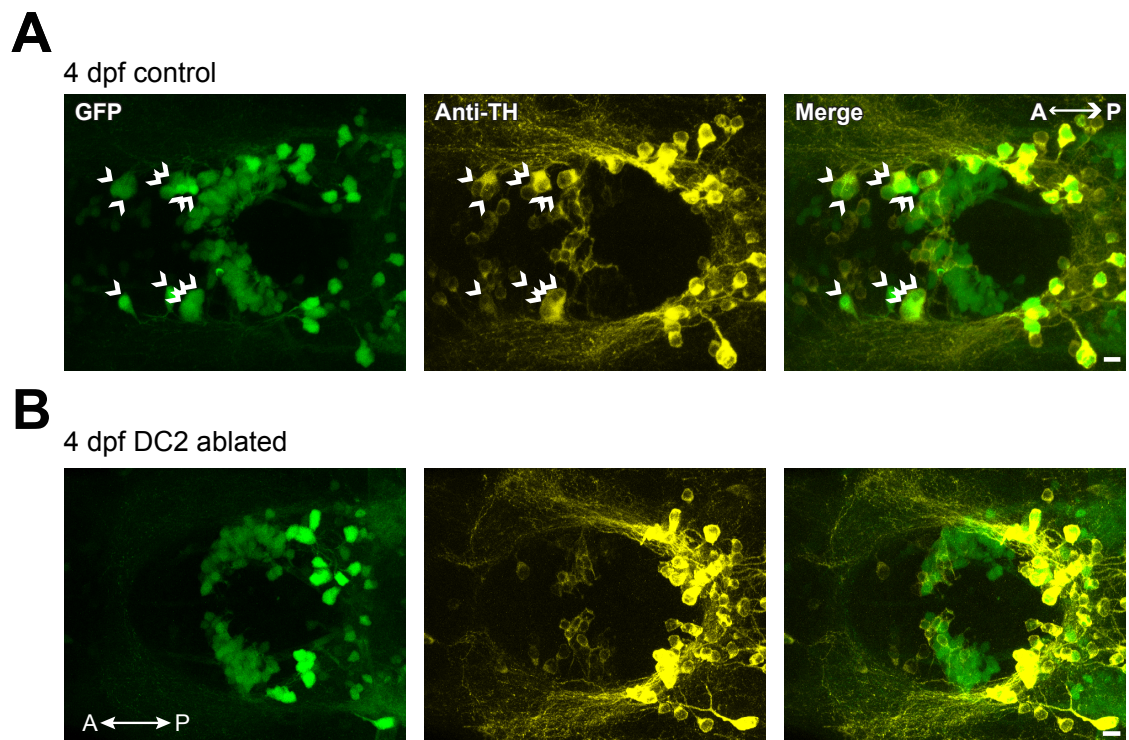


FIGURE 5.12
Selective loss of DDNs following ablation at 1 dpf. (A – B) Ventral view of GFP (left) anti-tyrosine hydroxylase (TH) staining (middle) and merged images (right) within the diencephalon of 4 dpf control (A) and 4 dpf larvae subject to ablation (B). Note that the anterior DDNs in DC2 (white arrowheads) are absent post-ablation. Scale bars in (A) and (B) = 10 μ m; anterior is left, posterior is right.

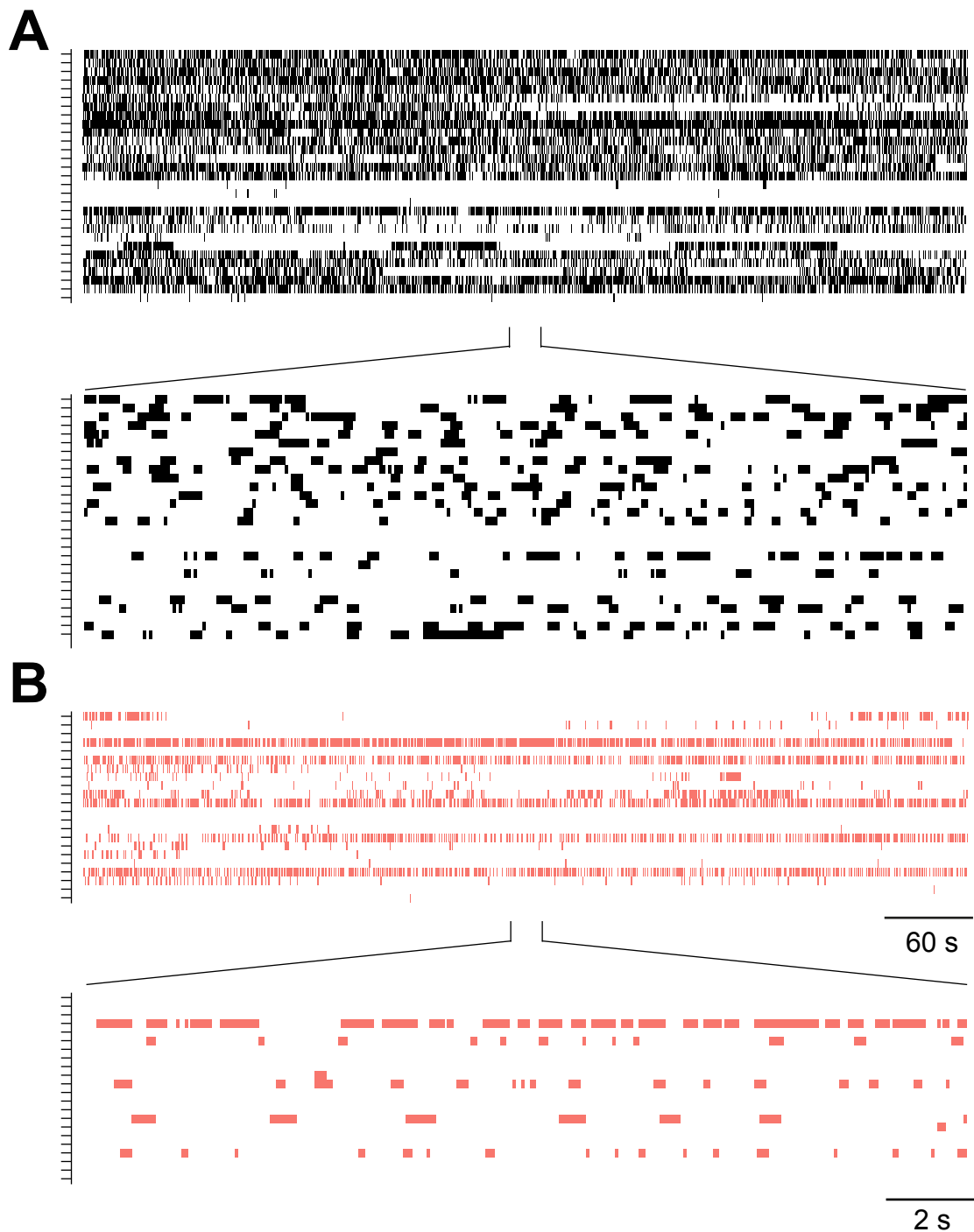


FIGURE 5.13
Identified beat-glide swim episodes in control and ablated larvae. (A – B) Raster plots of identified beat-glide swim episodes in control non-ablated (A) and ablated (B) larvae over a 10 min period. Each line represents individual larvae.

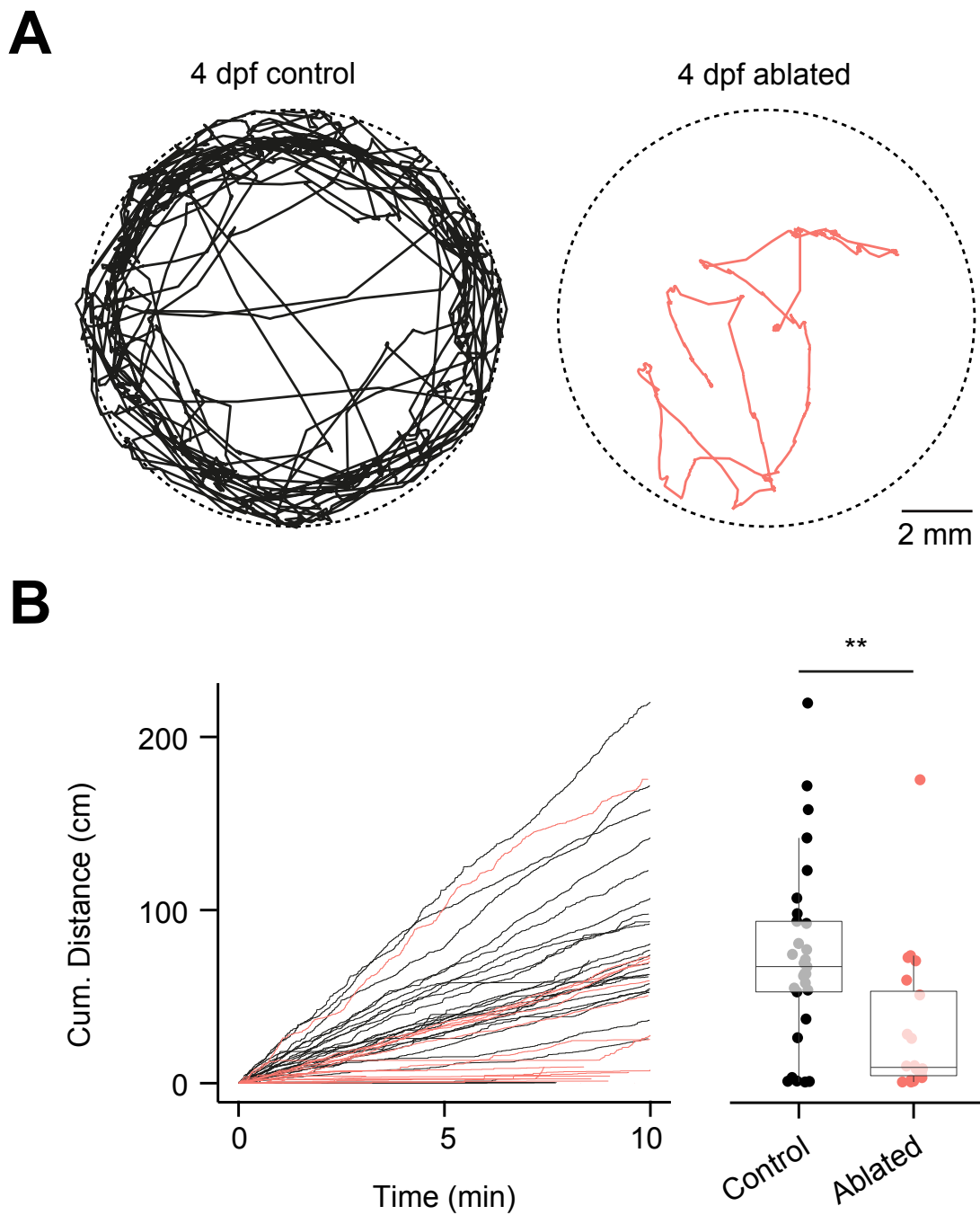


FIGURE 5.14
Selective loss of DDNs affects locomotor output. (A) Swimming trajectories of a 4 dpf control non-ablated and a laser ablated zebrafish recorded over a 10 min period. (B) Left: cumulative distance travelled over a 10 min period by control (black) and ablated (red) larvae. Right: box and whisker plots of total distance travelled.

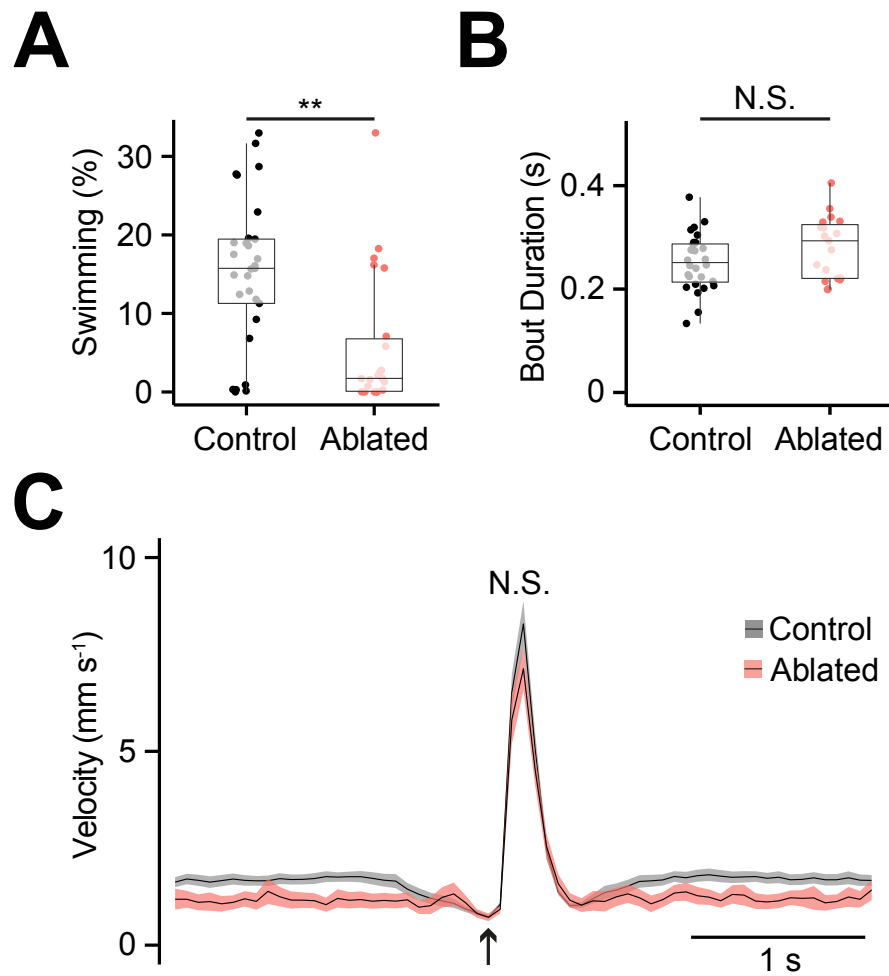


FIGURE 5.15

Parameters of swim episodes are unaffected by DDN ablation. (A – B) Box and whisker plots of percent time spent swimming (A) and the duration of individual beat-glide bouts (B). (C) Average velocity during the onset (arrow) of beat-glide swimming.

Since this caused effective loss of DDNs, the motor activity of freely behaving 4 dpf larvae was examined. During analysis of locomotor episodes, both control (28 of 29) and ablated (19 of 22) larvae exhibited bouts of beat-glide swimming (Figure 5.13A,B), which were characterised by alternating periods of motor activity and quiescence. However, a significant difference in distance swum was observed between control non-ablated and ablated conditions (Figure 5.14A,B). Control larvae travelled a total of 72.95 ± 9.95 cm in a 10 min period, while ablated larvae covered 30.37 ± 9.71 cm in the same duration (Figure 5.14B). Since this marked difference in distance covered could arise from changes in locomotor pattern, basic parameters of the swim episode were next considered. This analysis revealed that neither the duration (control = 0.25 ± 0.01 s, ablated = 0.28 ± 0.01 s, $p > 0.05$, Figure 5.15B) nor mean peak velocity (control = 8.35 ± 0.59 mm s⁻¹, ablated = 7.60 ± 0.64 mm s⁻¹, $p > 0.05$, Figure 5.15B) of beat-glide episodes was affected by DDN ablation. However, the proportion of time spent swimming was significantly affected: control larvae were engaged in beat-glide swimming for 15.34 ± 1.75 % of time while ablated larvae swam for only 5.81 ± 1.86 % of the 10 min period ($p < 0.01$, Figure 5.15A).

5.3.7 Effects of DC2 and DC4/5 ablation on motor behaviour

Since a proportion of DDNs are also located in the DC4/5 population, I next asked whether ablation of GFP-positive neurons in the posterior tuberculum of late 1 dpf (30–32) *ETvmat2:GFP* larvae was sufficient to abolish these cells by 4 dpf. Examination of larvae subject to this treatment revealed that all large intensely fluorescent GFP-positive cells in DC2 and DC4/5 were lost (Figure 5.16A,B cf. Figure 5.12A,B). Again, the locomotor output of these larvae were examined over a 10 min period. This

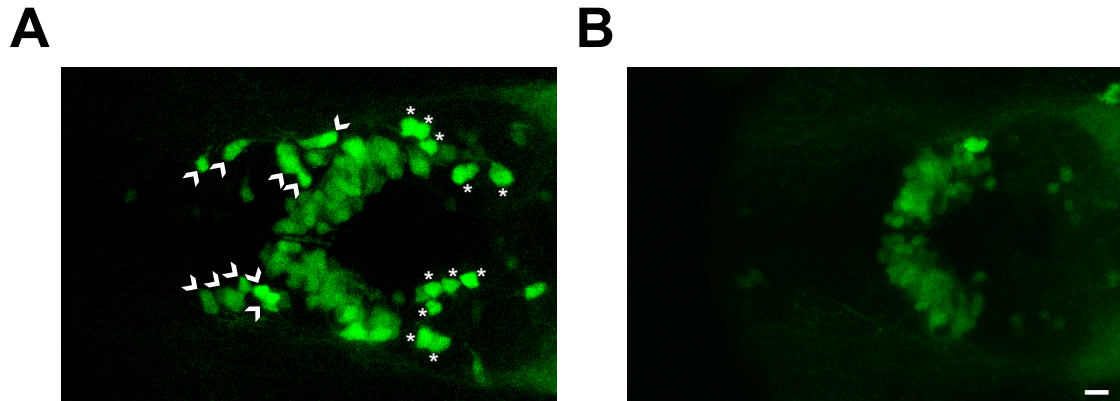


FIGURE 5.16

Selective loss of DC2/4/5 GFP-positive neurons at 4 dpf following ablation at 1 dpf. (A – B) Ventral view of GFP within the diencephalon of 4 dpf control (A) and 4 dpf larvae subject to ablation (B). Note the loss of all large *ETvmat2:GFP* cells (white arrowheads) toward the anterior and posterior (asterisks) aspects of the diencephalon. Scale bars of (A) and (B) = 10 μm ; anterior is left, posterior is right.

revealed broadly similar results relative to DC2 ablation. Neither the duration (control = 0.29 ± 0.01 s, DC2/4/5 ablated = 0.26 ± 0.03 s, $p > 0.05$) nor the mean peak velocity (control = 8.35 ± 0.64 mm s^{-1} , DC2/4/5 ablated = 6.74 ± 1.14 mm s^{-1}) of swim episodes were affected by this treatment (Figure 5.17B,C). However, the distance covered (control = 55.75 ± 10.61 cm, ablated = 2.27 ± 1.00 cm, $p < 0.001$) and percentage of time spent swimming (control = 13.50 ± 2.14 %, ablated = 0.84 ± 0.34 %) were markedly reduced (Figure 5.18, Figure 5.19). In sum, these findings suggest that ablation of DC2 and DC4/5 cells is sufficient to markedly reduce swim initiation.

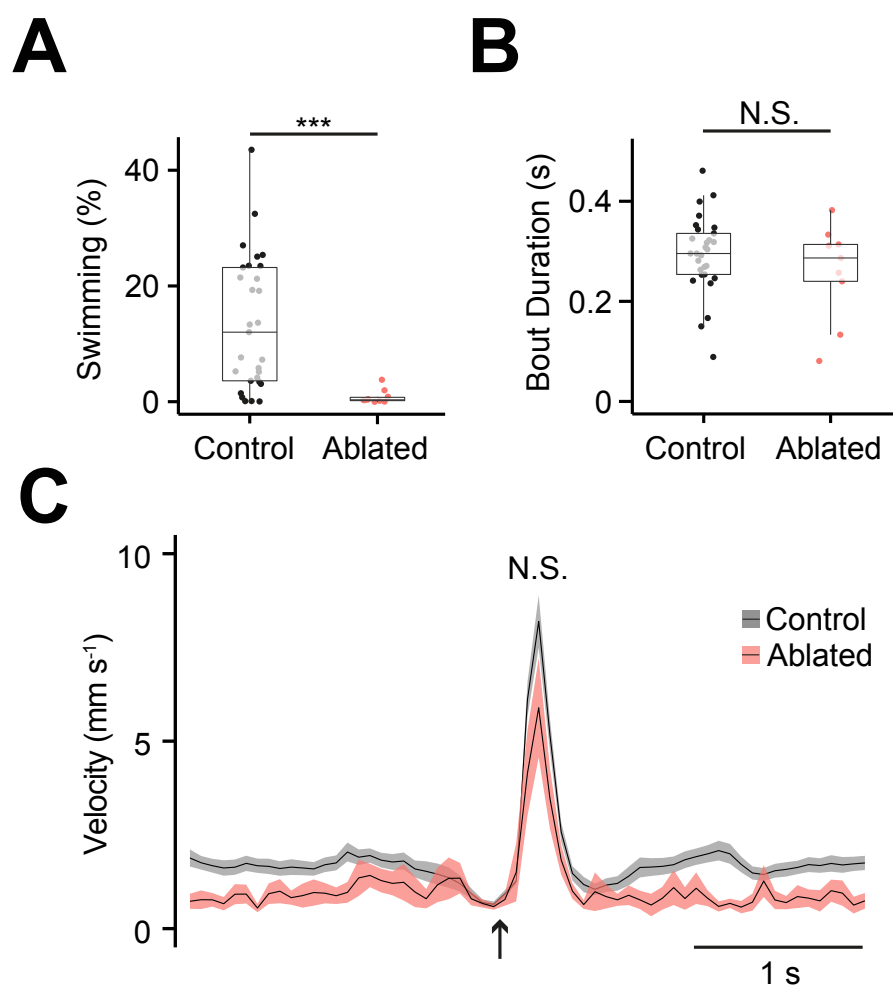


FIGURE 5.17

Parameters of swim episodes are unaffected by DC2/4/5 cell ablation. (A – B) Box and whisker plots of percent time spent swimming (A) and the duration of individual beat-glide bouts (B). (C) Average velocity during the onset (arrow) of beat-glide swimming.

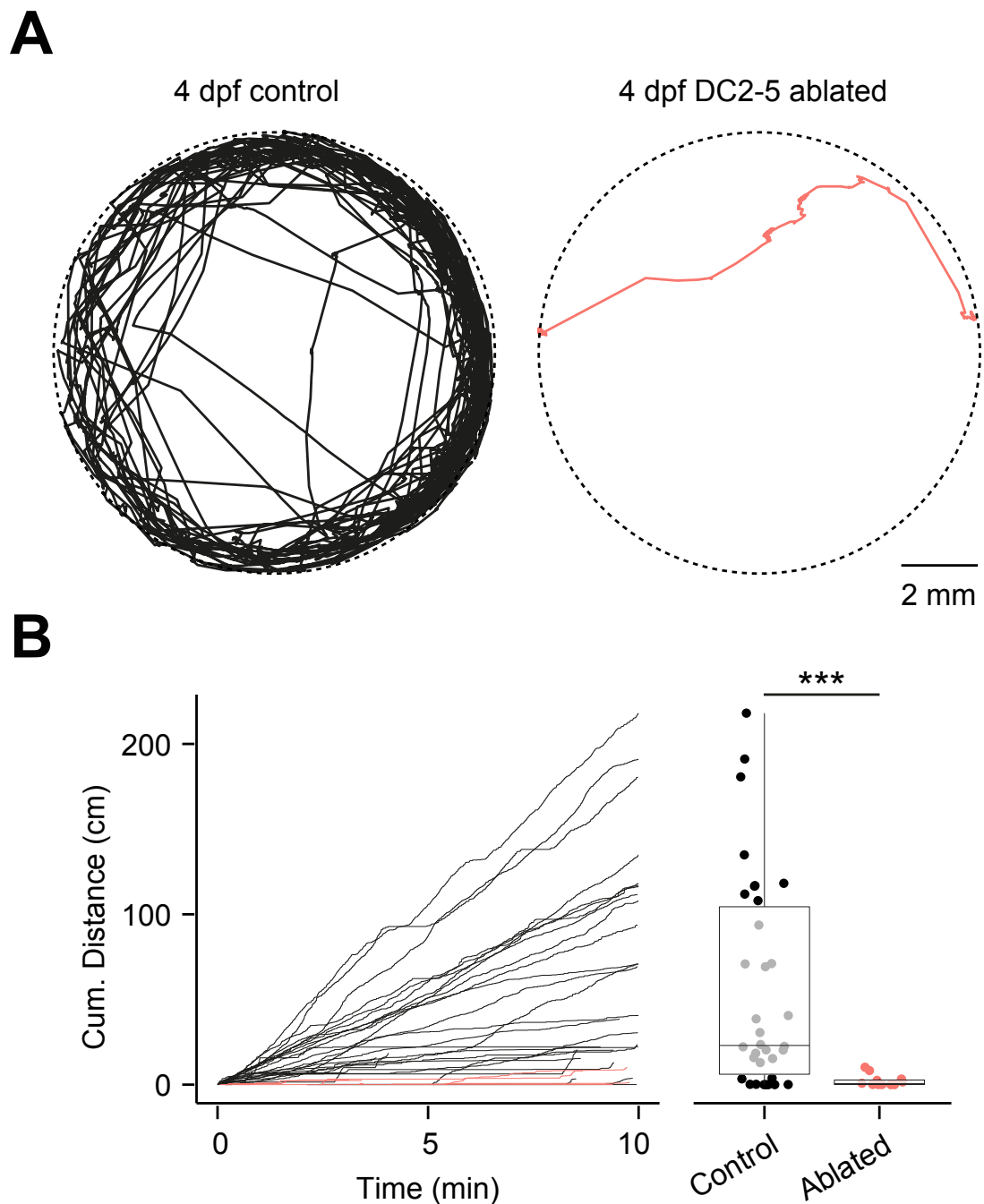


FIGURE 5.18

Selective loss of DC2/4/5 cells affects locomotor output. (A) Swimming trajectories of 4 dpf control and laser ablated zebrafish recorded over a 10 min period. (B) Left: cumulative distance travelled over a 10 min period by control (black) and ablated (red) larvae. Right: box and whisker plots of total distance travelled.

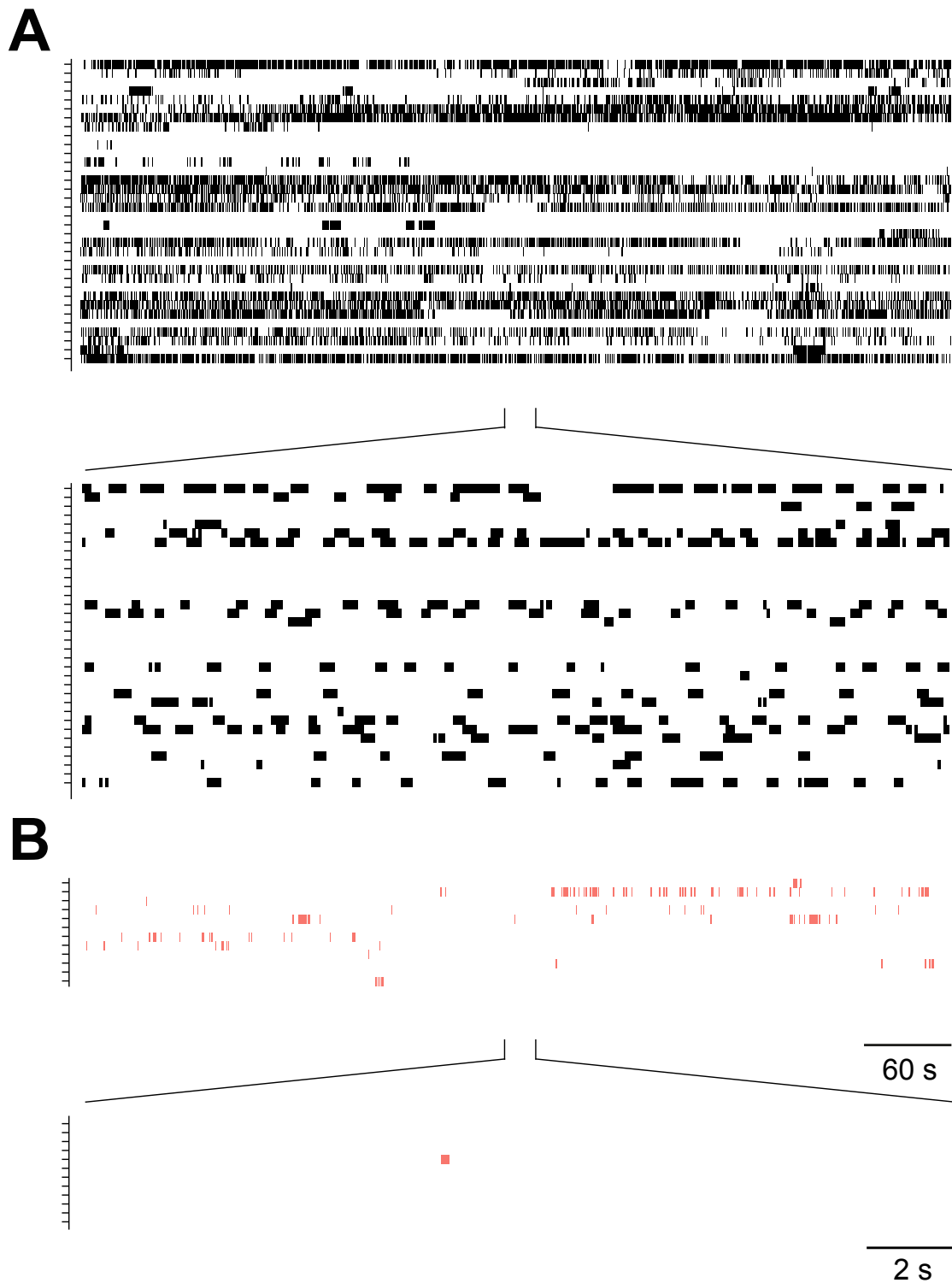


FIGURE 5.19
Identified beat-glide swim episodes in DC2/4/5 GFP-positive cell ablated larvae.
(A – B) Raster plots of identified beat-glide swim episodes in control non-ablated (A) and ablated (B) larvae over the 10 min period. Each line represents an individual larvae.

5.4 Discussion

In this chapter, I have examined the activity patterns of DDNs during development and examined the functional properties of these cells within the larval zebrafish. The results presented in this chapter demonstrate two key findings. Firstly, the synaptic inputs and endogenous activity patterns of DDNs mature progressively during early periods of motor network maturation and secondly, by 4 dpf, loss of DDNs is sufficient to significantly reduce the initiation of locomotor activity.

5.4.1 Ontogeny of endogenous DDN firing patterns and relationship to locomotor output

Since DDNs have been implicated in early stages of neurogenesis (Reimer et al., 2013), I first sought to examine when DDNs become functionally active. In order to do this, a series of *in vivo* non-invasive loose-patch recordings were performed across 18–30 hpf, a time when zebrafish embryos engage in coiling. These experiments revealed that during the early stages of coiling (18–20 hpf), DDNs are inactive. However, during mid coiling stages (21–24 hpf), a proportion of DDNs become functionally active and begin to fire sparse, unitary action potentials (mean frequency \approx 0.3 Hz). By late-stage coiling (25 hpf onward), all DDNs are active and still fire unitary, but more frequent (mean frequency \approx 1.3 Hz) action potentials. Loose patch DDN and whole-cell interneuron/motoneuron recordings were then conducted in order to examine the temporal relationship between DDN activity patterns and locomotor output. At coiling stages, there was no clear relationship between the low frequency spike activity within

DDNs and the periodic depolarisations that drive coiling. Given that coiling is driven by a network of spinally located neurons which do not require supraspinal inputs (Saint-Amant and Drapeau, 2001; Tong and McDearmid, 2012), it is perhaps unsurprising there was no observable correlation. Nonetheless, a modulatory role of DA release on spinal networks cannot be dismissed. Between 16–24 hpf, DA receptors are located throughout the hindbrain and spinal cord (Boehmler et al., 2004, 2007). Notably, D₄ receptors are densely distributed within the rostral aspect of the spinal cord by 16 hpf (Boehmler et al., 2007) which suggests that locomotor networks may be competent to DAergic signalling at the onset of coiling. A population of spinal interneurons which drive coiling (ipsilateral caudal (IC) cells) are known to be inhibited by dopamine (Tong and McDearmid, 2012) and these cells are also located within rostral segments of the spinal cord (Mendelson, 1986). Coiling is a transient behaviour which emerges at ≈ 17 hpf, peaks shortly thereafter and then slowly declines in frequency as fish begin to engage in swim-like behaviours (Saint-Amant and Drapeau, 1998). Since IC cells drive coiling (Tong and McDearmid, 2012), one possible mechanism by which the decline in coiling is mediated may be DA-mediated inhibition. However, whether IC cells have DA receptors or whether DDNs release appreciable amounts of DA at this age has yet to be resolved.

As the embryo matured to burst swimming stages, tonic spiking persisted and was of a similar frequency to that observed at late coiling stages. However, low frequency tonic spike discharge was now accompanied by high frequency bursts which were characterised by periods of short, high intensity spiking. By beat-glide swimming stages, two modes of firing activity were also observed: low frequency (≈ 2 Hz) tonic spiking and high-frequency (≈ 20 – 30 Hz) bursts. Interestingly, these modes of activity

mirror those seen during *in vivo* recordings from midbrain dopaminergic neurons of awake, behaving mammalian preparations (Schultz et al., 1997; Schultz, 1998; Hyland et al., 2002). While the DDN population is likely to encode different types of information in comparison to the ascending populations which arise from midbrain DAergic cell populations [which zebrafish do not possess (McLean and Fetcho, 2004a; Rink and Wullimann, 2002; Schweitzer and Driever, 2009)], it would appear that DDNs encode information in a manner that is broadly consistent with other DAergic populations of the mammalian brain.

In order to gain insight into the possible functions of these different modes of output, paired recordings were conducted between DDNs and spinal neurons at 2 and 4 dpf. These investigations revealed that DDN bursts correlated with the onset of swimming. Specifically, DDN bursts began ≈ 0.3 s prior to swim onset and with an average duration of ≈ 0.35 s, terminated shortly after recruitment of the spinal network. Additionally, at this age, tonic spiking was observed primarily during periods of locomotor inactivity and was often depressed for the duration of the swim episode. These data therefore suggest that the correlation between DDN bursting and motor activity first emerges as zebrafish begin to enter swimming stages. By 4 dpf, a similar relationship between DDN activity and locomotor output was observed such that tonic spiking was observed during periods of locomotor inactivity whilst bursts were observed when the larvae engaged in beat-glide swimming episodes. However, at beat-glide swimming stages, the structure of the swim episode has fundamentally changed such that the beat components of the swim episode are short, approximately ≈ 1 s in duration, and separated by periods of silence. At this stage, DDNs burst in register with the beat components and fall silent during the intervening glides. Additionally, DDN bursts no

longer terminate before the onset of swim episodes but are ongoing when motoneurons and muscle fibres are recruited. Nonetheless, despite this correlation between DDN bursting and locomotor output, DDN output is neither necessary nor sufficient for locomotion: at both 2 and 4 dpf, not all motor episodes are accompanied by bursts (56 % and 39 % at 2 and 4 dpf, respectively). Furthermore, burst onset is variable and sometimes precedes onset of locomotor activity. These findings strongly suggest that, in contrast to the descending DAergic pathways that innervate the lamprey brainstem (Ryczko et al., 2013), zebrafish DDNs are not necessary for swim generation. Within this chapter, paired recordings were performed between a single DDN and spinal neuron (or muscle fibre). One caveat worth consideration is whether other DDNs within the DC2 cluster exhibited bursting when the larvae engaged in locomotor activity. While this possibility cannot be excluded, paired recordings between both ipsilateral and contralateral DDN pairs suggest that the entire population of DDNs within the DC2 population burst in synchrony (in $\approx 98\%$ of cases) which suggests the whole DDN population is recruited contemporaneously.

Nonetheless, DDNs may contribute to swim initiation by co-release of glutamate. It has recently been shown that all DAergic (and NAergic) cell clusters in larval and adult zebrafish coexpress either GABA or glutamate as a second neurotransmitter (Filippi et al., 2014). Co-release of glutamate has also been established in midbrain DAergic neurons (Trudeau, 2004; Descarries et al., 2008; Chuhma et al., 2009; Hnasko et al., 2010; Gu, 2010; Tecuapetla et al., 2010; Stuber et al., 2010). Furthermore, some evidence suggests that DA neurons exhibit specialised terminals for glutamate and DA release, where DA is released from varicosities distributed along axonal projections while both glutamate and DA are released at classical synapses (Trudeau, 2004; Descar-

ries et al., 2008; Hnasko et al., 2010; Tecuapetla et al., 2010; Stuber et al., 2010). Interestingly, in zebrafish, those DAergic populations which project caudally to hindbrain and spinal regions [DC2,DC4/5,DC6 (Tay et al., 2011)] are glutamatergic while the remaining DAergic populations are GABAergic (Filippi et al., 2014). Given the extensive innervation of the spinal cord with TH-positive fibres (McLean and Fetcho, 2004a; Kastenhuber et al., 2010), the majority of which appear to arise from DAergic neurons (Kastenhuber et al., 2010), activation of DDNs may release appreciable levels of glutamate which could activate spinal locomotor networks. However, it should be noted that activation of ipsilateral, caudally projecting glutamatergic inputs in the spinal cord is insufficient to robustly elicit swim episodes, but activation of hindbrain glutamatergic inputs can efficiently induce locomotion (Kimura et al., 2013). Thus, DDNs could serve two synergistic roles within spinal networks: one which acts via DA to provide a tonic level of excitability down the entire extent of the spinal cord that facilitates neuronal recruitment (see subsection 5.4.2 for discussion) and a second which acts via glutamate to activate hindbrain neurons which drive swimming.

5.4.2 Effects of DDN ablation at beat-glide swimming stages

Given the correlation between DDN activity patterns and locomotor output, I next sought to address the question of whether disruption of DA signalling affects locomotor output. Standard approaches to disrupting DA signalling include the bath application of DA receptor agonists or antagonists. However, one caveat of this approach is that DA receptors are also expressed throughout the developing brain (Boehmler et al., 2004, 2007; Li et al., 2007). Thus, application of pharmacological reagents is likely to have off-target effects. Furthermore, given the nature of DDN firing patterns, prolonged and

uniform application of agonists is unlikely to simulate endogenous DA release. Additionally, since spinal networks are exposed to a basal level of DA on account of DDN autonomous spike capability, antagonist application is unlikely to mimic physiological conditions. Since DDN development is dependent upon orthopedia (*otp*) (Ryu et al., 2007), research groups have eliminated DDNs from the nervous system by chemogenetic ablation of *otpb* cells (Lambert et al., 2012) or by using *otp* mutants (Reimer et al., 2013). However, while these methods are sufficient to reduce DA projections to the spinal cord they also affect other DAergic (and non-DAergic) cell populations known to contribute to locomotor output (Mendelson, 1986; Faraco et al., 2006; Ryu et al., 2007; Lillesaar et al., 2009; Kastenhuber et al., 2010; Fernandes et al., 2013).

I therefore sought a more specific method to elucidate the behavioural significance of the DDN population. Since DDNs within DC2 are amongst the earliest developing DAergic cell populations in the brain (McLean and Fetcho, 2004a; Mahler et al., 2010; Reimer et al., 2013), *ETvmat2:GFP* positive cells were ablated at early embryonic stages. This caused a marked reduction in the number of GFP positive cells located toward the anterior aspect of the posterior tuberculum at both embryonic and larval (4 dpf) stage. Anti-TH immunohistochemical stains confirmed that TH-positive (and thus DAergic) cells were deleted following ablation. Analysis of swimming in freely behaving larvae revealed a significant reduction in total time spent swimming (and distance travelled) following ablation. When DC2 and DC4/5 neurons were ablated in order to examine more widespread loss of DDNs, a similar but stronger effect on motor output was observed which suggests that DDNs of DC2 and DC4/5 have equivalent functions in modulating motor network activity. However, within this chapter, the relationships between DC4/5 DDN firing patterns and locomotor activity

have not been examined. Nonetheless, both treatments did not affect the structure (bout duration and velocity) of beat-glide episodes. These findings stand in contrast to previous reports which demonstrate a reversion from mature to immature modes of output following chemogenetic ablation of *otpb*-expressing cells, block of D₄ receptors or spinal transection (Lambert et al., 2012). The reason for this discrepancy has yet to be determined. However, chemogenetic ablation, spinal transection and bath application of DA receptor antagonists are likely to be less specific than the methods employed in this chapter and therefore the previously observed changes may be attributable to perturbation of other descending inputs.

One possible explanation for the observed changes in levels of locomotor initiation is that DA may maintain a level of excitability within spinal networks which facilitates initiation of swim episodes. In the lamprey, DA has several effects. A population of DAergic neurons has been implicated in the control of locomotor output by providing excitatory drive to the MLR which evokes bouts of swimming (Ryczko et al., 2013). However, the zebrafish DDNs and this population of descending DAergic inputs in the lamprey are unlikely to be homologous since the lamprey DAergic cells terminate in the MLR (Ryczko et al., 2013). Nonetheless, in isolated lamprey spinal preparations, low concentrations of DA can produce locomotor output and increase swim frequency (McPherson and Kemnitz, 1994; Schotland et al., 1995). Thus, the low frequency tonic release of DA may serve to excite spinal networks.

How then do bursts contribute to endogenous activity patterns within spinal networks? Consideration must be given to DA release dynamics, the distribution of DA receptors and their affinity for DA. Computational experiments suggest firstly, that DA release increases in a non-linear fashion following high frequency bursting (Gonon,

1988; Wightman and Zimmerman, 1990; Kawagoe et al., 1992) and secondly that DA, when released under tonic conditions, will occupy the high-affinity D₂-like receptors while the lower affinity D₁-like receptors will remain largely unoccupied (Dreyer et al., 2010). In contrast, phasic bursts of activity will transiently increase concentrations of extracellular DA and, since D₂-like receptors are already occupied, this will preferentially increase the occupancy of D₁-like receptors (Dreyer et al., 2010). However, a recent study suggests that D₂ receptors can also exist in a low affinity state and still resolve phasic burst activity in the presence of tonic low levels of DA (Marcott et al., 2014). To investigate D₂-receptor function, G-protein-coupled inwardly rectifying potassium (GIRK) channels were expressed in medium spiny neurons (MSNs). These channels were found to couple to D₂-receptors, which when bathed in DA or DA receptor agonists produced an outward current. Therefore, this provided a means to infer D₂-receptor function (Marcott et al., 2014). Surprisingly, low levels of DA (1 μ M), which would ordinarily be expected to activate D₂-receptors were unable to elicit inhibitory currents. Furthermore, relatively high concentrations (10 μ M) could evoke inhibitory currents but were insufficient to saturate D₂ receptors which could still resolve phasic DA release (Marcott et al., 2014).

Within the context of zebrafish swimming, DDN activity patterns are characterised by high frequency bursts which will presumably release phasic, high concentrations of DA. Given that both D₁- and D₂-like receptors are distributed throughout the developing spinal cord (Boehmler et al., 2004, 2007; Li et al., 2007), this is likely to have important and complex functional consequences for spinal network output. Finally, given the heterogeneity of cell populations within the spinal CPG network, it is also important to consider which DA receptors are expressed on different cell types.

This issue has yet to be addressed but given the relatively low number of cell types in the zebrafish spinal cord, future detailed *in situ* hybridisation or immunohistochemical approaches could conceivably determine DA receptor distribution in different cell populations which contribute to output.

5.4.3 Contribution of synaptic inputs to activity patterns

In order to examine how glutamatergic and GABAergic inputs may contribute to endogenous activity patterns, cells were voltage clamped at the reversal potential for cationic and chloride-mediated currents which isolated presumed GABAergic and glutamatergic inputs, respectively. These findings suggest that burst discharges are driven by powerful bouts of glutamatergic input while tonic spike activity is driven by a combination of glutamate, GABA and autonomous spiking (see subsection 4.3.5).

Midbrain DAergic neurons derived from cell or tissue culture generate autonomous spiking whereas those recorded extracellularly in awake-behaving animals exhibit both tonic and burst modes of firing. These differences are thought to arise as a consequence of losing afferent synaptic inputs. Support for this hypothesis is derived from *in vitro* dynamic clamp studies, which show that burst firing can be elicited by introduction of NMDA and/or removal of GABAergic conductances (Deister et al., 2009; Lobb et al., 2010, 2011; Paladini and Roeper, 2014). Additionally, application of bicuculline, a GABA receptor antagonist can also induce burst firing *in vivo* (Tepper et al., 1995).

Within the mammalian substantia nigra pars compacta (SNc), GABAergic inputs arise from a number of regions including the striatum (Bolam and Smith, 1990),

globus pallidus (GP) (Smith and Bolam, 1990) and local SNc GABAergic interneurons (Tepper and Lee, 2007). Here, GABAergic inputs contribute up to 70 % of the synapses on DAergic neurons (Bolam and Smith, 1990). Application of GABA or GABA receptor agonists can strongly hyperpolarise the DA neuron membrane potential and inhibit firing (Pinnock, 1984; Lacey et al., 1988; Erhardt et al., 2002). Similarly, stimulation of the GABAergic afferents in the GP is sufficient to elicit long-lasting inhibition of DAergic neuron activity (Brazhnik et al., 2008). While these studies suggest a prominent role for GABAergic inputs, the voltage-clamp studies reported here reveal that DDNs receive little GABAergic input during endogenous activity patterns. Rather, DDNs receive barrages of glutamatergic input which likely underpin the bursts of spike activity observed during current clamp and extracellular recordings. DAergic neurons in the midbrain also receive glutamatergic inputs which can transiently increase the rate of firing and induce bursts of activity (Christoffersen and Meltzer, 1995; Zhang et al., 1997; Deister et al., 2009) which can be blocked by addition of NMDA (Chergui et al., 1994; Christoffersen and Meltzer, 1995; Tong et al., 1996), and in some instances AMPA (Blythe et al., 2007) receptor antagonists. Moreover, genetic inactivation or knockout of NMDA receptors can impair bursting and affect tonic modes of firing in DAergic neurons (Zweifel et al., 2009; Wang et al., 2011). Consistent with these results, stimulation of glutamatergic afferent inputs to SNc DAergic neurons can also elicit bursts that are subsequently lost following NMDA receptor antagonist application (Deister et al., 2009).

In both the ventral tegmental area (VTA) and SNc, DAergic neurons also receive inputs from noradrenergic and serotonergic inputs. The contributions of these neuromodulatory systems were not examined in this thesis but may be worthy of

consideration since these systems have profound effects upon midbrain DAergic neuron activity patterns. Noradrenaline (NA), acting via α_1 adrenergic receptors can alter the firing patterns of VTA DAergic neurons (Grenhoff and Svensson, 1993; Grenhoff et al., 1995). Here, increases in NA signalling can depolarise the membrane potential and increase the spontaneous firing rates of dopaminergic neurons. Some evidence also suggests that dopaminergic neurons in the VTA express α_2 adrenergic receptors which can regulate firing properties (Lee et al., 1998; Georges and Aston-Jones, 2003). In contrast, serotonergic inputs play inhibitory roles. Application of serotonin receptor antagonists (specifically SB 206553, a serotonin-2B/2C receptor antagonist) causes a dose-dependent increase in the firing rate of dopaminergic neurons in the VTA and SNc (Di Giovanni et al., 1999). However, the role of serotonin may be receptor-dependent. Application of a serotonin-1A receptor agonist markedly increased the firing rate in the majority of DAergic cells in the VTA while a serotonin-1B agonist failed to change basal firing rates (Prisco et al., 1994).

In the zebrafish, the serotonergic system projects throughout the posterior tuberculum, in close proximity to DAergic neurons in the same region (McLean and Fetcho, 2004a), which may include DDNs arising from the DC2 population. At larval stages, noradrenergic cells of the locus coeruleus (LC) send ascending projections toward the telencephalon (Kastenhuber et al., 2010), although the precise contribution of noradrenergic pathways at this age is unknown due to methodological issues [see discussions in McLean and Fetcho (2004a); Kastenhuber et al. (2010)]. However, by adult stages, noradrenergic fibres from the LC contribute to the longitudinal and periventricular pathways which innervate hypothalamic regions including the periventricular nucleus (Kaslin and Panula, 2001) where DC2 DAergic neurons are located.

Thus, DDN activity patterns may be modulated by other neuromodulatory systems, reminiscent of the “metamodulation” of spinal networks where one neuromodulatory system influences another to modulate output (Miles and Sillar, 2011).

In sum, the work presented in this chapter provides *in vivo* evidence demonstrating that synaptic input is necessary for tonic and burst modes of firing. Specifically, glutamatergic input appears to drive burst modes of output while sparse glutamatergic (and possibly GABAergic) inputs contribute to tonic modes of output.

5.4.4 Afferent inputs to DDNs

Whilst direct afferent inputs to identified DDNs have yet to be identified, this cell population may integrate inputs from a range of regions. For instance, the HCRT system, which has been implicated in the regulation of arousal states and locomotor activity levels, is known to branch extensively within the PT in both zebrafish (Faraco et al., 2006; Prober et al., 2006; Appelbaum et al., 2009; Elbaz et al., 2012) and mammals (Peyron et al., 1998; Sakurai et al., 1998; Marcus et al., 2001). In adult zebrafish, the HCRT system comprises of only $\approx 20-60$ cells concentrated toward the posterior hypothalamus (Appelbaum et al., 2009) which project to monoaminergic (and cholinergic) nuclei (Kaslin et al., 2004). At larval stages, HCRT receptors are distributed throughout the telencephalon, hypothalamus, PT and hindbrain (Yokogawa et al., 2007) and HCRT expressing neurons form putative synapses with TH-positive cells in the PT (Prober et al., 2006).

By 5 dpf, zebrafish larvae engage in sleep/wake-like behaviours. Under constant dark conditions, wildtype larvae will remain relatively immobile. Overexpression

of HCRT can markedly increase levels of locomotor output during periods of low light (Prober et al., 2006). However, genetic ablation of HCRT neurons does not affect activity levels in similar conditions, but rather affects locomotor levels during the transition between sleep and wake states (Elbaz et al., 2012). Specifically, wild type larvae showed reduced activity, whereas HCRT neuron-ablated larvae showed increased activity during the transition from dark to light conditions (Elbaz et al., 2012). By adult stages, loss of HCRT receptors induces short and fragmented sleep in the dark (Yokogawa et al., 2007). Interestingly, a recent drug screen identifying compounds which disrupt normal wake/sleep patterns has identified D₂-like receptor antagonists (specifically haloperidol and clozapine) as promoters of states of wakefulness at night (Rihel et al., 2010). Thus, the descending DAergic inputs described in this chapter may interact with the HCRT pathway in a presently unidentified mechanism to modulate locomotor activity. The contributions of DDN low frequency tonic spiking and high frequency bursting to locomotor output have yet to be resolved. However, loss of both modes is sufficient to reduce initiation of spontaneous swim episodes as revealed by the ablation experiments performed here. This suggests that at least tonic DA release may be necessary for maintaining some level of excitability within spinal networks that facilitates swim initiation. Loss of afferent inputs to DDNs reveals pacemaker like activity, but importantly, the frequency of this output is markedly slower than when synaptic inputs are intact. Thus, HCRT may act to reduce afferent inputs to DDNs to lower DA levels in spinal networks.

Interestingly, HCRT neurons also project to spinal networks (Faraco et al., 2006; Prober et al., 2006; Appelbaum et al., 2009) and may therefore directly modulate motor network components. Indeed, HCRT receptors are localised to glycinergic

interneurons in dorsal regions of the zebrafish spinal cord (Yokogawa et al., 2007). In rats, HCRT receptors are distributed throughout the dorsal horn and central canal (Date et al., 2000; Grudt et al., 2002) and whole cell recordings from rat superficial dorsal horn interneurons revealed exogenous HCRT application can increase inhibitory post synaptic currents (IPSCs) in a glycinergic-dependent manner (Grudt et al., 2002). In the zebrafish spinal cord, the effects of DA and DA receptor distribution are unknown. However, DAergic axons course medially down the rostral-caudal extent of the spinal cord, at approximately the level of the motoneuron pool (McLean and Fetcho, 2004a). DA is known to increase excitability in mammalian motoneurons (Han et al., 2007; Han and Whelan, 2009) and may therefore serve similar roles here. Thus, at the level of the spinal cord, HCRT could serve broadly inhibitory roles while DA has the opposite effect.

In lamprey, it has recently been demonstrated that olfactory signals are relayed through the posterior tuberculum to reticulospinal cells in the hindbrain, which subsequently generate locomotor output (Derjean et al., 2010). Similarly, the posterior tuberculum of zebrafish also receives extensive input from the olfactory bulb (OB) where axons form close associations with DAergic cells (Miyasaka et al., 2014). Thus, DDNs may relay information evoked by olfactory signals directly to spinal locomotor networks in a similar fashion.

Finally, at least a proportion of DC2 and DC4 DA neurons also express the melanopsin *opn4a*, suggesting that these cells are intrinsically photosensitive (Fernandes et al., 2012). Zebrafish engage in a behaviour known as the visual motor response (VMR) which is characterised by a transient increase in activity following loss of light. This behaviour is driven by *opn4a* positive neurons just rostral to DC2 neurons (Fer-

ndes et al., 2012). While a proportion of DC2/4 cells also express this opsin, they're unlikely to contribute to the VMR since loss of these cells is insufficient to disrupt the VMR (Fernandes et al., 2012). If the DC2/DC4 DAergic neurons are light sensitive but do not contribute to this behaviour, then what function do they serve? Exposure of melanopsin-containing cells to light in other systems can strongly depolarise the membrane potential and increase spike activity (Berson et al., 2002; Hattar et al., 2002; Qiu et al., 2005; Brown et al., 2010). If *opn4a*-positive DDNs respond in a similar manner, then under light conditions autonomous spike activity, which is strongly voltage dependent, would increase in frequency due to melanopsin-dependent membrane depolarisation. Under dark conditions, melanopsin would be inactive and DDN spike activity would presumably be relatively lower. Within this chapter, loss of DDNs arising from the DC2 and DC4/5 cluster strongly reduces the initiation of locomotor episodes, suggesting that DA may set a basal level of excitability within the spinal cord. If DDNs arising from these populations are light sensitive, then changes in illumination (such as during the day or night) may modulate DA release and affect recruitment of spinal networks.

In sum, the findings presented in this chapter demonstrate that DDNs integrate into the spinal network as zebrafish enter swimming stages of development. Paired recordings between DDNs revealed that the whole population of DDNs in both ipsi- and contralateral hemispheres are recruited during locomotor episodes, suggesting that these cells may play fundamental roles during motor output. Ablation of DDNs in the DC2 population was sufficient to significantly perturb normal levels of locomotor output without affecting structure of locomotor episodes. Thus, the role of DAergic inputs to spinal networks may be to maintain some level of excitability which facilitates

initiation of swim episodes.

General Discussion

Within this thesis, the roles of two neuromodulators, dopamine (DA) and nitric oxide (NO) were considered. In the first results chapter, the role of NO during neuromuscular junction development was examined. Previously, it had been demonstrated that NO is a potent modulator of axonal outgrowth (Bradley et al., 2010). The work within this chapter forms a logical extension of these investigations by examining the anatomical and functional consequences at the level of the neuromuscular junction. Here it is demonstrated that neuromuscular junction formation was markedly reduced following increases in NO levels. In contrast, inhibition of NO-dependent signalling significantly increased the number of neuromuscular junctions (NMJs). On a physiological level, innervation to both embryonic slow (ES) and embryonic fast (EF) muscle fibre populations was significantly altered. Since the density of NMJ puncta was not affected following NO-dependent signalling perturbation, it is thought that these effects arise because of the previously reported reduction in axonal branching.

Within the developing mammalian and *Xenopus* musculature, NO has also been identified as a contributor to proper NMJ development. A vital step for appropriate NMJ formation is the clustering of acetylcholine receptors (AChRs). In both mammals and zebrafish, this occurs before innervation by the outgrowing motoneuron (Lin et al., 2001; Flanagan-Steet et al., 2005; Panzer et al., 2006). In the case of embryonic *Xenopus* musculature, overexpression of either NOS1, NOS2 or NOS3 is sufficient to increase AChR aggregation (Godfrey and Schwarte, 2003) whilst inhibition of NOS signalling can, in some cases, reduce AChR aggregation by up to 90 % (Godfrey and Schwarte, 2003; Schwarte and Godfrey, 2004; Godfrey et al., 2007). Similar NO-dependent effects have also been identified in mouse (Godfrey and Schwarte, 2010) and chick (Jones and Werle, 2000) preparations. Whilst these results suggest that NO

has a conserved role during NMJ formation, specifically in modulating AChR aggregation, NO is likely to serve a different role during zebrafish NMJ maturation. This is for the following reasons. Firstly, aneural ACh receptor aggregation occurs as early as \approx 16 hours post fertilisation (hpf) (Panzer et al., 2005, 2006), before NO-expressing cells are observed within the developing spinal cord (Bradley et al., 2010). Indeed, by the time NO-positive cells are found within the zebrafish spinal cord, extensive NMJ maturation has already occurred. Secondly, in mammals all three isoforms of NOS are expressed within the developing musculature (Stamler and Meissner, 2001) which is not the case for zebrafish (Poon, 2003; Holmqvist et al., 2004; Bradley et al., 2010). Instead, the primary role for NO within the context of this work is to control axonal outgrowth [as previously described (Bradley et al., 2010)] which consequently affects NMJ number.

Irrespective of the mechanisms, these findings raise the question of whether perturbation of NO signalling has functional consequences. The work within this chapter revealed that elevated NO levels during development tended to slow miniature end plate current (mEPC) kinetics whilst the opposite was generally true for decreased NO levels. These changes could be attributable to a number of factors (see subsection 3.4.4), but importantly, end plate potential (EPP) kinetics were also affected which would have functional consequences during locomotor episodes. Whilst free swimming was not examined in this study, previous reports have demonstrated that the velocity, frequency and maximal bend amplitude during swim episodes were significantly altered by chronically perturbed NO signalling (Bradley et al., 2010), in line with the results reported here. NO has also been identified as an modulator of locomotor episodes in other species (McLean et al., 2001; McLean and Sillar, 2002; McLean and Fetcho,

2004a; Kyriakatos and El Manira, 2007; Kyriakatos et al., 2009). However, these latter studies examined the acute effects of perturbing NO levels. In this work, the developmental effects of perturbing NO on fictive locomotor output were examined. This demonstrated that increased NO levels tended to slow the rise, decay and frequency of EPPs. In order to investigate whether these effects were driven by changes in spinal locomotor network components, the properties of motoneurons were examined. These results showed that there were no NO-dependent modulation of intrinsic motoneuron properties. Nonetheless, the observed effects upon locomotor output may still arise from changes within interneuron populations. Further investigations examining the effect of perturbed NO signalling on interneuron populations are necessary to identify the mechanisms responsible for the observed changes in fictive locomotor patterns.

In chapters two and three, I examined the anatomical and functional characteristics of a population of developing dopaminergic neurons which project from the posterior tuberculum to both the developing spinal networks and to peripheral mechanosensory structures. Previous works have already identified a population of dopaminergic neurons which innervate the periphery (Bricaud et al., 2001) and a population of dopaminergic neurons which innervate the spinal cord (McLean and Fetcho, 2004a,b; Tay et al., 2011). However, the work presented in this chapter demonstrates that both the spinal and peripheral axonal projections arise from the same cells. This suggests that DA may have fundamental roles in modulating both mechanosensory processes and spinal networks.

Paired dopaminergic diencephalospinal neuron (DDN) and motoneuron/muscle fibre recordings revealed that these cells exhibit low frequency tonic spiking during periods of locomotor network inactivity but engage in discrete high

frequency bursts that are separated by periods of silence during swimming. In the vast majority of cases, bursts were rarely observed outside of this locomotor context. These findings strongly suggest that both the locomotor network and sensory systems receive a large bolus of dopamine during swim episodes. The lateral line system receives inhibitory inputs during locomotor output and the DAergic neurons characterised here may serve this role, presumably to inhibit self-induced flow signals.

What then is DA doing to spinal networks? To elucidate the role(s) of descending DAergic cells, DC2 DDNs (and DC2/4/5 cells) were subjected to laser ablation. Previous reports suggest that developmental loss of these cells (or DAergic signalling) was sufficient to markedly decrease motoneuron (and increase interneuron) number (Reimer et al., 2013) or change mature modes of output to immature modes (Lambert et al., 2012). Thus, it was surprising that loss of DDN projections did not change motor pattern structure. Instead of altering the structure of swim episodes, loss of DDNs affected the incidence of spontaneous swim episodes, which suggests that DA may act to maintain some level of excitability within the spinal network to facilitate swim initiation. In other preparations, DA can initiate or strengthen ongoing fictive locomotor patterns. For example, in spinalised cats, local spinal injections of L-3,4-dihydroxyphenylalanine (L-DOPA) can elicit locomotion. In mice spinal preparations, DA appears to be necessary but not sufficient for normal locomotor output (Han et al., 2007). Previous reports in zebrafish suggest that increases in DA signalling, either by bath application of DA or DA-receptor agonists can significantly inhibit spontaneous swim episodes (Thirumalai and Cline, 2008). How can the results reported here be reconciled with previous investigations? The effects of agonists and antagonists have been discussed previously (see subsection 5.4.2), but briefly, bath application of these

drugs is likely to have off target effects: DA receptors are expressed throughout the developing nervous system, and therefore bath application of DA, DA receptor agonists or antagonists is likely to have off target effects. Finally, application of these agonists and antagonists is unlikely to recapitulate the fine temporal kinetics of *in vivo* DA release.

DDNs have also been examined within a developmental context. Since previous reports have suggested the DAergic pathway which arises from these cells is fundamental to nervous system ontogeny (Reimer et al., 2013) and reconfiguration from immature to mature modes of output (Lambert et al., 2012), it was of interest to examine DDN firing properties during the course of development when: a) spinal networks mature and the number of cell populations increase; and b) the output from these networks changes markedly. At embryonic stages when zebrafish produce a transient behaviour known as coiling, DDNs exhibit low frequency tonic firing. This emerges at ≈ 21 hpf and appears to have no obvious temporal relationship with coiling behaviour. This is not surprising for several reasons. Firstly, coiling is driven by a small network of electrically coupled cells that do not require supraspinal inputs (Saint-Amant and Drapeau, 2001; Tong and McDermid, 2012). Indeed, spinal transection is insufficient to perturb this behaviour. Secondly, coiling emerges at approximately 17 hpf, while DDNs do not engage in spike activity until mid (≈ 21 hpf) coiling stages. Thus, while a modulatory role for DDN activity at mid-late stage coiling cannot be dismissed, DDN firing is unlikely to be necessary or sufficient to initiate coiling.

As zebrafish enter free swimming stages, low frequency tonic firing of DDNs is accompanied by high frequency bursting. Bursting is relatively infrequent at 2 days post fertilisation (dpf) in comparison to 4 dpf where the incidence of DDN bursts is significantly increased. Interestingly, these bursts occur coincident with periods of

locomotor activity. Specifically, at 2 dpf, DDN bursts occur just prior to the onset of a burst-swim episode. By 4 dpf, fish engage in beat-glide swimming and DDN bursts are associated with the beat component of the locomotor episode. Thus, while bursts occur contemporaneously with swimming there are subtle differences. At 4 dpf, bursts occur during the active component of a swim episode, while at 2 dpf, DDN bursts occur at the start of the swim episode, and then fall silent. How these DDN bursts contribute to locomotor output requires further investigation. Specifically, since zebrafish spinal neuron cell populations have been relatively well characterised, understanding which DA receptors are expressed on specific cell types would help elucidate the effects of DA on this spinal network.

Previous reports have suggested that DDNs do not have autoreceptors (Pappas et al., 2008). These conclusions were based on the observation that addition of sulpiride, a D₂ receptor agonist, did not decrease the levels of DA within the spinal cord. Since autoinhibition is typically mediated by D₂ receptors, the authors concluded that, unlike the canonical dopamine neuron, DDNs do not possess autoreceptors. However, DDNs appear to undergo autoinhibition: loss of glutamatergic and GABAergic input reveals autonomous spiking which is sensitive to extracellular DA concentrations. Addition of DA to the bath markedly reduced the membrane potential, inhibited slow subthreshold oscillations and autonomous spiking. This was reversible since wash off with normal Evan's extracellular saline was sufficient to recover autonomous spiking. In sum, these findings strongly suggest that DDNs express autoreceptors.

In sum, this thesis examined two known neuromodulators, DA and NO within the context of zebrafish locomotor network ontogeny and output. The work presented here demonstrates that perturbation of NO dependent signalling is sufficient to sig-

nificantly alter NMJ development and locomotor network output whilst disruption of DA signalling can significantly alter the generation of spontaneous swim episodes. Additionally, the work presented in this thesis represents the first examination of DDN activity patterns in a developmental and behavioural context. These findings will help inform future investigations into the role of dopamine in spinal network ontogeny and ongoing locomotor output.

References

- Adams, L., Franco, M. C., and Estevez, A. G. (2015). Reactive nitrogen species in cellular signaling. *Experimental Biology and Medicine*, 240(6):711–7.
- Albin, R. L., Young, a. B., and Penney, J. B. (1989). The functional anatomy of basal ganglia disorders. *Trends in Neurosciences*, 12(10):366–375.
- Alderton, W. K., Cooper, C. E., and Knowles, R. G. (2001). Nitric oxide synthases: structure, function and inhibition. *The Biochemical Journal*, 357(Pt 3):593–615.
- Alessandri-Haber, N., Paillart, C., Arsac, C., Gola, M., Couraud, F., and Crest, M. (1999). Specific distribution of sodium channels in axons of rat embryo spinal motoneurons. *Journal of Physiology*, 518(1):203–214.
- Alexander, G. E. and Crutcher, M. D. (1990). Functional architecture of basal ganglia circuits: neural substrates of parallel processing. *Trends in Neurosciences*, 13(7):266–271.
- Anzalone, A., Lizardi-Ortiz, J. E., Ramos, M., De Mei, C., Hopf, F. W., Iaccarino, C., Halbout, B., Jacobsen, J., Kinoshita, C., Welter, M., Caron, M. G., Bonci, A., Sulzer, D., and Borrelli, E. (2012). Dual Control of Dopamine Synthesis and Release by Presynaptic and Postsynaptic Dopamine D2 Receptors. *Journal of Neuroscience*, 32(26):9023–9034.
- Appel, S. B., Wise, L., McDaid, J., Koyama, S., McElvain, M. A., and Brodie, M. S. (2006). The effects of long chain-length n-alcohols on the firing frequency of dopaminergic neurons of the ventral tegmental area. *Journal of Pharmacology and Experimental Therapeutics*, 318(3):1137–1145.
- Appelbaum, L., Wang, G. X., Maro, G. S., Mori, R., Tovin, A., Marin, W., Yokogawa, T., Kawakami, K., Smith, S. J., Gothilf, Y., Mignot, E., and Mourrain, P. (2009). Sleep-wake regulation and hypocretin-melatonin interaction in zebrafish. *Proceedings of the National Academy of Sciences of the United States of America*, 106(51):21942–7.
- Arenzana, F. J., Arévalo, R., Sánchez-González, R., Clemente, D., Aijón, J., and Porteros, A. (2006). Tyrosine hydroxylase immunoreactivity in the developing visual pathway of the zebrafish. *Anatomy and embryology*, 211(4):323–34.
- Arnaiz, C. O., Taylor, L. L., Stehouwer, D. J., and Van Hartesveldt, C. (1996). An aromatic L-amino acid decarboxylase inhibitor blocks L-dopa-induced air-stepping in neonatal rats. *Developmental Brain Research*, 94(2):234–237.

REFERENCES

- Arnold, W. P., Mittal, C. K., Katsuki, S., and Murad, F. (1977). Nitric oxide activates guanylate cyclase and increases guanosine 3':5'-cyclic monophosphate levels in various tissue preparations. *Proceedings of the National Academy of Sciences of the United States of America*, 74(8):3203–3207.
- Ayali, A. and Harris-Warrick, R. M. (1999). Monoamine control of the pacemaker kernel and cycle frequency in the lobster pyloric network. *Journal of Neuroscience*, 19(15):6712–22.
- Baker, L. L., Chandler, S. H., and Goldberg, L. J. (1984). L-dopa-induced locomotor-like activity in ankle flexor and extensor nerves of chronic and acute spinal cats. *Experimental Neurology*, 86(3):515–526.
- Balligand, J. L., Ungureanu-Longrois, D., Simmons, W. W., Pimental, D., Malinski, T. A., Kapturczak, M., Taha, Z., Lowenstein, C. J., Davidoff, A. J., and Kelly, R. A. (1994). Cytokine-inducible nitric oxide synthase (iNOS) expression in cardiac myocytes. Characterization and regulation of iNOS expression and detection of iNOS activity in single cardiac myocytes in vitro. *Journal of Biological Chemistry*, 269(44):27580–8.
- Barbeau, H. and Rossignol, S. (1991). Initiation and modulation of the locomotor pattern in the adult chronic spinal cat by noradrenergic, serotonergic and dopaminergic drugs. *Brain Research*, 546(2):250–260.
- Barraud, Q., Obeid, I., Aubert, I., Barrière, G., Contamin, H., McGuire, S., Ravenscroft, P., Porras, G., Tison, F., Bezard, E., and Ghorayeb, I. (2010). Neuroanatomical study of the A11 diencephalospinal pathway in the non-human primate. *PloS one*, 5(10):e13306.
- Barreiro-Iglesias, A., Villar-Cerviño, V., Anadón, R., and Rodicio, M. C. (2008). Descending brain-spinal cord projections in a primitive vertebrate, the lamprey: Cerebrospinal fluid-contacting and dopaminergic neurons. *Journal of Comparative Neurology*, 511(6):711–723.
- Barrière, G., Mellen, N., and Cazalets, J. R. (2004). Neuromodulation of the locomotor network by dopamine in the isolated spinal cord of newborn rat. *European Journal of Neuroscience*, 19(5):1325–1335.
- Baruscotti, M., Bucchi, A., and DiFrancesco, D. (2005). Physiology and pharmacology of the cardiac pacemaker (“funny”) current. *Pharmacology & Therapeutics*, 107(1):59–79.
- Bean, B. P. (2007). The action potential in mammalian central neurons. *Nature Reviews Neuroscience*, 8(6):451–465.

REFERENCES

- Beaulieu, J.-M. and Gainetdinov, R. R. (2011). The physiology, signaling, and pharmacology of dopamine receptors. *Pharmacological Reviews*, 63(1):182–217.
- Beckstead, M. J., Ford, C. P., Phillips, P. E. M., and Williams, J. T. (2007). Presynaptic regulation of dendrodendritic dopamine transmission. *European Journal of Neuroscience*, 26(6):1479–1488.
- Beckstead, M. J., Grandy, D. K., Wickman, K., and Williams, J. T. (2004). Vesicular dopamine release elicits an inhibitory postsynaptic current in midbrain dopamine neurons. *Neuron*, 42(6):939–946.
- Bellamy, T. C. and Garthwaite, J. (2002). The receptor-like properties of nitric oxide-activated soluble guanylyl cyclase in intact cells. *Molecular and Cellular Biochemistry*, 230(1-2):165–176.
- Ben-Ari, Y., Gaiarsa, J.-l., Tyzio, R., and Khazipov, R. (2007). GABA: a pioneer transmitter that excites immature neurons and generates primitive oscillations. *Physiological reviews*, 87(4):1215–84.
- Ben-Jonathan, N. and Hnasko, R. (2001). Dopamine as a prolactin (PRL) inhibitor. *Endocrine Reviews*, 22(6):724–763.
- Benninger, F., Beck, H., Wernig, M., Tucker, K. L., Brüstle, O., and Scheffler, B. (2003). Functional integration of embryonic stem cell-derived neurons in hippocampal slice cultures. *Journal of Neuroscience*, 23(18):7075–7083.
- Benoit-Marand, M., Borrelli, E., and Gonon, F. (2001). Inhibition of dopamine release via presynaptic D2 receptors: time course and functional characteristics in vivo. *Journal of Neuroscience*, 21(23):9134–9141.
- Bernhardt, R. R., Chitnis, a. B., Lindamer, L., and Kuwada, J. Y. (1990). Identification of spinal neurons in the embryonic and larval zebrafish. *Journal of Comparative Neurology*, 302(3):603–616.
- Berson, D. M., Dunn, F. A., and Takao, M. (2002). Phototransduction by retinal ganglion cells that set the circadian clock. *Science*, 295(5557):1070–1073.
- Bhatt, D. H., McLean, D. L., Hale, M. E., and Fetcho, J. R. (2007). Grading Movement Strength by Changes in Firing Intensity versus Recruitment of Spinal Interneurons. *Neuron*, 53(1):91–102.
- Bicker, G. (2005). STOP and GO with NO: nitric oxide as a regulator of cell motility in simple brains. *BioEssays*, 27(5):495–505.

REFERENCES

- Biel, M., Wahl-Schott, C., Michalakis, S., and Zong, X. (2009). Hyperpolarization-activated cation channels: from genes to function. *Physiological reviews*, 89(3):847–85.
- Björklund, A. and Dunnett, S. B. (2007). Dopamine neuron systems in the brain: an update. *Trends in Neurosciences*, 30(5):194–202.
- Björklund, A. and Skagerberg, G. (1979). Evidence for a major spinal cord projection from the diencephalic A11 dopamine cell group in the rat using transmitter-specific fluorescent retrograde tracing. *Brain Research*, 177(1):170–175.
- Blackshaw, S., Eliasson, M. J. L., Sawa, A., Watkins, C. C., Krug, D., Gupta, A., Arai, T., Ferrante, R. J., and Snyder, S. H. (2003). Species, strain and developmental variations in hippocampal neuronal and endothelial nitric oxide synthase clarify discrepancies in nitric oxide-dependent synaptic plasticity. *Neuroscience*, 119(4):979–990.
- Blanke, M. L. and VanDongen, A. M. (2009). *Activation Mechanisms of the NMDA Receptor*.
- Blechman, J., Borodovsky, N., Eisenberg, M., Nabel-Rosen, H., Grimm, J., and Levkowitz, G. (2007). Specification of hypothalamic neurons by dual regulation of the homeodomain protein Orthopedia. *Development (Cambridge, England)*, 134(24):4417–26.
- Blythe, S. N., Atherton, J. F., and Bevan, M. D. (2007). Synaptic activation of dendritic AMPA and NMDA receptors generates transient high-frequency firing in substantia nigra dopamine neurons in vitro. *Journal of Neurophysiology*, 97(4):2837–50.
- Blythe, S. N., Wokosin, D., Atherton, J. F., and Bevan, M. D. (2009). Cellular mechanisms underlying burst firing in substantia nigra dopamine neurons. *Journal of Neuroscience*, 29(49):15531–15541.
- Boehmler, W., Carr, T., Thisse, C., Thisse, B., Canfield, V. a., and Levenson, R. (2007). D4 Dopamine receptor genes of zebrafish and effects of the antipsychotic clozapine on larval swimming behaviour. *Genes, Brain and Behavior*, 6(2):155–166.
- Boehmler, W., Obrecht-Pflumio, S., Canfield, V., Thisse, C., Thisse, B., and Levenson, R. (2004). Evolution and expression of D2 and D3 dopamine receptor genes in zebrafish. *Developmental Dynamics*, 230(3):481–93.
- Bolam, J. P. and Smith, Y. (1990). The GABA and substance P input to dopaminergic neurones in the substantia nigra of the rat. *Brain Research*, 529(1-2):57–78.

REFERENCES

- Borla, M. A., Palecek, B., Budick, S., and O'Malley, D. M. (2002). Prey capture by larval zebrafish: Evidence for fine axial motor control. *Brain, Behavior and Evolution*, 60(4):207–229.
- Boyd, I., Martin, A. R., and Boyd, B. I. A. (1956). Spontaneous subthreshold activity at mammalian neuromuscular junctions. *The Journal of Physiology*, 132(1):61–73.
- Bradley, S., Tossell, K., Lockley, R., and McDearmid, J. R. (2010). Nitric oxide synthase regulates morphogenesis of zebrafish spinal cord motoneurons. *Journal of Neuroscience*, 30(50):16818–31.
- Branson, K., Robie, A. a., Bender, J., Perona, P., and Dickinson, M. H. (2009). High-throughput ethomics in large groups of *Drosophila*. *Nature Methods*, 6(6):451–7.
- Brazhnik, E., Shah, F., and Tepper, J. M. (2008). GABAergic afferents activate both GABAA and GABAB receptors in mouse substantia nigra dopaminergic neurons in vivo. *Journal of Neuroscience*, 28(41):10386–10398.
- Bredt, D. S., Glatt, C. E., Hwang, P. M., Fotuhi, M., Dawson, T. M., and Snyder, S. H. (1991a). Nitric oxide synthase protein and mRNA are discretely localized in neuronal populations of the mammalian CNS together with NADPH diaphorase. *Neuron*, 7(4):615–624.
- Bredt, D. S., Hwang, P. M., Glatt, C. E., Lowenstein, C., Reed, R. R., and Snyder, S. H. (1991b). Cloned and expressed nitric oxide synthase structurally resembles cytochrome P-450 reductase. *Nature*, 351(6329):714–718.
- Bredt, D. S. and Snyder, S. H. (1990). Isolation of nitric oxide synthetase, a calmodulin-requiring enzyme. *Proceedings of the National Academy of Sciences of the United States of America*, 87(2):682–685.
- Bricaud, O., Char, V., Dambly-Chaudiere, C., and Ghysen, A. (2001). Early efferent innervation of the zebrafish lateral line. *Journal of Comparative Neurology*, 434(3):253–261.
- Brocard, F. and Dubuc, R. (2003). Differential contribution of reticulospinal cells to the control of locomotion induced by the mesencephalic locomotor region. *Journal of Neurophysiology*, 90(3):1714–1727.
- Brocard, F., Ryczko, D., Fénelon, K., Hatem, R., Gonzales, D., Auclair, F., and Dubuc, R. (2010). The transformation of a unilateral locomotor command into a symmetrical bilateral activation in the brainstem. *Journal of Neuroscience*, 30(2):523–533.

REFERENCES

- Brown, M. T. C., Henny, P., Bolam, J. P., and Magill, P. J. (2009). Activity of neurochemically heterogeneous dopaminergic neurons in the substantia nigra during spontaneous and driven changes in brain state. *Journal of Neuroscience*, 29(9):2915–2925.
- Brown, T. G. (1911). The Intrinsic Factors in the Act of Progression in the Mammal. *Proceedings of the Royal Society B: Biological Sciences*, 84(572):308–319.
- Brown, T. M., Gias, C., Hatori, M., Keding, S. R., Semo, M., Coffey, P. J., Gigg, J., Piggins, H. D., Panda, S., and Lucas, R. J. (2010). Melanopsin contributions to irradiance coding in the thalamo-cortical visual system. *PLoS Biology*, 8(12).
- Brüning, G. and Mayer, B. (1996). Prenatal development of nitric oxide synthase in the mouse spinal cord. *Neuroscience letters*, 202:189–192.
- Brunston, T. (1867). On the use of nitrite of amyl in angina pectoris. *Lancet*, 2:97.
- Brustein, E., Chong, M., Holmqvist, B., and Drapeau, P. (2003). Serotonin Patterns Locomotor Network Activity in the Developing Zebrafish by Modulating Quiescent Periods. *Journal of Neurobiology*, 57(3):303–322.
- Brustein, E. and Drapeau, P. (2005). Serotonergic modulation of chloride homeostasis during maturation of the locomotor network in zebrafish. *Journal of Neuroscience*, 25(46):10607–16.
- Buchanan, J. T. (1982). Identification of interneurons with contralateral, caudal axons in the lamprey spinal cord: synaptic interactions and morphology. *Journal of Neurophysiology*, 47(5):961–975.
- Buchanan, J. T. and Cohen, A. H. (1982). Activities of identified interneurons, motoneurons, and muscle fibers during fictive swimming in the lamprey and effects of reticulospinal and dorsal cell stimulation. *Journal of Neurophysiology*, 47(5):948–960.
- Buchanan, J. T. and Grillner, S. (1987). Newly identified 'glutamate interneurons' and their role in locomotion in the lamprey spinal cord. *Science*, 236(4799):312–4.
- Buchanan, J. T., Grillner, S., Cullheim, S., and Risling, M. (1989). Identification of excitatory interneurons contributing to generation of locomotion in lamprey: structure, pharmacology, and function. *Journal of Neurophysiology*, 62(1):59–69.
- Budick, S. A. and O'Malley, D. M. (2000). Locomotor repertoire of the larval zebrafish: swimming, turning and prey capture. *Journal of Experimental Biology*, 203(Pt 17):2565–79.

REFERENCES

- Bunney, B. S., Walters, J. R., Roth, R. H., and Aghajanian, G. K. (1973). Dopaminergic neurons: effect of antipsychotic drugs and amphetamine on single cell activity. *Journal of Pharmacology and Experimental Therapeutics*, 185(3):560–571.
- Buss, R. R., Bourque, C. W., and Drapeau, P. (2003). Membrane properties related to the firing behavior of zebrafish motoneurons. *Journal of Neurophysiology*, 89(2):657–64.
- Buss, R. R. and Drapeau, P. (2000). Physiological properties of zebrafish embryonic red and white muscle fibers during early development. *Journal of Neurophysiology*, 84(3):1545.
- Buss, R. R. and Drapeau, P. (2001). Synaptic drive to motoneurons during fictive swimming in the developing zebrafish. *Journal of Neurophysiology*, 86:197–210.
- Buss, R. R. and Drapeau, P. (2002). Activation of embryonic red and white muscle fibers during fictive swimming in the developing zebrafish. *Journal of Neurophysiology*, 87(3):1244.
- Cabelguen, J.-M., Bourcier-Lucas, C., and Dubuc, R. (2003). Bimodal locomotion elicited by electrical stimulation of the midbrain in the salamander *Notophthalmus viridescens*. *Journal of Neuroscience*, 23(6):2434–2439.
- Caine, S. B. and Koob, G. F. (1994). Effects of mesolimbic dopamine depletion on responding maintained by cocaine and food. *Journal of the Experimental Analysis of Behavior*, 61(2):133–149.
- Campello-Costa, P., Fosse, A., Ribeiro, J., Paes-de Carvalho, R., and Serfaty, C. (2000). Acute blockade of nitric oxide synthesis induces disorganization and amplifies lesion-induced plasticity in the rat retinotectal projection. *Journal of Neurobiology*, 44(4):371–381.
- Cangiano, L. and Grillner, S. (2003). Fast and slow locomotor burst generation in the hemispinal cord of the lamprey. *Journal of Neurophysiology*, 89(6):2931–2942.
- Cantrell, A. R., Smith, R. D., Goldin, A. L., Scheuer, T., and Catterall, W. A. (1997). Dopaminergic modulation of sodium current in hippocampal neurons via cAMP-dependent phosphorylation of specific sites in the sodium channel alpha subunit. *Journal of Neuroscience*, 17(19):7330–8.
- Carr, D. B. and Sesack, S. R. (2000). Projections from the rat prefrontal cortex to the ventral tegmental area: target specificity in the synaptic associations with mesoaccumbens and mesocortical neurons. *Journal of Neuroscience*, 20(10):3864–3873.

REFERENCES

- Carreira, B. P., Morte, M. I., Lourenço, A. S., Santos, A. I., Inácio, Â., Ambrósio, A. F., Carvalho, C. M., and Araújo, I. M. (2013). Differential Contribution of the Guanylyl Cyclase-Cyclic GMP-Protein Kinase G Pathway to the Proliferation of Neural Stem Cells Stimulated by Nitric Oxide. *Neurosignals*, 21(1-2):1–13.
- Ceccatelli, S., Lundberg, J. M., Zhang, X., Aman, K., and Hökfelt, T. (1994). Immunohistochemical demonstration of nitric oxide synthase in the peripheral autonomic nervous system. *Brain Research*, 656(2):381–395.
- Chagnaud, B. P., Banchi, R., Simmers, J., and Straka, H. (2015). Spinal corollary discharge modulates motion sensing during vertebrate locomotion. *Nature Communications*, 6:7982.
- Chan, C. S., Guzman, J. N., Ilijic, E., Mercer, J. N., Rick, C., Tkatch, T., Meredith, G. E., and Surmeier, D. J. (2007). 'Rejuvenation' protects neurons in mouse models of Parkinson's disease. *Nature*, 447(7148):1081–1086.
- Chang, J. W., Wachtel, S. R., Young, D., and Kang, U. J. (1999). Biochemical and anatomical characterization of forepaw adjusting steps in rat models of Parkinson's disease: Studies on medial forebrain bundle and striatal lesions. *Neuroscience*, 88(2):617–628.
- Chao, D. S., Silvagno, F., Xia, H., Cornwell, T. L., Lincoln, T. M., and Brecht, D. S. (1996). Nitric oxide synthase and cyclic GMP-dependent protein kinase concentrated at the neuromuscular endplate. *Neuroscience*, 76(3):665–672.
- Charbit, A. R., Akerman, S., Holland, P. R., and Goadsby, P. J. (2009). Neurons of the dopaminergic/calcitonin gene-related peptide A11 cell group modulate neuronal firing in the trigeminocervical complex: an electrophysiological and immunohistochemical study. *Journal of Neuroscience*, 29(40):12532–12541.
- Chen, H. T. and Kandasamy, S. B. (1996). Effect of chloral hydrate on in vivo KCl-induced striatal dopamine release in the rat. *Neurochemical Research*, 21(6):695–700.
- Chen, N. and Reith, M. E. (2000). Structure and function of the dopamine transporter. *European Journal of Pharmacology*, 405(1-3):329–339.
- Cheng, A., Wang, S., Cai, J., Rao, M. S., and Mattson, M. P. (2003). Nitric oxide acts in a positive feedback loop with BDNF to regulate neural progenitor cell proliferation and differentiation in the mammalian brain. *Developmental Biology*, 258(2):319–333.

REFERENCES

- Chergui, K., Akaoka, H., Charléty, P. J., Saunier, C. F., Buda, M., and Chouvet, G. (1994). Subthalamic nucleus modulates burst firing of nigral dopamine neurones via NMDA receptors.
- Chergui, K., Charléty, P. J., Akaoka, H., Saunier, C. F., Brunet, J. L., Buda, M., Svensson, T. H., and Chouvet, G. (1993). Tonic activation of NMDA receptors causes spontaneous burst discharge of rat midbrain dopamine neurons in vivo. *European Journal of Neuroscience*, 5(2):137–144.
- Chiodo, L. A. and Bunney, B. S. (1983). Typical and atypical neuroleptics: differential effects of chronic administration on the activity of A9 and A10 midbrain dopaminergic neurons. *Journal of Neuroscience*, 3(8):1607–1619.
- Choi, Y. B., Tenneti, L., Le, D. A., Ortiz, J., Bai, G., Chen, H. S., and Lipton, S. A. (2000). Molecular basis of NMDA receptor-coupled ion channel modulation by S-nitrosylation. *Nature Neuroscience*, 3(1):15–21.
- Chrisman, T. D., Garbers, D. L., Parks, M. A., and Hardman, J. G. (1975). Characterization of particulate and soluble guanylate cyclases from rat lung. *Journal of Biological Chemistry*, 250(2):374–381.
- Christoffersen, C. L. and Meltzer, L. T. (1995). Evidence for N-methyl-d-aspartate and AMPA subtypes of the glutamate receptor on substantia nigra dopamine neurons: Possible preferential role for N-methyl-d-aspartate receptors. *Neuroscience*, 67(2):373–381.
- Chuhma, N., Choi, W. Y., Mingote, S., and Rayport, S. (2009). Dopamine neuron glutamate cotransmission: frequency-dependent modulation in the mesoventromedial projection. *Neuroscience*, 164(3):1068–1083.
- Ciani, E. (2004). Nitric oxide negatively regulates proliferation and promotes neuronal differentiation through N-Myc downregulation. *Journal of Cell Science*, 117(20):4727–4737.
- Ciani, E. (2006). Proliferation of cerebellar precursor cells is negatively regulated by nitric oxide in newborn rat. *Journal of Cell Science*, 119(15):3161–3170.
- Ciliax, B. J., Drash, G. W., Staley, J. K., Haber, S., Mobley, C. J., Miller, G. W., Mufson, E. J., Mash, D. C., and Levey, A. I. (1999). Immunocytochemical localization of the dopamine transporter in human brain. *Journal of Comparative Neurology*, 409(1):38–56.

REFERENCES

- Clemens, S., Belin-Rauscent, A., Simmers, J., and Combes, D. (2012). Opposing modulatory effects of D1- and D2-like receptor activation on a spinal central pattern generator. *Journal of Neurophysiology*, 107(8):2250–9.
- Clemens, S. and Hochman, S. (2004). Conversion of the modulatory actions of dopamine on spinal reflexes from depression to facilitation in D3 receptor knock-out mice. *Journal of Neuroscience*, 24(50):11337–11345.
- Clemens, S., Rye, D., and Hochman, S. (2006). Restless legs syndrome: revisiting the dopamine hypothesis from the spinal cord perspective. *Neurology*, 67(1):125–30.
- Cohen, A. H. and Harris-Warrick, R. M. (1984). Strychnine eliminates alternating motor output during fictive locomotion in the lamprey. *Brain Research*, 293(1):164–167.
- Contestabile, A. and Ciani, E. (2004). Role of nitric oxide in the regulation of neuronal proliferation, survival and differentiation. *Neurochemistry international*, 45(6):903–14.
- Courtney, N. A., Mamaligas, A. A., and Ford, C. P. (2012). Species Differences in Somatodendritic Dopamine Transmission Determine D2-Autoreceptor-Mediated Inhibition of Ventral Tegmental Area Neuron Firing. *Journal of Neuroscience*, 32(39):13520–13528.
- Cowley, K. C. and Schmidt, B. (1995). Effects of inhibitory amino acid antagonists on reciprocal inhibitory interactions during rhythmic motor activity in the in vitro neonatal rat spinal cord. *Journal of Neurophysiology*, 74(3):1109–1117.
- Crossman, A. (1987). Primate models of dyskinesia: The experimental approach to the study of basal ganglia-related involuntary movement disorders. *Neuroscience*, 21(1):1–40.
- Dahlstroem, A. and Fuxe, K. (1964). Evidence for the existence of monoamine-containing neurons in the central nervous system. I. Demonstration of monoamines in the cell bodies of brain stem neurons. *Acta physiologica Scandinavica. Supplementum*, pages SUPPL 232:1–55.
- Dale, N. (1985). Reciprocal inhibitory interneurons in the *Xenopus* embryo spinal cord. *The Journal of Physiology*, 363:61–70.
- Dale, N. (1986). Excitatory synaptic drive for swimming mediated by amino acid receptors in the lamprey. *Journal of Neuroscience*, 6(9):2662–2675.

REFERENCES

- Dale, N. and Grillner, S. (1986). Dual-component synaptic potentials in the lamprey mediated by excitatory amino acid receptors. *Journal of Neuroscience*, 6(9):2653–2661.
- Dale, N., Ottersen, O. P., Roberts, a., and Storm-Mathisen, J. (1986). Inhibitory neurones of a motor pattern generator in *Xenopus* revealed by antibodies to glycine. *Nature*, 324(6094):255–257.
- Dale, N. and Roberts, A. (1985). Dual-component amino-acid-mediated synaptic potentials: excitatory drive for swimming in *Xenopus* embryos. *The Journal of Physiology*, 363:35–59.
- Date, Y., Mondal, M. S., Matsukura, S., and Nakazato, M. (2000). Distribution of orexin-A and orexin-B (hypocretins) in the rat spinal cord. *Neuroscience Letters*, 288(2):87–90.
- Davidson, J. S. and Baumgarten, I. M. (1988). Glycyrrhetic acid derivatives: a novel class of inhibitors of gap-junctional intercellular communication. Structure-activity relationships. *Journal of Pharmacology and Experimental Therapeutics*, 246(3):1104–7.
- Dawson, T. E. D. M., Bredt, D. S., Fotuhi, M., Hwang, P. M., and Snyder, S. H. (1991). Nitric oxide synthase and neuronal NADPH. *Neurobiology*, 88(September):7797–7801.
- Deister, C. A., Teagarden, M. A., Wilson, C. J., and Paladini, C. A. (2009). An intrinsic neuronal oscillator underlies dopaminergic neuron bursting. *Journal of Neuroscience*, 29(50):15888–97.
- Delcomyn, F. (1980). Neural basis of rhythmic behavior in animals. *Science*, 210(4469):492–8.
- Derjean, D., Moussaddy, A., Atallah, E., St-Pierre, M., Auclair, F., Chang, S., Ren, X., Zielinski, B., and Dubuc, R. (2010). A novel neural substrate for the transformation of olfactory inputs into motor output. *PLoS Biology*, 8(12).
- Descarries, L., Bérubé-Carrière, N., Riad, M., Bo, G. D., Mendez, J. A., and Trudeau, L. É. (2008). Glutamate in dopamine neurons: Synaptic versus diffuse transmission. *Brain Research Reviews*, 58(2):290–302.
- Devoto, S. H., Melançon, E., Eisen, J. S., and Westerfield, M. (1996). Identification of separate slow and fast muscle precursor cells in vivo, prior to somite formation. *Development (Cambridge, England)*, 122(11):3371–80.

REFERENCES

- Di Forti, M., Lappin, J. M., and Murray, R. M. (2007). Risk factors for schizophrenia - All roads lead to dopamine. *European Neuropsychopharmacology*, 17(SUPPL. 2):101–107.
- Di Giovanni, G., De Deurwaerdère, P., Di Mascio, M., Di Matteo, V., Esposito, E., and Spampinato, U. (1999). Selective blockade of serotonin-2C/2B receptors enhances mesolimbic and mesostriatal dopaminergic function: A combined in vivo electrophysiological and microdialysis study. *Neuroscience*, 91(2):587–597.
- Di Prisco, G. V., Pearlstein, E., Le Ray, D., Robitaille, R., and Dubuc, R. (2000). A cellular mechanism for the transformation of a sensory input into a motor command. *Journal of Neuroscience*, 20(21):8169–8176.
- Dinerman, J. L., Dawson, T. M., Schell, M. J., Snowman, A., and Snyder, S. H. (1994). Endothelial nitric oxide synthase localized to hippocampal pyramidal cells: implications for synaptic plasticity. *Proceedings of the National Academy of Sciences of the United States of America*, 91(10):4214–4218.
- Ding, A. H., Nathan, C. F., and Stuehr, D. J. (1988). Release of reactive nitrogen intermediates and reactive oxygen intermediates from mouse peritoneal macrophages. Comparison of activating cytokines and evidence for independent production. *Journal of immunology (Baltimore, Md. : 1950)*, 141(7):2407–2412.
- Ditlevsen, D. K., Køhler, L. B., Berezin, V., and Bock, E. (2007). Cyclic guanosine monophosphate signalling pathway plays a role in neural cell adhesion molecule-mediated neurite outgrowth and survival. *Journal of Neuroscience Research*, 85(4):703–711.
- Doig, N. M., Moss, J., and Bolam, J. P. (2010). Cortical and thalamic innervation of direct and indirect pathway medium-sized spiny neurons in mouse striatum. *Journal of Neuroscience*, 30(44):14610–14618.
- Doreulee, N., Sergeeva, O. A., Yanovsky, Y., Chepkova, A. N., Selbach, O., Gödecke, A., Schrader, J., and Haas, H. L. (2003). Cortico-striatal synaptic plasticity in endothelial nitric oxide synthase deficient mice. *Brain Research*, 964(1):159–63.
- Dossi, R. C., Nuñez, A., and Steriade, M. (1992). Electrophysiology of a slow (0.5-4 Hz) intrinsic oscillation of cat thalamocortical neurones in vivo. *The Journal of Physiology*, 447:215–234.
- Downes, G. B. and Granato, M. (2006). Supraspinal input is dispensable to generate glycine-mediated locomotive behaviors in the zebrafish embryo. *Journal of Neurobiology*, 66(5):437–451.

REFERENCES

- Doyle, C. A. and Slater, P. (1997). Localization of neuronal and endothelial nitric oxide synthase isoforms in human hippocampus. *Neuroscience*, 76(2):387–95.
- Drapeau, P., Ali, D. W., Buss, R. R., and Saint-Amant, L. (1999). In vivo recording from identifiable neurons of the locomotor network in the developing zebrafish. *Journal of Neuroscience Methods*, 88(1):1–13.
- Drapeau, P., Buss, R. R., Ali, D. W., Legendre, P., and Rotundo, R. L. (2001). Limits to the development of fast neuromuscular transmission in zebrafish. *Journal of Neurophysiology*, 86(6):2951–2956.
- Dreyer, J. K., Herrik, K. F., Berg, R. W., and Hounsgaard, J. D. (2010). Influence of phasic and tonic dopamine release on receptor activation. *Journal of Neuroscience*, 30(42):14273–83.
- Dubois, A., Savasta, M., Curet, O., and Scatton, B. (1986). Autoradiographic distribution of the D1 agonist [3H]SKF 38393, in the rat brain and spinal cord. Comparison with the distribution of D2 dopamine receptors. *Neuroscience*, 19(1):125–137.
- Dun, N., Dun, S., Forstermann, U., and Tseng, L. (1992). Nitric oxide synthase immunoreactivity in rat spinal cord. *Neuroscience Letters*, 147(2):217–220.
- Earley, C. J., Allen, R. P., Connor, J. R., Ferrucci, L., and Troncoso, J. (2009). The dopaminergic neurons of the A11 system in RLS autopsy brains appear normal. *Sleep Medicine*, 10(10):1155–1157.
- Easley-Neal, C., Fierro, J., Buchanan, J., and Washbourne, P. (2013). Late Recruitment of Synapsin to Nascent Synapses Is Regulated by Cdk5. *Cell Reports*, 3(4):1199–1212.
- Ebadi, M., Sharma, S. K., Ghafourifar, P., Brown-Borg, H., and El ReFaey, H. (2005). Peroxynitrite in the pathogenesis of Parkinson's disease and the neuroprotective role of metallothioneins. *Methods in Enzymology*, 396(05):276–298.
- Eisen, J. S. and Marder, E. (1982). Mechanisms underlying pattern generation in lobster stomatogastric ganglion as determined by selective inactivation of identified neurons. III. Synaptic connections of electrically coupled pyloric neurons. *Journal of Neurophysiology*, 48(6).
- Eisen, J. S., Pike, S. H., and Romancier, B. (1990). An identified motoneuron with variable fates in embryonic zebrafish. *Journal of Neuroscience*, 10(1):34–43.
- El Manira, A. (2014). Dynamics and plasticity of spinal locomotor circuits. *Current Opinion in Neurobiology*, 29:133–141.

REFERENCES

- El Manira, A. and Kyriakatos, A. (2010). The Role of Endocannabinoid Signaling in Motor Control. *Physiology*, 25(4):230–238.
- Elbaz, I., Yelin-Bekerman, L., Nicenboim, J., Vatine, G., and Appelbaum, L. (2012). Genetic Ablation of Hypocretin Neurons Alters Behavioral State Transitions in Zebrafish. *Journal of Neuroscience*, 32(37):12961–12972.
- Emran, F., Rihel, J., Adolph, A. R., and Dowling, J. E. (2010). Zebrafish larvae lose vision at night. *Proceedings of the National Academy of Sciences of the United States of America*, 107(13):6034–6039.
- Erhardt, S., Mathé, J. M., Chergui, K., Engberg, G., and Svensson, T. H. (2002). GABA(B) receptor-mediated modulation of the firing pattern of ventral tegmental area dopamine neurons in vivo. *Naunyn-Schmiedeberg's archives of pharmacology*, 365(3):173–80.
- Eriksen, J., Jørgensen, T. N., and Gether, U. (2010). Regulation of dopamine transporter function by protein-protein interactions: New discoveries and methodological challenges. *Journal of Neurochemistry*, 113(1):27–41.
- Faraco, J. H., Appelbaum, L., Marin, W., Gaus, S. E., Mourrain, P., and Mignot, E. (2006). Regulation of hypocretin (orexin) expression in embryonic zebrafish. *Journal of Biological Chemistry*, 281(40):29753–29761.
- Fedele, E., Fontana, G., Munari, C., Cossu, M., and Raiteri, M. (1999). Native human neocortex release-regulating dopamine D2 type autoreceptors are dopamine D2 subtype. *European Journal of Neuroscience*, 11(7):2351–8.
- Feil, S., Zimmermann, P., Knorn, A., Brummer, S., Schlossmann, J., Hofmann, F., and Feil, R. (2005). Distribution of cGMP-dependent protein kinase type I and its isoforms in the mouse brain and retina. *Neuroscience*, 135(3):863–868.
- Fernandes, A. M., Beddows, E., Filippi, A., and Driever, W. (2013). Orthopedia transcription factor *otpa* and *otpb* paralogous genes function during dopaminergic and neuroendocrine cell specification in larval zebrafish. *PloS one*, 8(9):e75002.
- Fernandes, A. M., Fero, K., Arrenberg, A. B., Bergeron, S. A., Driever, W., and Burgess, H. A. (2012). Deep Brain Photoreceptors Control Light-Seeking Behavior in Zebrafish Larvae. *Current Biology*, 22(21):2042–2047.
- Fero, K., Yokogawa, T., and Burgess, H. A. (2011). The Behavioral Repertoire of Larval Zebrafish. In Kalueff, A. V. and Cachat, J. M., editors, *NeuroMethods*, volume 52 of *Neuromethods*, pages 249–291. Humana Press, Totowa, NJ.

REFERENCES

- Fesenko, E. E., Kolesnikov, S. S., and Lyubarsky, A. L. (1985). Induction by cyclic GMP of cationic conductance in plasma membrane of retinal rod outer segment. *Nature*, 313(6000):310–3.
- Filippi, A., Mueller, T., and Driever, W. (2014). *vglut2* and *gad* expression reveal distinct patterns of dual GABAergic versus glutamatergic cotransmitter phenotypes of dopaminergic and noradrenergic neurons in the zebrafish brain. *Journal of Comparative Neurology*, 522(9):2019–37.
- Flamm, R. E. and Harris-Warrick, R. M. (1986a). Aminergic modulation in lobster stomatogastric ganglion. I. Effects on motor pattern and activity of neurons within the pyloric circuit. *Journal of Neurophysiology*, 55(5):847–865.
- Flamm, R. E. and Harris-Warrick, R. M. (1986b). Aminergic modulation in lobster stomatogastric ganglion. II. Target neurons of dopamine, octopamine, and serotonin within the pyloric circuit. *Journal of Neurophysiology*, 55(5):866–881.
- Flanagan-Steet, H., Fox, M. A., Meyer, D., and Sanes, J. R. (2005). Neuromuscular synapses can form in vivo by incorporation of initially aneural postsynaptic specializations. *Development (Cambridge, England)*, 132(20):4471–81.
- Flock, A. and Russell, I. J. (1973). The post-synaptic action of efferent fibres in the lateral line organ of the burbot *Lota lota*. *The Journal of Physiology*, 235(3):591–605.
- Floresco, S. B., West, A. R., Ash, B., Moore, H., and Grace, A. A. (2003). Afferent modulation of dopamine neuron firing differentially regulates tonic and phasic dopamine transmission. *Nature Neuroscience*, 6(9):968–973.
- Ford, C. (2014). The role of D2-autoreceptors in regulating dopamine neuron activity and transmission. *Neuroscience*, 282(January):13–22.
- Ford, C. P., Phillips, P. E. M., and Williams, J. T. (2009). The time course of dopamine transmission in the ventral tegmental area. *Journal of Neuroscience*, 29(42):13344–13352.
- Förstermann, U., Mülsch, A., Böhme, E., and Busse, R. (1986). Stimulation of soluble guanylate cyclase by an acetylcholine-induced endothelium-derived factor from rabbit and canine arteries. *Circulation research*, 58(4):531–538.
- Foster, J. D., Dunford, C., Sillar, K. T., and Miles, G. B. (2014). Nitric oxide-mediated modulation of the murine locomotor network. *Journal of Neurophysiology*, 111(3):659–74.

REFERENCES

- Francis, S. H., Busch, J. L., and Corbin, J. D. (2010). cGMP-Dependent Protein Kinases and cGMP Phosphodiesterases in Nitric Oxide and cGMP Action. *Pharmacological Reviews*, 62(3):525–563.
- Fukao, M., Mason, H. S., Britton, F. C., Kenyon, J. L., Horowitz, B., and Keef, K. D. (1999). Cyclic GMP-dependent protein kinase activates cloned BKCa channels expressed in mammalian cells by direct phosphorylation at serine 1072. *Journal of Biological Chemistry*, 274(16):10927–35.
- Furchgott, R. F. and Zawadzki, J. V. (1980). The obligatory role of endothelial cells in the relaxation of arterial smooth muscle by acetylcholine. *Nature*, 288(5789):373–376.
- Fye, W. B. (1986). T. Lauder Brunton and amyl nitrite: a Victorian vasodilator. *Circulation*, 74(2):222–229.
- Gabriel, J. P., Mahmood, R., Kyriakatos, A., Söll, I., Hauptmann, G., Calabrese, R. L., and El Manira, A. (2009). Serotonergic modulation of locomotion in zebrafish: endogenous release and synaptic mechanisms. *Journal of Neuroscience*, 29(33):10387–10395.
- Gahtan, E. and O'Malley, D. M. (2003). Visually guided injection of identified reticulospinal neurons in Zebrafish: A survey of spinal arborization patterns. *Journal of Comparative Neurology*, 459(2):186–200.
- Gallo, G., Ernst, A. F., McLoon, S. C., and Letourneau, P. C. (2002). Transient PKA activity is required for initiation but not maintenance of BDNF-mediated protection from nitric oxide-induced growth-cone collapse. *Journal of Neuroscience*, 22(12):5016–5023.
- Gao, B. X. and Ziskind-Conhaim, L. (1998). Development of ionic currents underlying changes in action potential waveforms in rat spinal motoneurons. *Journal of Neurophysiology*, 80(6):3047–3061.
- Gao, C. and Wolf, M. E. (2007). Dopamine alters AMPA receptor synaptic expression and subunit composition in dopamine neurons of the ventral tegmental area cultured with prefrontal cortex neurons. *Journal of Neuroscience*, 27(52):14275–14285.
- Garcia-Rill, E., Kinjo, N., Atsuta, Y., Ishikawa, Y., Webber, M., and Skinner, R. D. (1990). Posterior midbrain-induced locomotion. *Brain Research Bulletin*, 24(3):499–508.
- Garcia-Rill, E., Skinner, R., and Fitzgerald, J. (1985). Chemical activation of the mesencephalic locomotor region. *Brain Research*, 330(1):43–54.

REFERENCES

- Garcia-Rill, E. and Skinner, R. D. (1987). The mesencephalic locomotor region. II. Projections to reticulospinal neurons. *Brain Research*, 411(1):13–20.
- Garraway, S. M. and Hochman, S. (2001). Modulatory actions of serotonin, norepinephrine, dopamine, and acetylcholine in spinal cord deep dorsal horn neurons. *Journal of Neurophysiology*, 86(5):2183–2194.
- Garthwaite, G., Bartus, K., Malcolm, D., Goodwin, D., Kollb-Sielecka, M., Dooldeniya, C., and Garthwaite, J. (2006). Signaling from blood vessels to CNS axons through nitric oxide. *Journal of Neuroscience*, 26(29):7730–7740.
- Garthwaite, J. (1991). Glutamate, nitric oxide and cell-cell signalling in the nervous system. *Trends in Neurosciences*, 14(2):60–67.
- Garthwaite, J. (2008). Concepts of neural nitric oxide-mediated transmission. *European Journal of Neuroscience*, 27(11):2783–802.
- Garthwaite, J., Garthwaite, G., Palmer, R. M., and Moncada, S. (1989). NMDA receptor activation induces nitric oxide synthesis from arginine in rat brain slices. *European Journal of Pharmacology*, 172(4-5):413–416.
- Georges, F. and Aston-Jones, G. (2003). Prolonged activation of mesolimbic dopaminergic neurons by morphine withdrawal following clonidine: participation of imidazoline and norepinephrine receptors. *Neuropsychopharmacology : official publication of the American College of Neuropsychopharmacology*, 28(6):1140–1149.
- Gerzer, R., Böhme, E., Hofmann, F., and Schultz, G. (1981). Soluble guanylate cyclase purified from bovine lung contains heme and copper. *FEBS letters*, 132(1):71.
- Ghosh, Dipak, K. (2003). Nitric oxide synthases: domain structure and alignment in enzyme function and control. *Frontiers in Bioscience*, 8(1-3):d193.
- Giaid, A. and Saleh, D. (1995). Reduced Expression of Endothelial Nitric Oxide Synthase in the Lungs of Patients with Pulmonary Hypertension. *New England Journal of Medicine*, 333(4):214–221.
- Giros, B., Jaber, M., Jones, S. R., Wightman, R. M., and Caron, M. G. (1996). Hyperlocomotion and indifference to cocaine and amphetamine in mice lacking the dopamine transporter. *Nature*, 379(6566):606–12.
- Giuli, G., Luzi, A., Poyard, M., and Guellaën, G. (1994). Expression of mouse brain soluble guanylyl cyclase and NO synthase during ontogeny. *Developmental Brain Research*, 81(2):269–283.

REFERENCES

- Godfrey, E. W., Longacher, M., Neiswender, H., Schwarte, R. C., and Browning, D. D. (2007). Guanylate cyclase and cyclic GMP-dependent protein kinase regulate agrin signaling at the developing neuromuscular junction. *Developmental biology*, 307(2):195–201.
- Godfrey, E. W. and Schwarte, R. C. (2003). The role of nitric oxide signaling in the formation of the neuromuscular junction. *Journal of Neurocytology*, 32(5-8):591–602.
- Godfrey, E. W. and Schwarte, R. C. (2010). Nitric oxide and cyclic GMP regulate early events in agrin signaling in skeletal muscle cells. *Experimental Cell Research*, 316(12):1935–1945.
- Goldman-Rakic, P. S. (1992). Dopamine-mediated mechanisms of the prefrontal cortex. *Seminars in Neuroscience*, 4(2):149–159.
- Gonon, F. G. (1988). Nonlinear relationship between impulse flow and dopamine released by rat midbrain dopaminergic neurons as studied by in vivo electrochemistry. *Neuroscience*, 24(1):19–28.
- González-Hernández, T. and Rodríguez, M. (2000). Compartmental organization and chemical profile of dopaminergic and GABAergic neurons in the substantia nigra of the rat. *Journal of Comparative Neurology*, 421(1):107–135.
- Gordon, I. T. and Whelan, P. J. (2006). Monoaminergic control of cauda-equina-evoked locomotion in the neonatal mouse spinal cord. *Journal of Neurophysiology*, 96(6):3122–3129.
- Goulding, M. (2009). Circuits controlling vertebrate locomotion: moving in a new direction. *Nature Reviews Neuroscience*, 10(7):507–518.
- Grace, A. (1991). Regulation of spontaneous activity and oscillatory spike firing in rat midbrain dopamine neurons recorded in vitro. *Synapse*, 7(3):221–34.
- Grace, A. (1992). The depolarization block hypothesis of neuroleptic action: implications for the etiology and treatment of schizophrenia. *Journal of Neural Transmission Supplementum*, 36:91–131.
- Grace, A. and Bunney, B. (1980). Nigral dopamine neurons: intracellular recording and identification with L-dopa injection and histofluorescence. *Science*, 210(4470):654–656.
- Grace, A. and Bunney, B. (1983a). Intracellular and extracellular electrophysiology of nigral dopaminergic neurons–2. Action potential generating mechanisms and morphological correlates. *Neuroscience*, 10(2):317–31.

REFERENCES

- Grace, A. and Bunney, B. (1983b). Intracellular and extracellular electrophysiology of nigral dopaminergic neurons—1. Identification and characterization. *Neuroscience*, 10(2).
- Grace, A. and Bunney, B. (1983c). Intracellular and extracellular electrophysiology of nigral dopaminergic neurons—3. Evidence for electrotonic coupling. *Neuroscience*, 10(2).
- Grace, A. and Bunney, B. (1984a). The control of firing pattern in nigral dopamine neurons: burst firing. *Journal of Neuroscience*, 4(11):2877–2890.
- Grace, A. and Bunney, B. (1984b). The control of firing pattern in nigral dopamine neurons: single spike firing. *Journal of Neuroscience*, 4(11):2866–76.
- Grace, A. and Bunney, B. (1985). Opposing effects of striatonigral feedback pathways on midbrain dopamine cell activity. *Brain Research*, 333(2):271–284.
- Grace, A. and Bunney, B. (1986). Induction of depolarization block in midbrain dopamine neurons by repeated administration of haloperidol: analysis using in vivo intracellular recording. *Journal of Pharmacology and Experimental Therapeutics*, 238(3):1092–100.
- Grace, A. and Onn, S. (1989). Morphology and electrophysiological properties of immunocytochemically identified rat dopamine neurons recorded in vitro. *Journal of Neuroscience*, 9(10):3463–81.
- Granato, M., van Eeden, F. J., Schach, U., Trowe, T., Brand, M., Furutani-Seiki, M., Haffter, P., Hammerschmidt, M., Heisenberg, C. P., Jiang, Y. J., Kane, D. a., Kelsh, R. N., Mullins, M. C., Odenthal, J., and Nüsslein-Volhard, C. (1996). Genes controlling and mediating locomotion behavior of the zebrafish embryo and larva. *Development (Cambridge, England)*, 123:399–413.
- Grenhoff, J., North, R. A., and Johnson, S. W. (1995). Alpha 1 -adrenergic Effects on Dopamine Neurons Recorded Intracellularly in the Rat Midbrain Slice. *European Journal of Neuroscience*, 7(8):1707–1713.
- Grenhoff, J. and Svensson, T. H. (1993). Prazosin modulates the firing pattern of dopamine neurons in rat ventral tegmental area. *European Journal of Pharmacology*, 233(1):79–84.
- Grillner, S. (2003). The motor infrastructure: from ion channels to neuronal networks. *Nature Reviews Neuroscience*, 4(7):573–586.
- Grillner, S. (2006). Biological Pattern Generation: The Cellular and Computational Logic of Networks in Motion. *Neuron*, 52(5):751–766.

REFERENCES

- Grillner, S., Deliagina, T., Ekeberg, O. ., El Manira, a., Hill, R. H., Lansner, a., Orlovsky, G. N., and Wallén, P (1995). Neural networks that co-ordinate locomotion and body orientation in lamprey. *Trends in Neurosciences*, 18(6):270–279.
- Grillner, S. and Matsushima, T. (1991). The neural network underlying locomotion in lamprey—synaptic and cellular mechanisms. *Neuron*, 7(1):1–15.
- Grillner, S. and Robertson, B. (2015). The basal ganglia downstream control of brainstem motor centres—an evolutionarily conserved strategy. *Current Opinion in Neurobiology*, 33:47–52.
- Grillner, S. and Wallén, P. (1980). Does the central pattern generation for locomotion in lamprey depend on glycine inhibition? *Acta physiologica Scandinavica*, 110(1):103–105.
- Grillner, S. and Zangger, P. (1979). On the central generation of locomotion in the low spinal cat. *Experimental Brain Research*, 34(2):241–261.
- Groves, P. M., Wilson, C. J., Young, S. J., and Rebec, G. V. (1975). Self-inhibition by dopaminergic neurons. *Science*, 190(4214):522–8.
- Grozdanovic, Z. (1999). Nitric oxide synthase in skeletal muscle fibers: A signaling component of the dystrophin-glycoprotein complex.
- Grozdanovic, Z. and Gossrau, R. (1998). Co-localization of nitric oxide synthase I (NOS I) and NMDA receptor subunit 1 (NMDAR-1) at the neuromuscular junction in rat and mouse skeletal muscle. *Cell and tissue research*, 291(1):57–63.
- Grudt, T. J., van den Pol, A. N., and Perl, E. R. (2002). Hypocretin-2 (orexin-B) modulation of superficial dorsal horn activity in rat. *The Journal of Physiology*, 538(Pt 2):517–525.
- Gruetter, C. A., Barry, B. K., McNamara, D. B., Gruetter, D. Y., Kadowitz, P. J., and Ignarro, L. (1979). Relaxation of bovine coronary artery and activation of coronary arterial guanylate cyclase by nitric oxide, nitroprusside and a carcinogenic nitrosoamine. *Journal of Cyclic Nucleotide Research*, 5(3):211–224.
- Gu, X.-L. (2010). Deciphering the corelease of glutamate from dopaminergic terminals derived from the ventral tegmental area. *Journal of Neuroscience*, 30(41):13549–13551.
- Gu, Y. and Hall, Z. W. (1988). Immunological evidence for a change in subunits of the acetylcholine receptor in developing and denervated rat muscle. *Neuron*, 1(2):117–125.

REFERENCES

- Guertin, P. A. (2009). The mammalian central pattern generator for locomotion. *Brain Research Reviews*, 62(1):45–56.
- Guirado, S., Real, M. A., Olmos, J. L., and Dávila, J. C. (2003). Distinct types of nitric oxide-producing neurons in the developing and adult mouse claustrum. *Journal of Comparative Neurology*, 465(3):431–444.
- Guo, S., Wilson, S. W., Cooke, S., Chitnis, A. B., Driever, W., and Rosenthal, A. (1999). Mutations in the zebrafish unmask shared regulatory pathways controlling the development of catecholaminergic neurons. *Developmental biology*, 208(2):473–87.
- Haase, A. and Bicker, G. (2003). Nitric oxide and cyclic nucleotides are regulators of neuronal migration in an insect embryo. *Development (Cambridge, England)*, 130(17):3977–3987.
- Hale, M. E., Ritter, D. A., and Fetcho, J. R. (2001). A confocal study of spinal interneurons in living larval zebrafish. *Journal of Comparative Neurology*, 437(1):1–16.
- Hall, S. K. and Armstrong, D. L. (2000). Conditional and unconditional inhibition of calcium-activated potassium channels by reversible protein phosphorylation. *Journal of Biological Chemistry*, 275(6):3749–3754.
- Hammerschmidt, M., Bitgood, M. J., and McMahon, A. P. (1996). Protein kinase A is a common negative regulator of Hedgehog signaling in the vertebrate embryo. *Genes and Development*, 10(6):647–658.
- Han, P., Nakanishi, S. T., Tran, M. A., and Whelan, P. J. (2007). Dopaminergic modulation of spinal neuronal excitability. *Journal of Neuroscience*, 27(48):13192–204.
- Han, P. and Whelan, P. J. (2009). Modulation of AMPA currents by D1-like but not D2-like receptors in spinal motoneurons. *Neuroscience*, 158(4):1699–1707.
- Hanafy, K. A., Krumenacker, J. S., and Murad, F. (2001). NO, nitrotyrosine, and cyclic GMP in signal transduction. *Medical science monitor : international medical journal of experimental and clinical research*, 7(4):801–819.
- Hansson, G. K., Geng, Y. J., Holm, J., Hårdhammar, P., Wennmalm, A., and Jennische, E. (1994). Arterial smooth muscle cells express nitric oxide synthase in response to endothelial injury. *The Journal of experimental medicine*, 180(2):733–738.
- Hardingham, N., Dachtler, J., and Fox, K. (2013). The role of nitric oxide in pre-synaptic plasticity and homeostasis. *Frontiers in Cellular Neuroscience*, 7(October):190.

REFERENCES

- Hardman, J. G. and Sutherland, E. W. (1969). Guanyl cyclase, an enzyme catalyzing the formation of guanosine 3',5'-monophosphate from guanosine triphosphate. *Journal of Biological Chemistry*, 244(23):6363–6370.
- Harris, N. (1992). Sensitivity of transient outward rectification to ion channel blocking agents in guinea-pig substantia nigra pars compacta neurones in vitro. *Brain Research*, 596(1-2):325–329.
- Harris-Warrick, R. M. (2011). Neuromodulation and flexibility in Central Pattern Generator networks. *Current Opinion in Neurobiology*, 21(5):685–692.
- Harris-Warrick, R. M. and Cohen, A. H. (1985). Serotonin modulates the central pattern generator for locomotion in the isolated lamprey spinal cord. *Journal of Experimental Biology*, 116:27–46.
- Harris-Warrick, R. M., Coniglio, L. M., Barazangi, N., Guckenheimer, J., and Gueron, S. (1995). Dopamine modulation of transient potassium current evokes phase shifts in a central pattern generator network. *Journal of Neuroscience*, 15(1 Pt 1):342–358.
- Hattar, S., Liao, H. W., Takao, M., Berson, D. M., and Yau, K. W. (2002). Melanopsin-containing retinal ganglion cells: architecture, projections, and intrinsic photosensitivity. *Science*, 295(5557):1065–1070.
- Haul, S., Gödecke, A., Schrader, J., Haas, H. L., and Luhmann, H. J. (1999). Impairment of neocortical long-term potentiation in mice deficient of endothelial nitric oxide synthase. *Journal of Neurophysiology*, 81(2):494–497.
- He, Y., Yu, W., and Baas, P. W. (2002). Microtubule reconfiguration during axonal retraction induced by nitric oxide. *Journal of Neuroscience*, 22(14):5982–5991.
- Hell, J. W., Appleyard, S. M., Yokoyama, C. T., Warner, C., and Catterall, W. A. (1994). Differential phosphorylation of two size forms of the N-type calcium channel $\alpha 1$ subunit which have different COOH termini. *Journal of Biological Chemistry*, 269(10):7390–7396.
- Hell, J. W., Yokoyama, C. T., Wong, S. T., Warner, C., Snutch, T. P., and Catterall, W. A. (1993). Differential phosphorylation of two size forms of the neuronal class C L-type calcium channel $\alpha 1$ subunit. *Journal of Biological Chemistry*, 268(26):19451–19457.
- Henny, P., Brown, M. T. C., Northrop, A., Faunes, M., Ungless, M. A., Magill, P. J., and Bolam, J. P. (2012). Structural correlates of heterogeneous in vivo activity of midbrain dopaminergic neurons. *Nature Neuroscience*, 15(4):613–619.

REFERENCES

- Herberich, E., Sikorski, J., and Hothorn, T. (2010). A robust procedure for comparing multiple means under heteroscedasticity in unbalanced designs. *PLoS one*, 5(3):e9788.
- Hess, D. T., Patterson, S. I., Smith, D. S., and Skene, J. H. (1993). Neuronal growth cone collapse and inhibition of protein fatty acylation by nitric oxide. *Nature*, 366(6455):562–565.
- Hibbs, J. B., Vavrin, Z., and Taintor, R. R. (1987). L-arginine is required for expression of the activated macrophage effector mechanism causing selective metabolic inhibition in target cells. *Journal of immunology (Baltimore, Md. : 1950)*, 138(2):550–565.
- Hietala, J. and Syvälahti, E. (1996). Dopamine in Schizophrenia. *Annals of Medicine*, 28(6):557–561.
- Higashijima, S.-I., Mandel, G., and Fetcho, J. R. (2004a). Distribution of prospective glutamatergic, glycinergic, and GABAergic neurons in embryonic and larval zebrafish. *Journal of Comparative Neurology*, 480(1):1–18.
- Higashijima, S.-I., Schaefer, M., and Fetcho, J. R. (2004b). Neurotransmitter properties of spinal interneurons in embryonic and larval zebrafish. *Journal of Comparative Neurology*, 480(1):19–37.
- Hinckley, C. A., Hartley, R., Wu, L., Todd, A., and Ziskind-Conhaim, L. (2005). Locomotor-like rhythms in a genetically distinct cluster of interneurons in the mammalian spinal cord. *Journal of Neurophysiology*, 93(3):1439–1449.
- Hirata, H., Saint-Amant, L., Downes, G. B., Cui, W. W., Zhou, W., Granato, M., and Kuwada, J. Y. (2005). Zebrafish bandoneon mutants display behavioral defects due to a mutation in the glycine receptor beta-subunit. *Proceedings of the National Academy of Sciences of the United States of America*, 102(23):8345–8350.
- Hnasko, T. S., Chuhma, N., Zhang, H., Goh, G. Y., Sulzer, D., Palmiter, R. D., Rayport, S., and Edwards, R. H. (2010). Vesicular Glutamate Transport Promotes Dopamine Storage and Glutamate Corelease In Vivo. *Neuron*, 65(5):643–656.
- Hökfelt, T., Phillipson, O., and Goldstein, M. (1979). Evidence for a dopaminergic pathway in the rat descending from the A11 cell group to the spinal cord. *Acta physiologica Scandinavica*, 107(4):393–395.
- Holmqvist, B., Ebbesson, L., and Alm, P. (2007). Nitric oxide and the zebrafish (*Danio rerio*): Developmental neurobiology and brain neurogenesis. *Advances in Experimental Biology*, 1(07).

REFERENCES

- Holmqvist, B., Ellingsen, B., Alm, P., Forsell, J., Oyan, A. M., Goksøyr, A., Fjose, A., and Seo, H. C. (2000). Identification and distribution of nitric oxide synthase in the brain of adult zebrafish. *Neuroscience letters*, 292(2):119–22.
- Holmqvist, B., Ellingsen, B., Forsell, J., Zhdanova, I., and Alm, P. (2004). The early ontogeny of neuronal nitric oxide synthase systems in the zebrafish. *Journal of Experimental Biology*, 207(Pt 6):923–35.
- Holzschuh, J., Ryu, S., Aberger, F., and Driever, W. (2001). Dopamine transporter expression distinguishes dopaminergic neurons from other catecholaminergic neurons in the developing zebrafish embryo. *Mechanisms of Development*, 101(1-2):237–43.
- Hopper, R., Lancaster, B., and Garthwaite, J. (2004). On the regulation of NMDA receptors by nitric oxide. *European Journal of Neuroscience*, 19(7):1675–1682.
- Howe, K., Clark, M. D., Torroja, C. F., Torrance, J., Berthelot, C., Muffato, M., Collins, J. E., Humphray, S., McLaren, K., Matthews, L., McLaren, S., Sealy, I., Caccamo, M., Churcher, C., Scott, C., Barrett, J. C., Koch, R., Rauch, G.-J., White, S., Chow, W., Kilian, B., Quintais, L. T., Guerra-Assunção, J. a., Zhou, Y., Gu, Y., Yen, J., Vogel, J.-H., Eyre, T., Redmond, S., Banerjee, R., Chi, J., Fu, B., Langley, E., Maguire, S. F., Laird, G. K., Lloyd, D., Kenyon, E., Donaldson, S., Sehra, H., Almeida-King, J., Loveland, J., Trevanion, S., Jones, M., Quail, M., Willey, D., Hunt, A., Burton, J., Sims, S., McLay, K., Plumb, B., Davis, J., Clee, C., Oliver, K., Clark, R., Riddle, C., Elliott, D., Threadgold, G., Harden, G., Ware, D., Mortimore, B., Kerry, G., Heath, P., Phillimore, B., Tracey, A., Corby, N., Dunn, M., Johnson, C., Wood, J., Clark, S., Pelan, S., Griffiths, G., Smith, M., Glithero, R., Howden, P., Barker, N., Stevens, C., Harley, J., Holt, K., Panagiotidis, G., Lovell, J., Beasley, H., Henderson, C., Gordon, D., Auger, K., Wright, D., Collins, J., Raisen, C., Dyer, L., Leung, K., Robertson, L., Ambridge, K., Leongamornlert, D., McGuire, S., Gilderthorp, R., Griffiths, C., Manthravadi, D., Nichol, S., Barker, G., Whitehead, S., Kay, M., Brown, J., Murnane, C., Gray, E., Humphries, M., Sycamore, N., Barker, D., Saunders, D., Wallis, J., Babbage, A., Hammond, S., Mashreghi-Mohammadi, M., Barr, L., Martin, S., Wray, P., Ellington, A., Matthews, N., Ellwood, M., Woodmansey, R., Clark, G., Cooper, J., Tromans, A., Grafham, D., Skuce, C., Pandian, R., Andrews, R., Harrison, E., Kimberley, A., Garnett, J., Fosker, N., Hall, R., Garner, P., Kelly, D., Bird, C., Palmer, S., Gehring, I., Berger, A., Dooley, C. M., Ersan-Ürün, Z., Eser, C., Geiger, H., Geisler, M., Karotki, L., Kirn, A., Konantz, J., Konantz, M., Oberländer, M., Rudolph-Geiger, S., Teucke, M., Osoegawa, K., Zhu, B., Rapp, A., Widaa, S., Langford, C., Yang, F., Carter, N. P., Harrow, J., Ning, Z., Herrero, J., Searle, S. M. J., Enright, A., Geisler, R., Plasterk, R. H. a., Lee, C., Westerfield, M., de Jong, P. J., Zon, L. I., Postlethwait, J. H., Nüsslein-Volhard, C., Hubbard, T. J. P., Crollius, H. R., Rogers, J., and Stemple, D. L. (2013).

REFERENCES

- The zebrafish reference genome sequence and its relationship to the human genome. *Nature*, 496(7446):498–503.
- Huber, K. A., Kriegstein, K., and Unsicker, K. (1995). The neurotrophins BDNF, NT-3 and -4, but not NGF, TGF-beta 1 and GDNF, increase the number of NADPH-diaphorase-reactive neurons in rat spinal cord cultures. *Neuroscience*, 69(3):771–779.
- Humphreys, J. M. and Whelan, P. J. (2012). Dopamine exerts activation-dependent modulation of spinal locomotor circuits in the neonatal mouse. *Journal of Neurophysiology*, 108(12):3370–81.
- Hyland, B. I., Reynolds, J. N. J., Hay, J., Perk, C. G., and Miller, R. (2002). Firing modes of midbrain dopamine cells in the freely moving rat. *Neuroscience*, 114(2):475–92.
- Ichitani, Y., Okamura, H., Nakahara, D., Nagatsu, I., and Ibata, Y. (1994). Biochemical and immunocytochemical changes induced by intrastriatal 6OHDA injection.
- Ignarro, L. J., Buga, G. M., Wood, K. S., Byrns, R. E., and Chaudhuri, G. (1987). Endothelium-derived relaxing factor produced and released from artery and vein is nitric oxide. *Proceedings of the National Academy of Sciences of the United States of America*, 84(24):9265–9.
- Irons, T., Kelly, P., Hunter, D., MacPhail, R., and Padilla, S. (2013). Acute administration of dopaminergic drugs has differential effects on locomotion in larval zebrafish. *Pharmacology Biochemistry and Behavior*, 103(4):792–813.
- Iversen, S. D. and Iversen, L. L. (2007). Dopamine: 50 years in perspective. *Trends in Neurosciences*, 30(5):188–193.
- Iwase, K., Takemura, M., Shimada, T., Wakisaka, S., Nokubi, T., and Shigenaga, Y. (1998). Ontogeny of NADPH-diaphorase in rat forebrain and midbrain. *Anatomy and Embryology*, 197(3):229–247.
- Jaber, M., Robinson, S. W., Missale, C., and Caron, M. G. (1996). Dopamine receptors and brain function. *Neuropharmacology*, 35(11):1503–19.
- Jackson, D. M. and Westlind-Danielsson, A. (1994). Dopamine receptors: Molecular biology, biochemistry and behavioural aspects. *Pharmacology & Therapeutics*, 64(2):291–370.
- Jankowska, E., Jukes, M. G., Lund, S., and Lundberg, a. (1967a). The effect of DOPA on the spinal cord. 5. Reciprocal organization of pathways transmitting excitatory action to alpha motoneurons of flexors and extensors. *Acta physiologica Scandinavica*, 70(3):369–388.

REFERENCES

- Jankowska, E., Jukes, M. G., Lund, S., and Lundberg, A. (1967b). The effect of DOPA on the spinal cord. 6. Half-centre organization of interneurons transmitting effects from the flexor reflex afferents. *Acta physiologica Scandinavica*, 70(3):389–402.
- Jing, L., Gordon, L. R., Shtibin, E., and Granato, M. (2010). Temporal and spatial requirements of unplugged/MuSK function during zebrafish neuromuscular development. *PLoS ONE*, 5(1).
- Jing, L., Lefebvre, J. L., Gordon, L. R., and Granato, M. (2009). Wnt Signals Organize Synaptic Prepattern and Axon Guidance through the Zebrafish unplugged/MuSK Receptor. *Neuron*, 61(5):721–733.
- Joh, T. H. and Weiser, M. (1993). Early and late molecular events occurring following neuronal degeneration in the dopamine system. *Advances in Neurology*, 60:316–320.
- Johnson, B., Peck, J., and Harris-Warrick, R. (1993a). Amine modulation of electrical coupling in the pyloric network of the lobster stomatogastric ganglion. *Journal of Comparative Physiology A*, 172(6):715–732.
- Johnson, B., Peck, J., and Harris-Warrick, R. (1994). Differential modulation of chemical and electrical components of mixed synapses in the lobster stomatogastric ganglion. *Journal of Comparative Physiology A*, 175(2):233–249.
- Johnson, B. R., Peck, J. H., and Harris-Warrick, R. M. (1993b). Dopamine induces sign reversal at mixed chemical-electrical synapses. *Brain Research*, 625(1):159–164.
- Johnson, B. R., Peck, J. H., and Harris-Warrick, R. M. (1995). Distributed amine modulation of graded chemical transmission in the pyloric network of the lobster stomatogastric ganglion. *Journal of Neurophysiology*, 74(1):437–452.
- Jones, M. A. and Werle, M. J. (2000). Nitric Oxide Is a Downstream Mediator of Agrin-Induced Acetylcholine Receptor Aggregation. *Molecular and Cellular Neuroscience*, 16(5):649–660.
- Jones, S. R., Gainetdinov, R. R., Jaber, M., Giros, B., Wightman, R. M., and Caron, M. G. (1998). Profound neuronal plasticity in response to inactivation of the dopamine transporter. *Proceedings of the National Academy of Sciences of the United States of America*, 95(7):4029–4034.
- Joseph, J. D., Wang, Y. M., Miles, P. R., Budygin, E. a., Picetti, R., Gainetdinov, R. R., Caron, M. G., and Wightman, R. M. (2002). Dopamine autoreceptor regulation of release and uptake in mouse brain slices in the absence of D3 receptors. *Neuroscience*, 112(1):39–49.

REFERENCES

- Kabra, M., Robie, A. a., Rivera-Alba, M., Branson, S., and Branson, K. (2013). JAABA: interactive machine learning for automatic annotation of animal behavior. *Nature Methods*, 10(1):64–7.
- Kalueff, A. V., Gebhardt, M., Stewart, A. M., Cachat, J. M., Brimmer, M., Chawla, J. S., Craddock, C., Kyzar, E. J., Roth, A., Landsman, S., Gaikwad, S., Robinson, K., Bastrup, E., Tierney, K., Shamchuk, A., Norton, W., Miller, N., Nicolson, T., Braubach, O., Gilman, C. P., Pittman, J., Rosemberg, D. B., Gerlai, R., Echevarria, D., Lamb, E., Neuhauss, S. C. F., Weng, W., Bally-Cuif, L., and Schneider, H. (2013). Towards a comprehensive catalog of zebrafish behavior 1.0 and beyond. *Zebrafish*, 10(1):70–86.
- Kamisaki, Y., Saheki, S., Nakane, M., Palmieri, J. A., Kuno, T., Chang, B. Y., Waldman, S. A., and Murad, F. (1986). Soluble guanylate cyclase from rat lung exists as a heterodimer. *Journal of Biological Chemistry*, 261(16):7236–7241.
- Kang, Y. and Kitai, S. T. (1993). Calcium spike underlying rhythmic firing in dopaminergic neurons of the rat substantia nigra. *Neuroscience Research*, 18(3):195–207.
- Kapur, S., Bédard, S., Marcotte, B., Côté, C. H., and Marette, A. (1997). Expression of nitric oxide synthase in skeletal muscle: a novel role for nitric oxide as a modulator of insulin action. *Diabetes*, 46(11):1691–1700.
- Kaslin, J., Nystedt, J. M., Ostergård, M., Peitsaro, N., and Panula, P. (2004). The orexin/hypocretin system in zebrafish is connected to the aminergic and cholinergic systems. *Journal of Neuroscience*, 24(11):2678–2689.
- Kaslin, J. and Panula, P. (2001). Comparative anatomy of the histaminergic and other aminergic systems in zebrafish (*Danio rerio*). *Journal of Comparative Neurology*, 440(4):342–77.
- Kasthuber, E., Kratochwil, C. F., Ryu, S., Schweitzer, J., and Driever, W. (2010). Genetic dissection of dopaminergic and noradrenergic contributions to catecholaminergic tracts in early larval zebrafish. *Journal of Comparative Neurology*, 518(4):439–458.
- Kato, M. (1990). Chronically isolated lumbar half spinal cord generates locomotor activities in the ipsilateral hindlimb of the cat. *Neuroscience research*, 9(1):22–34.
- Katsuki, S., Arnold, W. P., and Murad, F. (1977). Effects of sodium nitroprusside, nitroglycerin, and sodium azide on levels of cyclic nucleotides and mechanical activity of various tissues. *Journal of Cyclic Nucleotide Research*, 3(4):239–247.

REFERENCES

- Katsuki, S. and Murad, F. (1977). Regulation of adenosine cyclic 3',5'-monophosphate and guanosine cyclic 3',5'-monophosphate levels and contractility in bovine tracheal smooth muscle. *Molecular pharmacology*, 13(2):330–341.
- Katz, B. and Miledi, R. (1967). A study of synaptic transmission in the absence of nerve impulses. *The Journal of Physiology*, 192:407–436.
- Kaupp, U. B. and Seifert, R. (2002). Cyclic nucleotide-gated ion channels. *Physiological reviews*, 82(3):769–824.
- Kawagoe, K. T., Garris, P. A., Wiedemann, D. J., and Wightman, R. M. (1992). Regulation of transient dopamine concentration gradients in the microenvironment surrounding nerve terminals in the rat striatum. *Neuroscience*, 51(1):55–64.
- Kebabian, J. W. and Calne, D. B. (1979). Multiple receptors for dopamine. *Nature*, 277(5692):93–96.
- Kemnitz, C. P. (1997). Dopaminergic modulation of spinal neurons and synaptic potentials in the lamprey spinal cord. *Journal of Neurophysiology*, 77(1):289–298.
- Khaliq, Z. M. and Bean, B. P. (2010). Pacemaking in dopaminergic ventral tegmental area neurons: depolarizing drive from background and voltage-dependent sodium conductances. *Journal of Neuroscience*, 30(21):7401–13.
- Khan, J. A. and Roberts, A. (1982). Experiments on the Central Pattern Generator for Swimming in Amphibian Embryos. *Philosophical Transactions of the Royal Society B: Biological Sciences*, 296(1081):229–243.
- Kiehn, O. and Butt, S. J. B. (2003). Physiological, anatomical and genetic identification of CPG neurons in the developing mammalian spinal cord. *Progress in Neurobiology*, 70(4):347–361.
- Kiehn, O. and Kjaerulff, O. (1996). Spatiotemporal characteristics of 5-HT and dopamine-induced rhythmic hindlimb activity in the in vitro neonatal rat. *Journal of Neurophysiology*, 75(4):1472–1482.
- Kim, K. M., Nakajima, Y., and Nakajima, S. (1995). G protein-coupled inward rectifier modulated by dopamine agonists in cultured substantia nigra neurons. *Neuroscience*, 69(4):1145–1158.
- Kim, S. W., Jang, Y. J., Chang, J. W., and Hwang, O. (2003). Degeneration of the nigrostriatal pathway and induction of motor deficit by tetrahydrobiopterin: An in vivo model relevant to Parkinson's disease. *Neurobiology of Disease*, 13(2):167–176.

REFERENCES

- Kimmel, C. B., Ballard, W. W., Kimmel, S. R., Ullmann, B., and Schilling, T. F. (1995). Stages of embryonic development of the zebrafish. *Developmental Dynamics*, 203(3):253–310.
- Kimura, Y., Okamura, Y., and Higashijima, S.-i. (2006). *alx*, a zebrafish homolog of Chx10, marks ipsilateral descending excitatory interneurons that participate in the regulation of spinal locomotor circuits. *Journal of Neuroscience*, 26(21):5684–97.
- Kimura, Y., Satou, C., Fujioka, S., Shoji, W., Umeda, K., Ishizuka, T., Yawo, H., and Higashijima, S. I. (2013). Hindbrain V2a neurons in the excitation of spinal locomotor circuits during zebrafish swimming. *Current Biology*, 23(10):843–849.
- Kinugawa, K.-i., Shimizu, T., Yao, A., Kohmoto, O., Serizawa, T., and Takahashi, T. (1997). Transcriptional Regulation of Inducible Nitric Oxide Synthase in Cultured Neonatal Rat Cardiac Myocytes. *Circulation Research*, 81(6):911–921.
- Kita, T., Kita, H., and Kitai, S. T. (1986). Electrical membrane properties of rat substantia nigra compacta neurons in an in vitro slice preparation. *Brain Research*, 372(1):21–30.
- Kjaerulff, O. and Kiehn, O. (1997). Crossed rhythmic synaptic input to motoneurons during selective activation of the contralateral spinal locomotor network. *Journal of Neuroscience*, 17(24):9433–9447.
- Knipp, S. and Bicker, G. (2009). A developmental study of enteric neuron migration in the grasshopper using immunological probes. *Developmental Dynamics*, 238(11):2837–49.
- Knogler, L. D. and Drapeau, P. (2014). Sensory gating of an embryonic zebrafish interneuron during spontaneous motor behaviors. *Frontiers in Neural Circuits*, 8(September):1–16.
- Knogler, L. D., Ryan, J., Saint-Amant, L., and Drapeau, P. (2014). A Hybrid Electrical/Chemical Circuit in the Spinal Cord Generates a Transient Embryonic Motor Behavior. *Journal of Neuroscience*, 34(29):9644–9655.
- Koblinger, K., Füzesi, T., Ejdrygiewicz, J., Krajacic, A., Bains, J. S., and Whelan, P. J. (2014). Characterization of a11 neurons projecting to the spinal cord of mice. *PLoS one*, 9(10):e109636.
- Kobzik, L., Reid, M. B., Brecht, D. S., and Stamler, J. S. (1994). Nitric oxide in skeletal muscle. *Nature*, 372(6506):546–548.

REFERENCES

- Koesling, D., Russwurm, M., Mergia, E., Mullershausen, F., and Friebe, A. (2004). Nitric oxide-sensitive guanylyl cyclase: structure and regulation. *Neurochemistry international*, 45(6):813–9.
- Koga, E. and Momiyama, T. (2000). Presynaptic dopamine D2-like receptors inhibit excitatory transmission onto rat ventral tegmental dopaminergic neurones. *The Journal of Physiology*, 523 Pt 1:163–173.
- Kopp-Scheinflug, C., Pigott, B. M., and Forsythe, I. D. (2015). Nitric oxide selectively suppresses I H currents mediated by HCN1-containing channels. *The Journal of Physiology*, 593(7):1685–1700.
- Kostrzewa, R. M. and Jacobowitz, D. M. (1974). Pharmacological actions of 6-hydroxydopamine. *Pharmacological Reviews*, 26(3):199–288.
- Kravitz, A. V. and Kreitzer, A. C. (2012). Striatal Mechanisms Underlying Movement, Reinforcement, and Punishment. *Physiology*, 27(3):167–177.
- Kullberg, R. W., Mikelberg, F. S., and Cohen, M. W. (1980). Contribution of cholinesterase to developmental decreases in the time course of synaptic potentials at an amphibian neuromuscular junction. *Developmental biology*, 75(2):255–267.
- Kuwada, J. Y., Bernhardt, R. R., and Chitnis, A. B. (1990a). Pathfinding by identified growth cones in the spinal cord of zebrafish embryos. *Journal of Neuroscience*, 10(4):1299–1308.
- Kuwada, J. Y., Bernhardt, R. R., and Nguyen, N. (1990b). Development of spinal neurons and tracts in the zebrafish embryo. *Journal of Comparative Neurology*, 302(3):617–628.
- Kuzhikandathil, E. V., Yu, W., and Oxford, G. S. (1998). Human dopamine D3 and D2L receptors couple to inward rectifier potassium channels in mammalian cell lines. *Molecular and Cellular Neuroscience*, 12(6):390–402.
- Kuznetsova, A. Y., Huertas, M. a., Kuznetsov, A. S., Paladini, C. a., and Canavier, C. C. (2010). Regulation of firing frequency in a computational model of a midbrain dopaminergic neuron. *Journal of Computational Neuroscience*, 28(3):389–403.
- Kyriakatos, A. and El Manira, A. (2007). Long-term plasticity of the spinal locomotor circuitry mediated by endocannabinoid and nitric oxide signaling. *Journal of Neuroscience*, 27(46):12664–12674.
- Kyriakatos, A., Mahmood, R., Ausborn, J., Porres, C. P., Büschges, A., and El Manira, A. (2011). Initiation of locomotion in adult zebrafish. *Journal of Neuroscience*, 31(23):8422–8431.

REFERENCES

- Kyriakatos, A., Molinari, M., Mahmood, R., Grillner, S., Sillar, K. T., and El Manira, A. (2009). Nitric oxide potentiation of locomotor activity in the spinal cord of the lamprey. *Journal of Neuroscience*, 29(42):13283–91.
- Lacey, M. G., Mercuri, N. B., and North, R. A. (1987). Dopamine acts on D2 receptors to increase potassium conductance in neurones of the rat substantia nigra zona compacta. *The Journal of Physiology*, 392:397–416.
- Lacey, M. G., Mercuri, N. B., and North, R. A. (1988). On the potassium conductance increase activated by GABAB and dopamine D2 receptors in rat substantia nigra neurones. *The Journal of Physiology*, 401:437–453.
- Lambert, A. M., Bonkowsky, J. L., and Masino, M. A. (2012). The conserved dopaminergic diencephalospinal tract mediates vertebrate locomotor development in zebrafish larvae. *Journal of Neuroscience*, 32(39):13488–500.
- Lammel, S., Hetzel, A., Häckel, O., Jones, I., Liss, B., and Roeper, J. (2008). Unique properties of mesoprefrontal neurons within a dual mesocorticolimbic dopamine system. *Neuron*, 57(5):760–73.
- Lammel, S., Lim, B. K., and Malenka, R. C. (2014). Reward and aversion in a heterogeneous midbrain dopamine system. *Neuropharmacology*, 76(PART B):351–359.
- Lancaster, J. (1997). A Tutorial on the Diffusibility and Reactivity of Free Nitric Oxide. *Nitric Oxide*, 1(1):18–30.
- Lancaster, J. R. (1994). Simulation of the diffusion and reaction of endogenously produced nitric oxide. *Proceedings of the National Academy of Sciences of the United States of America*, 91(17):8137–41.
- Lapointe, N. P., Rouleau, P., Ung, R.-V., and Guertin, P. a. (2009). Specific role of dopamine D1 receptors in spinal network activation and rhythmic movement induction in vertebrates. *The Journal of Physiology*, 587(Pt 7):1499–1511.
- Le Ray, D., Juvin, L., Ryczko, D., and Dubuc, R. (2011). *Supraspinal control of locomotion. The mesencephalic locomotor region*, volume 188. Elsevier BV, 1 edition.
- Lee, A., Wissekerke, A. E., Rosin, D. L., and Lynch, K. R. (1998). Localization of alpha2C-adrenergic receptor immunoreactivity in catecholaminergic neurons in the rat central nervous system. *Neuroscience*, 84(4):1085–1096.
- Lefebvre, J. L., Ono, F., Puglielli, C., Seidner, G., Franzini-Armstrong, C., Brehm, P., and Granato, M. (2004). Increased neuromuscular activity causes axonal defects and muscular degeneration. *Development (Cambridge, England)*, 131(11):2605–2618.

REFERENCES

- Lei, S. Z., Pan, Z. H., Aggarwal, S. K., Chen, H. S., Hartman, J., Sucher, N. J., and Lipton, S. A. (1992). Effect of nitric oxide production on the redox modulatory site of the NMDA receptor-channel complex. *Neuron*, 8(6):1087–1099.
- Lenka, N., Lu, Z. J., Sasse, P., Hescheler, J., and Fleischmann, B. K. (2002). Quantitation and functional characterization of neural cells derived from ES cells using nestin enhancer-mediated targeting in vitro. *Journal of Cell Science*, 115(Pt 7):1471–1485.
- Levant, B. and McCarson, K. E. (2001). D(3) dopamine receptors in rat spinal cord: implications for sensory and motor function. *Neuroscience letters*, 303(1):9–12.
- Li, K. and Xu, E. (2008). The role and the mechanism of γ -aminobutyric acid during central nervous system development. *Neuroscience Bulletin*, 24(3):195–200.
- Li, M., West, J. W., Lai, Y., Scheuer, T., and Catterall, W. A. (1992). Functional modulation of brain sodium channels by cAMP-dependent phosphorylation. *Neuron*, 8(6):1151–1159.
- Li, P., Shah, S., Huang, L., Carr, A. L., Gao, Y., Thisse, C., Thisse, B., and Li, L. (2007). Cloning and spatial and temporal expression of the zebrafish dopamine D1 receptor. *Developmental Dynamics*, 236(5):1339–1346.
- Liao, J. C. (2010). Organization and physiology of posterior lateral line afferent neurons in larval zebrafish. *Biology letters*, 6(3):402–5.
- Liao, J. C. and Fetcho, J. R. (2008). Shared versus specialized glycinergic spinal interneurons in axial motor circuits of larval zebrafish. *Journal of Neuroscience*, 28(48):12982–12992.
- Liley, A. (1956a). An investigation of spontaneous activity at the neuromuscular junction of the rat. *The Journal of Physiology*, 132:650–666.
- Liley, A. (1956b). The quantal components of the mammalian end-plate potential. *The Journal of Physiology*, 133(3):571–587.
- Lillesaar, C., Stigloher, C., Tannhäuser, B., Wullmann, M. F., and Bally-Cuif, L. (2009). Axonal projections originating from raphe serotonergic neurons in the developing and adult Zebrafish, *Danio Rerio*, using transgenics to visualize Raphe-specific pet1 expression. *Journal of Comparative Neurology*, 512(2):158–182.
- Lin, W., Burgess, R. W., Dominguez, B., Pfaff, S. L., Sanes, J. R., and Lee, K. F. (2001). Distinct roles of nerve and muscle in postsynaptic differentiation of the neuromuscular synapse. *Nature*, 410(6832):1057–1064.

REFERENCES

- Lipton, S. A., Choi, Y.-B., Pan, Z.-H., Lei, S. Z., Chen, H.-S. V., Sucher, N. J., Loscalzo, J., Singel, D. J., and Stamler, J. S. (1993). A redox-based mechanism for the neuroprotective and neurodestructive effects of nitric oxide and related nitroso-compounds. *Nature*, 364(6438):626–632.
- Lipton, S. A., Choi, Y.-B., Takahashi, H., Zhang, D., Li, W., Godzik, A., and Bankston, L. A. (2002). Cysteine regulation of protein function—as exemplified by NMDA-receptor modulation. *Trends in Neurosciences*, 25(9):474–80.
- Liu, D. W. and Westerfield, M. (1990). The formation of terminal fields in the absence of competitive interactions among primary motoneurons in the zebrafish. *Journal of Neuroscience*, 10(December):3947–3959.
- Liu, D. W. and Westerfield, M. (1992). Clustering of muscle acetylcholine receptors requires motoneurons in live embryos, but not in cell culture. *Journal of Neuroscience*, 12(5):1859–1866.
- Liu, D. W., Westerfield, M., and Vainio (1988). Function of identified motoneurons and co-ordination of primary and secondary motor systems during zebra fish swimming. *The Journal of Physiology*, 403(1):73–89.
- Liu, L., Shen, R. Y., Kapatos, G., and Chiodo, L. A. (1994). Dopamine neuron membrane physiology: characterization of the transient outward current (IA) and demonstration of a common signal transduction pathway for IA and IK. *Synapse*, 17(4):230–40.
- Lobb, C. J., Troyer, T. W., Wilson, C. J., and Paladini, C. A. (2011). Disinhibition bursting of dopaminergic neurons. *Frontiers in systems neuroscience*, 5(May):25.
- Lobb, C. J., Wilson, C. J., and Paladini, C. A. (2010). A dynamic role for GABA receptors on the firing pattern of midbrain dopaminergic neurons. *Journal of Neurophysiology*, 104(1):403–13.
- López, J. M. and González, A. (2002). Ontogeny of NADPH diaphorase/nitric oxide synthase reactivity in the brain of *Xenopus laevis*. *Journal of Comparative Neurology*, 445(1):59–77.
- Lorang, D., Amara, S. G., and Simerly, R. B. (1994). Cell-type-specific expression of catecholamine transporters in the rat brain. *Journal of Neuroscience*, 14(8):4903–4914.
- Lowery, L. A. and Vactor, D. V. (2009). The trip of the tip: understanding the growth cone machinery. *Nature Reviews Molecular Cell Biology*, 10(5):332–343.

REFERENCES

- Luna, V. M. and Brehm, P. (2006). An electrically coupled network of skeletal muscle in zebrafish distributes synaptic current. *The Journal of general physiology*, 128(1):89–102.
- Luskin, M. B. (1993). Restricted proliferation and migration of postnatally generated neurons derived from the forebrain subventricular zone. *Neuron*, 11(1):173–89.
- Lüthi, A. and McCormick, D. A. (1998). H-Current. *Neuron*, 21(1):9–12.
- Lynch, J. W. (2004). Molecular structure and function of the glycine receptor chloride channel. *Physiological reviews*, 84(4):1051–1095.
- Lyness, W. H., Friedle, N. M., and Moore, K. E. (1979). Destruction of dopaminergic nerve terminals in nucleus accumbens: Effect on d-amphetamine self-administration. *Pharmacology Biochemistry and Behavior*, 11(5):553–556.
- Ma, P. M. (1994a). Catecholaminergic systems in the zebrafish. I. Number, morphology, and histochemical characteristics of neurons in the locus coeruleus. *Journal of Comparative Neurology*, 344(2):242–255.
- Ma, P. M. (1994b). Catecholaminergic systems in the zebrafish. II. Projection pathways and pattern of termination of the locus coeruleus. *Journal of Comparative Neurology*, 344(2):256–269.
- Ma, P. M. (1997). Catecholaminergic systems in the zebrafish. III. Organization and projection pattern of medullary dopaminergic and noradrenergic neurons. *Journal of Comparative Neurology*, 381(4):411–427.
- Maccaferri, G. and McBain, C. J. (1996). The hyperpolarization-activated current (I_h) and its contribution to pacemaker activity in rat CA1 hippocampal stratum oriens-alveus interneurons. *The Journal of Physiology*, 497:119–130.
- MacDonald, R. B., Debiais-Thibaud, M., Talbot, J. C., and Ekker, M. (2010). The relationship between dlx and gad1 expression indicates highly conserved genetic pathways in the zebrafish forebrain. *Developmental Dynamics*, 239(8):2298–2306.
- Mahler, J., Filippi, A., and Driever, W. (2010). DeltaA/DeltaD regulate multiple and temporally distinct phases of notch signaling during dopaminergic neurogenesis in zebrafish. *Journal of Neuroscience*, 30(49):16621–16635.
- Maitra, K. K., Seth, P., Thewissen, M., Ross, H. G., and Ganguly, D. K. (1993). Dopaminergic influence on the excitability of antidromically activated Renshaw cells in the lumbar spinal cord of the rat. *Acta physiologica Scandinavica*, 148(2):101–107.

REFERENCES

- Mandal, S., Stanco, A., Buys, E. S., Enikolopov, G., and Rubenstein, J. L. R. (2013). Soluble guanylate cyclase generation of cGMP regulates migration of MGE neurons. *Journal of Neuroscience*, 33(43):16897–914.
- Manzoni, O., Prezeau, L., Marin, P., Desagher, S., Deshager, S., Bockaert, J., and Fagni, L. (1992). Nitric oxide-induced blockade of NMDA receptors. *Neuron*, 8(4):653–62.
- Marcott, P., Mamaligas, A., and Ford, C. (2014). Phasic Dopamine Release Drives Rapid Activation of Striatal D2-Receptors. *Neuron*, 84(1):164–176.
- Marcus, J. N., Aschkenasi, C. J., Lee, C. E., Chemelli, R. M., Saper, C. B., Yanagisawa, M., and Elmquist, J. K. (2001). Differential expression of orexin receptors 1 and 2 in the rat brain. *Journal of Comparative Neurology*, 435(1):6–25.
- Marder, E. and Bucher, D. (2001). Central pattern generators and the control of rhythmic movements. *Current Biology*, 11(23):986–996.
- Margolis, E. B., Lock, H., Hjelmstad, G. O., and Fields, H. L. (2006). The ventral tegmental area revisited: is there an electrophysiological marker for dopaminergic neurons? *The Journal of Physiology*, 577(Pt 3):907–924.
- Margolis, E. B., Mitchell, J. M., Ishikawa, J., Hjelmstad, G. O., and Fields, H. L. (2008). Midbrain dopamine neurons: projection target determines action potential duration and dopamine D(2) receptor inhibition. *Journal of Neuroscience*, 28(36):8908–8913.
- Marletta, M. a. (1993). Nitric oxide synthase structure and mechanism. *Journal of Biological Chemistry*, 268(17):12231–12234.
- Marletta, M. A., Yoon, P. S., Iyengar, R., Leaf, C. D., and Wishnok, J. S. (1988). Macrophage oxidation of L-arginine to nitrite and nitrate: nitric oxide is an intermediate. *Biochemistry*, 27(24):8706–8711.
- Marsh, N. and Marsh, A. (2000). A short history of nitroglycerine and nitric oxide in pharmacology and physiology. *Clinical and Experimental Pharmacology and Physiology*, 27(4):313–319.
- Martin, S. C., Heinrich, G., and Sandell, J. H. (1998). Sequence and expression of glutamic acid decarboxylase isoforms in the developing zebrafish. *Journal of Comparative Neurology*, 396(2):253–266.
- März, M., Schmidt, R., Rastegar, S., and Strähle, U. (2010). Expression of the transcription factor Olig2 in proliferating cells in the adult zebrafish telencephalon. *Developmental Dynamics*, 239(12):3336–49.

REFERENCES

- Matarredona, E. R., Murillo-Carretero, M., Moreno-López, B., and Estrada, C. (2004). Nitric oxide synthesis inhibition increases proliferation of neural precursors isolated from the postnatal mouse subventricular zone. *Brain Research*, 995(2):274–284.
- Mayer, M. L. and Westbrook, G. L. (1987). The physiology of excitatory amino acids in the vertebrate central nervous system. *Progress in neurobiology*, 28(3):197–276.
- Maynard, D. M. and Selverston, A. I. (1975). Organization of the stomatogastric ganglion of the spiny lobster IV. The Pyloric System. *Journal of Comparative Physiology A*, 100(2):161–182.
- McCormick, D. A. and Pape, H. C. (1990). Properties of a hyperpolarization-activated cation current and its role in rhythmic oscillation in thalamic relay neurones. *The Journal of Physiology*, 431(1):291–318.
- McCrea, A. E., Stehouwer, D. J., and Van Hartesveldt, C. (1997). Dopamine D1 and D2 antagonists block L-DOPA-induced air-stepping in decerebrate neonatal rats. *Developmental Brain Research*, 100(1):130–132.
- McDearmid, J. R., Liao, M., and Drapeau, P. (2006). Glycine receptors regulate interneuron differentiation during spinal network development. *Proceedings of the National Academy of Sciences of the United States of America*, 103(25):9679–84.
- McDearmid, J. R., Scrymgeour-Wedderburn, J. F., and Sillar, K. T. (1997). Aminergic modulation of glycine release in a spinal network controlling swimming in *Xenopus laevis*. *Journal of Physiology*.
- McEwen, M. L., Van Hartesveldt, C., and Stehouwer, D. J. (1997). L-DOPA and quipazine elicit air-stepping in neonatal rats with spinal cord transections. *Behavioral Neuroscience*, 111(4):825–833.
- McLean, D. L., Fan, J., Higashijima, S.-i., Hale, M. E., and Fetcho, J. R. (2007). A topographic map of recruitment in spinal cord. *Nature*, 446(7131):71–5.
- McLean, D. L. and Fetcho, J. R. (2004a). Ontogeny and innervation patterns of dopaminergic, noradrenergic, and serotonergic neurons in larval zebrafish. *Journal of Comparative Neurology*, 480(1):38–56.
- McLean, D. L. and Fetcho, J. R. (2004b). Relationship of tyrosine hydroxylase and serotonin immunoreactivity to sensorimotor circuitry in larval zebrafish. *Journal of Comparative Neurology*, 480(1):57–71.
- McLean, D. L., Masino, M. a., Koh, I. Y. Y., Lindquist, W. B., and Fetcho, J. R. (2008). Continuous shifts in the active set of spinal interneurons during changes in locomotor speed. *Nature Neuroscience*, 11(12):1419–1429.

REFERENCES

- McLean, D. L., McDearmid, J. R., and Sillar, K. T. (2001). Induction of a non-rhythmic motor pattern by nitric oxide in hatchling *Rana temporaria* embryos. *Journal of Experimental Biology*, 204:1307–1317.
- McLean, D. L. and Sillar, K. T. (2000). The distribution of NADPH-diaphorase-labelled interneurons and the role of nitric oxide in the swimming system of *Xenopus laevis* larvae. *Journal of Experimental Biology*, 203(Pt 4):705–13.
- McLean, D. L. and Sillar, K. T. (2001). Spatiotemporal pattern of nicotinamide adenine dinucleotide phosphate-diaphorase reactivity in the developing central nervous system of premetamorphic *Xenopus laevis* tadpoles. *Journal of Comparative Neurology*, 437(3):350–362.
- McLean, D. L. and Sillar, K. T. (2002). Nitric oxide selectively tunes inhibitory synapses to modulate vertebrate locomotion. *Journal of Neuroscience*, 22(10):4175–4184.
- McLean, D. L. and Sillar, K. T. (2004). Metamodulation of a spinal locomotor network by nitric oxide. *Journal of Neuroscience*, 24(43):9561–9571.
- McPherson, D. R. and Kemnitz, C. P. (1994). Modulation of lamprey fictive swimming and motoneuron physiology by dopamine, and its immunocytochemical localization in the spinal cord. *Neuroscience Letters*, 166(1):23–26.
- Mehler-Wex, C., Riederer, P., and Gerlach, M. (2006). Dopaminergic dysbalance in distinct basal ganglia neurocircuits: Implications for the pathophysiology of parkinson's disease, schizophrenia and attention deficit hyperactivity disorder. *Neurotoxicity Research*, 10(3-4):167–179.
- Meinkoth, J. L., Alberts, a. S., Went, W., Fantozzi, D., Taylor, S. S., Hagiwara, M., Montminy, M., and Feramisco, J. R. (1993). Signal transduction through the cAMP-dependent protein kinase. *Molecular and cellular biochemistry*, 127-128(1):179–86.
- Meldrum, B. S. (2000). Glutamate as a neurotransmitter in the brain: review of physiology and pathology. *The Journal of nutrition*, 130(4S Suppl):1007S–15S.
- Mendelson, B. (1986). Development of reticulospinal neurons of the zebrafish. II. Early axonal outgrowth and cell body position. *Journal of Comparative Neurology*, 251(2):172–184.
- Menelaou, E. and McLean, D. L. (2012). A gradient in endogenous rhythmicity and oscillatory drive matches recruitment order in an axial motor pool. *Journal of Neuroscience*, 32(32):10925–39.

REFERENCES

- Menelaou, E., VanDunk, C., and McLean, D. L. (2014). Differences in the morphology of spinal V2a neurons reflect their recruitment order during swimming in larval zebrafish. *Journal of Comparative Neurology*, 522(6):1232–48.
- Menniti, F. S., Faraci, W. S., and Schmidt, C. J. (2006). Phosphodiesterases in the CNS: targets for drug development. *Nature Reviews Drug Discovery*, 5(8):660–670.
- Mereu, G., Lilliu, V., Vicini, S., Casula, A., Francesconi, W., and Gessa, G. (1995). Ontogeny of firing patterns of dopamine neurons in rat midbrain slices. Role of NMDA receptor activation. *European Neuropsychopharmacology*, 5(3):237–238.
- Mergia, E., Russwurm, M., Zoidl, G., and Koesling, D. (2003). Major occurrence of the new alpha2beta1 isoform of NO-sensitive guanylyl cyclase in brain. *Cellular signalling*, 15(2):189–195.
- Meriney, S. D., Gray, D. B., and Pilar, G. R. (1994). Somatostatin-induced inhibition of neuronal Ca²⁺ current modulated by cGMP-dependent protein kinase. *Nature*, 369(6478):336–339.
- Metcalf, W. K., Kimmel, C. B., and Schabtach, E. (1985). Anatomy of the posterior lateral line system in young larvae of the zebrafish. *Journal of Comparative Neurology*, 233(3):377–389.
- Metcalf, W. K., Mendelson, B., and Kimmel, C. B. (1986). Segmental homologies among reticulospinal neurons in the hindbrain of the zebrafish larva. *Journal of Comparative Neurology*, 251(2):147–159.
- Metcalf, W. K., Myers, P. Z., Trevarrow, B., Bass, M. B., and Kimmel, C. B. (1990). Primary neurons that express the L2/HNK-1 carbohydrate during early development in the zebrafish. *Development (Cambridge, England)*, 110(2):491–504.
- Miles, G. B. and Sillar, K. T. (2011). Neuromodulation of Vertebrate Locomotor Control Networks. *Physiology*, 26(6):393–411.
- Milescu, L. S., Yamanishi, T., Ptak, K., and Smith, J. C. (2010). Kinetic properties and functional dynamics of sodium channels during repetitive spiking in a slow pacemaker neuron. *Journal of Neuroscience*, 30(36):12113–12127.
- Miller, E. K., Freedman, D. J., and Wallis, J. D. (2002). The prefrontal cortex: categories, concepts and cognition. *Philosophical Transactions of the Royal Society B: Biological Sciences*, 357(1424):1123–1136.
- Miller, J. P. and Selverston, A. I. (1982a). Mechanisms underlying pattern generation in lobster stomatogastric ganglion as determined by selective inactivation of identified

REFERENCES

- neurons. II. Oscillatory properties of pyloric neurons. *Journal of Neurophysiology*, 48(6).
- Miller, J. P. and Selverston, A. I. (1982b). Mechanisms underlying pattern generation in lobster stomatogastric ganglion as determined by selective inactivation of identified neurons. IV. Network properties of pyloric system. *Journal of Neurophysiology*, 48(6):1416–1432.
- Milner, K. L. and Mogenson, G. J. (1988). Electrical and chemical activation of the mesencephalic and subthalamic locomotor regions in freely moving rats. *Brain Research*, 452(1-2):273–285.
- Mishina, M., Takai, T., Imoto, K., Noda, M., Takahashi, T., Numa, S., Methfessel, C., and Sakmann, B. (1986). Molecular distinction between fetal and adult forms of muscle acetylcholine receptor. *Nature*, 321(6068):406–411.
- Missale, C., Nash, S. R., Robinson, S. W., Jaber, M., and Caron, M. G. (1998). Dopamine receptors: from structure to function. *Physiological reviews*, 78(1):189–225.
- Missias, A. C., Chu, G. C., Klocke, B. J., Sanes, J. R., and Merlie, J. P. (1996). Maturation of the acetylcholine receptor in skeletal muscle: regulation of the AChR gamma-to-epsilon switch. *Developmental biology*, 179(1):223–238.
- Miyasaka, N., Arganda-Carreras, I., Wakisaka, N., Masuda, M., Sümbül, U., Seung, H. S., and Yoshihara, Y. (2014). Olfactory projectome in the zebrafish forebrain revealed by genetic single-neuron labelling. *Nature Communications*, 5:3639.
- Moncada, S. and Higgs, E. A. (2006). The discovery of nitric oxide and its role in vascular biology. *British journal of pharmacology*, 147 Suppl:S193–S201.
- Mongeon, R., Walogorsky, M., Urban, J., Mandel, G., Ono, F., and Brehm, P. (2011). An acetylcholine receptor lacking both γ and ϵ subunits mediates transmission in zebrafish slow muscle synapses. *The Journal of general physiology*, 138(3):353–66.
- Moreno-López, B., Noval, J. A., González-Bonet, L. G., and Estrada, C. (2000). Morphological bases for a role of nitric oxide in adult neurogenesis. *Brain Research*, 869(1-2):244–250.
- Moreno-López, B., Romero-Grimaldi, C., Noval, J. A., Murillo-Carretero, M., Matarredona, E. R., and Estrada, C. (2004). Nitric oxide is a physiological inhibitor of neurogenesis in the adult mouse subventricular zone and olfactory bulb. *Journal of Neuroscience*, 24(1):85–95.

REFERENCES

- Mueller, B. K., Yamashita, T., Schaffar, G., and Mueller, R. (2006). The role of repulsive guidance molecules in the embryonic and adult vertebrate central nervous system. *Philosophical Transactions of the Royal Society B: Biological Sciences*, 361(1473):1513–1529.
- Mueller, T., Wullimann, M. F., and Guo, S. (2008). Early teleostean basal ganglia development visualized by zebrafish *Dlx2a*, *Lhx6*, *Lhx7*, *Tbr2* (*eomesa*), and *GAD67* gene expression. *Journal of Comparative Neurology*, 507(2):1245–1257.
- Murphy, B. J., Rossie, S., De Jongh, K. S., and Catterall, W. a. (1993). Identification of the sites of selective phosphorylation and dephosphorylation of the rat brain Na⁺ channel α subunit by cAMP-dependent protein kinase and phosphoprotein phosphatases. *Journal of Biological Chemistry*, 268(36):27355–27362.
- Murphy, K. P. and Bliss, T. V. (1999). Photolytically released nitric oxide produces a delayed but persistent suppression of LTP in area CA1 of the rat hippocampal slice. *The Journal of Physiology*, 515:453–462.
- Murphy, K. P., Williams, J. H., Bettache, N., and Bliss, T. V. (1994). Photolytic release of nitric oxide modulates NMDA receptor-mediated transmission but does not induce long-term potentiation at hippocampal synapses. *Neuropharmacology*, 33(11):1375–1385.
- Murthy, K. S. (2001). cAMP inhibits IP(3)-dependent Ca(2+) release by preferential activation of cGMP-primed PKG. *American journal of physiology. Gastrointestinal and liver physiology*, 281(5):G1238–G1245.
- Myers, P.Z. (1985). Spinal motoneurons of the larval zebrafish. *Journal of Comparative Neurology*, 236(4):555–561.
- Myers, P. Z., Eisen, J. S., and Westerfield, M. (1986). Development and axonal outgrowth of identified motoneurons in the zebrafish. *Journal of Neuroscience*, 6(8):2278–89.
- Nakanishi, H., Kita, H., and Kitai, S. T. (1987). Intracellular study of rat substantia nigra pars reticulata neurons in an in vitro slice preparation: electrical membrane properties and response characteristics to subthalamic stimulation. *Brain Research*, 437(1):45–55.
- Nambu, A. (2015). Functional Circuitry of the Basal Ganglia. In *Deep Brain Stimulation for Neurological Disorders*, pages 1–11. Springer International Publishing, Cham.
- Naranjo, D. and Brehm, P. (1993). Modal shifts in acetylcholine receptor channel gating confer subunit-dependent desensitization. *Science*, 260(5115):1811–4.

REFERENCES

- Nathan, C. (1992). Nitric oxide as a secretory product of mammalian cells. *The FASEB journal : official publication of the Federation of American Societies for Experimental Biology*, 6(12):3051–3064.
- Nathan, C. and Xie, Q.-w. (1994). Nitric Oxide Synthases: Roles, Tolls, and Controls. *Cell*, 78(Table 1):915–918.
- Nedergaard, S., Flatman, J. A., and Engberg, I. (1993). Nifedipine- and omega-conotoxin-sensitive Ca²⁺ conductances in guinea-pig substantia nigra pars compacta neurones. *The Journal of Physiology*, 466:727–747.
- Nelson, R. J., Demas, G. E., Huang, P. L., Fishman, M. C., Dawson, V. L., Dawson, T. M., and Snyder, S. H. (1995). Behavioural abnormalities in male mice lacking neuronal nitric oxide synthase. *Nature*, 378(6555):383–6.
- Neuhoff, H., Neu, A., Liss, B., and Roeper, J. (2002). I(h) channels contribute to the different functional properties of identified dopaminergic subpopulations in the midbrain. *Journal of Neuroscience*, 22(4):1290–302.
- Nguyen, P. V., Aniksztejn, L., Catarsi, S., and Drapeau, P. (1999). Maturation of neuromuscular transmission during early development in zebrafish. *Journal of Neurophysiology*, 81(6):2852–61.
- Nishimura, T., Akasu, T., and Krier, J. (1992). Guanosine 3',5'-cyclic monophosphate regulates calcium channels in neurones of rabbit vesical pelvic ganglia. *The Journal of Physiology*, 457:559–574.
- Oberlander, C., Euvrard, C., Dumont, C., and Boissier, J. R. (1979). Circling behaviour induced by dopamine releasers and/or uptake inhibitors during degeneration of the nigrostriatal pathway. *European Journal of Pharmacology*, 60(2-3):163–170.
- O'Dell, T. J., Huang, P. L., Dawson, T. M., Dinerman, J. L., Snyder, S. H., Kandel, E. R., and Fishman, M. C. (1994). Endothelial NOS and the blockade of LTP by NOS inhibitors in mice lacking neuronal NOS. *Science*, 265(5171):542–6.
- Ohlstein, E. H., Barry, B. K., Gruetter, D. Y., and Ignarro, L. J. (1979). Methemoglobin blockade of coronary arterial soluble guanylate cyclase activation by nitroso compounds and its reversal with dithiothreitol. *FEBS Letters*, 102(2):316–320.
- Ohta, Y. and Grillner, S. (1989). Monosynaptic excitatory amino acid transmission from the posterior rhombencephalic reticular nucleus to spinal neurons involved in the control of locomotion in lamprey. *Journal of Neurophysiology*, 62(5):1079–1089.

REFERENCES

- Ohyama, K., Ellis, P., Kimura, S., and Placzek, M. (2005). Directed differentiation of neural cells to hypothalamic dopaminergic neurons. *Development (Cambridge, England)*, 132(23):5185–5197.
- Ondo, W. G., He, Y., Rajasekaran, S., and Le, W. D. (2000). Clinical correlates of 6-hydroxydopamine injections into A11 dopaminergic neurons in rats: a possible model for restless legs syndrome. *Movement disorders : official journal of the Movement Disorder Society*, 15(1):154–158.
- Oster, A., Faure, P., and Gutkin, B. S. (2015). Mechanisms for multiple activity modes of VTA dopamine neurons. *Frontiers in Computational Neuroscience*, 9(July):1–17.
- Overton, P. G. and Clark, D. (1997). Burst firing in midbrain dopaminergic neurons. *Brain Research Reviews*, 25(3):312–34.
- Pacher, P., Beckman, J. S., and Liaudet, L. (2007). Nitric Oxide and Peroxynitrite in Health and Disease. *Physiological Reviews*, 87(1):315–424.
- Packer, M. A., Stasiv, Y., Benraiss, A., Chmielnicki, E., Grinberg, A., Westphal, H., Goldman, S. A., and Enikolopov, G. (2003). Nitric oxide negatively regulates mammalian adult neurogenesis. *Proceedings of the National Academy of Sciences of the United States of America*, 100(16):9566–9571.
- Paladini, C. and Roeper, J. (2014). Generating bursts (and pauses) in the dopamine midbrain neurons. *Neuroscience*, 282:109–121.
- Paladini, C. A. and Tepper, J. M. (1999). GABA(A) and GABA(B) antagonists differentially affect the firing pattern of substantia nigra dopaminergic neurons in vivo. *Synapse*, 32(3):165–76.
- Palmer, R. M., Ferrige, A. G., and Moncada, S. (1987). Nitric oxide release accounts for the biological activity of endothelium-derived relaxing factor. *Nature*, 327(6122):524–6.
- Palmer, R. M., Rees, D. D., Ashton, D. S., and Moncada, S. (1988a). L-arginine is the physiological precursor for the formation of nitric oxide in endothelium-dependent relaxation. *Biochemical and biophysical research communications*, 153(3):1251–6.
- Palmer, R. M. J., Ashton, D. S., and Moncada, S. (1988b). Vascular endothelial cells synthesize nitric oxide from L-arginine. *Nature*, 333(6174):664–666.
- Panzer, J. A., Gibbs, S. M., Dosch, R., Wagner, D., Mullins, M. C., Granato, M., and Balice-Gordon, R. J. (2005). Neuromuscular synaptogenesis in wild-type and mutant zebrafish. *Developmental Biology*, 285:340–357.

REFERENCES

- Panzer, J. a., Song, Y., and Balice-Gordon, R. J. (2006). In vivo imaging of preferential motor axon outgrowth to and synaptogenesis at prepatterned acetylcholine receptor clusters in embryonic zebrafish skeletal muscle. *Journal of Neuroscience*, 26(3):934–47.
- Pappas, S. S., Behrouz, B., Janis, K. L., Goudreau, J. L., and Lookingland, K. J. (2008). Lack of D2 receptor mediated regulation of dopamine synthesis in A11 diencephalospinal neurons in male and female mice. *Brain Research*, 1214:1–10.
- Park, H.-C., Shin, J., and Appel, B. (2004). Spatial and temporal regulation of ventral spinal cord precursor specification by Hedgehog signaling. *Development (Cambridge, England)*, 131(23):5959–5969.
- Park, J.-Y., Mott, M., Williams, T., Ikeda, H., Wen, H., Linhoff, M., and Ono, F. (2014). A Single Mutation in the Acetylcholine Receptor Subunit Causes Distinct Effects in Two Types of Neuromuscular Synapses. *Journal of Neuroscience*, 34(31):10211–10218.
- Parker, D. and Grillner, S. (1999). Activity-dependent metaplasticity of inhibitory and excitatory synaptic transmission in the lamprey spinal cord locomotor network. *Journal of Neuroscience*, 19(5):1647–1656.
- Parker, D. and Grillner, S. (2000). The activity-dependent plasticity of segmental and intersegmental synaptic connections in the lamprey spinal cord. *European Journal of Neuroscience*, 12(6):2135–2146.
- Pautz, A., Art, J., Hahn, S., Nowag, S., Voss, C., and Kleinert, H. (2010). Regulation of the expression of inducible nitric oxide synthase. *Nitric Oxide*, 23(2):75–93.
- Peck, J. H., Gaier, E., Stevens, E., Repicky, S., and Harris-Warrick, R. M. (2006). Amine modulation of Ih in a small neural network. *Journal of Neurophysiology*, 96(6):2931–2940.
- Pendino, K. J., Laskin, J. D., Shuler, R. L., Punjabi, C. J., and Laskin, D. L. (1993). Enhanced production of nitric oxide by rat alveolar macrophages after inhalation of a pulmonary irritant is associated with increased expression of nitric oxide synthase. *Journal of immunology (Baltimore, Md. : 1950)*, 151(12):7196–7205.
- Perkel, D. H. and Mulloney, B. (1974). Motor pattern production in reciprocally inhibitory neurons exhibiting postinhibitory rebound. *Science*, 185(4146):181–3.
- Perrins, R., Walford, A., and Roberts, A. (2002). Sensory activation and role of inhibitory reticulospinal neurons that stop swimming in hatchling frog tadpoles. *Journal of Neuroscience*, 22(10):4229–4240.

REFERENCES

- Peunova, N., Scheinker, V., Cline, H., and Enikolopov, G. (2001). Nitric oxide is an essential negative regulator of cell proliferation in *Xenopus* brain. *Journal of Neuroscience*, 21(22):8809–8818.
- Peyron, C., Tighe, D. K., van den Pol, A. N., de Lecea, L., Heller, H. C., Sutcliffe, J. G., and Kilduff, T. S. (1998). Neurons containing hypocretin (orexin) project to multiple neuronal systems. *Journal of Neuroscience*, 18(23):9996–10015.
- Piazza, M., Guillemette, J. G., and Dieckmann, T. (2015). Dynamics of Nitric Oxide Synthase–Calmodulin Interactions at Physiological Calcium Concentrations. *Biochemistry*, page 150316104511002.
- Pickel, V. M., Chan, J., and Nirenberg, M. J. (2002). Region-specific targeting of dopamine D2-receptors and somatodendritic vesicular monoamine transporter 2 (VMAT2) within ventral tegmental area subdivisions. *Synapse*, 45(2):113–24.
- Pietri, T., Manalo, E., Ryan, J., Saint-Amant, L., and Washbourne, P. (2009). Glutamate drives the touch response through a rostral loop in the spinal cord of zebrafish embryos. *Developmental Neurobiology*, 69(12):780–95.
- Pike, S. H., Melancon, E. F., and Eisen, J. S. (1992). Pathfinding by zebrafish motoneurons in the absence of normal pioneer axons. *Development (Cambridge, England)*, 114(4):825–31.
- Pinault, D. (1996). A novel single-cell staining procedure performed in vivo under electrophysiological control: Morpho-functional features of juxtacellularly labeled thalamic cells and other central neurons with biocytin or Neurobiotin. *Journal of Neuroscience Methods*, 65(2):113–136.
- Pineda, R. H. (2005). Developmental, Molecular, and Genetic Dissection of INa In Vivo in Embryonic Zebrafish Sensory Neurons. *Journal of Neurophysiology*, 93(6):3582–3593.
- Pinnock, R. D. (1984). Hyperpolarizing action of baclofen on neurons in the rat substantia nigra slice. *Brain Research*, 322(2):337–340.
- Plazas, P. V., Nicol, X., and Spitzer, N. C. (2013). Activity-dependent competition regulates motor neuron axon pathfinding via PlexinA3. *Proceedings of the National Academy of Sciences of the United States of America*, 110(4):1524–9.
- Poon, K. (2003). Expression pattern of neuronal nitric oxide synthase in embryonic zebrafish. *Gene Expression Patterns*, 3(4):463–466.

REFERENCES

- Price, C. J., Kim, P., and Raymond, L. a. (1999). D1 dopamine receptor-induced cyclic AMP-dependent protein kinase phosphorylation and potentiation of striatal glutamate receptors. *Journal of Neurochemistry*, 73(6):2441–2446.
- Prisco, S., Pagannone, S., and Esposito, E. (1994). Serotonin-dopamine interaction in the rat ventral tegmental area: an electrophysiological study in vivo. *Journal of Pharmacology and Experimental Therapeutics*, 271(1):83–90.
- Prober, D. A., Rihel, J., Onah, A. A., Sung, R.-J., and Schier, A. F. (2006). Hypocretin/orexin overexpression induces an insomnia-like phenotype in zebrafish. *Journal of Neuroscience*, 26(51):13400–13410.
- Qiu, X., Kumbalasiri, T., Carlson, S. M., Wong, K. Y., Krishna, V., Provencio, I., and Berson, D. M. (2005). Induction of photosensitivity by heterologous expression of melanopsin. *Nature*, 433(7027):745–749.
- Qu, S., Le, W., Zhang, X., Xie, W., Zhang, A., and Ondo, W. G. (2007). Locomotion Is Increased in A11-Lesioned Mice With Iron Deprivation. *Journal of Neuropathology and Experimental Neurology*, 66(5):383–388.
- Qu, S., Ondo, W. G., Zhang, X., Xie, W. J., Pan, T. H., and Le, W. D. (2006). Projections of diencephalic dopamine neurons into the spinal cord in mice. *Experimental Brain Research*, 168(1-2):152–6.
- Raamsdonk, W., Pool, C. W., and Kronnie, G. (1978). Differentiation of muscle fiber types in the teleost *Brachydanio rerio*. *Anatomy and Embryology*, 153(2):137–155.
- Raamsdonk, W., Veer, L., Veeken, K., Heyting, C., and Pool, C. W. (1982). Differentiation of muscle fiber types in the teleost *Brachydanio rerio*, the zebrafish. *Anatomy and Embryology*, 164(1):51–62.
- Rae, J., Cooper, K., Gates, P., and Watsky, M. (1991). Low access resistance perforated patch recordings using amphotericin B. *Journal of Neuroscience Methods*, 37(1):15–26.
- Raible, D. W. and Kruse, G. J. (2000). Organization of the lateral line system in embryonic zebrafish. *Journal of Comparative Neurology*, 421(2):189–198.
- Ramanathan, S., Combes, D., Molinari, M., Simmers, J., and Sillar, K. T. (2006). Developmental and regional expression of NADPH-diaphorase/nitric oxide synthase in spinal cord neurons correlates with the emergence of limb motor networks in metamorphosing *Xenopus laevis*. *European Journal of Neuroscience*, 24(7):1907–1922.

REFERENCES

- Rao, Y. M., Chaudhury, A., and Goyal, R. K. (2008). Active and inactive pools of nNOS in the nerve terminals in mouse gut: implications for nitrenergic neurotransmission. *American journal of physiology. Gastrointestinal and liver physiology*, 294(3):G627–G634.
- Rauscent, A., Einum, J., Le Ray, D., Simmers, J., and Combes, D. (2009). Opposing aminergic modulation of distinct spinal locomotor circuits and their functional coupling during amphibian metamorphosis. *Journal of Neuroscience*, 29(4):1163–1174.
- Reimer, M., Norris, A., Ohnmacht, J., Patani, R., Zhong, Z., Dias, T., Kuscha, V., Scott, A., Chen, Y.-C., Rozov, S., Frazer, S., Wyatt, C., Higashijima, S.-i., Patton, E., Panula, P., Chandran, S., Becker, T., and Becker, C. (2013). Dopamine from the Brain Promotes Spinal Motor Neuron Generation during Development and Adult Regeneration. *Developmental Cell*, pages 1–14.
- Reyes, R., Haendel, M., Grant, D., Melancon, E., and Eisen, J. S. (2004). Slow Degeneration of Zebrafish Rohon-Beard Neurons during Programmed Cell Death. *Developmental Dynamics*, 229(1):30–41.
- Ribera, J., Marsal, J., Casanovas, A., Hukkanen, M., Tarabal, O., and Esquerda, J. E. (1998). Nitric oxide synthase in rat neuromuscular junctions and in nerve terminals of Torpedo electric organ: Its role as regulator of acetylcholine release. *Journal of Neuroscience Research*, 51(1):90–102.
- Richards, C. D., Shiroyama, T., and Kitai, S. T. (1997). Electrophysiological and immunocytochemical characterization of GABA and dopamine neurons in the substantia nigra of the rat. *Neuroscience*, 80(2):545–557.
- Richardson, B. (1864). Report of the physiological action of nitrite of amyl. *British Association for the Advancement of Science*, 34:120.
- Rihel, J., Prober, D. A., Arvanites, A., Lam, K., Zimmerman, S., Jang, S., Haggarty, S. J., Kokel, D., Rubin, L. L., Peterson, R. T., and Schier, A. F. (2010). Zebrafish behavioral profiling links drugs to biological targets and rest/wake regulation. *Science*, 327(5963):348–51.
- Rink, E. and Wullimann, M. F. (2001). The teleostean (zebrafish) dopaminergic system ascending to the subpallium (striatum) is located in the basal diencephalon (posterior tuberculum). *Brain Research*, 889(1-2):316–30.
- Rink, E. and Wullimann, M. F. (2002). Development of the catecholaminergic system in the early zebrafish brain: An immunohistochemical study. *Developmental Brain Research*, 137(1):89–100.

REFERENCES

- Robbins, T. W. and Koob, G. F. (1980). Selective disruption of displacement behaviour by lesions of the mesolimbic dopamine system. *Nature*, 285(5764):409–412.
- Roberts, a. and Blight, a. R. (1975). Anatomy, Physiology and Behavioural Role of Sensory Nerve Endings in the Cement Gland of Embryonic *Xenopus*. *Proceedings of the Royal Society B: Biological Sciences*, 192(1106):111–127.
- Roberts, a. and Sillar, K. T. (1990). Characterization and function of spinal excitatory interneurons with commissural projections in *Xenopus laevis* embryos. *European Journal of Neuroscience*, 2(12):1051–1062.
- Roberts, D. C. and Koob, G. F. (1982). Disruption of cocaine self-administration following 6-hydroxydopamine lesions of the ventral tegmental area in rats. *Pharmacology Biochemistry and Behavior*, 17(5):901–904.
- Rodriguez-Oroz, M. C., Jahanshahi, M., Krack, P., Litvan, I., Macias, R., Bezard, E., and Obeso, J. a. (2009). Initial clinical manifestations of Parkinson's disease: features and pathophysiological mechanisms. *The Lancet Neurology*, 8(12):1128–1139.
- Romero-Grimaldi, C., Moreno-López, B., and Estrada, C. (2008). Age-dependent effect of nitric oxide on subventricular zone and olfactory bulb neural precursor proliferation. *Journal of Comparative Neurology*, 506(2):339–46.
- Russell, I. J. (1971). The role of the lateral-line efferent system in *Xenopus laevis*. *Journal of Experimental Biology*, 54(3):621–41.
- Russell, I. J. and Roberts, B. L. (1974). Active reduction of lateral-line sensitivity in swimming dogfish. *Journal of Comparative Physiology A*, 94(1):7–15.
- Russwurm, M. and Koesling, D. (2002). Isoforms of NO-sensitive guanylyl cyclase. *Molecular and cellular biochemistry*, 230(1-2):159–64.
- Ruth, P., Landgraf, W., Keilbach, a., May, B., Egleme, C., and Hofmann, F. (1991). The activation of expressed cGMP-dependent protein kinase isozymes I alpha and I beta is determined by the different amino-termini. *European journal of biochemistry / FEBS*, 202(3):1339–44.
- Ryczko, D., Grätsch, S., Auclair, F., Dubé, C., Bergeron, S., Alpert, M. H., Cone, J. J., Roitman, M. F., Alford, S., and Dubuc, R. (2013). Forebrain dopamine neurons project down to a brainstem region controlling locomotion. *Proceedings of the National Academy of Sciences of the United States of America*, 110(34):E3235–42.
- Ryu, S., Mahler, J., Acampora, D., Holzschuh, J., Erhardt, S., Omodei, D., Simeone, A., and Driever, W. (2007). Orthopedia Homeodomain Protein Is Essential for

REFERENCES

- Diencephalic Dopaminergic Neuron Development. *Current Biology*, 17(10):873–880.
- Saint-Amant, L. (2006). Development of motor networks in zebrafish embryos. *Zebrafish*, 3(2):173–90.
- Saint-Amant, L. and Drapeau, P. (1998). Time course of the development of motor behaviors in the zebrafish embryo. *Journal of Neurobiology*, 37:622–632.
- Saint-Amant, L. and Drapeau, P. (2000). Motoneuron activity patterns related to the earliest behavior of the zebrafish embryo. *Journal of Neuroscience*, 20(11):3964–3972.
- Saint-Amant, L. and Drapeau, P. (2001). Synchronization of an embryonic network of identified spinal interneurons solely by electrical coupling. *Neuron*, 31(6):1035–46.
- Saito, S., Kidd, G. J., Trapp, B. D., Dawson, T. M., Brecht, D. S., Wilson, D. A., Traystman, R. J., Snyder, S. H., and Hanley, D. F. (1994). Rat spinal cord neurons contain nitric oxide synthase. *Neuroscience*, 59(2):447–456.
- Sakuma, I., Stuehr, D. J., Gross, S. S., Nathan, C., and Levi, R. (1988). Identification of arginine as a precursor of endothelium-derived relaxing factor. *Proceedings of the National Academy of Sciences of the United States of America*, 85(22):8664–8667.
- Sakurai, T., Amemiya, A., Ishii, M., Matsuzaki, I., Chemelli, R. M., Tanaka, H., Williams, S. C., Richardson, J. A., Kozlowski, G. P., Wilson, S., Arch, J. R. S., Buckingham, R. E., Haynes, A. C., Carr, S. A., Annan, R. S., McNulty, D. E., Liu, W. S., Terrett, J. A., Elshourbagy, N. A., Bergsma, D. J., and Yanagisawa, M. (1998). Orexins and orexin receptors: A family of hypothalamic neuropeptides and G protein-coupled receptors that regulate feeding behavior. *Cell*, 92(4):573–585.
- Salerno, J. C., Harris, D. E., Irizarry, K., Patelf, B., Morales, A. J., Smith, S. M. E., Martasek, P., Roman, L. J., Masters, B. S. S., Jones, C. L., Weissman, B. A., Lane, P., Liu, Q., and Gross, S. S. (1997). An autoinhibitory control element defines calcium-regulated isoforms of nitric oxide synthase. *Journal of Biological Chemistry*, 272(47):29769–29777.
- Sallinen, V., Torkko, V., Sundvik, M., Reenilä, I., Khrustalyov, D., Kaslin, J., and Panula, P. (2009). MPTP and MPP+ target specific aminergic cell populations in larval zebrafish. *Journal of Neurochemistry*, 108(3):719–731.
- Samama, B., Chateau, D., and Boehm, N. (1995). Expression of NADPH-diaphorase in the rat forebrain during development. *Neuroscience letters*, 184(3):204–207.

REFERENCES

- Sanes, J. R. and Lichtman, J. W. (1999). Development of the vertebrate neuromuscular junction. *Annual review of neuroscience*, 22:389–442.
- Sardella, T. C. P., Polgár, E., Watanabe, M., and Todd, A. J. (2011). A quantitative study of neuronal nitric oxide synthase expression in laminae I-III of the rat spinal dorsal horn. *Neuroscience*, 192:708–720.
- Sato, T., Hamaoka, T., Aizawa, H., Hosoya, T., and Okamoto, H. (2007). Genetic single-cell mosaic analysis implicates ephrinB2 reverse signaling in projections from the posterior tectum to the hindbrain in zebrafish. *Journal of Neuroscience*, 27(20):5271–5279.
- Satou, C., Kimura, Y., and Higashijima, S.-i. (2012). Generation of multiple classes of V0 neurons in zebrafish spinal cord: progenitor heterogeneity and temporal control of neuronal diversity. *Journal of Neuroscience*, 32(5):1771–83.
- Satou, C., Kimura, Y., Kohashi, T., Horikawa, K., Takeda, H., Oda, Y., and Higashijima, S.-i. (2009). Functional role of a specialized class of spinal commissural inhibitory neurons during fast escapes in zebrafish. *Journal of Neuroscience*, 29(21):6780–6793.
- Satterlie, R. A. (1985). Reciprocal inhibition and postinhibitory rebound produce reverberation in a locomotor pattern generator. *Science*, 229(4711):402–4.
- Schiemann, J., Schlaudraff, F., Klose, V., Bingmer, M., Seino, S., Magill, P. J., Zaghoul, K. A., Schneider, G., Liss, B., and Roeper, J. (2012). K-ATP channels in dopamine substantia nigra neurons control bursting and novelty-induced exploration. SUPPLEMENTARY. *Nature Neuroscience*, 15(9):1272–80.
- Schlossmann, J. and Hofmann, F. (2005). cGMP-dependent protein kinases in drug discovery. *Drug discovery today*, 10(9):627–34.
- Schmidt, H. and Rathjen, F. G. (2010). Signalling mechanisms regulating axonal branching in vivo. *BioEssays*, 32(11):977–85.
- Schmidt, H., Werner, M., Heppenstall, P. A., Henning, M., Moré, M. I., Kühbandner, S., Lewin, G. R., Hofmann, F., Feil, R., and Rathjen, F. G. (2002). cGMP-mediated signaling via cGKI α is required for the guidance and connectivity of sensory axons. *Journal of Cell Biology*, 159(3):489–498.
- Schmidtko, A., Tegeder, I., and Geisslinger, G. (2009). No NO, no pain? The role of nitric oxide and cGMP in spinal pain processing. *Trends in Neurosciences*, 32(6):339–46.

REFERENCES

- Schotland, J., Shupliakov, O., Wikström, M., Brodin, L., Srinivasan, M., You, Z.-b., Herrera-Marschitz, M., Zhang, W., Hökfelt, T., and Grillner, S. (1995). Control of lamprey locomotor neurons by colocalized monoamine transmitters. *Nature*, 374(6519):266–268.
- Schultz, W. (1998). Predictive reward signal of dopamine neurons. *Journal of Neurophysiology*, 80:1–27.
- Schultz, W., Dayan, P., and Montague, P. R. (1997). A neural substrate of prediction and reward. *Science*, 275(5306):1593–9.
- Schwarte, R. C. and Godfrey, E. W. (2004). Nitric oxide synthase activity is required for postsynaptic differentiation of the embryonic neuromuscular junction. *Developmental biology*, 273(2):276–84.
- Schweitzer, J. and Driever, W. (2009). Development of the dopamine systems in zebrafish. *Advances in Experimental Medicine and Biology*, 651:1–14.
- Schweitzer, J., Lohr, H., Filippi, A., and Driever, W. (2012). Dopaminergic and noradrenergic circuit development in zebrafish. *Developmental Neurobiology*, 72(3):256–68.
- Schwentker, a., Vodovotz, Y., Weller, R., and Billiar, T. R. (2002). Nitric oxide and wound repair: role of cytokines? *Nitric Oxide*, 7(1):1–10.
- Scott, J. D. (1991). Cyclic nucleotide-dependent protein kinases. *Pharmacology & Therapeutics*, 50(1):123–145.
- Selverston, A. I. and Miller, J. P. (1982). Mechanisms underlying pattern generation in lobster stomatogastric ganglion as determined by selective inactivation of identified neurons. I. Pyloric system. *Journal of Neurophysiology*, 44(6):1102–1121.
- Sen, N., Hara, M. R., Kornberg, M. D., Cascio, M. B., Bae, B.-I., Shahani, N., Thomas, B., Dawson, T. M., Dawson, V. L., Snyder, S. H., and Sawa, A. (2008). Nitric oxide-induced nuclear GAPDH activates p300/CBP and mediates apoptosis. *Nature Cell Biology*, 10(7):866–873.
- Sesack, S. R. and Pickel, V. M. (1992). Prefrontal cortical efferents in the rat synapse on unlabeled neuronal targets of catecholamine terminals in the nucleus accumbens septi and on dopamine neurons in the ventral tegmental area. *Journal of Comparative Neurology*, 320(2):145–160.
- Seth, P., Gajendiran, M., Maitra, K. K., Ross, H. G., and Ganguly, D. K. (1993). Evidence for D1 dopamine receptor-mediated modulation of the synaptic transmission from

REFERENCES

- motor axon collaterals to Renshaw cells in the rat spinal cord. *Neuroscience Letters*, 158(2):217–220.
- Seutin, V., Verbanck, P., Massotte, L., and Dresse, A. (1990). Evidence for the presence of N-methyl-D-aspartate receptors in the ventral tegmental area of the rat: an electrophysiological in vitro study. *Brain Research*, 514(1):147–150.
- Sharp, A. H., Dawson, T. M., Ross, C. A., Fotuhi, M., Mourey, R. J., and Snyder, S. H. (1993). Inositol 1,4,5-trisphosphate receptors: immunohistochemical localization to discrete areas of rat central nervous system. *Neuroscience*, 53(4):927–942.
- Sharp, A. H., Nucifora, F. C., Blondel, O., Sheppard, C. A., Zhang, C., Snyder, S. H., Russell, J. T., Ryugo, D. K., and Ross, C. A. (1999). Differential cellular expression of isoforms of inositol 1,4,5-triphosphate receptors in neurons and glia in brain. *Journal of Comparative Neurology*, 406(2):207–20.
- Sharples, S. a., Humphreys, J. M., Jensen, a. M., Dhoopar, S., Delaloye, N., Clemens, S., and Whelan, P. J. (2015). Dopaminergic modulation of locomotor network activity in the neonatal mouse spinal cord. *Journal of Neurophysiology*, 113(7):2500–2510.
- Sharples, S. A., Koblinger, K., Humphreys, J. M., and Whelan, P. J. (2014). Dopamine: a parallel pathway for the modulation of spinal locomotor networks. *Frontiers in Neural Circuits*, 8(June):55.
- Shelly, M., Lim, B. K., Cancedda, L., Heilshorn, S. C., Gao, H., and Poo, M.-m. (2010). Local and long-range reciprocal regulation of cAMP and cGMP in axon/dendrite formation. *Science*, 327(5965):547–52.
- Sillar, K. T., Combes, D., Ramanathan, S., Molinari, M., and Simmers, J. (2008). Neuromodulation and developmental plasticity in the locomotor system of anuran amphibians during metamorphosis. *Brain Research Reviews*, 57(1):94–102.
- Sillar, K. T., Combes, D., and Simmers, J. (2014). Neuromodulation in developing motor microcircuits. *Current Opinion in Neurobiology*, 29C:73–81.
- Sillar, K. T., Woolston, A. M., and Wedderburn, J. F. (1995). Involvement of brainstem serotonergic interneurons in the development of a vertebrate spinal locomotor circuit. *Proceedings. Biological sciences / The Royal Society*, 259(1354):65–70.
- Silva, N. L. and Bunney, B. S. (1988). Intracellular studies of dopamine neurons in vitro: pacemakers modulated by dopamine. *European journal of pharmacology*, 149(3):307–315.

REFERENCES

- Sirota, M. G., Di Prisco, G. V., and Dubuc, R. (2000). Stimulation of the mesencephalic locomotor region elicits controlled swimming in semi-intact lampreys. *European Journal of Neuroscience*, 12(11):4081–4092.
- Skagerberg, G. and Lindvall, O. (1985). Organization of diencephalic dopamine neurones projecting to the spinal cord in the rat. *Brain Research*, 342(2):340–351.
- Sladek, S. M., Regenstein, A. C., Lykins, D., and Roberts, J. M. (1993). Nitric oxide synthase activity in pregnant rabbit uterus decreases on the last day of pregnancy. *American Journal of Obstetrics and Gynecology*, 169(5):1285–91.
- Smeets, W. J. a. J. and González, A. (2000). Catecholamine systems in the brain of vertebrates: New perspectives through a comparative approach. *Brain Research Reviews*, 33(2-3):308–379.
- Smith, R. D. and Goldin, a. L. (1997). Phosphorylation at a single site in the rat brain sodium channel is necessary and sufficient for current reduction by protein kinase A. *Journal of Neuroscience*, 17(16):6086–6093.
- Smith, Y. and Bolam, J. P. (1990). The output neurones and the dopaminergic neurones of the substantia nigra receive a GABA-Containing input from the globus pallidus in the rat. *Journal of Comparative Neurology*, 296(1):47–64.
- Snyder, S. (1992). Nitric oxide: first in a new class of neurotransmitters. *Science*, 257(5069):494–496.
- Soffe, S. R. (1989). Roles of glycinergic inhibition and N-methyl-D-aspartate receptor mediated excitation in the locomotor rhythmicity of one half of the *Xenopus* embryo central nervous system. *European Journal of Neuroscience*, 1(6):561–571.
- Son, H., Hawkins, R. D., Martin, K., Kiebler, M., Huang, P. L., Fishman, M. C., and Kandel, E. R. (1996). Long-term potentiation is reduced in mice that are doubly mutant in endothelial and neuronal nitric oxide synthase. *Cell*, 87(6):1015–23.
- Song, J., Kyriakatos, a., and El Manira, a. (2012). Gating the Polarity of Endocannabinoid-Mediated Synaptic Plasticity by Nitric Oxide in the Spinal Locomotor Network. *Journal of Neuroscience*, 32(15):5097–5105.
- Sorenson, C. a. and Ellison, G. D. (1970). Striatal organization of feeding behavior in the decorticate rat. *Experimental Neurology*, 29(1):162–174.
- Sotnikova, T. D., Beaulieu, J. M., Espinoza, S., Masri, B., Zhang, X., Salahpour, A., Barak, L. S., Caron, M. G., and Gainetdinov, R. R. (2010). The dopamine metabolite 3-methoxytyramine is a neuromodulator. *PLoS ONE*, 5(10).

REFERENCES

- Souza, B. R., Romano-Silva, M. A., and Tropepe, V. (2011). Dopamine D2 receptor activity modulates Akt signaling and alters GABAergic neuron development and motor behavior in zebrafish larvae. *Journal of Neuroscience*, 31(14):5512–25.
- Spano, P. F., Govoni, S., and Trabucchi, M. (1978). Studies on the pharmacological properties of dopamine receptors in various areas of the central nervous system. *Advances in Biochemical Psychopharmacology*, 19:155–165.
- Spielewoy, C., Roubert, C., Hamon, M., Nosten-Bertrand, M., Betancur, C., and Giros, B. (2000). Behavioural disturbances associated with hyperdopaminergia in dopamine-transporter knockout mice. *Behavioural pharmacology*, 11(3-4):279–290.
- Spike, R. C., Todd, A. J., and Johnston, H. M. (1993). Coexistence of NADPH diaphorase with GABA, glycine, and acetylcholine in rat spinal cord. *Journal of Comparative Neurology*, 335(3):320–333.
- Spitzer, N. C., Vincent, A., and Lautermilch, N. J. (2000). Differentiation of electrical excitability in motoneurons. *Brain Research Bulletin*, 53(5):547–552.
- Spratt, D. E., Newman, E., Mosher, J., Ghosh, D. K., Salerno, J. C., and Guillemette, J. G. (2006). Binding and activation of nitric oxide synthase isozymes by calmodulin EF hand pairs. *FEBS Journal*, 273(8):1759–1771.
- Stamler, J. S. and Meissner, G. (2001). Physiology of nitric oxide in skeletal muscle. *Physiological reviews*, 81(1):209–237.
- Stein, W. (2014). Sensory Input to Central Pattern Generators. In *Encyclopedia of Computational Neuroscience*, pages 1–11. Springer New York, New York, NY.
- Steinbach, K., Volkmer, H., and Schlosshauer, B. (2002). Semaphorin 3E/collapsin-5 inhibits growing retinal axons. *Experimental cell research*, 279(1):52–61.
- Steinfels, G. F., Heym, J., and Jacobs, B. L. (1981). Single unit activity of dopaminergic neurons in freely moving cuts. *Life sciences*, 29(14):1435–1442.
- Stephenson-Jones, M., Samuelsson, E., Ericsson, J., Robertson, B., and Grillner, S. (2011). Evolutionary conservation of the basal ganglia as a common vertebrate mechanism for action selection. *Current Biology*, 21(13):1081–1091.
- Stern, M. and Bicker, G. (2010). Nitric oxide as a regulator of neuronal motility and regeneration in the locust embryo. *Journal of insect physiology*, 56(8):958–65.
- Stern, M., Böger, N., Eickhoff, R., Lorbeer, C., Kerssen, U., Ziegler, M., Martinelli, G. P., Holstein, G. R., and Bicker, G. (2010). Development of nitrergic neurons

REFERENCES

- in the nervous system of the locust embryo. *Journal of Comparative Neurology*, 518(8):1157–75.
- Strübing, C., Ahnert-Hilger, G., Shan, J., Wiedenmann, B., Hescheler, J., and Wobus, A. M. (1995). Differentiation of pluripotent embryonic stem cells into the neuronal lineage in vitro gives rise to mature inhibitory and excitatory neurons. *Mechanisms of Development*, 53(2):275–287.
- Stuber, G. D., Hnasko, T. S., Britt, J. P., Edwards, R. H., and Bonci, A. (2010). Dopaminergic terminals in the nucleus accumbens but not the dorsal striatum corelease glutamate. *Journal of Neuroscience*, 30(24):8229–8233.
- Stuehr, D. J. (2004). Enzymes of the L-arginine to nitric oxide pathway. *The Journal of nutrition*, 134(10 Suppl):2748S–2751S; discussion 2765S–2767S.
- Sun, X., Zhao, Y., and Wolf, M. E. (2005). Dopamine receptor stimulation modulates AMPA receptor synaptic insertion in prefrontal cortex neurons. *Journal of Neuroscience*, 25(32):7342–7351.
- Swanson, L. W., Mogenson, G. J., Gerfen, C. R., and Robinson, P. (1984). Evidence for a projection from the lateral preoptic area and substantia innominata to the 'mesencephalic locomotor region' in the rat. *Brain Research*, 295(1):161–178.
- Taddese, A. and Bean, B. P. (2002). Subthreshold sodium current from rapidly inactivating sodium channels drives spontaneous firing of tuberomammillary neurons. *Neuron*, 33(4):587–600.
- Takemura, M., Wakisaka, S., Iwase, K., Yabuta, N. H., Nakagawa, S., Chen, K., Bae, Y. C., Yoshida, A., and Shigenaga, Y. (1996). NADPH-diaphorase in the developing rat: Lower brainstem and cervical spinal cord, with special reference to the trigemino-solitary complex. *Journal of Comparative Neurology*, 365(4):511–525.
- Tay, T. L., Ronneberger, O., Ryu, S., Nitschke, R., and Driever, W. (2011). Comprehensive catecholaminergic projectome analysis reveals single-neuron integration of zebrafish ascending and descending dopaminergic systems. *Nature Communications*, 2:171.
- Tazerart, S., Vinay, L., and Brocard, F. (2008). The persistent sodium current generates pacemaker activities in the central pattern generator for locomotion and regulates the locomotor rhythm. *Journal of Neuroscience*, 28(34):8577–89.
- Tecuapetla, F., Patel, J. C., Xenias, H., English, D., Tadros, I., Shah, F., Berlin, J., Deisseroth, K., Rice, M. E., Tepper, J. M., and Koos, T. (2010). Glutamatergic

REFERENCES

- signaling by mesolimbic dopamine neurons in the nucleus accumbens. *Journal of Neuroscience*, 30(20):7105–7110.
- Tegeder, I., Del Turco, D., Schmidtko, A., Sausbier, M., Feil, R., Hofmann, F., Deller, T., Ruth, P., and Geisslinger, G. (2004). Reduced inflammatory hyperalgesia with preservation of acute thermal nociception in mice lacking cGMP-dependent protein kinase I. *Proceedings of the National Academy of Sciences of the United States of America*, 101(9):3253–7.
- Tegenge, M. A. and Bicker, G. (2009). Nitric oxide and cGMP signal transduction positively regulates the motility of human neuronal precursor (NT2) cells. *Journal of Neurochemistry*, 110(6):1828–41.
- Tegenge, M. A., Rockel, T. D., Fritsche, E., and Bicker, G. (2011a). Nitric oxide stimulates human neural progenitor cell migration via cGMP-mediated signal transduction. *Cellular and molecular life sciences : CMLS*, 68(12):2089–99.
- Tegenge, M. A., Roloff, F., and Bicker, G. (2011b). Rapid differentiation of human embryonal carcinoma stem cells (NT2) into neurons for neurite outgrowth analysis. *Cellular and molecular neurobiology*, 31(4):635–43.
- Tepper, J. M. and Lee, C. R. (2007). GABAergic control of substantia nigra dopaminergic neurons. *Progress in Brain Research*, 160(06):189–208.
- Tepper, J. M., Martin, L. P., and Anderson, D. R. (1995). GABA_A receptor-mediated inhibition of rat substantia nigra dopaminergic neurons by pars reticulata projection neurons. *Journal of Neuroscience*, 15(4):3092–103.
- Tepper, J. M., Trent, F., and Nakamura, S. (1990). Postnatal development of the electrical activity of rat nigrostriatal dopaminergic neurons. *Developmental Brain Research*, 54(1):21–33.
- Tepper, J. M., Trent, F., and Nakamura, S. (1991). In Vivo Development of the Spontaneous Activity of Rat Nigrostriatal Dopaminergic Neurons. pages 259–268.
- Terada, H., Nagai, T., Kimura, H., Kitahama, K., and Okada, S. (1996). Distribution of nitric oxide synthase-immunoreactive neurons in fetal rat brains at embryonic day 15 and day 19. *Journal of Chemical Neuroanatomy*, 10(3-4):273–278.
- Terada, H., Nagai, T., Okada, S., Kimura, H., and Kitahama, K. (2001). Ontogenesis of neurons immunoreactive for nitric oxide synthase in rat forebrain and midbrain. *Developmental Brain Research*, 128(2):121–137.

REFERENCES

- Tertyshnikova, S., Yan, X., and Fein, A. (1998). cGMP inhibits IP₃-induced Ca²⁺ release in intact rat megakaryocytes via cGMP- and cAMP-dependent protein kinases. *Journal of Physiology*, 512(1):89–96.
- Thirumalai, V. and Cline, H. T. (2008). Endogenous dopamine suppresses initiation of swimming in prefeeding zebrafish larvae. *Journal of Neurophysiology*, 100(3):1635–48.
- Tong, H. and McDearmid, J. R. (2012). Pacemaker and Plateau Potentials Shape Output of a Developing Locomotor Network. *Current Biology*, 22(24):2285–2293.
- Tong, Z. Y., Overton, P. G., and Clark, D. (1996). Antagonism of NMDA receptors but not AMPA/kainate receptors blocks bursting in dopaminergic neurons induced by electrical stimulation of the prefrontal cortex. *Journal of Neural Transmission*, 103(8-9):889–904.
- Töpel, I., Stanarius, A., and Wolf, G. (1998). Distribution of the endothelial constitutive nitric oxide synthase in the developing rat brain: An immunohistochemical study. *Brain Research*, 788(1-2):43–48.
- Tran, S., Nowicki, M., Muraleetharan, A., and Gerlai, R. (2014). Differential effects of dopamine D1 and D2/3 receptor antagonism on motor responses. *Psychopharmacology*, 232(4):795–806.
- Traub, R. and Llinás, R. (1977). The spatial distribution of ionic conductances in normal and axotomized motoneurons. *Neuroscience*, 2(6):829–849.
- Tricoire, L. and Vitalis, T. (2012). Neuronal nitric oxide synthase expressing neurons: a journey from birth to neuronal circuits. *Frontiers in Neural Circuits*, 6(December):82.
- Trimm, K. R. and Rehder, V. (2004). Nitric oxide acts as a slow-down and search signal in developing neurites. *European Journal of Neuroscience*, 19(4):809–18.
- Trudeau, L. É. (2004). Glutamate co-transmission as an emerging concept in monoamine neuron function. *Journal of Psychiatry and Neuroscience*, 29(4):296–310.
- Tucker, K. R., Huertas, M. A., Horn, J. P., Canavier, C. C., and Levitan, E. S. (2012). Pacemaker rate and depolarization block in nigral dopamine neurons: a somatic sodium channel balancing act. *Journal of Neuroscience*, 32(42):14519–31.
- Uchida, S., Akaike, N., and Nabekura, J. (2000). Dopamine activates inward rectifier K⁺ channel in acutely dissociated rat substantia nigra neurones. *Neuropharmacology*, 39(2):191–201.

REFERENCES

- Ungless, M. A. and Grace, A. A. (2012). Are you or aren't you? Challenges associated with physiologically identifying dopamine neurons. *Trends in Neurosciences*, 35(7):422–30.
- Uteshev, V., Stevens, D., and Haas, H. (1995). A persistent sodium current in acutely isolated histaminergic neurons from rat hypothalamus. *Neuroscience*, 66(1):143–149.
- Valenti, O., Cifelli, P., Gill, K. M., and Grace, A. A. (2011). Antipsychotic drugs rapidly induce dopamine neuron depolarization block in a developmental rat model of schizophrenia. *Journal of Neuroscience*, 31(34):12330–12338.
- van den Pol, A. N. and Trombley, P. Q. (1993). Glutamate neurons in hypothalamus regulate excitatory transmission. *Journal of Neuroscience*, 13(7):2829–2836.
- van Dijken, H., Dijk, J., Voom, P., and Holstege, J. C. (1996). Localization of dopamine D2 receptor in rat spinal cord identified with immunocytochemistry and in situ hybridization. *European Journal of Neuroscience*, 8(3):621–628.
- Van Hartesveldt, C., Sickles, A. E., Porter, J. D., and Stehouwer, D. J. (1991). 1-DOPA-induced air-stepping in developing rats. *Developmental Brain Research*, 58(2):251–255.
- van Mier, P., Joosten, H. W., van Rheden, R., and ten Donkelaar, H. J. (1986). The development of serotonergic raphespinal projections in *Xenopus laevis*. *International journal of developmental neuroscience : the official journal of the International Society for Developmental Neuroscience*, 4(5):465–475.
- van Mier, P. and ten Donkelaar, H. J. (1989). Structural and functional properties of reticulospinal neurons in the early-swimming stage *Xenopus* embryo. *Journal of Neuroscience*, 9(1):25–37.
- Van Wagenen, S. and Rehder, V. (1999). Regulation of neuronal growth cone filopodia by nitric oxide. *Journal of neurobiology*, 39(2):168–185.
- Vodovotz, Y., Bogdan, C., Paik, J., Xie, Q. W., and Nathan, C. (1993). Mechanisms of suppression of macrophage nitric oxide release by transforming growth factor beta. *The Journal of experimental medicine*, 178(2):605–613.
- Walogorsky, M., Mongeon, R., Wen, H., Mandel, G., and Brehm, P. (2012a). Acetylcholine receptor gating in a zebrafish model for slow-channel syndrome. *Journal of Neuroscience*, 32(23):7941–8.

REFERENCES

- Walogorsky, M., Mongeon, R., Wen, H., Nelson, N. R., Urban, J. M., Ono, F., Mandel, G., and Brehm, P. (2012b). Zebrafish model for congenital myasthenic syndrome reveals mechanisms causal to developmental recovery. *Proceedings of the National Academy of Sciences of the United States of America*, 109(43):17711–6.
- Walsh, D., Perkins, J., and Krebs, E. (1968). An adenosine 3', 5'-monophosphate-dependant protein kinase from rabbit skeletal muscle. *Journal of Biological Chemistry*, 243(13):3763–3774.
- Wang, L. P., Li, F., Wang, D., Xie, K., Wang, D., Shen, X., and Tsien, J. Z. (2011). NMDA receptors in dopaminergic neurons are crucial for habit learning. *Neuron*, 72(6):1055–1066.
- Wang, W. and Lufkin, T. (2000). The murine *Otp* homeobox gene plays an essential role in the specification of neuronal cell lineages in the developing hypothalamus. *Developmental biology*, 227(2):432–449.
- Wang, W.-C. and McLean, D. L. (2014). Selective responses to tonic descending commands by temporal summation in a spinal motor pool. *Neuron*, 83(3):708–21.
- Wang, X. and Robinson, P. J. (1997). Cyclic GMP-dependent protein kinase and cellular signaling in the nervous system. *Journal of Neurochemistry*, 68(2):443–456.
- Warp, E., Agarwal, G., Wyart, C., Friedmann, D., Oldfield, C. S., Conner, A., Del Bene, F., Arrenberg, A. B., Baier, H., and Isacoff, E. Y. (2012). Emergence of Patterned Activity in the Developing Zebrafish Spinal Cord. *Current Biology*, 22(2):93–102.
- Warren, J. B. (1994). Nitric oxide and human skin blood flow responses to acetylcholine and ultraviolet light. *The FASEB journal : official publication of the Federation of American Societies for Experimental Biology*, 8(2):247–251.
- Weber, B., Schlicker, E., Sokoloff, P., and Stark, H. (2001). Identification of the dopamine autoreceptor in the guinea-pig retina as D(2) receptor using novel subtype-selective antagonists. *British journal of pharmacology*, 133(8):1243–1248.
- Wen, L., Wei, W., Gu, W., Huang, P., Ren, X., Zhang, Z., Zhu, Z., Lin, S., and Zhang, B. (2008). Visualization of monoaminergic neurons and neurotoxicity of MPTP in live transgenic zebrafish. *Developmental biology*, 314(1):84–92.
- Wenker, I. C., Benoit, J. P., Chen, X., Liu, H., Horner, R. L., and Mulkey, D. K. (2012). Nitric oxide activates hypoglossal motoneurons by cGMP-dependent inhibition of TASK channels and cGMP-independent activation of HCN channels. *Journal of Neurophysiology*, 107(5):1489–99.

REFERENCES

- Westerfield, M. (2000). *The Zebrafish Book: a Guide to the Laboratory Use of the Zebrafish (Brachydanio rerio)*. University of Oregon Press, Eugene, 4th edition.
- Westerfield, M., McMurray, J. V., and Eisen, J. S. (1986). Identified motoneurons and their innervation of axial muscles in the zebrafish. *Journal of Neuroscience*, 6(8):2267–77.
- Wetts, R., Phelps, P. E., and Vaughn, J. E. (1995). Transient and continuous expression of NADPH diaphorase in different neuronal populations of developing rat spinal cord. *Developmental Dynamics*, 202(3):215–228.
- White, C. R., Brock, T. A., Chang, L. Y., Crapo, J., Briscoe, P., Ku, D., Bradley, W. A., Gianturco, S. H., Gore, J., and Freeman, B. A. (1994). Superoxide and peroxynitrite in atherosclerosis. *Proceedings of the National Academy of Sciences of the United States of America*, 91(3):1044–1048.
- White, R. E., Lee, A. B., Shcherbatko, A. D., Lincoln, T. M., Schonbrunn, A., and Armstrong, D. L. (1993). Potassium channel stimulation by natriuretic peptides through cGMP-dependent dephosphorylation. *Nature*, 361(6409):263–266.
- Wienecke, J., Ren, L.-Q., Hultborn, H., Chen, M., Moller, M., Zhang, Y., and Zhang, M. (2014). Spinal Cord Injury Enables Aromatic L-Amino Acid Decarboxylase Cells to Synthesize Monoamines. *Journal of Neuroscience*, 34(36):11984–12000.
- Wightman, R. and Zimmerman, J. B. (1990). Control of dopamine extracellular concentration in rat striatum by impulse flow and uptake. *Brain Research Reviews*, 15(2):135–144.
- Wilson, J. M. (2005). Conditional Rhythmicity of Ventral Spinal Interneurons Defined by Expression of the Hb9 Homeodomain Protein. *Journal of Neuroscience*, 25(24):5710–5719.
- Wilson, R. I., Gödecke, A., Brown, R. E., Schrader, J., and Haas, H. L. (1999). Mice deficient in endothelial nitric oxide synthase exhibit a selective deficit in hippocampal long-term potentiation. *Neuroscience*, 90(4):1157–1165.
- Wise, R. A. (2004). Dopamine, learning and motivation. *Nature Reviews Neuroscience*, 5(6):483–494.
- Wolfart, J., Neuhoff, H., Franz, O., and Roeper, J. (2001). Differential expression of the small-conductance, calcium-activated potassium channel SK3 is critical for pacemaker control in dopaminergic midbrain neurons. *Journal of Neuroscience*, 21(10):3443–3456.

REFERENCES

- Wu, H. H., Cork, R. J., Huang, P. L., Shuman, D. L., and Mize, R. R. (2000). Refinement of the ipsilateral retinocollicular projection is disrupted in double endothelial and neuronal nitric oxide synthase gene knockout mice. *Developmental Brain Research*, 120(1):105–111.
- Wu, H. H., Selski, D. J., El-Fakahany, E. E., and McLoon, S. C. (2001). The role of nitric oxide in development of topographic precision in the retinotectal projection of chick. *Journal of Neuroscience*, 21(12):4318–25.
- Wu, H. H., Williams, C. V., and McLoon, S. C. (1994). Involvement of nitric oxide in the elimination of a transient retinotectal projection in development. *Science*, 265(5178):1593–6.
- Wu, J., Xiao, H., Sun, H., Zou, L., and Zhu, L. Q. (2012). Role of dopamine receptors in ADHD: A systematic meta-analysis. *Molecular Neurobiology*, 45(3):605–620.
- Wu, K. K. (2002). Regulation of endothelial nitric oxide synthase activity and gene expression. *Annals of the New York Academy of Sciences*, 962:122–130.
- Wyart, C., Del Bene, F., Warp, E., Scott, E. K., Trauner, D., Baier, H., and Isacoff, E. Y. (2009). Optogenetic dissection of a behavioural module in the vertebrate spinal cord. *Nature*, 461(7262):407–410.
- Xi, Y., Yu, M., Godoy, R., Hatch, G., Poitras, L., and Ekker, M. (2011). Transgenic zebrafish expressing green fluorescent protein in dopaminergic neurons of the ventral diencephalon. *Developmental Dynamics*, 240(11):2539–47.
- Xiang, Y., Li, Y., Zhang, Z., Cui, K., Wang, S., Yuan, X.-b., Wu, C.-p., Poo, M.-m., and Duan, S. (2002). Nerve growth cone guidance mediated by G protein-coupled receptors. *Nature Neuroscience*, 5(9):843–848.
- Xiong, G., Mojsilovic-Petrovic, J., Pérez, C. a., and Kalb, R. G. (2007). Embryonic motor neuron dendrite growth is stunted by inhibition of nitric oxide-dependent activation of soluble guanylyl cyclase and protein kinase G. *European Journal of Neuroscience*, 25(7):1987–97.
- Xue, C., Botkin, S. J., and Johns, R. A. (1996). Localization of Endothelial NOS at the Basal Microtubule Membrane in Ciliates Epithelium of Rat Lung. *Journal of Histochemistry & Cytochemistry*, 44(5):463–471.
- Yamada, R. X., Matsuki, N., and Ikegaya, Y. (2006). Nitric oxide/cyclic guanosine monophosphate-mediated growth cone collapse of dentate granule cells. *Neuroreport*, 17(6):661–665.

REFERENCES

- Yamada-Hanff, J. and Bean, B. P. (2013). Persistent sodium current drives conditional pacemaking in CA1 pyramidal neurons under muscarinic stimulation. *Journal of Neuroscience*, 33(38):15011–21.
- Yokogawa, T., Marin, W., Faraco, J., Pézeron, G., Appelbaum, L., Zhang, J., Rosa, F., Mourrain, P., and Mignot, E. (2007). Characterization of sleep in zebrafish and insomnia in hypocretin receptor mutants. *PLoS Biology*, 5(10):2379–2397.
- Yokoyama, C., Okamura, H., Nakajima, T., Taguchi, J., and Ibata, Y. (1994). Autoradiographic distribution of [³H]YM-09151-2, a high-affinity and selective antagonist ligand for the dopamine D2 receptor group, in the rat brain and spinal cord. *Journal of Comparative Neurology*, 344(1):121–136.
- Zhang, X. F., Hu, X. T., White, F. J., and Wolf, M. E. (1997). Increased responsiveness of ventral tegmental area dopamine neurons to glutamate after repeated administration of cocaine or amphetamine is transient and selectively involves AMPA receptors. *Journal of Pharmacology and Experimental Therapeutics*, 281(2):699–706.
- Zhao, H., Zhu, W., Pan, T., Xie, W., Zhang, A., Ondo, W. G., and Le, W. (2007). Spinal cord dopamine receptor expression and function in mice with 6-OHDA lesion of the A11 nucleus and dietary iron deprivation. *Journal of Neuroscience Research*, 85(5):1065–1076.
- Zhao, Z., Wang, Z., Gu, Y., Feil, R., Hofmann, F., and Ma, L. (2009). Regulate axon branching by the cyclic GMP pathway via inhibition of glycogen synthase kinase 3 in dorsal root ganglion sensory neurons. *Journal of Neuroscience*, 29(5):1350–60.
- Zhu, H., Clemens, S., Sawchuk, M., and Hochman, S. (2007). Expression and distribution of all dopamine receptor subtypes (D1-D5) in the mouse lumbar spinal cord: A real-time polymerase chain reaction and non-autoradiographic in situ hybridization study. *Neuroscience*, 149(4):885–897.
- Zhu, H., Clemens, S., Sawchuk, M., and Hochman, S. (2008). Unaltered D1, D2, D4, and D5 dopamine receptor mRNA expression and distribution in the spinal cord of the D3 receptor knockout mouse. *Journal of Comparative Physiology A*, 194(11):957–962.
- Zhu, J.-H., Zhang, X., McClung, J. P., and Lei, X. G. (2006). Impact of Cu, Zn-superoxide dismutase and Se-dependent glutathione peroxidase-1 knockouts on acetaminophen-induced cell death and related signaling in murine liver. *Experimental Biology and Medicine*, 231(11):1726–1732.

REFERENCES

Zweifel, L. S., Parker, J. G., Lobb, C. J., Rainwater, A., Wall, V. Z., Fadok, J. P., Darvas, M., Kim, M. J., Mizumori, S. J. Y., Paladini, C. A., Phillips, P. E. M., and Palmiter, R. D. (2009). Disruption of NMDAR-dependent burst firing by dopamine neurons provides selective assessment of phasic dopamine-dependent behavior. *Proceedings of the National Academy of Sciences of the United States of America*, 106(18):7281–7288.